A. R. JENSEN: Permo-Triassic Stratigraphy and Sedimentation in the Bowen Basin, Queensland—BMR Bulletin 154

BUREAU OF MINERAL RESOURCES
GEOLOGY AND GEOPHYSICS
DEPARTMENT OF MINERALS AND ENERGY
AUSTRALIA

Bulletin 154

Permo-Triassic Stratigraphy and Sedimentation in the Bowen Basin, Queensland

A. R. Jensen

BMR
S55(94)
BUL.45
Copy 4

DEPARTMENT OF MINERALS AND ENERGY
BUREAU OF MINERAL RESOURCES, GEOLOGY AND GEOPHYSICS

BULLETIN 154

Permo-Triassic Stratigraphy and Sedimentation in the Bowen Basin, Queensland

A. R. JENSEN

AUSTRALIAN GOVERNMENT PUBLISHING SERVICE
CANBERRA, 1975

DEPARTMENT OF MINERALS AND ENERGY

MINISTER: THE HON. R. F. X. CONNOR, M.P.

SECRETARY: SIR LENOX HEWITT, O.B.E.

BUREAU OF MINERAL RESOURCES, GEOLOGY AND GEOPHYSICS

ACTING DIRECTOR: L. C. NOAKES

ASSISTANT DIRECTOR, GEOLOGICAL BRANCH: J. N. CASEY

Published for the Bureau of Mineral Resources, Geology and Geophysics
by the Australian Government Publishing Service

ISBN 0 642 00968 6

MANUSCRIPT RECEIVED: DECEMBER 1972

REVISED MANUSCRIPT RECEIVED: NOVEMBER 1973

ISSUED: FEBRUARY 1975

Printed by Graphic Services Pty Ltd, 88 Pirie Street, Adelaide 5000

CONTENTS

	Page
SUMMARY	1
INTRODUCTION	3
Geological setting	3
Tectonic history	3
Depositional history	4
Structural elements	4
Conventions	6
Symbols and abbreviations	6
Arenite nomenclature	6
BLACKWATER GROUP	8
STRATIGRAPHY	8
Fair Hill Formation	8
Burngrove Formation	9
Rangal Coal Measures	11
PETROGRAPHY	12
Fair Hill Formation	12
Burngrove Formation	13
Rangal Coal Measures	15
SEDIMENTARY STRUCTURES	15
Description of structures	15
Orientation of cross-stratification	16
REWAN AND CLEMATIS GROUPS	18
STRATIGRAPHY	18
Southwestern area	18
Previous investigations	18
Description of stratigraphic units	23
Central area	34
Previous investigations	34
Description of stratigraphic units	36
Northern area	42
Previous investigations	42
Description of stratigraphic units	44
Southeastern area	55
Previous investigations	55
Description of stratigraphic units	57
Sequences farther west, on margin of Galilee Basin	63
Mantuan Downs area	63
Jericho and Lake Galilee area	63

Page

PETROGRAPHY 64

Lutite 64
Nomenclature 64
Rewan Group 64
Glenidal Formation 69
Expedition Sandstone 79
Origin of lutite suites 79

Arenite 82
Classification 82
Description of sandstone suites 84
Origin of petrological suites 100
Stratigraphic significance 105

ANALYSIS OF STRATIFICATION 107

Environmental significance of stratification 107
Classification sedimentation units 107
Recognition of patterns of sedimentation 108
Stratification in the Rewan Group 108
Stratification in the Clematis Group 116
Comparison with sequences of non-fluvial environments 126

Orientation of cross-stratification 129
Regional trends of palaeocurrents 132
Variability of azimuthal distribution 136

INTEGRATION OF RESULTS 137

Controls of sedimentation 137
Depositional environments—stratigraphic and tectonic implications 138
Blackwater Group 138
Rewan and Clematis Groups 139

Provenance—the significance of mineralogical changes 141

Conclusions 143

ACKNOWLEDGMENTS 144

REFERENCES 145

APPENDICES

1. Elongation function analysis 151

2. Table B. Location of samples 167
Table C. Modal analyses of arenite samples 176
Table D. Cross-stratification in Permian and Triassic Units 183

Page

TABLES

1. Thickness of Rewan and Clematis Groups 21
2. Stratigraphic nomenclature used in southwestern area 22
3. Stratigraphic sequence in southwestern area 24
4. Stratigraphic nomenclature used in central area 35
5. Stratigraphic sequence in central area 37
6. Stratigraphic nomenclature used in northern area 43
7. Stratigraphic sequence in northern area 47
8. Stratigraphic nomenclature used in southeastern area 56
9. Stratigraphic sequence in southeastern area 61
10. Main characteristics of lutites of Rewan Group and Glenidal Formation 65
11. Clay minerals in lutites 68
12. Chemical analyses of lutites 69
13. Fabric of mudstone in Glenidal Formation 70
14. Main petrographic characteristics of lutites 83
15. Main petrographic characteristics of sandstone suites 87
16. Clay minerals in sandstones 90
17. Bedding transitions in Rewan Group 109
18. Bedding transitions in Clematis Group 117

FIGURES

1. Outcrop distribution of Triassic rocks in the Bowen Basin 2
2. Structural elements of the Bowen Basin and surrounding areas 5
3. Symbols and abbreviations used in columnar sections 7
4. Silicified fossil stump, Fort Cooper Coal Measures 10
5. Glass shard in sandstone, Burngrove Formation. Photomicrograph 13
6. Crystal tuff, Kaloola Member of the Baralaba Coal Measures. Photomicrograph 14
7. Orientation of cross-stratification in the Blackwater Group 17
8. Original thickness of the Rewan Group 19
9. Original thickness of the Clematis Group 20
10. Rewan Group, measured sections and well logs in the southwestern area .... Between pages 22 & 23
11. Clematis Group, measured sections in the southwestern area Between pages 26 & 27
12. Sandstone of the Glenidal Formation, Carnarvon Ranges 27
13. Triangular-shaped cliff formed by landslide, Expedition Range 27
14. Type section of the Glenidal Formation, southwestern area 28
15. Red silty mudstone at top of the Glenidal Formation, Carnarvon Ranges 29

Page

16. Thin-bedded sandstone of the Glenidal Formation, Expedition Range 30
17. Planar stratification in sandstone of the Glenidal Formation, near Moolayember Dip 31
18. Ripple lamination in sandstone of the Glenidal Formation, southwestern area 31
19. Burrows and tracks in sandstone of the Glenidal Formation 32
20. Pebble conglomerate in very coarse pebbly sandstone at the base of the upper part of the Expedition Sandstone, southwestern area 33
21. Intraformational conglomerate near the base of the Sagittarius Sandstone. Central area 38
22. Faunal burrows near the base of the Sagittarius Sandstone. Central area 39
23. Clematis Group, measured sections in the central area 41
24. Rewan Group, measured sections in the northern area 45
25. Sagittarius Sandstone, measured sections in the northern area 48
26. Arcadia Formation showing cross-stratified sandstone overlain by a sequence fining up to mudstone. Southern end of Carborough Range 49
27. Arcadia Formation, Section GA46, northern area 50
28. Red mudstone of the Arcadia Formation with thin layers of green siltstone. Near Lake Elphinstone 51
29. Red mudstone of the Arcadia Formation with irregular patches of mottled green mudstone and silty mudstone. Near Lake Elphinstone 51
30. Clematis Group, measured sections in the northern area 52
31. Glenidal Formation, measured section in the northern area 54
32. Rewan Group, composite section in the southeastern area 58
33. Clematis Group, composite section in the southeastern area 59
34. Grainsize analysis of red and green lutite samples from the Rewan Group 66
35. Red mudstone of the Rewan Group showing distinct lamination. Photomicrograph 67
36. Graphic log of fabric and compositional changes in Triassic soil profiles. Based on core from BMR Mount Coolon 7 72
37. Fabric of mudstone at 33.57 m, BMR Mount Coolon 7. Photomicrograph 73
38. Inherited pedorelicts in mudstone from 33.76 m, BMR Mount Coolon 7. Photomicrograph 73
39. Striotubule in mudstone at 33.76 m, BMR Mount Coolon 7. Photomicrograph 74
40. Skew-plane sesquans in mudstone at 34.39 m, BMR Mount Coolan 7. Photomicrograph 74
41. Isotubule filled with s-matrix in mudstone at 34.39 m, BMR Mount Coolon 7. Photomicrograph 75

Page

42. Enlargement of part of isotubule in Figure 41. Photomicrograph 75
43. Faint lamination in red mudstone at 35.00 m, BMR Mount Coolon 7. Photomicrograph 76
44. Skew-plane sesquans and rounded sedimentary relicts in mudstone at 35.46 m, BMR Mount Coolon 7. Photomicrograph 76
45. Mudstone with an inundulic plasmic fabric at 35.76 m, BMR Mount Coolon 7. Photomicrograph 78
46. Framework composition (QRF plot) of sandstones of the Rewan and Clematis Groups 85
47. Typical quartzose sandstone. Photomicrograph 89
48. Sandstone from the Glenidal Formation showing well developed grain and channel argillans. Photomicrograph 91
49. Lithic sandstone. Photomicrograph 93
50. Pellet of fibrous to micritic carbonate, Sagittarius Sandstone. Photomicrograph 96
51. Pellet of micritic carbonate, Sagittarius Sandstone. Photomicrograph 96
52. Fine-grained sandstone with sparry carbonate. Photomicrograph 97
53. Kaolinitic ooliths, Sagittarius Sandstone. Photomicrograph 98
54. Vermicular kaolinite pellets, Sagittarius Sandstone. Photomicrograph 98
55. Phosphatic mud clast, Sagittarius Sandstone. Photomicrograph 99
56. Comparison of median grainsize with amount of quartz in framework of sandstones of the Rewan and Clematis Groups 104
57. Composition of sandstone framework in units within the Rewan and Clematis Groups 105
58. Progressive changes in the composition of the sandstones in successively younger units of the Rewan and Clematis Groups 106
59. Summary of cyclic pattern in the Rewan Group. (Based on Table 17d) 109
60. Arcadia Formation (Sect. GA10) in the Dawson River near Theodore, southwestern area 110
61. Cross-stratified sandstone of the Arcadia Formation showing upward decrease in the set size. Southwestern area 111
62. Stratification in the Arcadia Formation in Section GA11, southwestern area 112
63. Cumulative frequency curves of grainsize distribution of two samples from Bed G and one from Bed F in Section GA11 (Fig. 62) 113
64. Stratification in the Sagittarius Sandstone in Section GA34, northern area 115
65. Stratification in the Arcadia Formation in Section GA37-1, northern area 116
66. Cyclic pattern suggested by results of analysis in Table 18 116
67. Stratification in the Expedition Sandstone in Section GA05 (Spring Creek), southwestern area 119

		Page
68.	Section (GA05) in the Expedition Sandstone, southwestern area	120
69.	Stratification within a microdelta in the Expedition Sandstone, Expedition Range	121
70.	Solitary cross-stratified sandstone unit in small erosion hollow cut in planar stratified sandstone. Expedition Sandstone, southwestern area	122
71.	Stratification in the Expedition Sandstone in Section GA55, central area	123
72.	Solitary cross-stratified sandstone unit overlain by group cross-stratified unit. Expedition Sandstone, Raby Creek area	124
73.	Azimuthal distribution of cross-stratification in the Rewan Group	127
74.	Azimuthal distribution of cross-stratification in the Expedition Sandstone	128
75.	Histogram of dip angle of cross-strata	129
76.	Orientation of cross-stratification in the Sagittarius Sandstone	130
77.	Orientation of cross-stratification in the Arcadia Formation	130
78.	Orientation of cross-stratification in the Glenidal Formation	131
79.	Orientation of cross-stratification in the lower part of the Expedition Sandstone	131
80.	Orientation of cross-stratification in the upper part of the Expedition Sandstone	132
81.	Summary of cross-stratification trends in the Rewan and Clematis Groups	133
82.	Cumulative frequency histogram for azimuths of cross-stratification in units in the northern area	134
83.	Azimuthal distribution and vector means of cross-stratification in units in the northern area	135

SUMMARY

Part of the Permo-Triassic succession in the Bowen Basin consists of coal measures (Blackwater Group) overlain by a redbed sequence (Rewan Group) and a sequence composed essentially of quartz-rich sandstone (Clematis Group). The succession attains a maximum thickness of 3500 m. This study discusses the stratigraphy and controls of sedimentation, mainly from observations in the northern half of the basin.

The coal measures were formed at the close of the Permian when earth movements created a rapidly subsiding intermontane basin, possibly with an internal drainage system. The Rewan Group was laid down in the same drainage basin in a system of meandering and anastomosing channels, in response to a decreased rate of subsidence relative to the rate of supply of sediment. The red colour of the mudstone is due to the presence of finely divided hematite derived from red soils in the source area. When the rate of sediment supply exceeded the rate of subsidence, a major reorganization of the drainage system took place, together with a general increase in stream gradients as sandy sediment accumulated along the margin of the basin. Changes of relief in the source area, and in the type of vegetation, local climate, and rates of erosion and subsidence, led to podsolic weathering in both the source area and at the site of deposition; fossil soil profiles can now be recognized by the application of micro-pedological analysis to the mottled red and green mudstone of the basal part of the Clematis Group. The newly established system of braided and meandering channels spread sand from the northern and southwestern parts of the area towards the southeast, where the rate of subsidence was greatest.

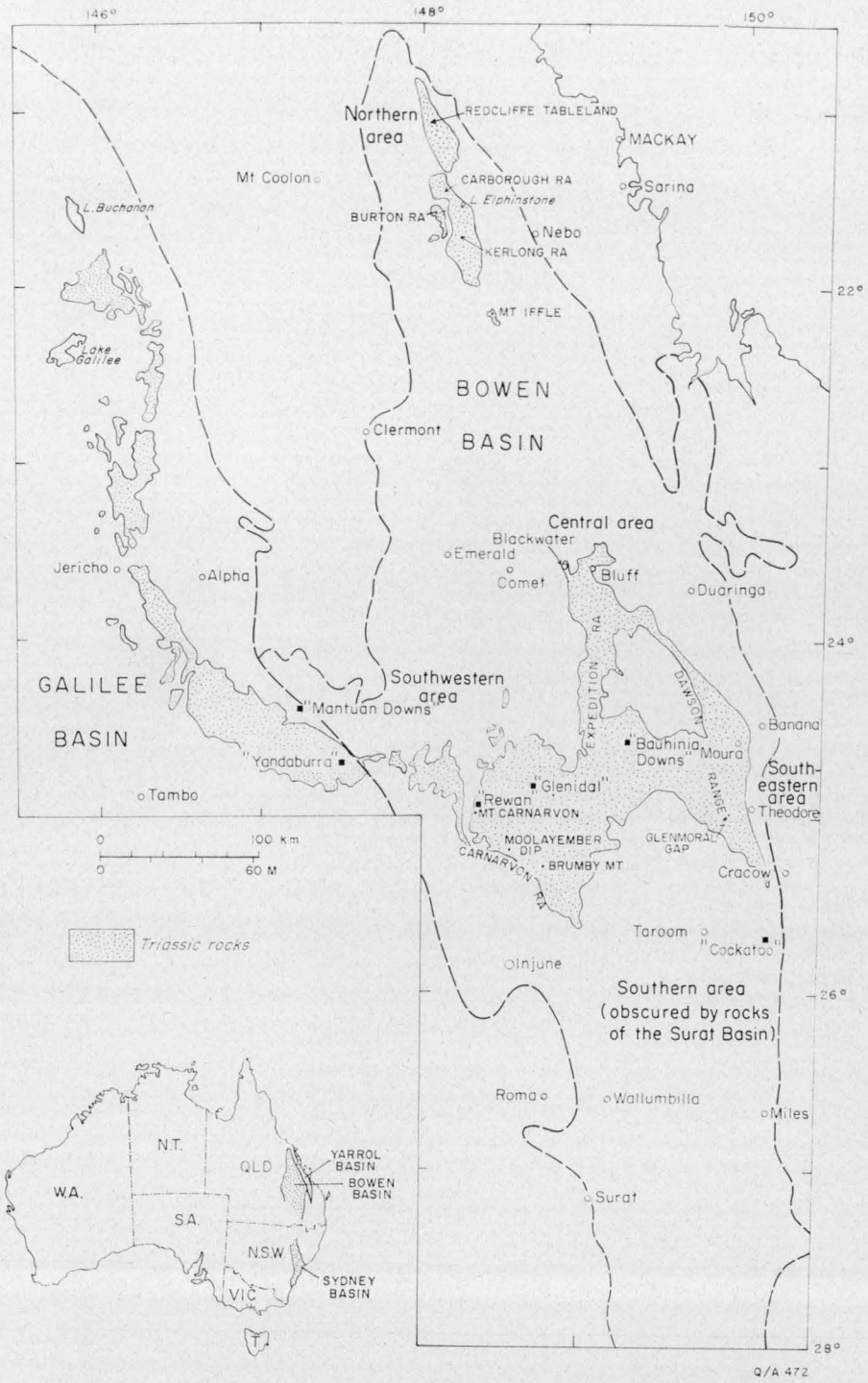


Fig. 1. Outcrop distribution of Triassic rocks in the Bowen Basin.

INTRODUCTION

A sequence of sedimentary rocks deposited during the Late Permian and Early to Middle Triassic in the Bowen Basin is here described and interpreted. The sequence comprises three lithostratigraphic units of basinwide extent—the Blackwater, Rewan, and Clematis Groups—and consists of coal measures at the base, overlain by redbeds, and quartz-rich sandstone at the top.

The purpose of the study was to investigate the nature of the Late Permian and Triassic succession and the factors controlling sedimentation in the basin. The study involved (a) the establishment of regional lithostratigraphic units as a basis for correlation in the well exposed northern half of the basin; (b) determination of the environment of deposition by the study of sedimentary structures; (c) determination of the regional palaeocurrent trends; and (d) a study of the mineral composition and fabric of the rocks with particular reference to features which reflect provenance, environment of deposition, and post-depositional changes.

The basin, which lies about 600 km northwest of Brisbane (Fig. 1), was formed during the Permian and Triassic, when a thick pile of marine and continental sediments accumulated over a wide area. It exists today as a structural basin, 900 km long and 250 km wide, the southern half of which is obscured by Jurassic and Cretaceous rocks of the Surat Basin. The present study is based on observations in five areas within the northern half (Fig. 1), where the Permo-Triassic succession crops out over an area of about 70 000 km^2.

The basin has become increasingly important over the last decade with the discovery of large deposits of coking coal within the Permian sequence. Much of the area is, however, sparsely populated, and most of the land is used for the raising of beef cattle. Unsealed roads and station tracks provide access to most areas, but the rugged country formed by the Clematis Group is accessible only on foot.

Geological Setting

Tectonic history

The folded rocks of eastern Australia were deformed by a number of partly overlapping tectonic events, ranging from the Cambrian to Late Triassic, which gave rise to subparallel belts elongated nearly north-south, with the older rocks to the west and the younger to the east (Warren, 1972, p. 46). These rocks, which constitute the East Australian Orogenic Province (Tectonic Map of Australia, 1971), are partly overlain by the Trans-Australian Platform Cover. The Bowen Basin is part of a depression in this platform cover.

The western side of the basin is bounded by sedimentary rocks and volcanics of the transitional North Queensland domain, which were deformed and intruded by granite in the Devonian and Carboniferous. Rocks of the same domain crop out to the east of the basin, but they are of relatively limited extent compared with those of the New England/Yarrol domain, in which the most intense deformation took place in the Permian. It was during this time that the Bowen Basin was filled, mainly with clastic detritus, presumably as an exogeosyncline (Voisey, 1959) or foredeep adjacent to a rising eastern margin, with a relatively stable cratonic block to the west.

In the Late Triassic the rocks of the Bowen Basin were deformed, most intensely along the eastern margin and in the areas now forming the Gogango Overthrust Zone.

Depositional history

In the Bowen Basin sedimentation began in Early Permian time and continued with little interruption into the Late Triassic. The earliest Permian rocks laid down comprise marine and continental sediments in the eastern part of the basin and continental beds in the southwest. The sequence in the east consists predominantly of intermediate volcanics. The sea transgressed westwards into the basin during the Early Permian and marine sedimentation continued into the Late Permian, with a partial regression late in the Early Permian. The earliest Late Permian was marked by a widespread transgression (Dickins, Malone, & Jensen, 1964) and the sea extended farther west than at any previous time during the Permian. During the Late Permian the sea finally withdrew and thick coal measures were formed on the newly emergent lowlands.

Little is known of the nature of the final marine regression. Alternative models based on relatively rapid or slow regression in various parts of the basin have been discussed by Jensen (1971), but in the absence of adequate time control their applicability cannot be tested. The palaeocurrent directions and mineral composition of arenites suggest that the regression was relatively rapid, and that there was only limited coeval marine deposition under its influence. In the southeast, the regression resulted in the westerly spread of shallow marine, deltaic, and finally non-marine sedimentation towards the centre of the basin. On the southwestern margin there is some evidence of non-deposition or possibly erosion before the non-marine beds were laid down.

During the regression in the north sediment was derived from source areas in the west and north, and possibly also from the east. The initial regression away from the western margin resulted in the spread of quartz-rich sand and associated paralic sediments towards the east, and in the east the shoreline probably migrated westwards from the folded and eroded eastern margin of the basin. In the final stage of regression a new drainage system was established, and most of the sediment was then derived from the north and northeast, with progressively smaller amounts from the west.

Structural elements

The Bowen Basin lies within an area of structural complexity, and the structure of the basin itself is also complex. The main structural elements as presented in Figure 2 are based on interpretations by Derrington (1962), Malone (1964), Traves (1966), Olgers (1973), and Dickins & Malone (1973).

The northwestern margin of the basin is bounded by the Anakie Inlier, which is flanked to the west by sediments of the Drummond Basin and the Carboniferous Bulgonunna Volcanics. The Anakie Inlier is a basement ridge consisting of pre-Devonian Anakie Metamorphics, Middle Devonian volcanics and sedimentary rocks, and Upper Devonian granite. It plunges south under the Bowen and Surat Basins to form the Nebine Ridge. In the Roma area the western margin of the basin is formed by the Roma Shelf, which consists of block-faulted metamorphosed Devonian rocks (Timbury Hills Formation) intruded by Carboniferous granite.

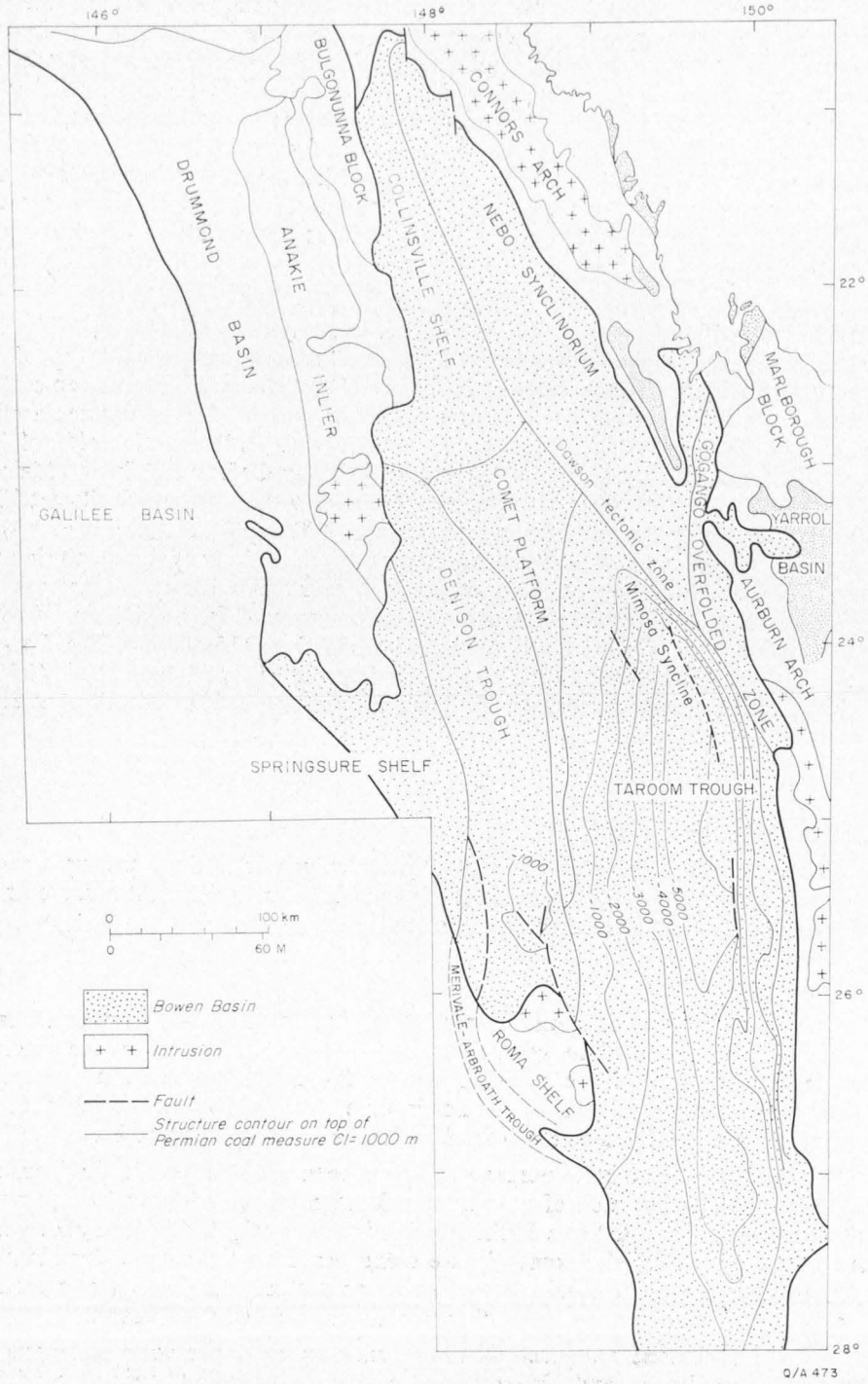


Fig. 2. Structural elements of the Bowen Basin and surrounding areas.

The eastern structural boundary is centred along the Connors and Auburn Arches, where the margin of the Bowen Basin is ill defined. The oldest rocks (the Marlborough Block), which are thought to be lower Palaeozoic, are extensively sheared and moderately to tightly folded. The relationship of small patches of Silurian and Devonian sedimentary rocks and volcanics to the Marlborough Block is unknown, but they were also folded before the formation of the Yarrol Basin. Elsewhere the Connors and Auburn Arches consist mainly of Carboniferous and Permian volcanics with some interbedded sedimentary rocks, which are moderately faulted and intruded by acid to basic plutonic rocks during the Permian and Mesozoic.

There is a wide range of structures within the Bowen Basin. The Taroom Trough, the northern continuation of which is known as the Mimosa Syncline, is a relatively simple deep elongate basin. The structure contours on the top of the uppermost Permian coal measures (Fig. 2) reveal that the basin has a steep eastern margin, a flat base, and a gently dipping western margin. The structures around the Comet Platform consist of a broad anticlinorium, with gentle folds of low amplitude, which merges into the structurally similar Collinsville Shelf (Malone, 1964; Malone et al., 1969). The Denison Trough, to the west of the Comet Platform, is a Lower Permian basin in which about 400 m of clastic sediments were deposited. To the west it is bounded in part by the relatively stable Springsure Shelf, from which a thin sequence of Permian rocks dips gently southwards. By way of contrast, the Nebo Synclinorium contains zones of intense isoclinal folding and overturned folds, particularly in the Gogango Overfolded Zone. The Dawson Tectonic Zone (Derrington, 1962) has been interpreted by Malone et al. (1969) as the result of gravity tectonics with detachment along a deep décollement zone.

Conventions

Symbols and abbreviations

The symbols and abbreviations used in the columnar sections are explained in Figure 3. The abbreviations opposite each symbol refer to the most common rock type at that level, unless otherwise indicated.

Arenite nomenclature

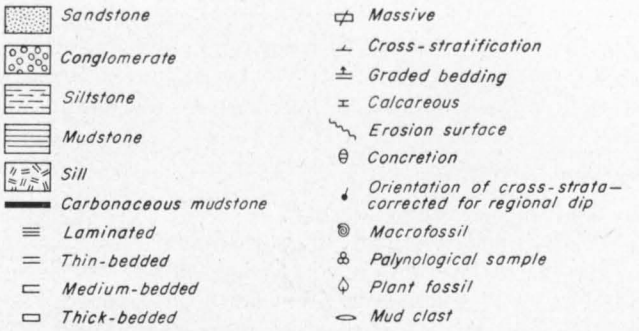
The great number of arenite classifications described in the literature (Okada, 1971) is an indication of the general dissatisfaction with all the available schemes. Part of the solution of the problem lies in the establishment of a universally acceptable nomenclature which does not involve classification, and which does not use terms already defined and redefined such as arkose and greywacke.

A brief code for arenite nomenclature has been adopted here in the form of a statement of the proportion of quartz to rock fragments to feldspar, calculated on a matrix-free and cement-free basis. To this is commonly added an indication of the amount of matrix, the nomenclature being based on the simple classification: A = less than 5 percent matrix, B = 5 to 15 percent matrix, C = greater than 15 percent matrix, although the limits of each class are somewhat arbitrary.

Thus a sandstone composed of 40 percent quartz, 30 percent rock fragments, 10 percent feldspar, and 20 percent matrix is described as a sandstone (50:38:12C), or in a shorter form (541C). Some use is also made of terms such as 'lithic' and 'sublabile', which are defined on page 84.

Conventions

SYMBOLS



ABBREVIATIONS

abd	*Abundant*	*mass*	*Massive*
ang	*Angular*	*max*	*Maximum*
Bd, Bdg, bdd	*Bed(ing)(ed)*	*Md, md*	*Mud(dy)*
biot	*Biotitic*	*Mdst*	*Mudstone*
bl (bl)	*Blue(ish)*	*Mic, mic*	*Mica(ceous)*
blk (blk)	*Black(ish)*	*mnr*	*Minor*
blky	*Blocky*	*Mrl, mrl*	*Marl(y)*
Bnd, Bndg, bndd	*Band(ing)(ed)*	*mtl*	*Mottled*
brn (brn)	*Brown(ish)*	*Mtx*	*Matrix*
C	*Coal*	*No*	*Number*
c	*Coarse*	*nr*	*Nearly, near*
c	*With*	*num*	*Numerous*
Calc, calc	*Calcite (areous)*	*O/c*	*Outcrop*
carb	*Carbonaceous*	*p*	*Poorly, poor*
Cgl, cgl	*Conglomerate(ic)*	*Pbl, pbl*	*Pebble(y)*
choc	*Chocolate*	*Pel, pel*	*Pellet(al)*
Cl, cl	*Clay(ey)*	*pk (pk)*	*Pink(ish)*
Clst	*Claystone*	*Plt*	*Plant*
com	*Common(ly)*	*Plt debris*	*Plant debris*
Conc	*Concretion*	*purp(purp)*	*Purple(ish)*
dk	*Dark(er)*	*Qz, qtz, qzs*	*Quartz(itic)(ose)*
Dolr, dolr	*Dolerite(ic)*	*Qzt*	*Quartzite*
f	*Fine(ly)*	*red-bd*	*Red-bed*
fe, fed	*Ferruginous(ised)*	*rnd, rndd*	*Round (ed)*
festnd	*Ironstained*	*Rub, rub*	*Rubble(y)*
fib	*Fibrous*	*scatd*	*Scattered*
Fld, fld	*Feldspar(thic)*	*Sd, sd*	*Sand(y)*
Frag, frag	*Fragment(al)*	*sft*	*Soft*
fri	*Friable*	*Sh, sh*	*Shale(y)*
gn (gn)	*Green(ish)*	*Si, si*	*Silica(eous)(ified)*
grd, grdd, grdg	*Grade(ed)(ing)*	*Sid, sid*	*Siderite(ic)*
Grn, grnd	*Grain(ed)*	*sl*	*Slight(ly)*
Grnl, grnl	*Granule(ar)*	*Slt, slt*	*Silt(y)*
gy (gy)	*Grey(ish)*	*Sltst*	*Siltstone*
hd	*Hard*	*Spl*	*Sample*
hvy, hvly	*Heavy(ily)*	*Sst*	*Sandstone*
Intbd, intbdd	*Interbed(ed)*	*stnd*	*Stained*
irreg	*Irregular*	*tk*	*Thick(ly)*
kao	*Kaolinitic*	*tn*	*Thin(ly)*
kh	*Khaki*	*Unconf, unconf*	*Unconformity(able)*
lab	*Labile*	*v*	*Very*
Lam, lam	*Laminae(tion)(ted)*	*vrtl*	*Vertical*
Len, len	*Lens(ticular)*	*wh (wh)*	*White(ish)*
lrg	*Largely*	*Wthrg, wthrd*	*Weathering(ed)*
lt	*Light(er)*	*yel*	*Yellow*
m	*Medium*	*&*	*And*

Fig. 3. Symbols and abbreviations used in columnar sections.

BLACKWATER GROUP

STRATIGRAPHY

The term Blackwater Group was proposed by Malone et al. (1969) for the sequence between the Back Creek Group and the Rewan Group (Formation) in the Blackwater area. Its use has been extended throughout the basin. In the Blackwater area, the group comprises three formations: the Fair Hill and Burngrove Formations and the Rangal Coal Measures. Local names have been applied to equivalents of each of these units in various parts of the basin.

Fair Hill Formation

The term 'Fairhill' was originally used by Utah Development Co. in unpublished reports for a unit between their Burngrove Shale and the German Creek Coal Measures. The name was later published (Malone et al., 1969) as Fair Hill, with the type section in a small gully about 6 km north of Cooroorah homestead in the Duaringa Sheet area. In this area, the formation is relatively homogeneous and consists of about 85 m of fine to coarse-grained, micaceous, calcareous sandstone (442B), which is conglomeratic in places, interbedded with very minor brown calcareous mudstone. Pebble conglomerate is restricted to thin beds in the sequence, but scattered pebbles are distributed throughout. Fossil logs are common; they have generally been replaced by siderite or limonite, and as they lie along bedding planes they were not buried in situ.

In the southeast, near Cracow, the Fair Hill Formation is represented by the Gyranda Formation which was defined originally by Derrington & Morgan (1960). The Gyranda Formation, which is about 400 m thick, consists essentially of sandstone and mudstone with thin beds of conglomerate and conglomeratic sandstone. The formation rests conformably on the Mount Steel Formation, but the boundary is defined by a sharp change in lithology from hard buff argillite to green-brown sandstone. The sandstones forming the lower part of the unit are overlain by a mudstone sequence followed by sandstone and conglomeratic sandstone at the top. The base of the overlying formation is taken at the first beds of tuff and conglomerate which contain numerous silicified fossil logs. The tuff beds were originally included in the Gyranda Formation by Derrington & Morgan (1960) and the conglomerate in the overlying Kia Ora Formation. To avoid confusion and to facilitate lithological correlation in other parts of the basin, however, the tuff beds are now excluded from the Gyranda Formation.

In the far northern part of the basin, the Fair Hill Formation is represented by the Hail Creek Beds (Jensen, 1971), which lie between the Blenheim Subgroup and the Fort Cooper Coal Measures. In marked contrast to the Blenheim Sub-group, the Hail Creek Beds consist of lithic sandstone (262C-091A), brown carbonaceous mudstone, and petromict conglomerate. The name is derived from Hail Creek, a tributary of Bee Creek, in the headwaters of which the beds crop out. The type section is along the Lake Elphinstone/Homevale road (between grid reference points 6766319 and 68083179 in the Mount Coolon Sheet area). The distribution and thickness of the beds are not known precisely. The thickness was originally estimated at 1360 m. The estimate was based on a composite section in the type area, but as parts of the sequence are probably repeated by faulting the

true thickness is probably considerably less. Farther north near Exmoor homestead, where the structure is less complex, the lower part of the unit is known to be 425 m thick, but the upper part is concealed. West of the type section the unit thins to 210 m (Davis, 1971).

In the type area, the base of the sequence consists of brown calcareous sandstone (15:60:25C), containing scattered pebbles of shale and volcanic rocks, with some conglomerate lenses up to 12 m thick. The conglomerate is composed of rounded pebbles and cobbles of volcanic rocks, sandstone, and shale set in a sandy matrix; subangular pieces of fossil wood are also common. Higher in the sequence conglomerate is rare and the unit consists of alternating lithic sandstone (2:90:8A) and mudstone. The mudstone is generally dark grey to brown, and in places it contains a high proportion of carbonaceous material, which suggests that some coal may be present. Discoidal calcareous concretions up to 50 cm in diameter are present in this part of the sequence. A similar succession is exposed in tributaries of the Bowen River near Exmoor homestead.

In the southwest no lithostratigraphic equivalent of the Fair Hill Formation is present, and the Black Alley Shale at the top of the Blenheim Sub-group is overlain by equivalents of the Burngrove Formation.

Burngrove Formation

In the Blackwater area, the sequence between the Fair Hill Formation and the Rewan Group comprises the Burngrove Formation and Rangal Coal Measures. The Burngrove Formation grades up into the coal measures, and the boundary is difficult to select.

In the type section, in a small creek about 9.5 km north of Cooroorah homestead, the Burngrove Formation is about 90 m thick. At the boundary between the Fair Hill Formation and the overlying Burngrove Formation there is generally a sudden change from cross-stratified calcareous sandstone to greyish brown carbonaceous mudstone with thin beds of green chert, extremely carbonaceous shale or shaly coal, and light green claystone. The basal beds are overlain by hard fine-grained sandstone thinly interbedded with hard grey or green mudstone. The sandstone is almost invariably laminated with thin mudstone partings and the mudstone commonly contains thin lenses of sandstone. In the upper part of the unit the hard green mudstone that predominates in this part of the section is crowded with well preserved leaf impressions. Silicified logs with simple growth rings or the complex structure of tree-ferns (*Palaeosmunda*) are restricted to one horizon at the top of the unit.

In the southeast the Burngrove Formation is represented by the Kaloola Member of the Baralaba Coal Measures. The type section is in a tributary of Kianga Creek, 13 km south of the Moura coal mine in the Monto Sheet area (Dear, McKellar, & Tucker, 1971), where it is reported to be between 90 and 120 m thick, and to consist of 'siltstone, feldspathic and lithic sandstone, tuff, and conglomerate'. Farther south, near Cracow, where the unit is 350 m thick, it consists of labile sandstone (5:75:20B), conglomerate, siltstone, volcanic breccia, tuff, and carbonaceous mudstone grading into shaly coal. The sandstone is commonly light brown to yellow in contrast to the greenish brown sandstone of the underlying

Gyranda Formation, the difference probably being attributable to the lack of chlorite in the Kaloola Member and the presence of kaolinite. Unweathered biotite flakes are commonly visible in the sandstone. The volcanic breccia is composed of a mixture of angular and rounded fragments of light-coloured banded acid volcanic rock up to 5 cm in diameter, but with the addition of rounded clasts it grades into volcanic-pebble conglomerate, which is present throughout the Baralaba Coal Measures in this area. Unlike the volcanic breccia, which has an open framework, the pebble conglomerate has a matrix of lithic sandstone. Most of the pebbles consist of banded volcanic rocks, but well rounded pebbles of biotite-rich fine tuff, similar to the crystal tuff interbedded with the unit, are relatively abundant. The crystal tuff is generally grey or brown, and the fine-grained varieties contain an abundance of well preserved fossil leaves and stems. In hand specimen the coarser variety closely resembles a microdiorite composed of plagioclase and biotite, and it is only the presence of plant fossils that provides proof of its clastic origin. Thin shaly coals are interbedded with the tuffs in a road cutting about 7 km southwest of Theodore. Silicified fossil logs are common in both the tuff and the labile sandstone.

In the northern part of the basin, the Burngrove Formation can be correlated with the Fort Cooper Coal Measures, a unit named but not rigidly defined by Reid (1946). A type section has therefore been selected in the headwaters of Hail Creek (between grid reference points 67533209 and 67413188 in the Mount



Fig. 4. Silicified fossil stump standing in its growth position within mudstone of the Fort Cooper Coal Measures. Headwaters of Hail Creek, northern area. The circular structures on either side of the stump are concretions.

Coolon Sheet area). The sequence in the type section is about 400m thick, and is composed of green lithic sandstone, conglomerate, mudstone, carbonaceous shale, coal, and thin beds of greyish white cherty tuff containing abundant leaf impressions. The base of the coal measures is taken at the lowest bed of pebbly lithic sandstone interbedded with thin beds of fine cherty tuff. Carbonaceous shale and thin coal are more common towards the top of the sequence. Fossil logs are common throughout, but particularly in conglomerate and tuff beds; fossil stumps standing in their growth position are present in a few places (Fig. 4).

Pebble and cobble conglomerate marker beds and conglomeratic sandstone are common at the base and near the top of the unit. Most of the pebbles, which are generally rounded, are composed of acid and intermediate volcanic rocks, but pebbles of quartz-rich sandstone (901A), hornfels, and phyllite are also present. The clasts are commonly cemented with calcite or fibrous chlorite, or both. The matrix is composed of the same type of rock fragments as the framework, with the addition of large subrounded feldspar grains and minor quartz.

The weathered sandstones in the coal measures appear to be highly limonitic, and develop a distinctive rectangular 'onion skin' on weathered surfaces; beds up to 3 m thick are present near St Albans homestead.

A separate equivalent of the Burngrove Formation has not been differentiated in the southwestern area, but the thin-bedded sandy limestone at the top of the Blenheim Sub-group is overlain by fine-grained sandstone interbedded with siliceous leaf-bearing tuff similar to the tuff in the Kaloola Member of the Baralaba Coal Measures. This part of the sequence in the southwest also contains numerous silicified fossil logs, and has been used to mark the base of the Blackwater Group (Mollan et al., 1969). It is overlain by soft shale, coarse conglomerate, carbonate-cemented sandstone (12:75:13A), and by a few beds of green montmorillonitic claystone.

Rangal Coal Measures

The Rangal Coal Measures form the upper unit of the Blackwater Group; the type section is in Deep Creek in the Duaringa Sheet area (Malone et al., 1969). Near the Utah Development Co. mine at Blackwater they are 107 to 137 m thick (Staines, 1972). There are few outcrops of the coal measures in the Blackwater area, and the best exposures are in the newly developed open-cut mines, where the sequence consists of sandstone, coal, shale and carbonaceous shale, siltstone, and thin kaolinitic clay bands or tonsteins. The sandstone is generally greyish white to dark grey, moderately well sorted, and fine to coarse-grained. In the lower part of the unit the sandstone is coarse-grained and trough cross-stratified, but the sandstone interbedded with the coal seams is generally very fine to fine-grained and laminated or cross-laminated. The thickness of the coal seams varies from about 10 m down to a few centimetres, and seam splits are common. The interbedded siltstone and shale are generally laminated and full of carbonaceous plant debris.

In the southeast the Rangal Coal Measures, which can be correlated with the upper part of the Baralaba Coal Measures as defined by Dear et al. (1971), are 240 m thick. The lithology is similar to that in the Blackwater area, except for the presence of thick lenses of pebble conglomerate, particularly around Cracow,

and of coarse-grained thickly bedded sandstone, such as the Bridge Sandstone of Reid (1944), between the coal seams. Laminated fine sandstone and mudstone are common, however, as in the Blackwater area.

In the north, the Fort Copper Coal Measures are overlain by a sequence, about 120 m thick, which is equivalent to the Rangal Coal Measures. The sequence consists of light brown calcareous sandstone, carbonaceous shale, mudstone, coal, and yellow-brown concretionary limestone, which has been referred to, but not precisely defined as, the Elphinstone Coal Measures by Reid (1946). Although the coal measures near Lake Elphinstone crop out fairly well, correlation with the Blackwater Group elsewhere is difficult because much of the sequence, especially the coal seams, is never seen in continuous section. The best exposures are probably farther west in the headwaters of Hail Creek within a syncline recognized by Jensen & Arman (1966).

In both the southeastern and central areas, the coal measures have in places been considerably altered by heat. In the southeast, as for example at Hill View homestead and near Lake Nash, cross-stratified sandstone and carbonaceous mudstone of the coal measures have been baked, fused, and brecciated. At both localities there are large blocks of black and brown cross-stratified sandstone with a vesicular texture. In places the blocks are composed of angular fragments of the sandstone, which have been fused together after brecciation. King & Jensen (1966) have suggested that the combustion of coal seams at or near the surface generated enough heat and explosive force to bake and shatter the surrounding sedimentary rocks.

PETROGRAPHY

Petrographic analysis of rocks from the Blackwater Group has been confined mainly to sandstone and pyroclastic rocks. Modal analyses of sandstone samples are listed in Appendix 2.

Fair Hill Formation

In all parts of the basin, the composition of the framework of the sandstones in the Fair Hill Formation and its lithostratigraphic equivalents is dominated by lithic fragments, and in particular, by fragments of volcanic rock. It is only in the central and northern areas, where the framework includes fragments of metamorphic and sedimentary rocks, that the quartz content exceeds 65 percent. In the north, where there is a progressive decrease from base to top in the amount of quartz, there is a corresponding increase in the number of volcanic-lithic fragments relative to sedimentary and metamorphic rocks. In the southeast, the sandstone of the Gyranda Formation is commonly devoid of quartz, and the lithic fragments consist exclusively of volcanic rocks. Many of the volcanic rocks are porphyritic and holocrystalline; others are holohyaline and contain perlitic cracks and are partly replaced by chlorite. The most distinctive feature of the sandstone in the southeast, however, is the presence of large subhedral grains of clinopyroxene and occasional small flakes of biotite and euhedral grains of apatite.

Burngrove Formation

The most typical rock type of the Burngrove Formation in the central area is fine-grained sandstone (25:30:45B) with black mudstone laminae. It is composed of subrounded fragments of highly altered greenish brown volcanic rock and angular grains of quartz and feldspar cemented by microcrystalline silica which is responsible for the toughness of the rock. The black mudstone laminae consist of a dark green phyllosilicate and cryptocrystalline material. The presence of devitrified glass shards, which have been replaced by microcrystalline silica, in the finer bands (Fig. 5)

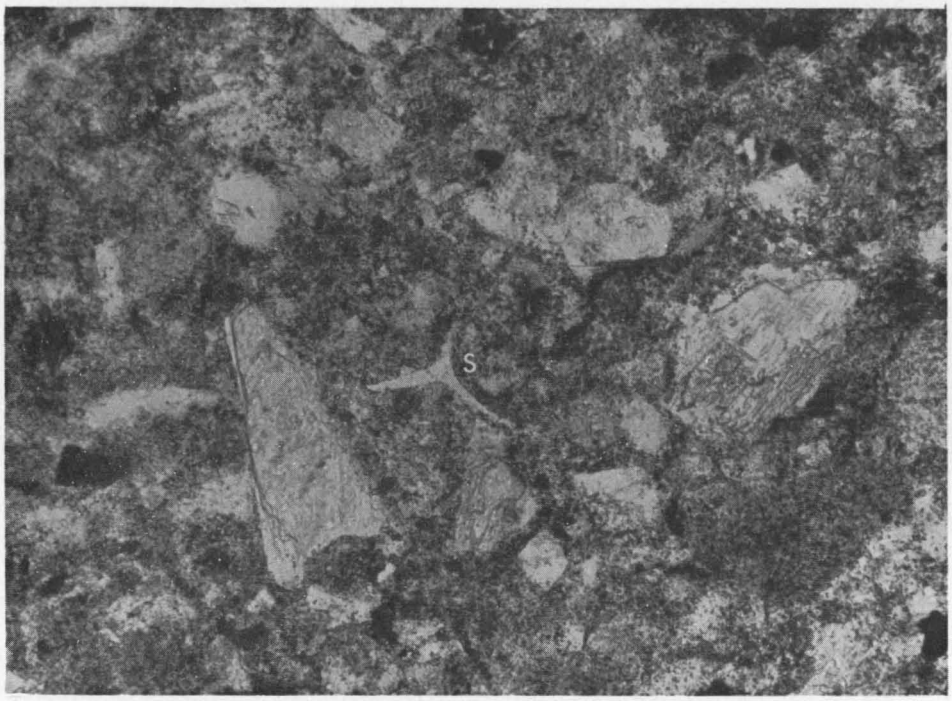


Fig. 5. A glass shard (S) in very fine-grained sandstone of the Burngrove Formation. Central area. Plane polarized light, x 160.

suggests that the microcrystalline cement of the coarser fraction is recrystallized volcanic dust. Recrystallized glass shards are also present in the green cherty tuffaceous mudstone, which consists mainly of silt-size quartz and feldspar grains set in a matrix of brown cryptocrystalline material interspersed with recrystallized zones composed of microcrystalline quartz-feldspar intergrowths.

The crystal tuff in the Kaloola Member of the Baralaba Coal Measures (Fig. 6) consists of subhedral laths of andesine, averaging 2 mm in length, which commonly have a shattered appearance, together with deep reddish brown subhedral to euhedral plates of biotite. The matrix, which forms up to 15 percent of the rock, consists of fine polycrystalline aggregates of potassium feldspar and possibly quartz. The fine conglomerate interbedded with the crystal tuff consists mainly of rounded fragments of volcanic rock cemented by sparry calcite or, in some places, analcite. As some of the clasts are identical with the biotite tuff interbedded



Fig. 6. Crystal tuff of the Kaloola Member of the Baralaba Coal Measures. The rock consists of crystals of andesine (A) and biotite (B) set in recrystallized glassy groundmass (G). Crossed polarizers, x 40.

with the conglomerate it is concluded that most of the detritus was derived by erosion of penecontemporaneous ash deposits and flows. The composition of the parent volcanic rocks is uncertain, but Joplin (1968, p. 130) has described a tuff belonging to the shoshonite association from Central Tilba in New South Wales which is similar to the biotite crystal tuff of the Kaloola Member. The fragments of volcanic rock in the conglomerate of the Kaloola Member contain very little quartz, and analysis of one pebble has shown it to have a high potassium content (3.5%). The composition is possibly consistent with the high-potassium calc-alkaline association of Jakes & Smith (1970), although the K/Na ratio is low (0.8%) and silica totals 65 percent.

Pyroclastic detritus and epiclastic detritus of volcanic origin are abundant in the Fort Cooper Coal Measures, the northern equivalent of the Burngrove Formation. Fragments of volcanic rock and large laths of plagioclase predominate in the sandstone (2:54:44B), which ranges from fine to very coarse-grained, but it is generally well sorted, with a chloritic or carbonate cement. The coarse epiclastic rocks cropping out between Turrawalla and Blenheim homesteads consist of sub-rounded and rounded clasts, ranging from about 5 mm to 1 cm in diameter, of devitrified holohyaline volcanic rock, which are probably reworked lapilli, set in a sparry carbonate cement. The finer-grained rocks within the Fort Cooper Coal Measures are commonly altered tuffs, with scattered clasts of pumice and laths of

feldspar set in a matrix of cryptocrystalline material and microcrystalline quartz and feldspar intergrowths formed by devitrification of volcanic ash.

Although pyroclastic rocks are very common no lavas have been recognized in the sequence. In the north, fine-grained igneous rocks are interbedded not only with the Fort Cooper Coal Measures, but also with the rest of the Blackwater Group. Some of the interbedded igneous rocks have been shown to be sills, but some flow rocks may be present. The contacts of some of the sills transgress the bedding, but there is no alteration of the surrounding sedimentary rocks. In places some of the sills are parallel to bedding and could be mistaken for interbedded flow rocks.

Rangal Coal Measures

The sandstone (343B) of the Rangal Coal Measures is generally moderately well sorted and fine to coarse-grained. The characteristic greyish white colour is due to the abundance of kaolinitic cement, and to the replacement of feldspar and rock fragments by kaolin. Most of the fragments that can be identified are of volcanic origin, but fragments of fine-grained sedimentary rocks are also present. A few of the rock fragments and feldspar grains have been replaced by dolomite, and small euhedral rhombs of dolomite replace the matrix. The sandstone (1:94:5A) of the Baralaba Coal Measures and the sandstone (5:61:34B) of the Elphinstone Coal Measures are similar to that of the Rangal Coal Measures at Blackwater, the only difference being that they contain less quartz in the framework.

SEDIMENTARY STRUCTURES

Description of structures

The sandstones of the Fair Hill Formation, and of equivalent formations in other parts of the basin, are generally either trough cross-stratified or horizontally stratified, but the environmental significance of the structures is unknown. In the southeast, the Gyranda Formation consists partly of repeated cyclic sequences, averaging 30 m, comprising mudstone, horizontally stratified sandstone, and trough cross-stratified sandstone. Insufficient data are available to determine the origin of the cycles.

In outcrop, the most striking feature of the Burngrove Formation in the Blackwater area, apart from its hardness, is its thin and regular bedding, which ranges from a few centimetres to about half a metre. Many of the beds, no matter how thin, are laminated and in places cross-stratified; slumping of the laminae is common. Some of the thin beds appear to be graded. The uniform bedding, hardness of the rocks, and low dip, have resulted in the development of flat rock platforms in parts of Burngrove Creek and in the type area.

One of the platforms, about 10 km north of Cooroorah homestead, bears a multitude of trails and impressions. The most common type of impression is current crescents, which consist of small scoop-shaped depressions, about 5 cm long, many of which have an elongate median platform. They are randomly distributed over the whole exposure, about 20 per square metre, and oriented north-south with the shallow fanned-out part of the depression at the southern end.

Measurements at two other localities show that small fragments of fossil wood are also roughly aligned in the same direction. No pebbles or obstructions that could have caused the current crescents are visible, but the bed immediately above consists of angular mud clasts, and water flowing around mud pellets lying on a muddy surface could have scoured out the depressions. The two main varieties of tracks preserved on the rock surface were evidently made by amphibians or fish (Warren, 1972, p. 160).

Elsewhere in the basin, the equivalents of the Burngrove Formation are not characterized by thin and regular bedding, mainly because the lithology is more variable, with a range from conglomerate to fine tuff. Most of the conglomerate beds appear to be massive, and the thick-bedded sandstones are commonly cross-stratified; only the mudstone and shale are thinly bedded.

The coarse sandstone of the Rangal Coal Measures in the central area is trough cross-stratified. The fine sandstone commonly found within seam splits is characteristically laminated or cross-laminated, with the size of sets of cross-strata not exceeding a few centimetres; the interbedded mudstone and siltstone are also laminated. The rocks within the splits are commonly disposed in a number of domes and basins produced by differential compaction (Burgis, 1973) during deposition of the coal measures. As a result of this differential movement the interseam rocks dip at high angles relative to the flat-lying or gently dipping coal seams, and the structures superficially resemble large foresets up to 30 m thick. The same type of structure is present in the Baralaba Coal Measures at Moura.

Orientation of cross-stratification

Method. The orientation of cross-stratification was measured as it was encountered because outcrop in much of the sequence is too sparse for systematic grid sampling to be carried out. Where possible measurements were also made throughout each stratigraphic section to check for differences within each unit. About 25 measurements were made at each locality; fewer where outcrop was poor, and more in some places to give a better idea of variability. All readings were automatically corrected for magnetic declination. Orientation data were processed by computer using a program developed by Jones (1970) which, after correcting for regional tilt, gives the arithmetic and vector means and variance (Appendix 2, table D). A modified version of the Rayleigh test of significance (Durrand & Greenwood, 1958) was applied, and if the distribution of azimuthal orientation was found to be random the result has not been used in further calculations or on maps. The data were organized at three hierarchial levels, one representing measurements taken at one sample site, the second from a few closely spaced sites but at slightly different stratigraphic levels, and a third including all measurements from particular stratigraphic units within each area. The palaeocurrent maps use vector means of azimuthal orientation computed from the first and second level of grouping.

Results. Measurements of the orientation of cross-stratification from scattered localities in the northern, central, and southeastern areas show that the Fair Hill Formation was deposited by currents moving south-southeast through the basin (Fig. 7a). In the southeast, however, the results are based on only a few measurements and are not particularly reliable.

Measurements of the orientation of cross-stratification in the Burngrove Formation and Rangal Coal Measures in a number of locations throughout the basin (Fig. 7b) indicate a change in the direction of sediment transport from that operative during the deposition of the Fair Hill Formation. The flow in the north was still directed southwards, but in the south and centre it was directed to the north or northwest. It is therefore possible that an internal drainage system existed or, alternatively, that there was some flow westwards from the centre of the basin.

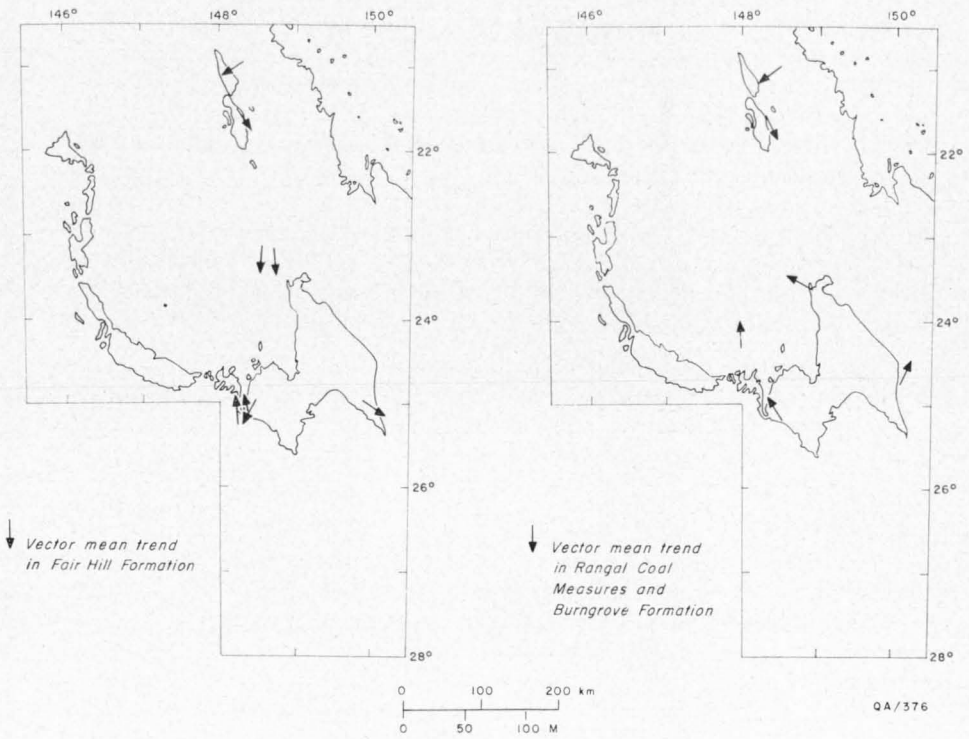


Fig. 7. Orientation of cross-stratification in the Blackwater Group.

REWAN AND CLEMATIS GROUPS

STRATIGRAPHY

The Triassic Rewan Formation, Clematis Sandstone, and Moolayember Formation were combined by Malone et al. (1969) to form the Mimosa Group because of a postulated change of climate after the deposition of the coal measures, a 'drastic change in locus and environment of deposition', and presumably because the three units were considered to be lithogenetically related. The effect of this nomenclature is a restriction of the status of divisions within each unit to member rank. Thus, the Sagittarius Sandstone, which is recognizable over the whole basin, is regarded as a member of the Rewan Formation, even though it is just as widespread and distinctive as the Rangal Coal Measures or Burngrove Formation. Secondly, the grouping implies that there is a closer genetic relationship between the Rewan Formation and the Clematis Sandstone than between the Rewan Formation and the Rangal Coal Measures, whereas in actual fact the Rangal Coal Measures and Rewan Formation were laid down in the same drainage basin, and the major change in palaeocurrent directions occurred when deposition of the Clematis Sandstone began. It is therefore proposed that the Rewan Formation be elevated to group rank by the recognition of two constituent formations—the Sagittarius Sandstone and the Arcadia Formation (see p. 25). Similarly, the Clematis Sandstone has been upgraded to the Clematis Group, which comprises the newly defined Glenidal Formation and the Expedition Sandstone.

No detailed isopach map of either the Rewan or Clematis Groups can be drawn, for lack of data, but the general variation of thickness is shown in Figures 8 and 9. The information is based on measured stratigraphic sections and unpublished well completion reports (Table 1).

Southwestern Area

For many years the attention of geologists was concentrated on the southwestern part of the basin, primarily because it was considered to be more prospective for petroleum. Many of the stratigraphic terms, such as Rewan Formation and Clematis Sandstone, have their origins in this area. This has turned out to be rather unfortunate because the sequences are much better developed in other parts of the basin.

Previous Investigations

Nomenclature. A summary of the changes in stratigraphic nomenclature of this part of the basin is presented in Table 2.

Use of the terms Upper, Middle, and Lower Bowen for divisions of the Bowen Series in the northern part of the basin were well established by the turn of the century, and in his reconnaissance of the southwestern area H. I. Jensen (1926) recognized a sequence equivalent to the Upper Bowen. He named the unit lying conformably above it the Clematis Sandstone, and later specified the gorge on Clematis Creek as the type area (Whitehouse, 1955). Reeves (1947) divided the Upper Bowen in the southwest into a basal coal measures overlain by a variegated clay shale. In cross-sections, he included a marker horizon, the Brumby Sandstone, at the boundary between the two units, but did not define it. Isbell (1955) and Hill (1957) used the term Rewan Formation for the sequence between the top of

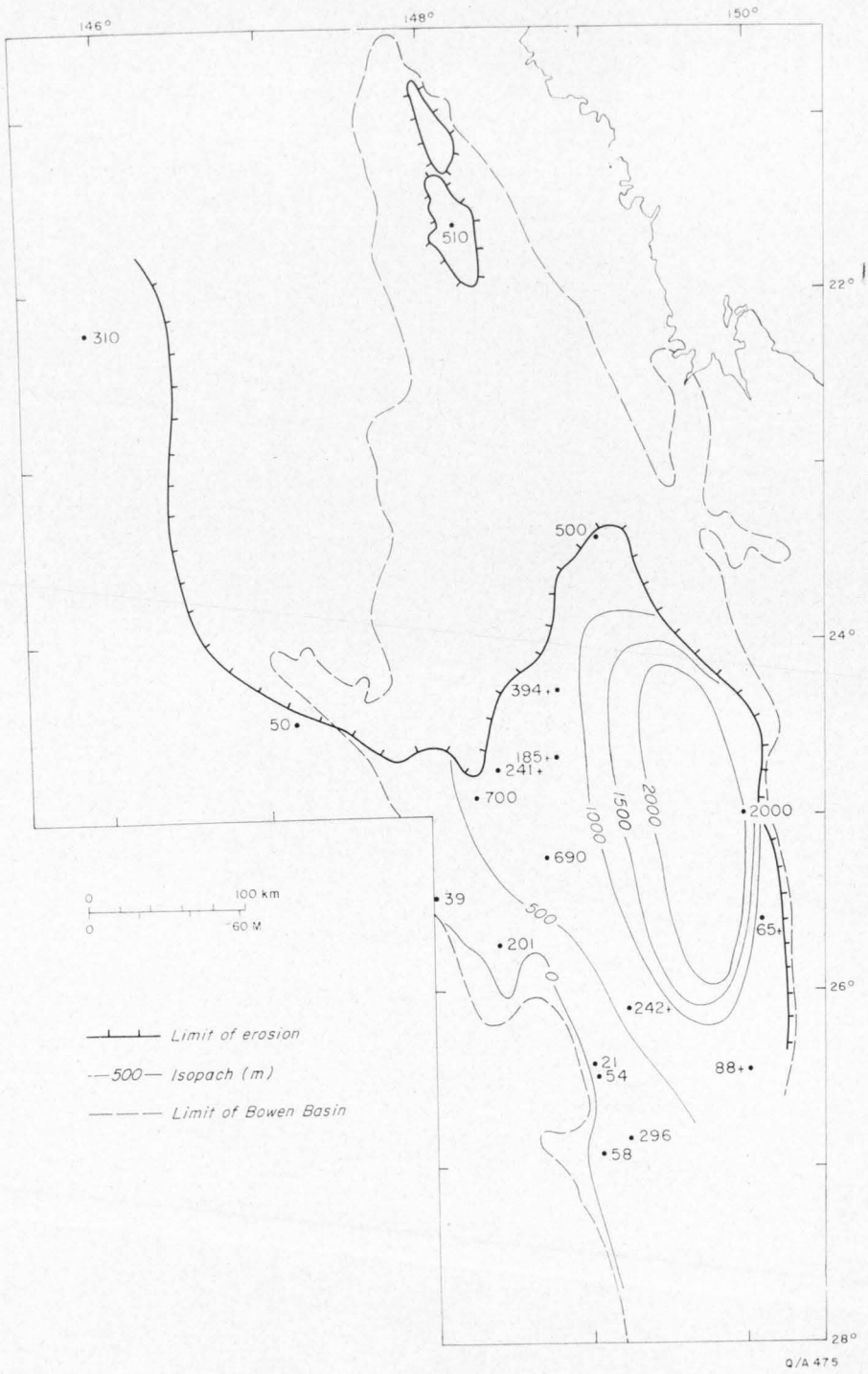


Fig. 8. Original thickness of the Rewan Group.

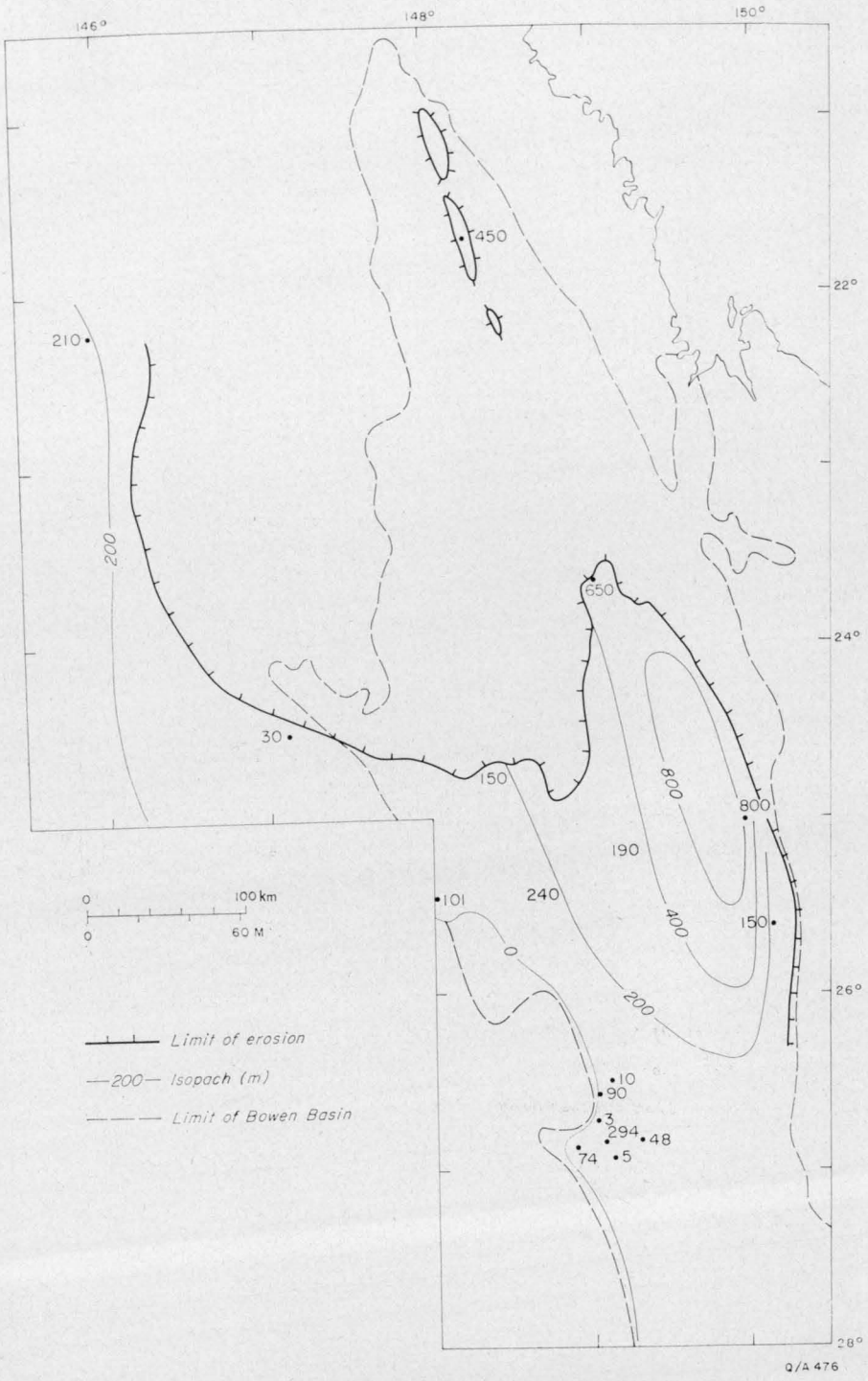


Fig. 9. Original thickness of the Clematis Group.

TABLE 1. THICKNESS OF REWAN AND CLEMATIS GROUPS

Location	*Rewan Group* (m)	*Clematis Group* (m)
Farmout Drillers Alice River No. 1	—	253
AAO Bardloming No. 1	—	3
Basin Creek outcrop	—	240
AAO Boondara No. 1	58	5
AAO Brucedale No. 1	—	74
Central area of outcrop	500?	650
Clematis Creek outcrop	—	240
UKA Cockatoo Creek No. 1	650	150
Amalgamated Petroleum Cometside No. 1	185	—
UKA Conloi No. 1	58	—
Planet Crystalbrook No. 1	39	101
AAO Dalmuir No. 1	21	—
Marathon-Continental Glenhaughton No. 1	1120	190
AAO Kildare No. 1	201	—
Exoil Lake Galilee No. 1	310	—
AAO Lorelle No. 1	296	48
Mantuan Downs outcrop area	50	30
AAO Meeleebee No. 1	242	—
SQD Morella No. 1	241	—
Northern area of outcrop	510	450
AAO Raslie No. 1	54	10
Amalgamated Petroleum Snake Creek No. 1	—	90
Southeastern area of outcrop	2000	800
Southwestern area of outcrop	690	—
AAO Sunlight No. 1	394	—

the coal measures and the base of the Clematis Sandstone. Mollan et al. (1969) correlated a coarse sandstone in the vicinity of Rewan homestead with the Brumby Sandstone and used this as the base of their proposed type section of the Rewan Formation. At Brumby Mountain farther to the east, however, Mollan, Forbes, Jensen, Exon, & Gregory (1972) take the boundary between the coal measures and the Rewan Formation just above the youngest coal seam, thereby including a sequence of rocks beneath the Brumby Sandstone. In this Bulletin, the sequence from the top of the youngest coal seam of the Blackwater Group to the base of the stratigraphically lowest thick sequence of red mudstone of the newly defined Arcadia Formation is correlated with the Sagittarius Sandstone of the central area.

Petrographic studies. Bastian (1965a) examined six samples from the type section of the Rewan Formation as designated by Mollan et al. (1969) and reported them to be subgreywacke (415A), volcanic sandstone (Williams, Turner, & Gilbert, 1955), and protoquartzite (Pettijohn, 1957). He suggested that the rock fragments were derived from volcanic and plutonic source rocks. Bastian (1965b) also described a few samples from the Clematis Group, and concluded that the unit was derived from metamorphic rocks.

Palaeontological studies. Fossil spores and pollens have been recorded from both the Rewan and the Clematis Groups of the southwestern area, but much of the work is reported in unpublished well completion reports or Records of the Bureau of Mineral Resources. Important determinations given in a brief review by Evans (1962) include: (a) a Tr1 assemblage from the interval 15 m above the highest coal in AAO (Arcadia) No. 7 well, which contains *Quadrisporites horridus, Nuskoisporites radiatus,* and *Striatiti* spp. (Evans, 1964); (b) a Tr1 assemblage

TABLE 2. STRATIGRAPHIC NOMENCLATURE USED IN SOUTHWESTERN AREA

Jensen, H. I. (1926)	*Reeves* (1947)	*Hill* (1957)	*Mollan et al.* (1969)	*This Bulletin*	
Clematis Sandstone	Carnarvon Sandstone	Clematis Sandstone	Clematis Sandstone	Expedition Sandstone	Clematis Group
				Glenidal Formation	
Upper Bowen	Variegated clay shale	Rewan Formation	Rewan Formation	Arcadia Formation	Rewan Group
	Brumby Sandstone	Lower	Brumby Sandstone	Sagittarius Sandstone	
	Coal Measures	Bandanna Formation	Blackwater Group		Blackwater Group
			Black Alley Shale	Black Alley Shale	

in Planet Warrinilla No. 1, where in core 3 (402-407 m), 61 m above the highest coal, Evans (1963a) records *Q. horridus* and *Taeniaesporites* spp., and in core 1 (150-155 m) abundant *Taeniaesporites* spp., *Trizonaesporites* sp., and *N. radiatus*.

Samples from the uppermost part of the Clematis Group in the Expedition Range, west of Bauhinia Downs, were examined by de Jersey (1968), who reported assemblages dominated by *Alisporites,* but which contain *Leiotriletes directus, Osmundacidites,* and *Stereisporites*. In comparing the assemblages found in the Clematis Sandstone in the southeastern and southwestern parts of the basin, de Jersey noted that the species that he regards as survivals of the underlying Rewan Group—*Aratrisporites tenuispinosus, Indospora clara, I. reticulata,* and *Striatisaccus novimundi*—are all absent in the southwest. He concluded that the upper part of the Clematis Group in the Expedition Range is younger than most, if not all, of the Clematis Group sampled on the eastern side of the syncline.

The following fossil plants collected during the course of the present study were identified by J. F. Rigby of the Geological Survey of Queensland: *Cladophlebis johnstoni, Pteruchus rhaetica, Taeniopteris daintreei, Desmiophyllum* sp., and *Araucaria cutchensis?*. Rigby (pers. comm.) regards the assemblage as Middle or Late Triassic from the known distribution of *Cladophlebis johnstoni* and *Pteruchus rhaetica.*

No fossil shells have been recorded from outcrops of the Clematis or Rewan Groups in the southwestern area, but small shells were observed, but not described, in cuttings from OSL (Arcadia) No. 3 in the interval above the coal measures. These are almost certain to be conchostracans, which are common at the same stratigraphic level in the central part of the basin.

In the southwest the redbeds of the Rewan Group contain fossil lungfish, labyrinthodont amphibians, and reptiles (Bartholomai & Howie, 1970), which have not yet been described. The original find was south of Rewan homestead at a locality known as 'The Crater', but during the course of this study other localities around the Arcadia valley have been found where bone fragments have been concentrated by recent erosion and transportation.

MEASURED SECTION S29
Mt Carnarvon area—Type section
of Rewan Formation (Mollan et al., 1969)

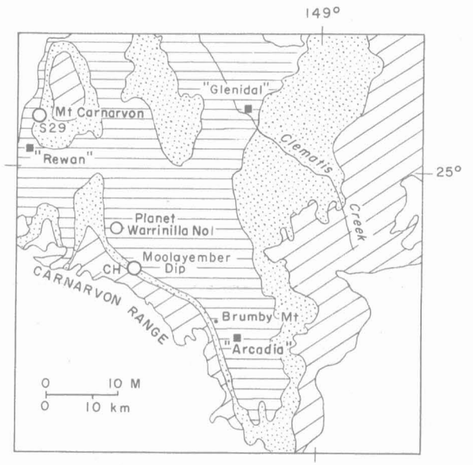
MEASURED SECTION CH
Near Moolayember Dip

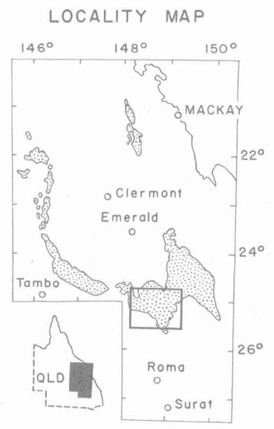
PLANET WARRINILLA No 1
Based on Planet Exploration Co Pty Ltd (1963)
Palynology by P. R. Evans

Parts of sections N6 & R6 measured about
4 miles NNW of Rewan Homestead by
A. R. Jensen. Palynology by P. R. Evans (1963)

SECTIONS R4 & R5 and OSL No 3 (ARCADIA)
BRUMBY MOUNTAIN

AA07 (ARCADIA)
Based on Derrington (1957)
Palynology by P. R. Evans (1964)





Rewan Group
Clematis Group
Moolayember Formation

ARCADIA FORMATION

SAGITTARIUS SANDSTONE
Upper part
Lower part

Fig. 10. Rewan Group, measured sections and well logs in the southwestern area.

M(S) 253

Description of Stratigraphic Units

A summary of the stratigraphic sequence in the southwestern area is present in Table 3.

Sagittarius Sandstone

The *lower part of the Sagittarius Sandstone* in the southwest (Fig. 10) lies directly above the coal measures, and the boundary is taken just above the youngest coal. Although both the sandstone and mudstone beds contain carbonaceous plant fragments, the unit is differentiated from the coal measures by the absence of coal seams. The lower part of the unit is seldom exposed in the southwest. On the eastern side of Reids Dome, where the dip is about 18°, the formation forms a narrow strip of gently undulating country. In the Arcadia valley most of the sequence is concealed at Brumby Mountain, and is known mainly from the two wells OSL (Arcadia) No. 3 and AAO (Arcadia) No. 7.

The sequence exposed north of Rewan homestead, which lies to the south of the type section of the Rewan Formation proposed by Mollan et al. (1969), consists of interbedded mudstone and sandstone. The sandstone is brown, calcareous, and generally fine to medium-grained, and contains scattered mud clasts and plant fragments. Rare beds of very coarse-grained sandstone are also present. The mudstone exposed is green to brown, with scattered black carbonaceous plant fragments. A similar sequence was penetrated in the wells at Brumby Mountain, except that the sandstone when fresh is light grey rather than brown, and, of more significance, some of the mudstone is mottled chocolate-brown and grey.

At Brumby Mountain the thickness of the lower part of the Sagittarius Sandstone, measured from the top of the coal measures to the base of the Brumby Sandstone, is 135 m. In the outcrop near Rewan homestead, the upper part of the unit is missing and the lower part is 165 m thick as measured from the top of the coal measures to the base of a thick sequence of chocolate-brown to red mudstone (Arcadia Formation). In this area, Mollan et al. (1969) used what they believed to be the base of the Brumby Sandstone as the boundary between their newly defined Rewan Formation and the Blackwater Group. However, in many places, the Brumby Sandstone was thought to be absent, and the boundary was placed either at the top of the youngest coal seam or at the base of the oldest red mudstone. Of the three alternative positions for the boundary, the only one which can be recognized over the entire basin is the one placed at the top of the youngest coal seam. This boundary has already been used in the regional mapping for the rest of the basin.

At both Brumby Mountain and north of Rewan homestead Evans (1963b, 1966a) has recorded assemblages in the lower part of the unit belonging to his palynological unit Tr1.

Upper part of Sagittarius Sandstone. One of the most important localities in the development (and subsequent confusion) of stratigraphic nomenclature in this part of the basin is Brumby Mountain, an isolated hill in the Arcadia valley. The lower slopes of the hill are composed of gently dipping rocks of the lower part of the Sagittarius Sandstone overlain by the Brumby Formation, which consists of about 4 m of grey-white lustre-mottled pebbly clayey sandstone (21:75:4B). In places this distinctive rock consists of reddish brown mud clasts together with fragments of green volcanic rock and large grains of glassy quartz. Woolley (1944) recognized the same bed, utilized it for much of his mapping in the valley, and

TABLE 3. STRATIGRAPHIC SEQUENCE IN SOUTHWESTERN AREA

Unit	Thickness (m)	Lithology			Definition of Base	Fossils
		Sand/Shale	Mudstone and Siltstone	Sandstone		
Expedition Sandstone upper part	240	1:0	Rare siltstone lenses	f-vc grading to granule cgl; (910B), (1000B)	Conglomeratic marker; change to unit coarser than lower part	
Expedition Sandstone lower part	95	1:0	Rare siltstone lenses	f-vc; (910B), (1000B)	Change to sequence without mudstone	
Glenidal Formation	80	3:2	Grey or red siltstone and mudstone	f-vc; (820B)	Change in composition of arenite framework	M. to U. Triassic plant fossils
Arcadia Formation	520	1:1	Red mudstone, green siltstone	f-m; (451C)	Change to unit with thick beds of red mudstone	Lungfish, labyrinthodonts, reptiles
	135	3:1?	Greyish white clayey siltstone and mudstone	m-vc; cgl; (281B)	Basal marker bed Brumby Sandstone	Fossil logs
Sagittarius Sandstone	165	1:1	Grey mudstone with rare mottled chocolate-brown and grey mudstone	f-m; (451C)	Absence of coal seams	Scattered plant fragments. Tr1 spore assemblage

called it the 'Malta Grit'. Woolley's mapping revealed that the 'Malta Grit' is underlain by a slight but distinct angular unconformity. In most places the unconformity is marked by a slight divergence of strike above and below the 'Malta Grit', but in two places where the 'Malta Grit' is almost horizontal, the unit below the unconformity dips at up to 15° to the west.

The unit above the unconformity, which includes the Brumby Sandstone (or 'Malta Grit') at its base, is here termed the upper part of the Sagittarius Sandstone. At Brumby Mountain much of the sequence is concealed, but judging from the rare outcrops and from Woolley's description it consists mainly of medium to coarse-grained greyish white calcareous sandstone, which is cross-stratified in places, interbedded with greyish white micaceous clayey siltstone and mudstone. The upper part of the unit is distinguished from the lower by the increased grainsize of the sandstone, and by the reduction in the amount of mudstone and carbonaceous plant debris.

The upper part of the unit reaches a maximum thickness of 135 m at Brumby Mountain, where it is approximately equivalent to Woolley's 'Lower Rewan Group'. Woolley records that this interval thins rapidly away from Brumby Mountain, and at a locality 3 km to the north it is reduced to 1 m of sandstone lying on about 4 m of 'Malta Grit'; 9 km northwest of Brumby Mountain it is represented only by the 'Malta Grit', which is a little under 4 m thick. The upper part of the unit cannot be recognized at the proposed type section of the Rewan Formation designated by Mollan et al. (1969), where the Arcadia Formation directly overlies the lower part of the Sagittarius Sandstone.

It seems probable from Woolley's mapping that there is some discordance at the base of the upper part of the unit, but the nature and significance of the break are uncertain. The relief developed on the coal measures, or on the lower part of the Sagittarius Sandstone, appears to have been substantial judged by the great change of thickness along the strike of the upper part of the unit, and this together with the coarse grain of the basal beds suggests some type of valley-fill deposit. It is possible that the change of base level which resulted in the formation of the valley was due to minor earth movements now recorded by the slight to moderate angular unconformity noted by Woolley (1944). On the other hand, the localized nature of the upper part of the unit and the unconformity suggests that some of the angular discordance is the result of the differential compaction in the underlying coal measures.

Arcadia Formation (new name)

The Arcadia Formation is the name proposed for all but the lower 50 m of the section given by Mollan et al. (1969) as the type section for the Rewan Formation. The lower 50 m is regarded as belonging to the Sagittarius Sandstone, and the sequence included in both units forms the new Rewan Group.

The Arcadia Formation, which is characterized by thick sequences of red mudstone, is relatively unresistant to erosion. This, coupled with the fact that it is overlain by relatively resistant sandstone beds, explains why it seldom crops out. It normally underlies gently undulating sand-covered plains dotted with small outliers of the Glenidal Formation. It is, however, exposed in some of the deep steep-sided creeks, such as the one in which Mollan et al. (1969) measured their type section, where the superficial cover of sand has been removed by erosion and the soft red-brown mudstone exposed. Such exposures are soon destroyed by undercutting and collapse of the banks of the creeks. The formation also crops out on

the lower slopes of ranges where there have been recent landslides, such as near Moolayember Dip and in the Expedition Range near Glenidal. Occasionally, small pinnacles composed of the Arcadia Formation and the overlying Glenidal Formation have been isolated from the main range, and exceedingly rapid headward erosion has produced at least one crater-like feature breached on one side. Fossil vertebrate remains are concentrated on the floor of the 'craters' in which the drainage is directed inwards towards the centre of the depressions.

The upper part of the Arcadia Formation is exposed in road cuttings at the southern end of the Arcadia valley where the road ascends from the Dawson River to the Carnarvon Ranges.

Near Rewan homestead the Arcadia Formation is about 520 m thick, and consists mainly of red-brown mudstone and silty mudstone with thin green bands of siltstone and very fine sandstone, interbedded with beds up to 15 m thick of green fine to medium-grained cross-stratified sandstone (451C). The sandstone is calcareous in places and commonly contains layers of well rounded clasts of green mudstone.

Glenidal Formation (new name)

The Glenidal Formation lies stratigraphically above the Arcadia Formation and beneath the Expedition Sandstone (Fig. 11). No angular discordance has been observed between the units, and there is no apparent disconformity at the base of the Glenidal Formation. The sequence, which in the past has been included in the Clematis Sandstone, consists of mudstone, some of which is red, siltstone, and sandstone. The lower boundary is taken at the change from labile sandstone to quartz-rich or sublabile sandstone, which corresponds with a decrease in the amount of interbedded mudstone.

The Glenidal Formation crops out strongly to form the scarps or upper slopes of many of the ranges in the southwestern area (Fig. 12). The scarps tend to be benched owing to the alternation of hard and soft layers. An unusual topographic feature has been found 18 km northwest of Glenidal homestead, where the nose of a high spur has slumped out and downwards (Fig. 13) to form a triangular-shaped cliff composed mainly of Glenidal Formation, which is separated from the nose of the original spur by a narrow deep slot.

The Glenidal Formation has been identified near Basin Creek towards the southern end of the Arcadia valley, where it is only about 30 m thick. It is known to extend into the Moolayember Dip area, which is regarded here as the type section (Fig. 14), where it attains a thickness of 68 m. It can be recognized in the section measured at Mount Carnarvon by Mollan et al. (1969), although they included it in the Clematis Sandstone, and it can be seen 70 km to the north of Moolayember Dip in a small range of hills near Rolleston. The formation is also well exposed around Clematis Creek gorge, the nominated type section of the Clematis Sandstone, and northwards along the Expedition Range.

The type section, which is named after Glenidal homestead, is in the Carnarvon Ranges 2.5 km northwest of Moolayember Dip (lat. 25°11′S, long. 148°35′E; Fig. 14). In the type section, if siltstone and muddy siltstone are included with mudstone, the sand/mudstone ratio is about 1.4, and although sandstone is predominant in outcrop, it only forms about 60 percent of the sequence. The sandstone ranges from white to shades of dark brown, in contrast to the more labile green sandstone of the underlying Arcadia Formation. It is commonly very fine-

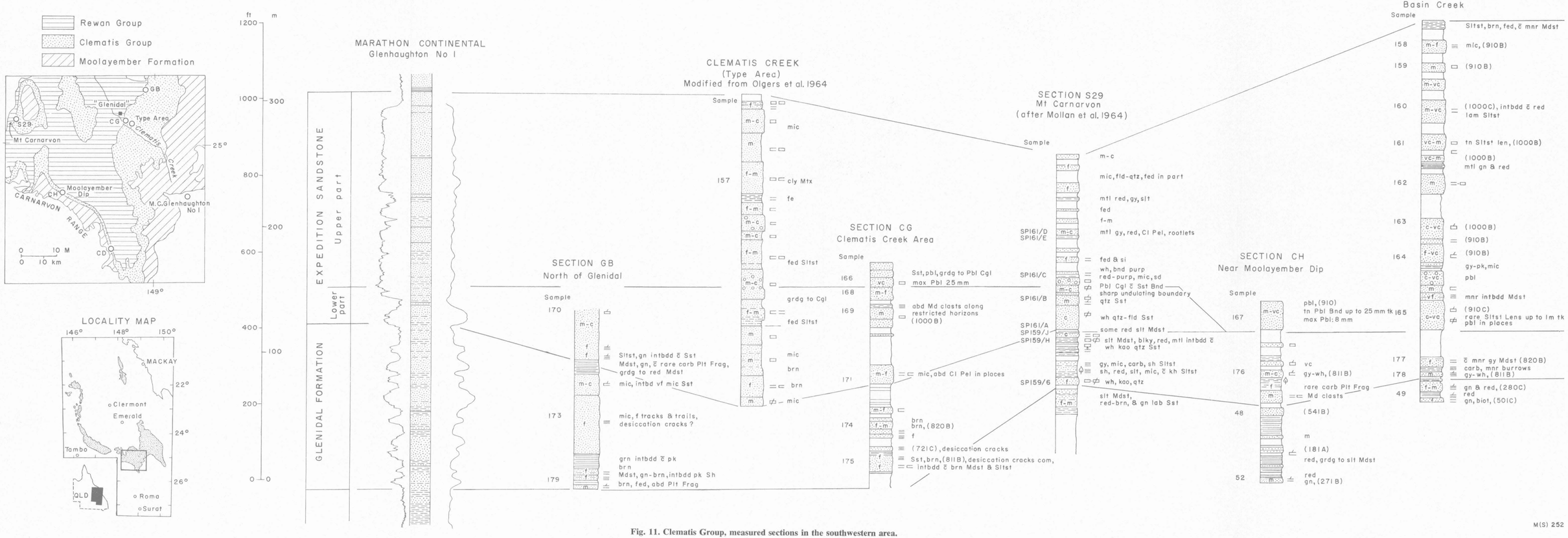


Fig. 11. Clematis Group, measured sections in the southwestern area.

M(S) 252

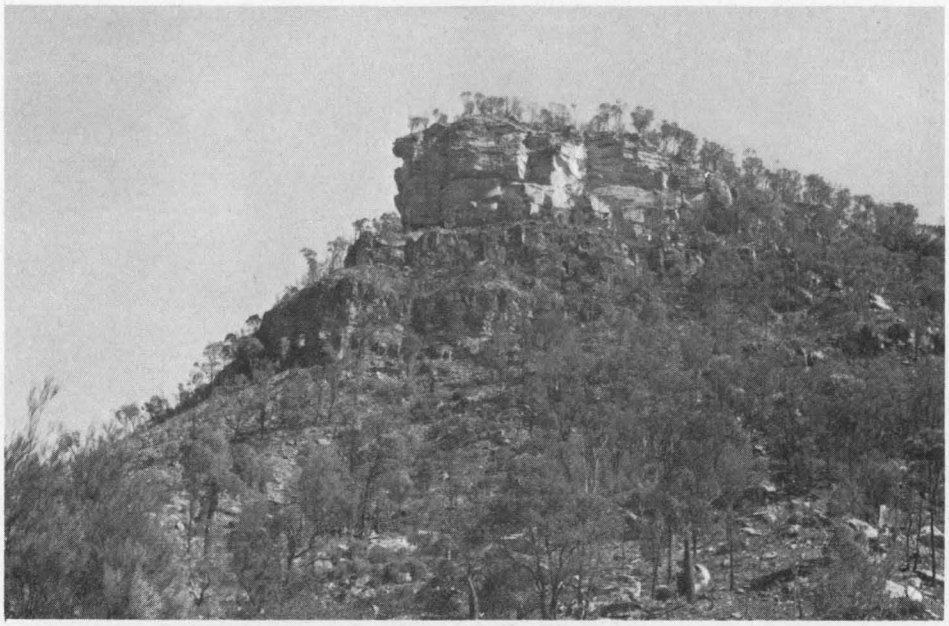


Fig. 12. Upper part of the type section of the Glenidal Formation cropping out as dark sandstone benches below the bluff of light-coloured Expedition Sandstone. Carnarvon Ranges, near Moolayember Dip, southwestern area.

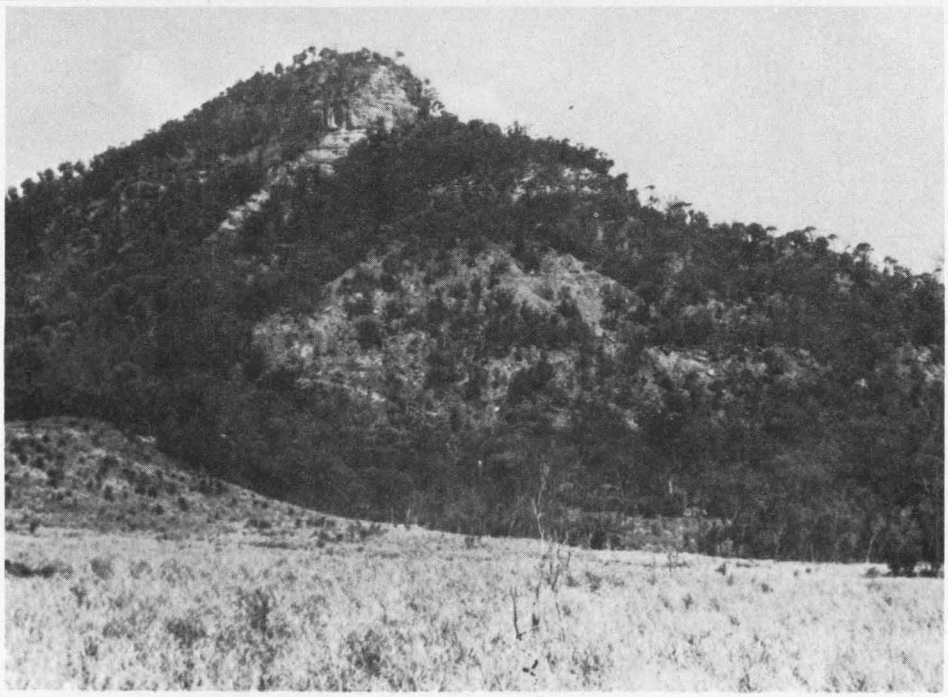


Fig. 13. Triangular-shaped cliff, formed by a landslide, composed of the Glenidal Formation overlain by basal beds of the Expedition Sandstone. Expedition Range, near Glenidal homestead.

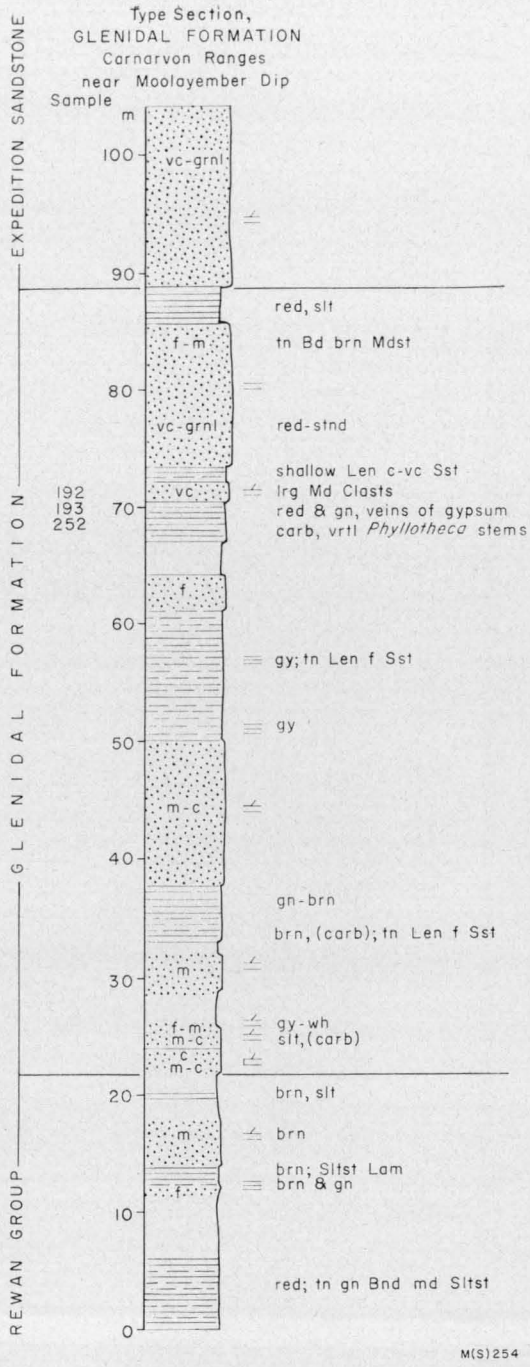


Fig. 14. Type section of the Glenidal Formation, southwestern area.



Fig. 15. Junction of red silty mudstone at the top of the Glenidal Formation and the overlying Expedition Sandstone. Carnarvon Ranges, near Moolayember Dip.

grained to medium-grained, but very coarse pebbly sand is present as thin lenses in the siltstone. Mud clasts are abundant along restricted intervals.

The siltstone is commonly grey, but also brown and mottled red, and forms about 10 percent of the formation. It is generally micaceous and laminated, and in places the grey siltstone contains numerous carbonaceous laminae composed of finely disseminated plant debris. In places, the laminated siltstone contains replaced stems of *Phyllotheca* standing in their growth position.

The mudstone in the Glenidal Formation is generally red or red-brown, but at certain levels it is yellow-green or grey and contains abundant carbonaceous plant material. Veins of gypsum are present in some of the grey non-carbonaceous mudstone. The most conspicuous mudstone sequence crops out at the top of the type section, where a 3-m bed of red silty mudstone, mottled yellow and white in places, lies between two thick sandstone beds (Fig. 15).

The sequence is characteristically thinly bedded (Fig. 16) and beds of sandstone with planar stratification are common (Fig. 17). Cross-stratification is present, but the sets are thin and generally planar to very slightly curved. Ripple lamination is common (Fig. 18). In places vertical feeding burrows are preserved in the thin flaggy sandstone (Fig. 19a); oscillation ripples, on which are superimposed desiccation cracks and fecal pellets (Fig. 19b), may also be present.

Expedition Sandstone (new name)

The Expedition Sandstone is a sequence between the top of the Glenidal Formation and the base of the Moolayember Formation. The proposed type section

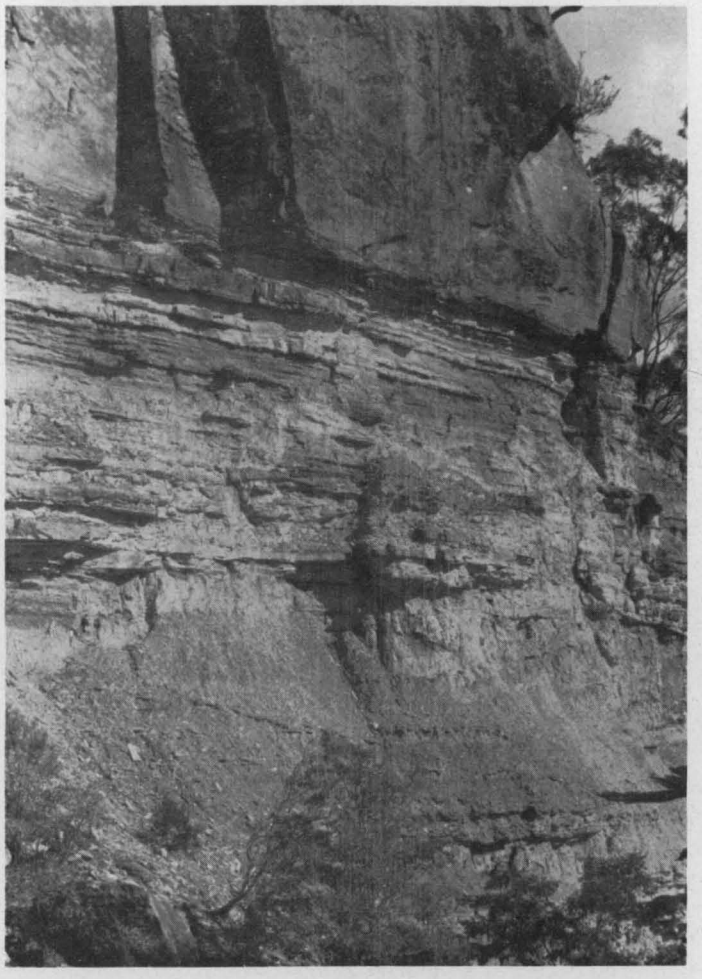


Fig. 16. Thin-bedded sandstone of the Glenidal Formation overlain by massive or thick-bedded Expedition Sandstone. Expedition Range, near Glenidal homestead.

(Fig. 11) is in the hills immediately east of Serocold homestead; the section was measured by Mollan et al. (1969, Sect. S29) and is about 145 m thick. The Expedition Sandstone has not been observed to rest directly on the Arcadia Formation, although the Glenidal Formation thins considerably from place to place; no angular unconformities have been reported in this part of the sequence.

In places the formation can be divided into two parts. The base of the lower part is taken at the change from a sequence of interbedded sandstone, mudstone, and siltstone, to one which is mainly sandstone. In practice it is taken at the top of the highest thick bed of mudstone in the Glenidal Formation. The base of the upper part is taken at the base of a pebble or granule conglomerate or very coarse pebbly sandstone; the upper part is slightly coarser than the lower. The two parts are described together because they are difficult to distinguish if the conglomerate at the base of the upper part is absent or poorly developed. The top of the upper

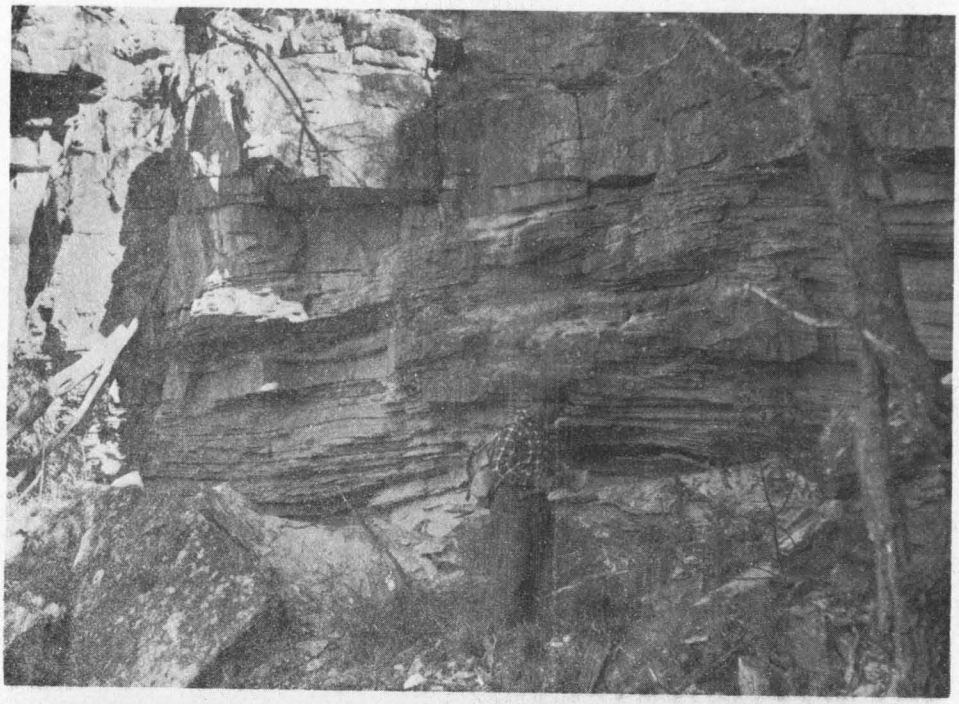


Fig. 17. Planar stratification in sandstone of the Glenidal Formation. Near Moolayember Dip, southwestern area.

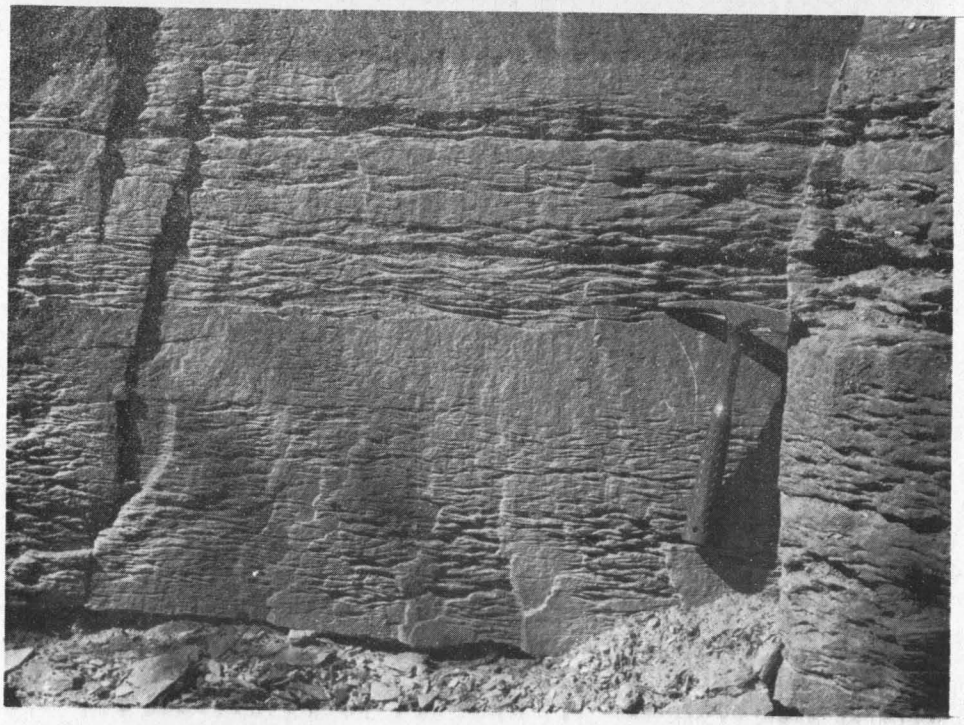


Fig. 18. Ripple lamination in sandstone of the Glenidal Formation. Southwestern area.

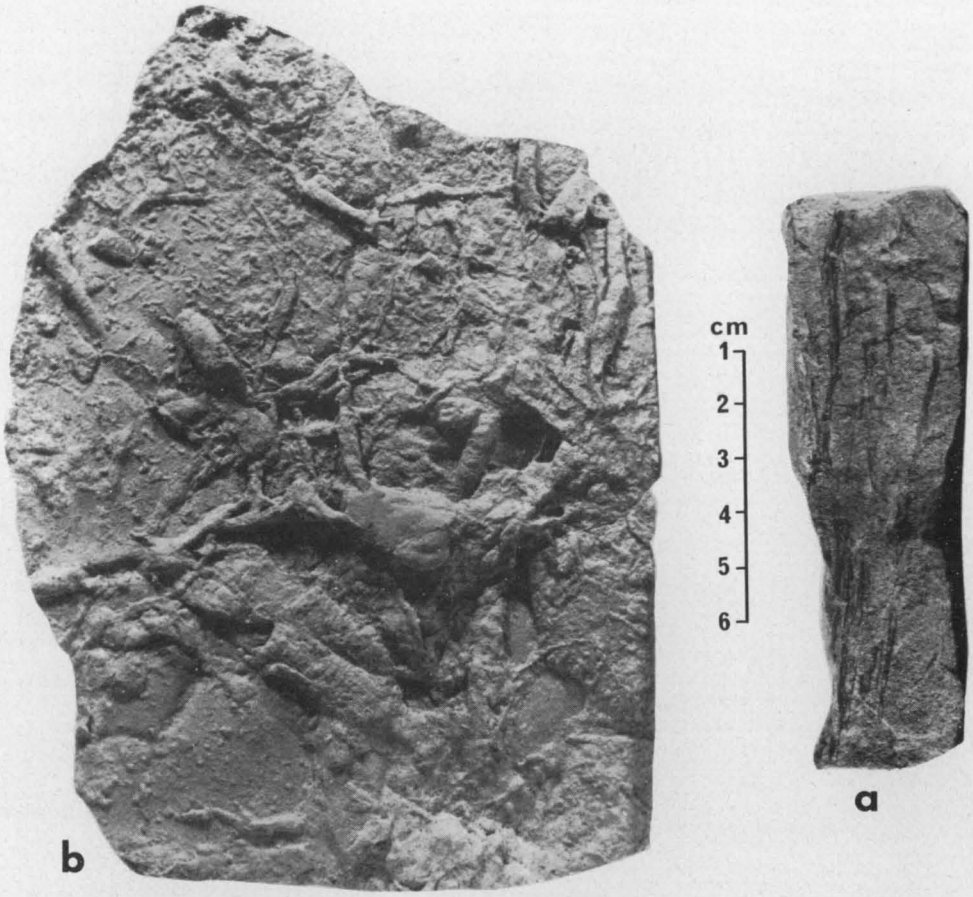


Fig. 19. Burrows and tracks in sandstone of the Glenidal Formation. (a) Vertical sand-filled burrows lined with iron oxide. (b) Convex hyporeliefs of nesting tracks on a bedding plane.

part is taken at the base of the lowest thick persistent bed of brown mudstone, where there is a distinct increase in the proportion of mudstone and siltstone, carbonaceous material, and labile sandstone.

The Expedition Sandstone is widespread, and crops out from the southern end of the Arcadia valley northeastwards along the Carnarvon Range, and northwards along the Expedition Range. It invariably forms deep steep-sided valleys topped by cliffs. The lower part is best developed around Mount Carnarvon, near Rewan homestead, and probably equates with Reid's (1930) 'Carnarvon Red Member', which was so named because of the red-stained joint planes that are visible for some distance from the ranges. The conglomerate at the base of the upper part is also best developed in this area, where it forms a small ridge, or in places a cliff, devoid of vegetation. This feature, which forms a distinctive pattern on the aerial photographs, can be traced along the western limb of the Rewan Syncline, and can also be recognized at many places in the Expedition Ranges.

The complete sequence is seldom exposed in outcrop. The section measured at Basin Creek (Fig. 11), from the top of the Glenidal Formation to the base of the Moolayember Formation, is 240 m thick, but the lower part appears to be absent. A minimum thickness of 180 m is present at Clematis Creek (Olgers et al., 1966), and the thickness appears to be about the same in the Marathon-Continental Glenhaughton No. 1 well. The lower part is only 35 m thick at Mount Carnarvon, and attains a maximum outcrop thickness of about 95 m in Clematis Creek. The thickness is estimated to be the same to the west of Planet Creek in the Expedition Range.

The Expedition Sandstone consists predominantly of sandstone (910B), with some lenses of grey or red siltstone and muddy siltstone up to 1 m thick. The sandstone ranges from very fine to very coarse, and in places the pebbly sand grades into granule and pebble conglomerate. The sandstone of the lower part ranges from medium to coarse and very coarse-grained, while the sandstone in the upper part, especially at the base, is coarse to very coarse and grades into conglomerate. Towards the top of the upper part, the sandstone becomes finer, and the average grainsize, if one can apply the concept to such a thick and variable sequence, is about that of medium sand. The sandstone ranges from dark brown to white, but the lower part tends to be dark brown or grey-brown owing to the greater proportion of iron oxide. Mud clasts are present in both units, but are more common in the lower.

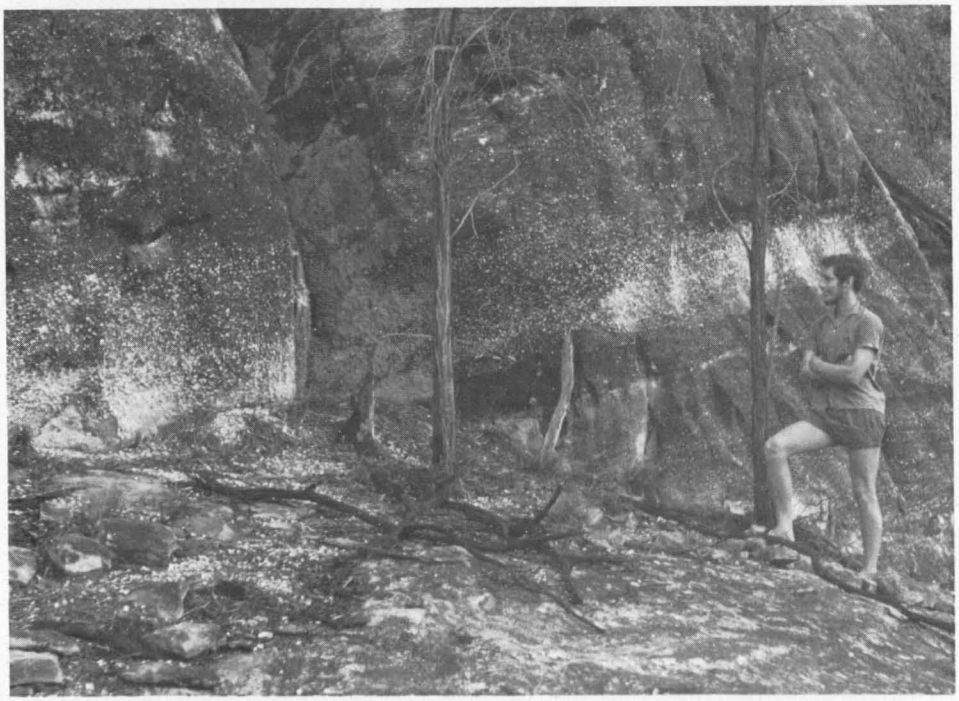


Fig. 20. Pebble conglomerate within very coarse pebbly sandstone at the base of the upper part of the Expedition Sandstone. Southwestern area.

In the upper part the conglomerate grades into very coarse sandstone, and forms beds several metres thick (Fig. 20). The thickest conglomeratic sequence observed is near Mount Carnarvon, where it is about 12 m thick, and consists of cross-stratified very coarse sandstone with thick layers of granule and pebble conglomerate.

The siltstone and muddy siltstone form lenses up to 1 m thick and 30 m across, although one 3-m bed of red muddy siltstone was noted near the top of the sequence near Mount Carnarvon.

The siltstone is commonly laminated, grey-white to pink and red, and where fresh, slightly friable. The gradation from grey-white slightly carbonaceous siltstone into thick lenses of red ferruginous siltstone overlain by sandstone suggests that the iron oxide was precipitated from groundwater. The siltstone lenses are truncated by erosion surfaces, and large blocks of siltstone and muddy siltstone are included in the overlying sandstone in addition to small rounded clasts.

Cross-stratification is ubiquitous in the Expedition Sandstone, although some of the sandstone beds particularly near the top of the unit, are horizontally stratified. The association of horizontal stratification and cross-stratification is discussed on page 107. Overturned cross-stratification is rare, and where it is present some of the laminae in the cross-stratified sets are contorted. Some thick beds appear massive, but it is difficult to ascertain if horizontal lamination or small-scale cross-stratification is present. Some of the thick lenses of sandstone filling large erosional troughs have a poorly developed horizontal lamination and ripple lamination on some surfaces.

Central Area

The central area lies, broadly speaking, at the northern end of the Dawson Range, and near Blackwater and Bluff (Fig. 1). It also includes the northern end of the Expedition Range.

Previous Investigations

Nomenclature. The area lies mainly within the Duaringa Sheet area, the geology of which has been described by Malone et al. (1969).

A summary of the changes in stratigraphic nomenclature is presented in Table 4. The sequence between the marine Permian unit known as the Crocker Sandstone and the Clematis Group in the central part of the basin was originally called the Taurus Formation by Mines Administration (1959). The upper part of the Taurus Formation, the Woodlands Member, was divided by Malone et al. (1969) into the Blackwater Group and Rewan Formation, and use of the terms 'Taurus' and 'Woodlands' was discontinued. The Blackwater Group contains the youngest coal measures in the district, and the overlying Rewan Formation was differentiated by the absence of carbonaceous material. The lower part of the Rewan Formation was called the Sagittarius Sandstone Member by Malone et al. (1969), who designated adjacent stretches of Blackwater, Taurus, and Deep Creeks, near

TABLE 4. STRATIGRAPHIC NOMENCLATURE USED IN CENTRAL AREA

Minad (1959)		*Malone et al.* (1969)		*This Bulletin*	
Clematis Sandstone		Clematis Sandstone		Expedition Sandstone	Clematis Group
				Glenidal Formation	
Taurus Formation	Woodlands Member	Rewan Formation		Arcadia Formation	Rewan Group
			Sagittarius Sandstone Member	Sagittarius Sandstone	
		Blackwater Group		Blackwater Group	

Blackwater, as the type section. The Sagittarius Sandstone Member was reported to consist mainly of lithic sandstone interbedded with red-brown, green, and rarely dark grey mudstone, and was said to be distinguished from the rest of the Rewan Formation only by the predominance of sandstone. The top of the member, however, was taken at the base of the stratigraphically lowest thick bed of massive red-brown mudstone.

Malone et al. (1969) referred the rocks forming the Expedition, Shotover, and Dawson Ranges and the Blackdown Tableland to the Clematis Sandstone of H. I. Jensen (1926). They described it as a medium to coarse-grained quartz sandstone containing thin beds and pockets of angular granules, pebbles of quartz, and thin interbeds of micaceous siltstone with plant fragments. A thickness of 240 m was quoted for the Clematis Sandstone on the western limb of the Mimosa Syncline, and about 300 m in the Dawson Range farther east.

Palaeontological studies. The intraformational conglomerate near the base of the Sagittarius Sandstone and the cores of siltstone horizons in BHP holes contain accumulations of conchostracan shells. Preliminary examination of the material (Prof. P. Tasch, Wichita State Univ., pers. comm.) indicates that two genera are present in the outcrop sample, a paleolimnadid and a probable cyziciid. The core samples from slightly higher levels in the sequence contain *Cyzicus* (*Lioestheria*) sp. and a paleolimnadid type similar to *Paleolimnadia glabra* (Mitchell) from the Upper Permian Newcastle Coal Measures.

Evans (1966b) has shown that the lowermost part of the Sagittarius Sandstone contains *Striatopodocarpites cancellatus* and aff. *Striatoabietites* with *Nuskoisporites radiatus, Apiculatisporis,* and *Alisporites,* on the basis of which he assigned it to the palynological unit Tr1a, noting, however, that there was no sign of *Quadrisporites horridus.* The samples also contain recycled Late Carboniferous and Early Permian species apparently derived by erosion of Carboniferous and Permian strata. The samples from horizons higher in the Sagittarius Sandstone, and in the Rewan Group above, contain a Tr1b assemblage including saccate pollens such as Striatiti spp. and *A.* sp.

Description of Stratigraphic Units

A summary of the stratigraphic sequence in the central area is presented in Table 5.

Sagittarius Sandstone

The base of the Sagittarius Sandstone is taken immediately above the highest coal seam in the area, above which there is considerably less carbonaceous material. The thickness of the sequence is not known, but Malone et al. (1969) estimate that it is from 300 to 400 m. Outcrop in the type section is exceedingly poor. The sequence in the scattered outcrops south of Blackwater, which is stratigraphically almost immediately above the coal measures, consists mainly of medium-grained calcareous sandstone and mudstone, both of which grade into sandy marlstone. At least one thin bed of intraformational conglomerate crops out near the base of the unit (Fig. 21); the clasts are commonly phosphatic and both clasts and matrix contain abundant conchostracans in places. The matrix of the conglomerate is commonly oolitic.

A far better description of the sequence can be obtained from the logs of continuously cored holes drilled by the Broken Hill Pty Co. Ltd to explore for coal (Malone et al., 1969). The most striking feature of the sequence is the rarity of thick beds of any particular type: for example some of the beds of sandstone, up to 12 m thick, as shown on the graphic logs are described in the written logs as beds of sandstone containing shale bands up to 30 cm thick. Similarly, most of the shale and siltstone beds contain laminae and very thin beds of sandstone. The sand-shale ratio based on the description given in the written logs of holes 1 and 3, after including siltstone in shale and making certain generalizations (e.g. a sequence described as muddy sandstone is regarded as sandstone), is 1.6 for BHP No. 1 and 1.5 for BHP No. 3. Both holes were drilled through about 300 m of the lowest part of the unit. Hence the sequence is dominated by sandstone, but the name 'Sandstone Member' is somewhat misleading, as the unit probably contains about 40 percent of sediment finer than sand. Much of the thin-bedded sandstone ranges from fine to very fine-grained, with some medium-grained sand. In addition to the shale partings the sandstone also contains numerous shale and siltstone clasts, and in places grades into intraformational conglomerate. The shape, size, and composition of the clasts vary according to the composition of the material eroded and, presumably, the current strength. The size of the clasts ranges from a few millimetres to about 10 cm, and the shape from flat and angular to spherical and round. Examination of the cores from two holes shows that most of the clasts are discoidal,

TABLE 5. STRATIGRAPHIC SEQUENCE IN CENTRAL AREA

Unit	*Thickness* (m)	*Lithology*			*Definition of Base*	*Fossils*
		Sand/Shale	*Mudstone and Siltstone*	*Sandstone*		
Expedition Sandstone	300	1:0	Rare siltstone lenses	f-vc; (910-1000)	Increase in framework quartz	
Glenidal Formation	350	4:1	Grey and brown mudstone	f-c; (811B)	Change in arenite composition and sand/shale ratio	Carbonaceous plant material; minor woody fragments
Arcadia Formation	800?	1:1?	Red mudstone and green siltstone	f-c; (451B)	First appearance of thick sequences of red mudstone	Labyrinthodonts and reptiles
Sagittarius Sandstone	300-400	3:2	Grey mudstone and siltstone	f-m; (361C); interbedded intraformational conglomerate	Absence of coal seams	Conchostracans. Palynological stage Tr1a and Tr1b. Recycled U. Carboniferous and L. Permian spores



Fig. 21. Intraformational conglomerate (C) between mudstone and cross-stratified sandstone near the base of the Sagittarius Sandstone. Central area.

subrounded, and about 2 cm long. The grainsize of the clasts ranges from clay-size to silt-size, and most of them consist of laminated silty mudstone. Small phosphate nodules were noted at one horizon, but ooliths, similar to those in the intraformational conglomerate sampled in outcrop near the base of the unit, are rare.

The composition, fabric, and economic potential of the intraformational conglomerate suggest that a more detailed study of the rock may be warranted. Similar rocks occur in the Narrabeen Group of the Sydney Basin, and Lassak & Golding (1967) have reported beds of friable conglomerate with discoidal phosphatic nodules, up to 10 cm in diameter, in the Bulga Sandstone and phosphatic nodules in the Gosford Formation. They concluded that phosphate bands, nodules, and concretions are widespread in the upper part of the Narrabeen Group.

The description of the cores from the BHP holes indicates that thick sequences of red or chocolate-coloured mudstone are much less common than previously thought. Indeed, in the two holes for which written logs were available, purple shale is recorded only once, and green-grey to chocolate-coloured shale only twice, all probably in the upper part of the unit. The siltstone and mudstone beds are commonly light greenish grey, mid-grey, or dark grey to black.

Both the mudstone and siltstone are laminated, and the dark grey mudstone is commonly riddled with irregularly shaped faunal burrows up to 5 mm wide. Sand-filled desiccation cracks are preserved in some of the cores of grey and green-grey mudstone.

The sandstone is commonly cross-stratified, although at least some of the fine-grained sandstone is horizontally laminated; parting lineation can be seen in the laminated sandstone in outcrop. Small-scale group cross-stratification is present in some of the fine sandstone in the cores. The sandstone also contains vertically disposed cylindrical bodies from 5 mm to 7 cm in diameter and up to 11 cm long (Fig. 22). The top of the cylinder is flat and the base slightly convex downwards. Although single cylinders are most common, some are joined in pairs. The cylinders have an outer shell of fibrous carbonate about 2 to 3 mm wide, and the core is filled mainly with calcareous sandstone. Some of the cylinders were apparently hollow, but the central void has been filled with botryoidal carbonate. The bedding adjacent to the cylinders is curved downwards. The tubes are probably faunal burrows, in which the carbonate shell represents replacement of mucus secreted by the organism to bind the sediment wall.

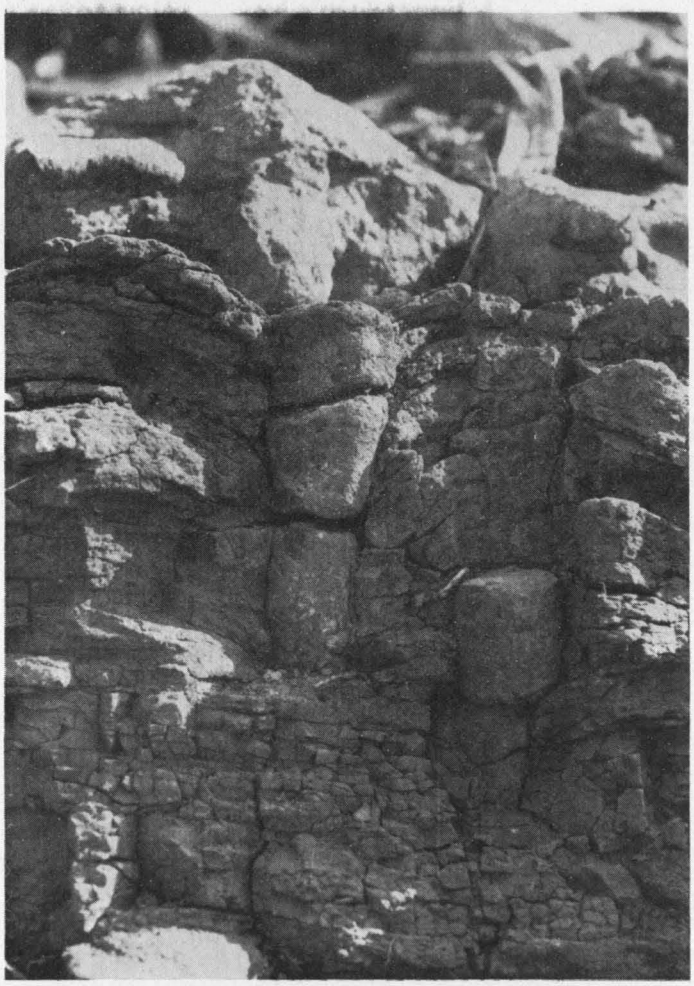


Fig. 22. Infilled faunal burrows (cylindrical structures) near the base of the Sagittarius Sandstone. Central area. The cylinders are about 4 cm in diameter.

Glenidal Formation

The Glenidal Formation lies stratigraphically well above the highest known occurrences of the Sagittarius Sandstone, but the intervening sequence, which is presumably equivalent to the Arcadia Formation, is poorly exposed and is not described. The poorly exposed sequence has not been drilled, and the only known outcrops consist of thick beds of red mudstone with interbedded green lithic sandstone (451B). On the basis of these outcrops the unit is considered to be similar to the Arcadia Formation in the southwest.

The lowest exposed beds of the Glenidal Formation form the foothills and, in some cases, part of the main scarps of the Dawson, Shotover, and Expedition Ranges. The terrain is moderately rugged, with deep valleys bordered with sheer cliffs and steep scree slopes, depending on the contrasting resistance to erosion of the relatively hard quartz-rich sandstone and the relatively soft red mudstone. There is considerably more topographic relief than in the underlying units, which are composed of more labile softer sandstone beds and soft mudstone.

The sequence was previously included in the Rewan Formation or Clematis Sandstone. Although three sections have been measured in the Raby Creek area and observations made at points between the sections (Fig. 23), the precise thickness of the formation is still unknown. It is at least 290 m thick at Raby Creek, and, assuming that the major break in slope between ranges and plains corresponds approximately with the base of the formation, the total thickness is probably about 350 m. The formation can be recognized in a section measured by Olgers et al. (1966) 20 km farther south in the Dawson Range, and it probably crops out for 35 km south of the Raby Creek area. The base of the formation, however, is apparently not exposed.

The formation consists predominantly of sandstone (811B), and the sand-shale ratio ranges from about 3 to 5. The sandstone is less labile than that of the Rewan Group and more labile than the overlying Expedition Sandstone. It is commonly medium or coarse-grained, but some fine and very fine-grained sandstone is present. The colour is generally grey or brown, although in places the rock is mottled brown and white. Colourless mica is abundant, and rounded discoidal clasts of brown mud are common along a few horizons. The bedding is characteristically medium to thin, and some of the fine-grained hard sandstone is flaggy. The sandstone beds are almost invariably cross-stratified.

The mudstone most commonly seen in outcrop is grey or brown, and forms beds up to 1 m thick. The red mudstone crops out poorly, but sequences up to 6 m thick have been observed. They contain thin but persistent beds of green siltstone or very fine sandstone. Carbonaceous plant debris and impressions of plant and woody material are common in the brown mudstone.

Expedition Sandstone

The Expedition Sandstone rests directly on the Glenidal Formation. It extends over the northern end of the Dawson Range as far west as the Blackdown Tableland, and then to the south along the Expedition Range. The sequence was examined in the Raby Creek area, at the northern end of the Dawson Range, where the Clematis Group lies within a south-plunging syncline, the axis of which lies

roughly along Raby Creek (Fig. 23). The boundary with the Glenidal Formation is taken immediately above the highest bed of mudstone or siltstone, where there is an increase in the proportion of framework quartz in the sandstones, and a decrease in the amount of feldspar. The boundary is also defined on the aerial

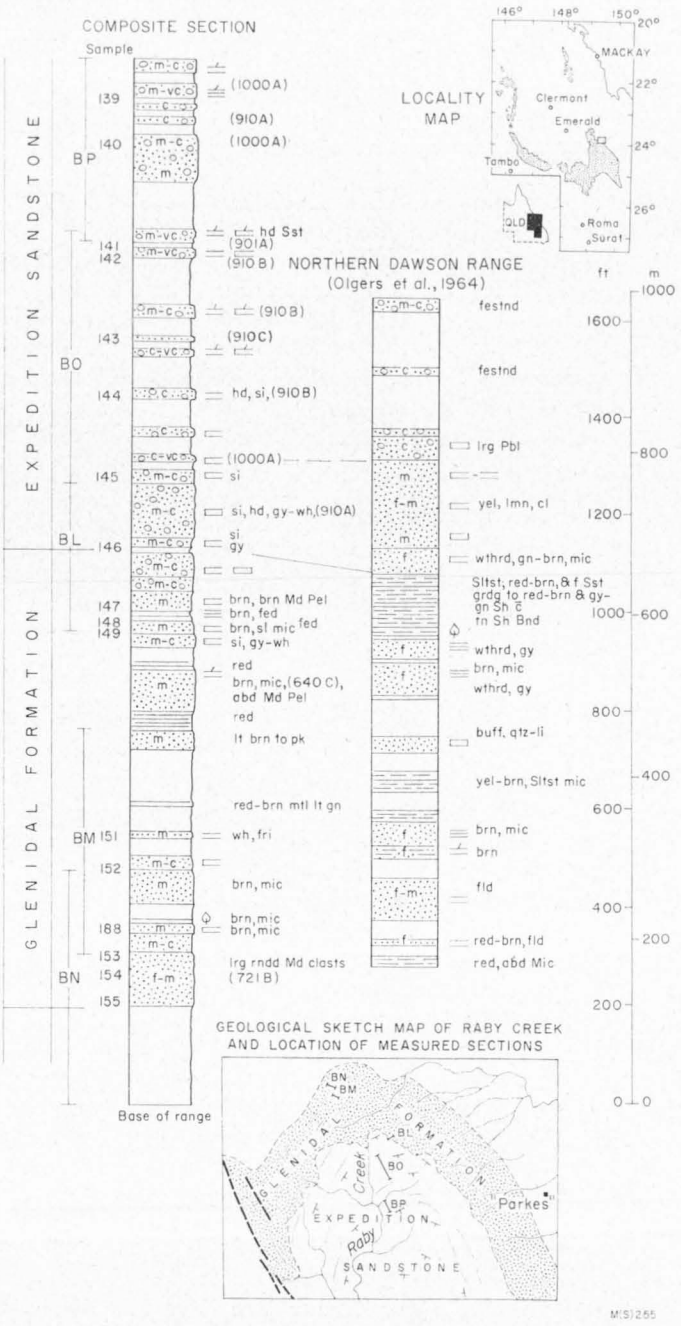


Fig. 23. Clematis Group, measured sections in the central area.

photographs by a change from a dark to a light grey tone. In the central part of the basin the Expedition Sandstone is generally overlain by Tertiary basalt or soil, and the top of the unit has probably been removed by erosion. The formation forms steep-sided cuestas or plateaux, depending on the dip of the beds. Most of the plateaux occur in the Expedition Range and Blackdown Tableland. The thickness of the sequence in the Raby Creek area is 300 m, but the total thickness is somewhat greater as the top is eroded.

Most of the sequence at Raby Creek is included in three sections measured near the axis of the syncline (Fig. 23). The dip near the lowest section (BL) is about 8°, but to the south the dip is no more than 4° in Section BP.

The formation is composed almost entirely of sandstone, with rare lenses of siltstone and mudstone not more than 1 m thick. The sandstone is generally white to yellow, and in outcrop it has a hard silicified appearance. It is generally coarse-grained, but ranges from fine to very coarse. There is an increase in the average grainsize about 50 m above the base of the sequence, but the change is not sharp and tends to be masked by silicification. Above this level, quartz and chert pebbles up to 1.5 cm in diameter are common in places. In the section measured by Olgers et al. (1966) in the Dawson Range, about 25 km south of the Raby Creek area, there is a similar increase in grainsize about 70 m above the highest siltstone in the Glenidal Formation.

Cross-stratification is the dominant sedimentary structure, and in the Raby Creek area doubly cross-stratified units are present. The sequence also includes some sandstone with parallel lamination. The sandstone is mainly medium to thick-bedded, but extremely thick beds are present in places. One solitary cross-stratified unit on the Blackdown Tableland is 7 m thick.

Northern Area

Previous Investigations

Nomenclature. In the northern area, the original threefold division of the Permian sequence by Jack & Etheridge (1892) into Lower, Middle, and Upper Bowen was adopted with little change by most subsequent authors (Table 6). Reid (1924-25) recognized a quartz-rich sandstone unit above the Upper Bowen (the Redcliffe Series), and later he subdivided the Upper Bowen into two provisional units—the Fort Cooper and Elphinstone Coal Measures (Reid, 1946). The term Elphinstone Coal Measures was intended to cover the sequence from the top of the Fort Cooper Coal Measures to the base of the Redcliffe Series. During the regional mapping of the Bowen Basin it was found that there is a considerable thickness of strata between the coal seams of the Elphinstone Coal Measures and the base of the Redcliffe Series; this interval contains red mudstone typical of the Rewan Formation in the southwestern part of the basin, and for this reason the most modern maps of the northern part of the basin show the Rewan Formation between the Permian coal measures and the sandstone of the Redcliffe Tableland.

Reid (1928) correlated his Redcliffe Series with the sandstone of the Carborough Range, and used the terms Carborough Sandstone, Carborough Range Sandstone, and Carborough Series. Later authors have used both Carborough and Redcliffe Sandstones (Isbell, 1955), Carborough Sandstone (Malone, Corbett, & Jensen, 1964), and more recently Clematis Sandstone (Dickins & Malone, 1973).

TABLE 6. STRATIGRAPHIC NOMENCLATURE USED IN NORTHERN AREA

<table>
<tr><th>Jack & Etheridge (1892)</th><th>Reid (1924-25)</th><th colspan="2">Reid (1946)</th><th colspan="2">Dickins & Malone (1973)</th><th colspan="2">This Bulletin</th></tr>
<tr><td rowspan="6">Upper Bowen Formation</td><td>Redcliffe Series</td><td colspan="2">Carborough Sandstone</td><td>Clematis Sandstone</td><td rowspan="2">Mimosa Group</td><td>Expedition Sandstone</td><td rowspan="2">Clematis Group</td></tr>
<tr><td rowspan="5">Upper Bowen Coal Measures</td><td rowspan="2">Elphinstone Coal Measures</td><td rowspan="5">Upper Bowen Coal Measures</td><td rowspan="2">Rewan Formation</td><td>Glenidal Formation</td></tr>
<tr><td>Arcadia Formation</td><td rowspan="2">Rewan Group</td></tr>
<tr><td>Sagittarius Sandstone</td></tr>
<tr><td rowspan="3">Fort Cooper Coal Measures</td><td>Rangal Coal Measures</td><td rowspan="3">Blackwater Group</td><td>Rangal Coal Measures</td><td rowspan="3">Blackwater Group</td></tr>
<tr><td>Burngrove Formation</td><td>Burngrove Formation</td></tr>
<tr><td>Fair Hill Formation</td><td>Fair Hill Formation</td></tr>
<tr><td>Middle Bowen Formation</td><td>Middle Bowen Marine Series</td><td colspan="2">Middle Bowen Series</td><td colspan="2">Back Creek Group</td><td colspan="2">Back Creek Group</td></tr>
</table>

Thus whereas the early workers would have referred the sequence under review to the upper part of the Upper Bowen Coal Measures and the Carborough Sandstone, the most recent workers equate it with the Rewan Formation and the overlying Clematis Sandstone.

Lithological studies. As redbeds equivalent to those of the Rewan Group have been discovered in the northern part of the basin only in the last six years, it is not surprising that very little has been published about their lithology. In addition, the sequence is poorly exposed in the north, especially the finer rocks which form a large part of the succession. The general lithology of the sequence is indicated by a section measured near Lake Elphinstone (Jensen & Arman, 1966), and most of the observations made during this study are based on this section (Fig. 24).

Previous descriptions of the Clematis Group in this area apply mainly to the resistant Expedition Sandstone which occupies the upper part of the ranges. Petrographic studies of a few samples from the group (Isbell, 1955) show that it consists of moderately well sorted quartz-rich sandstone (811B) with very minor interbedded siltstone. Cross-stratification is ubiquitous, and preliminary studies by Olgers et al. (1966) have shown a direction of sediment transport towards the south or south-southeast. Malone et al. (1964) established a thickness of 460 m for the group in the Carborough Range, and the suggestion of a possible Jurassic age for the upper part was discounted with the finding of Triassic plants in the overlying Moolayember Formation.

Description of Stratigraphic Units

A summary of the stratigraphic sequence in the northern area is presented in Table 7.

Sagittarius Sandstone

Two units can be recognized within the Sagittarius Sandstone in the northern part of the basin. The lower unit, which is 80 m thick, rests apparently conformably on the Elphinstone Coal Measures. It is distinguished from the coal measures by the presence of thin red mudstone beds, and by the absence of coal seams and tuffs. The sequence consists of mudstone and siltstone interbedded with about the same proportion of green lithic sandstone (361C). It is partly exposed in small road cuttings east of the Carborough Range near Lake Elphinstone (Fig. 25a), in the headwaters of Bee Creek, and also much farther north in the Blenheim area, where it crops out poorly in small creeks draining eastwards into the Bowen River. The formation generally forms low rounded ridges and cuestas. In the Lake Elphinstone area the base is marked by a ridge about 50 m above the level of the coal measures; the rest of the Rewan Group forms a moderately dissected plain sloping gently towards the base of the Carborough Range. Elsewhere there are no marked topographic differences between the areas underlain by the coal measures and the Sagittarius Sandstone.

The argillaceous rocks in the lower unit consist mainly of laminated brown and greenish brown mudstone and siltstone, with some thin beds up to 50 cm thick of red and mottled red-green mudstone and siltstone. The siltstone in the laminated brown and green-brown sequence is commonly cross-stratified in small

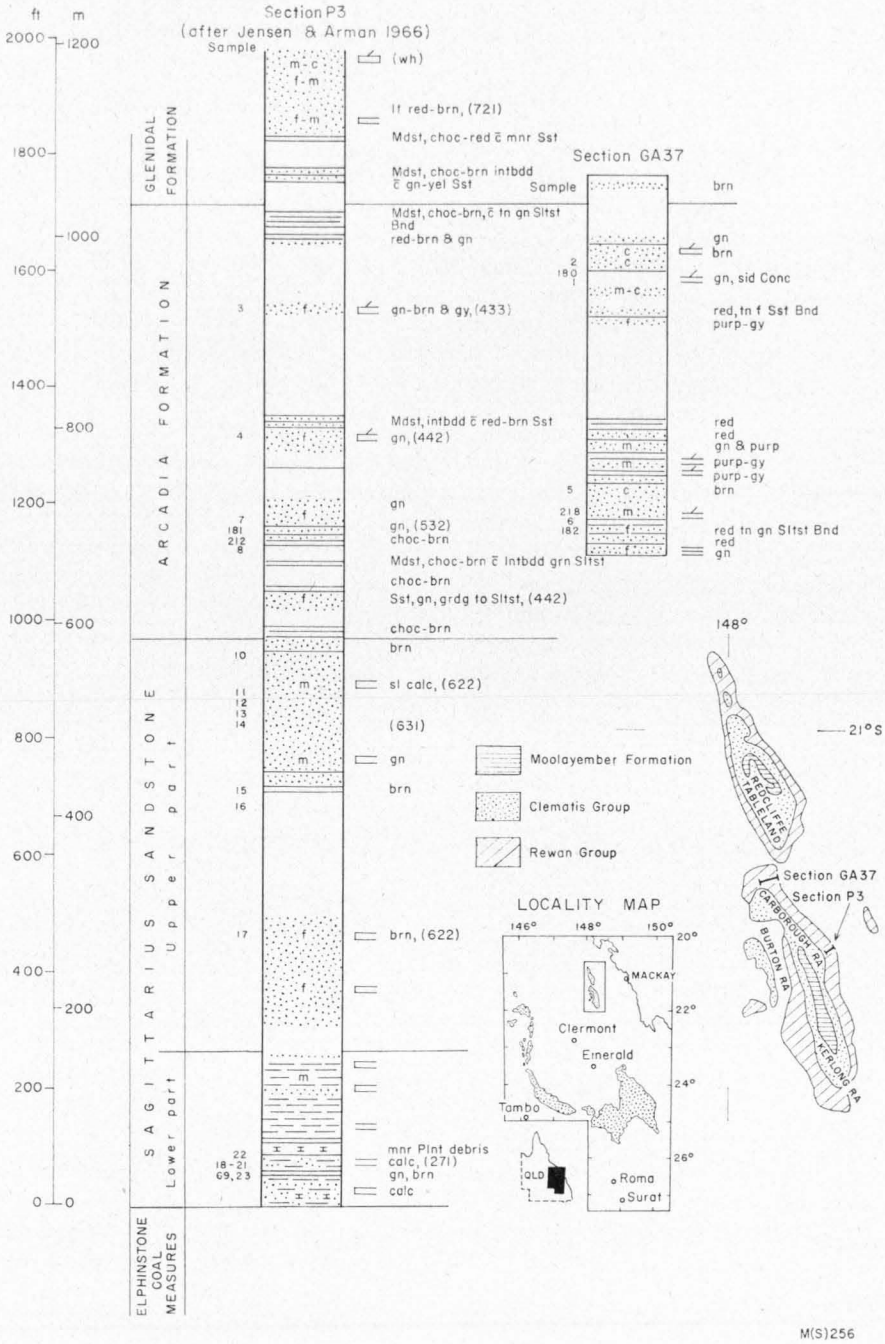


Fig. 24. Rewan Group, measured sections in the northern area.

solitary or grouped sets from 5 mm to 1.5 cm thick. Rare mud-cracks filled with siltstone are preserved in the interbedded brown mudstone, which in places is slightly carbonaceous.

The sandstone in the lower unit is generally green or brown and ranges from medium to fine-grained and from moderately to poorly sorted. Carbonaceous plant material is concentrated on some laminae; it consists mainly of small slightly rounded tabular coalified grains averaging 0.5 mm in diameter, but with some fragments up to 2 cm; although coalified, a fibrous woody texture is still apparent to the unaided eye. Rounded mud clasts are also common along restricted intervals. The sandstone is commonly group cross-stratified, with individual sets forming wedges up to 40 m long; the cosets extend over a greater distance because of overlapping constituent sets. The beds of fine and very fine sandstone are laminated in places, and parting lineation can be seen on bedding planes.

The main difference between the upper and lower parts of the Sagittarius Sandstone is the change in mineral composition of the sandstone framework, and as it would be difficult to map the boundary between them they are not considered to be formal rock units. The upper part of the formation is very poorly exposed. The best outcrops are in small creeks draining westwards about 3 km east of Lake Elphinstone, where the sequence is about 200 m thick. The only section measured (Fig. 25b) consists mainly of medium-grained sandstone (631C), containing scattered mud clasts, interbedded with brown and green mudstone. Finely disseminated carbonaceous material is common in the lower part of the sequence, but is absent in the upper.

The distribution of the upper part of the sequence is uncertain, but there is some evidence to suggest that it is present in the Blenheim area, 50 km to the north, where an isolated sandstone bar across a creek about 120 m above the top of the coal measures was found to have a framework composition consistent with that of the upper part.

The argillaceous rocks in the sequence consist of brown and green mudstone which is generally strongly weathered in outcrop. Where fresh the mudstone is laminated, and contains small mud clasts in places. Much of the concealed sequence (e.g. Fig. 15b, Sect. BB) is probably mudstone. The sandstone (631C) in the upper part of the sequence is generally green to green-brown, fine-grained, and moderately well sorted. It is either trough cross-stratified or, more rarely, laminated.

Arcadia Formation

Of the three units in the Rewan Group, the Arcadia Formation crops out most strongly, although it contains roughly equal amounts of sandstone and softer red-brown mudstone. The formation is 230 m thick (Fig. 24). It can be differentiated from the Sagittarius Sandstone by the decrease in framework quartz in the sandstones, and also by the appearance of thick sequences of red mudstone and the increase in the proportion of interbedded lutite. These features could be used to map the boundary between the Arcadia Formation and Sagittarius Sandstone where the sequence is sufficiently well exposed. The best natural exposures are in the Isaacs River east of the gorge through the Carborough Range, and in the creeks and gullies along the eastern side of the range to its southern extremity, where there are a few excellent exposures in recently made road cuttings on the Peak

TABLE 7. STRATIGRAPHIC SEQUENCE IN NORTHERN AREA

Unit		*Thickness* (m)	*Lithology*			*Definition of Base*	*Fossils*
			Sand/Shale	*Mudstone & Siltstone*	*Sandstone*		
Expedition Sandstone	Upper part	130	1:0	Rare siltstone lenses	vf-vc; (811C)	Basal granule conglomerate; generally coarser than Cn2	
	Lower part	170	1:0	Rare siltstone lenses	vf-vc; (910C)	Decrease in number and nature of argillaceous beds; increase in grain-size	
Glenidal Formation		150	4:1	Red, green, and grey mudstone	f-c; (811C)	Decrease in mudstone and change in arenite framework	Rare carbonaceous plant fragments
Arcadia Formation		230	1:1	Red mudstone, mottled green, green siltstone; minor brown and grey mudstone and siltstone	vf-c; (541C); green, very rarely grey or red	First appearance of thick sequence of red mudstone	Finely disseminated plant fragments. *Densoisporites playfordi*, *Taeniasporites* sp.
Sagittarius Sandstone	Upper part	200	1:1	Brown and green mudstone	f; (631C)	Increase in framework quartz	
	Lower part	80	1:1	Brown and greenish brown mudstone and siltstone; thin beds of red and mottled red and green mudstone and siltstone	f-m; (361C)	Presence of thin beds of red mudstone; absence of coal and tuff	Finely disseminated carbonaceous plant material in places

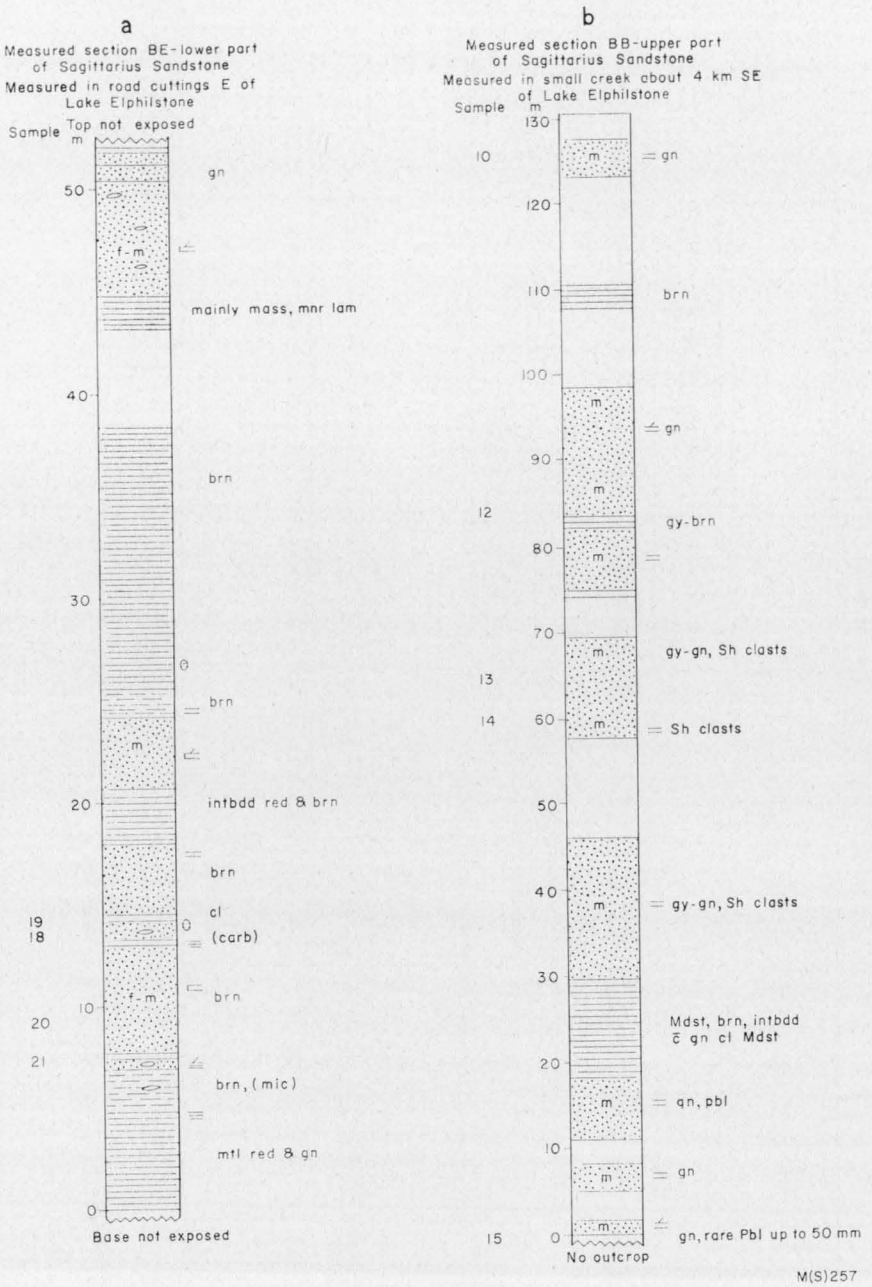


Fig. 25. Sagittarius Sandstone, measured sections in the northern area.

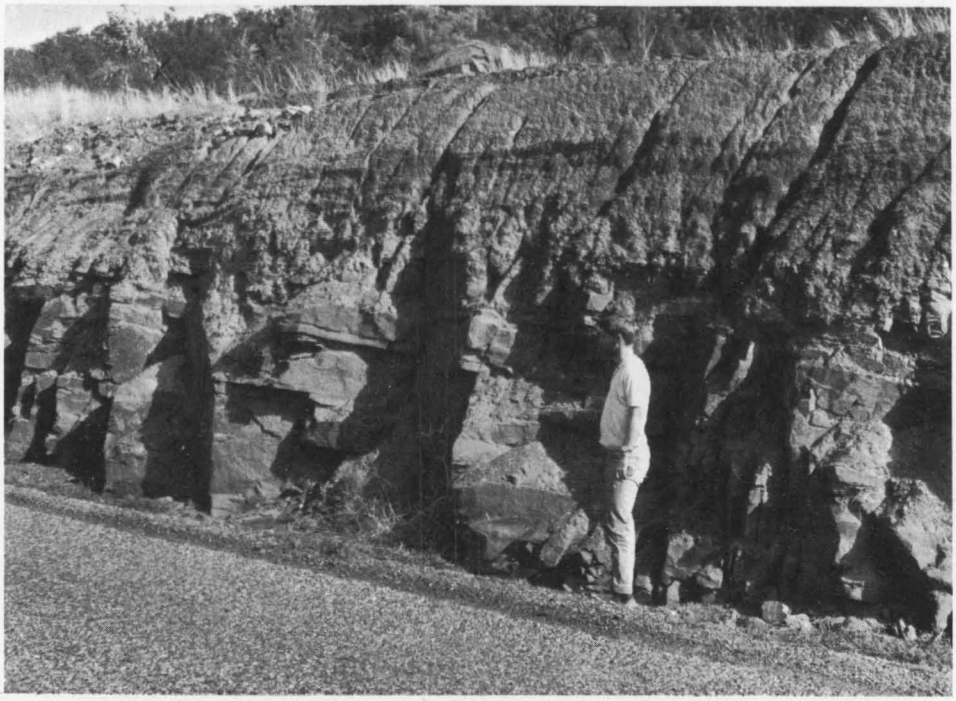


Fig. 26. Arcadia Formation showing cross-stratified sandstone overlain by a sequence fining up to mudstone at the top. Road cutting at southern end of Carborough Range, northern area.

Downs Highway (Fig. 26). The formation is also exposed in Exe Creek, between Turrawalla homestead and the eastern edge of the Redcliffe Tableland (Fig. 13, Sect. GA46). The thick sequences measured in Sections GA37 and GA46 (Figs 24, 27) are composed of alternating sandstone and mudstone, in which the sandstone commonly consists of group cross-stratified beds containing thin lenses of mudstone.

In the field the mudstone can be roughly classified into four types: (a) massive red mudstone; (b) mottled red and green mudstone and silty mudstone; (c) green siltstone; and (d) brown and grey mudstone and siltstone. The massive red mudstone, which forms the thickest sequence, is almost invariably interbedded with thin bands of bright green siltstone (Fig. 28) that are commonly associated with mottled red and green bands. Some of the small irregular patches of mottled red and green mudstone (Fig. 29) are associated with irregular joints in the massive red mudstone. Beds of brown and grey-brown mudstone and siltstone are rare, and generally occur as thin interbeds in sandstone sequences. They are invariably laminated, and commonly contain finely disseminated plant debris.

The sandstone (541C) in the Arcadia Formation is commonly green, but in places purple-grey and red. It is generally fine-grained, but ranges from coarse to very fine, and is moderately to poorly sorted. Rounded mud clasts are common, and rare sideritic concretions have been observed. Fine disseminated carbonaceous plant fragments are present in some beds.

Samples collected for palynology yielded a Tr2a assemblage (Evans, 1966b).

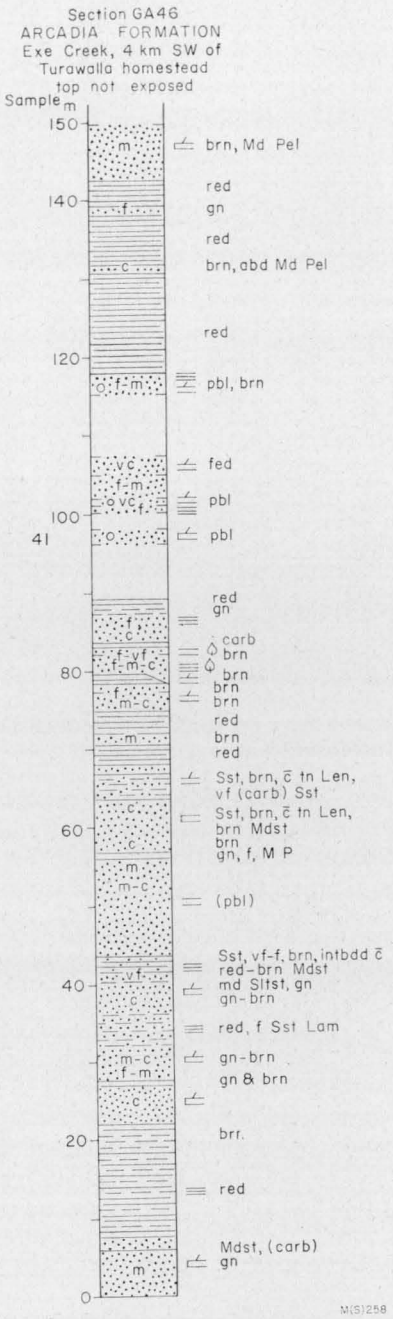


Fig. 27. Arcadia Formation, Section GA46, northern area.



Fig. 28. Red mudstone of the Arcadia Formation with thin green (white) layers of siltstone. Near Lake Elphinstone, northern area.

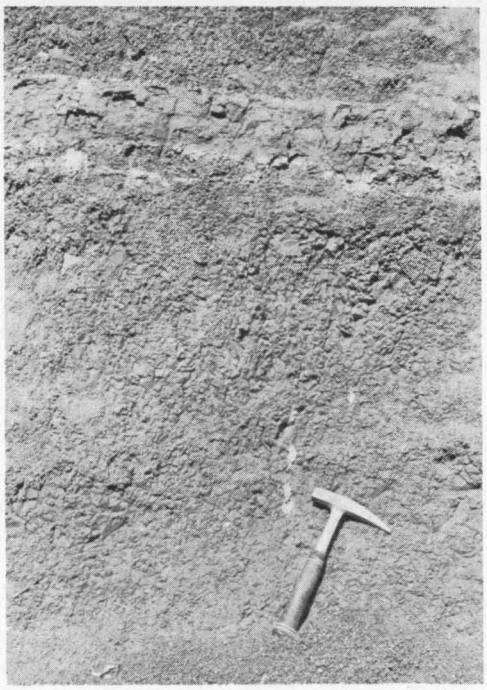


Fig. 29. Red mudstone of the Arcadia Formation with irregular patches of mottled green mudstone and silty mudstone. Near Lake Elphinstone, northern area.

Glenidal Formation

The Glenidal Formation is about 150 m thick in the northern part of the basin (Fig. 30), and rests apparently conformably on the Arcadia Formation, from which it is distinguished by a decrease in the proportion of mudstone and a change in the composition of the arenite framework. The two formations interfinger in places, but the boundary between them is generally relatively sharp, and of great stratigraphic importance. Mudstone generally forms only about one-fifth of the sequence, the rest consisting of fine to coarse sandstone, the framework of which contains substantially more quartz than the sandstone in the Rewan Group. There are also minor beds of granule conglomerate. The formation extends from the Red-

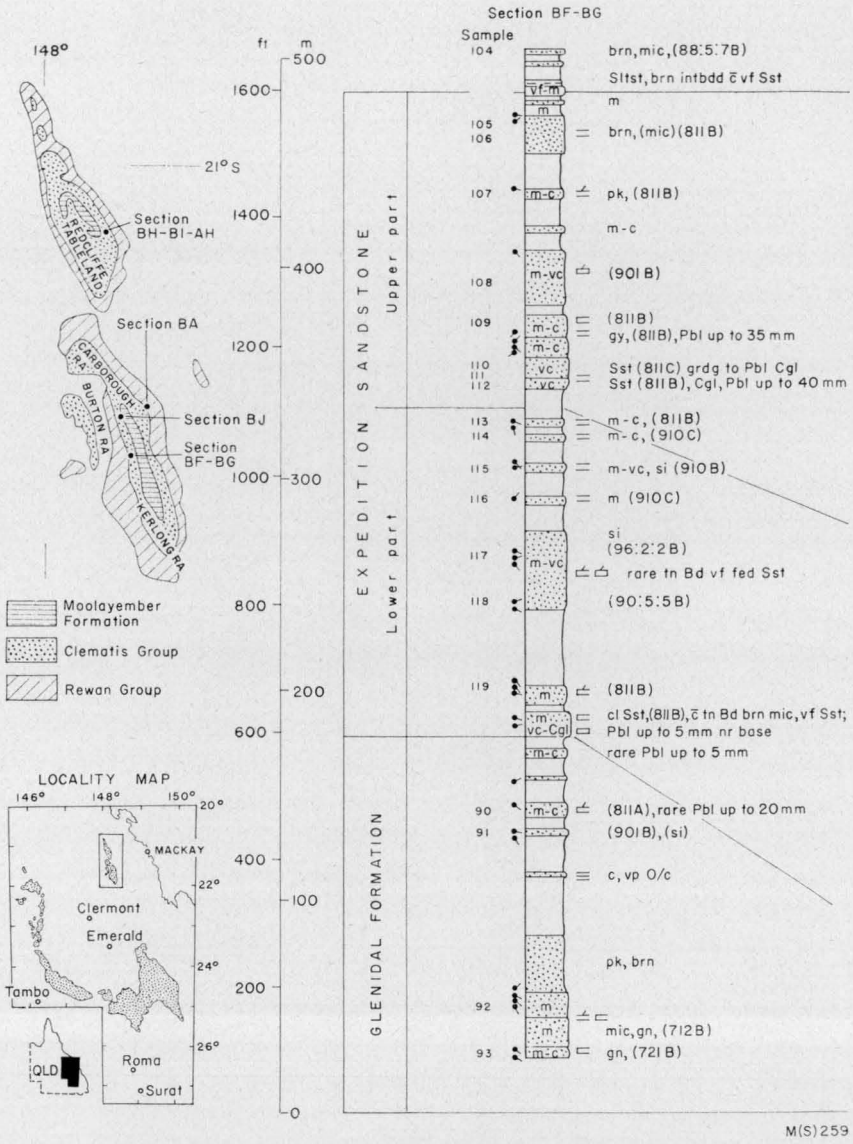


Fig. 30. Clematis Group, measured sections in the northern area.

cliffe Tableland to the Carborough Range, and westward to the Kerlong and Burton Ranges. It can also be recognized in the section measured by Veevers, Randal, Mollan, & Paten (1964) at Mount Iffle, some 30 km to the south of the southern end of the Carborough Range.

The Glenidal Formation almost invariably occupies the lower part of the ranges and tablelands formed by the Clematis Group, and is commonly covered by scree.

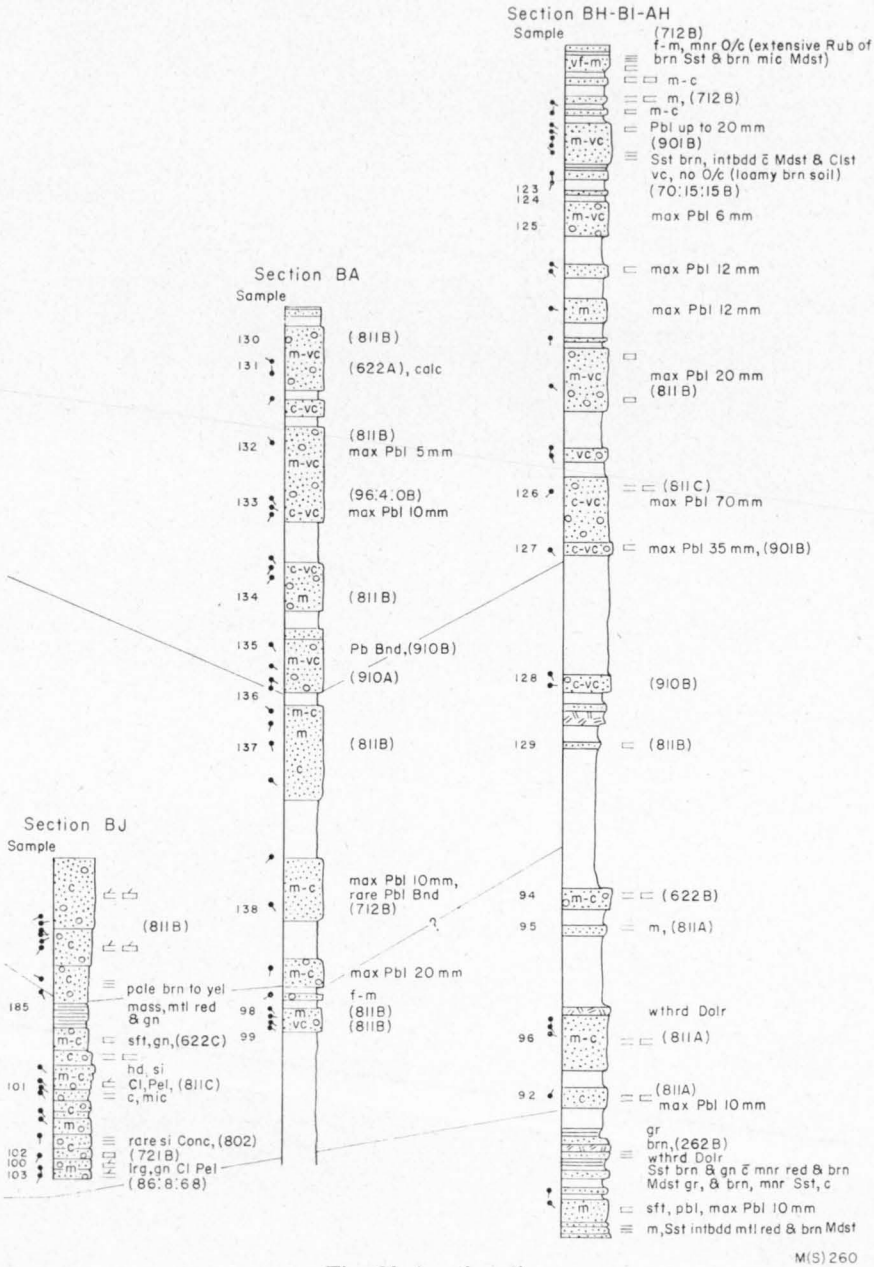


Fig. 30 (continued).

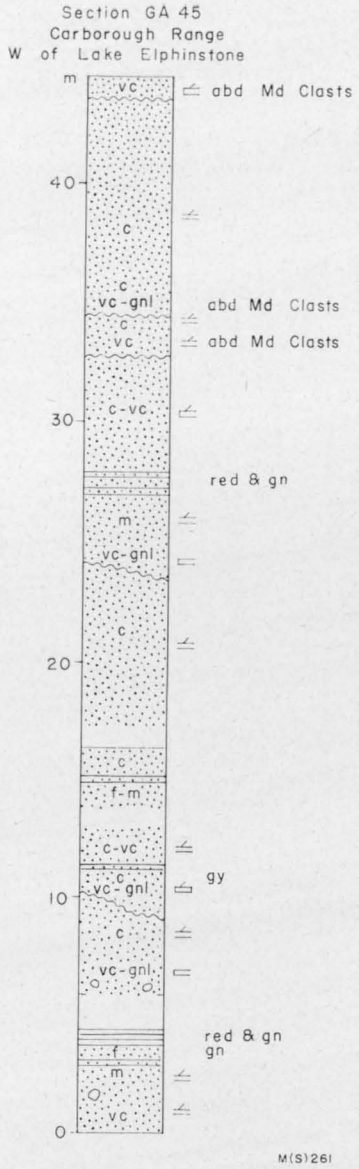


Fig 31. Glenidal Formation, measured section in the northern area.

Although it is reasonably distinct from the remainder of the Clematis Group, it has not been recognized before in this area owing to the paucity of outcrop. The best exposures occur in narrow near-vertical strips in a few places along the ranges where landslides and erosion have produced waterfall-like features with nearly continuous exposure. One of these outcrops lies on the western side of Lake Elphinstone in the Carborough Range, and another near Burton Downs homestead (Fig. 30, Sect. BJ). Section GA45 (Fig. 31) is fairly representative of the Glenidal Formation in the northern area.

A series of five shallow holes was drilled in the northern part of the basin to determine the lateral extent of the sandstone and mudstone bodies. The maximum distance between holes was 160 m, and over this distance there was little change in the thickness of the beds (Roddick, 1971). The sequence penetrated consists of interbedded fine to coarse sandstone and mottled grey, red, and green mudstone.

Expedition Sandstone

The Expedition Sandstone in the northern area forms ranges and tablelands about 200 m above the surrounding plain. The sequence is particularly well exposed in almost vertical cliffs up to 80 m high, which extend for many kilometres, but in the tablelands the formation is covered by sand or lateritic soil. The Expedition Sandstone is distinguished from the underlying Glenidal Formation by a decrease in the number and nature of argillaceous beds and by an overall increase in grainsize. Sandstone is predominant, but there are some beds of granule conglomerate. No mudstone has been recorded, and siltstone lenses are rare. The boundary with the overlying Moolayember Formation is taken at the lowest bed of brown mudstone, where on a regional scale there is a change to a more labile and more micaceous sandstone. Locally, however, beds of quartz-rich sandstone occur above the labile sandstones, and it is therefore unlikely that there is a disconformity between the two units.

Medium to very coarse sandstone (811C-910C) predominates in the northern area, but two subunits can be distinguished. The upper unit is generally slightly coarser and has a conglomerate or pebbly sandstone at the base. The coarser basal beds are not continuous throughout the area and cannot be correlated over long distances. The sandstone in both units is almost invariably cross-stratified. In places the cross-strata are graded, fining upwards over intervals of about 5 cm. Overturned cross-strata and convoluted laminae are common at restricted horizons.

The Expedition Sandstone is about 300 m thick between the Kerlong Range and the northern part of the Carborough Range, and the thickness appears to be the same in the Redcliffe Tableland, 50 km to the north (Fig. 30). In the Kerlong Range the lower subunit is about 170 m thick, and the upper 130 m.

Southeastern Area

Previous Investigations

Stratigraphic studies. A summary of changes in stratigraphic nomenclature in the southeastern area is presented in Table 8.

One of the most striking topographic features in this area, the Dawson Range, extends from the central part of the basin near Blackwater and Bluff, southeastwards towards Theodore and Cracow. The range is composed of a sequence called the Dawson Range Sandstone by Reid (1945), but later referred to as the Clematis Sandstone (Mollan et al., 1972; Derrington & Morgan, 1960). The sequence below the Dawson Range Sandstone was called the Isla Formation by Derrington & Morgan (1960), who described it as a sequence of 'interbedded olive green mudstone, siltstone, and sandy siltstone, and locally cross-bedded, biotitic, feldspathic lithic sandstone' lying conformably between the Clematis Sandstone and the Kia Ora Formation. Later, Jensen et al. (1964) demonstrated that the top of the Kia Ora Formation was equivalent to the Baralaba Coal Measures, and that the sequence between the coal measures and Dawson Range Sandstone was equated to the Rewan Formation; the use of the term 'Isla' was therefore discontinued.

TABLE 8. STRATIGRAPHIC NOMENCLATURE USED IN SOUTHEASTERN AREA

<table>
<tr><th>Reid (1945)</th><th>Derrington & Morgan (1960)</th><th>Jensen et al. (1964)</th><th colspan="2">This Bulletin</th></tr>
<tr><td rowspan="2">Dawson Range Sandstone</td><td rowspan="2">Clematis Sandstone</td><td rowspan="2">Clematis Sandstone</td><td rowspan="2"></td><td>Dawson Range Sandstone</td></tr>
<tr><td rowspan="3">Clematis Group</td><td>Unnamed equivalent of Glenidal Formation</td></tr>
<tr><td rowspan="3"></td><td rowspan="2">Rewan Group</td><td>Arcadia Formation</td></tr>
<tr><td></td><td>Sagittarius Sandstone</td></tr>
<tr><td></td><td>Kia Ora Formation</td><td>Baralaba Coal Measures</td><td></td><td>Rangal Coal Measures</td></tr>
</table>

Although the total thickness of the sequence is about 3700 m little was known of the lithology of this interval because it is so poorly exposed. Shallow stratigraphic holes were subsequently drilled into the base and at four other points higher in the sequence (Jensen et al., 1964), and the recovery of cores of chocolate-coloured mudstone confirmed the correlation with the Rewan Formation. From 1966 to 1968, the Geological Survey of Queensland drilled a series of deeper holes in the same interval and in the Dawson Range Sandstone.

Petrographic investigations. Thin sections of core and cuttings from the BMR shallow stratigraphic holes and of outcrop samples of the Rewan and Clematis Group were described by Arman (1965) and Bastian (1965a,b). The sandstone near the base and lower middle parts of the Rewan Group was found to be lithic (181C), and to consist mainly of fragments of volcanic rock. Samples from the upper part of the unit were found to contain less labile sandstone (442C). The Dawson Range Sandstone yielded labile sandstone (532B) and sublabile sandstone (721B), both with a volcanic provenance.

Palaeontological studies. The southern area is important stratigraphically because it is one of the few places with some palaeontological control. In many parts of eastern Australia it is difficult to distinguish the Triassic rocks from the Permian rocks because of the lack of marine faunas in critical sections. The upper limit of the *Glossopteris* flora has long been regarded as the end of Permian (David, 1950), and the stratigraphically highest occurrence of *Glossopteris* in the Bowen Basin is in the Blackwater Group. No collections of fossil plants are recorded between the coal horizons and the *Dicroidium* flora of the Clematis Group and Moolayember Formation, except from one locality near the base of the Rewan Group (Jensen et al., 1964). The specimens were poorly preserved, and White (1965) referred one fern frond to *Dicroidium odontopteroides* (Morr.) Gothan, which ranges from Triassic to Early Jurassic.

On the basis of palynology, de Jersey (1970) suggested that the Rewan Group is Early Triassic (Scythian). Assemblages from the Sagittarius Sandstone were only tentatively regarded as Triassic on the grounds that they have not been recorded in any Permian microflora. Equivalents of the Glenidal Formation in the southeast contain the first appearance of *Triadispora crassa* and on that basis are regarded as late Scythian. The upper part of the Clematis Group is correlated with the Scythian or early Anisian (de Jersey, 1968).

As a result of his studies of cores from the Geological Survey of Queensland stratigraphic holes (Figs 32, 33) in the southeast, de Jersey (1970) concluded that biostratigraphic subdivision of the sequence is possible on the basis of the successive appearance of selected species, but that it would be necessary to study the lateral distribution of the assemblages before attempting to define biostratigraphic units formally. Some difficulty was experienced in recognizing the units described by Evans (1964, 1966a) from the same section, partly because Evans' work was based on cores and cuttings from only a few shallow holes with a total sequence of 2000 m, and partly because his results were recorded before he subdivided units Tr1 and Tr2.

Considering the change from the coal measures to the Rewan Formation, de Jersey (1970) noted the decline of striate species such as *Protohaploxypinus limpidus,* but recorded the appearance of *Striatisaccus novimundi,* and the disappearance rather than the decline in numbers of *Dulhuntyispora parvithola.* De Jersey (1970) considers that the change could have been brought about equally well by a facies change as by a hiatus in sedimentation.

De Jersey records a relatively major microfloral change between the sequences in DRD No. 14 and DRD No. 15, with a marked upwards decline in the proportion of striate bisaccate pollens, and an increase in the percentages of *Alisporites* and *Aratrisporites.* He noted that his microfloral change corresponded with the change in lithology from a redbed sequence to a normal clastic sequence, and he appears to favour ecological control of the microfloral change. An abundance of apparently recycled Permian spores is recorded in DRD No. 13.

With regard to the Clematis Sandstone de Jersey (1968) noted a gradual change from the upper part of what is now regarded as Rewan Formation to the Clematis Sandstone, and that there is a gradual increase upwards in the proportion of *Alisporites* and a decrease in the proportion of *Osmundacidites.*

Description of Stratigraphic Units

A summary of the stratigraphic sequence in the southeastern area is presented in Table 9.

Rewan Group

The Rewan Group (Fig. 32) contains no horizons as resistant to weathering as the conglomerate and tuff of the underlying coal measures, and the boundary between the two units is marked by the change to a more subdued topography. The group crops out as rounded strike ridges. Some changes in vegetation are apparent on the aerial photographs, but almost all the bedrock is covered by a thin layer of soil. The boundary between the coal measures and the Rewan Group is taken above the youngest coal seam, but in places the youngest coal seam is overlain by a distinctive conglomerate composed of rounded cobbles of volcanic rocks. As

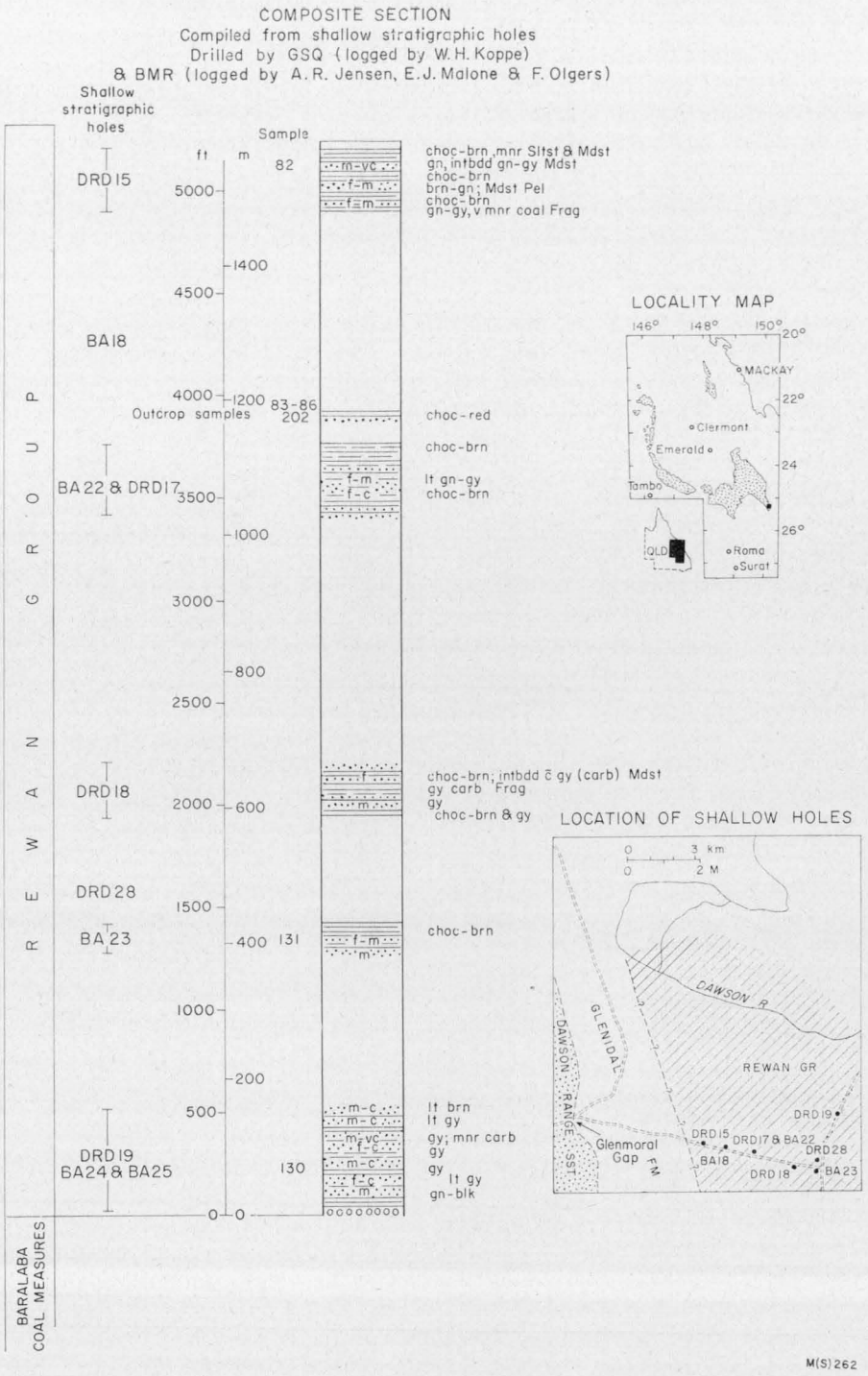


Fig. 32. Rewan Group, composite section in the southeastern area.

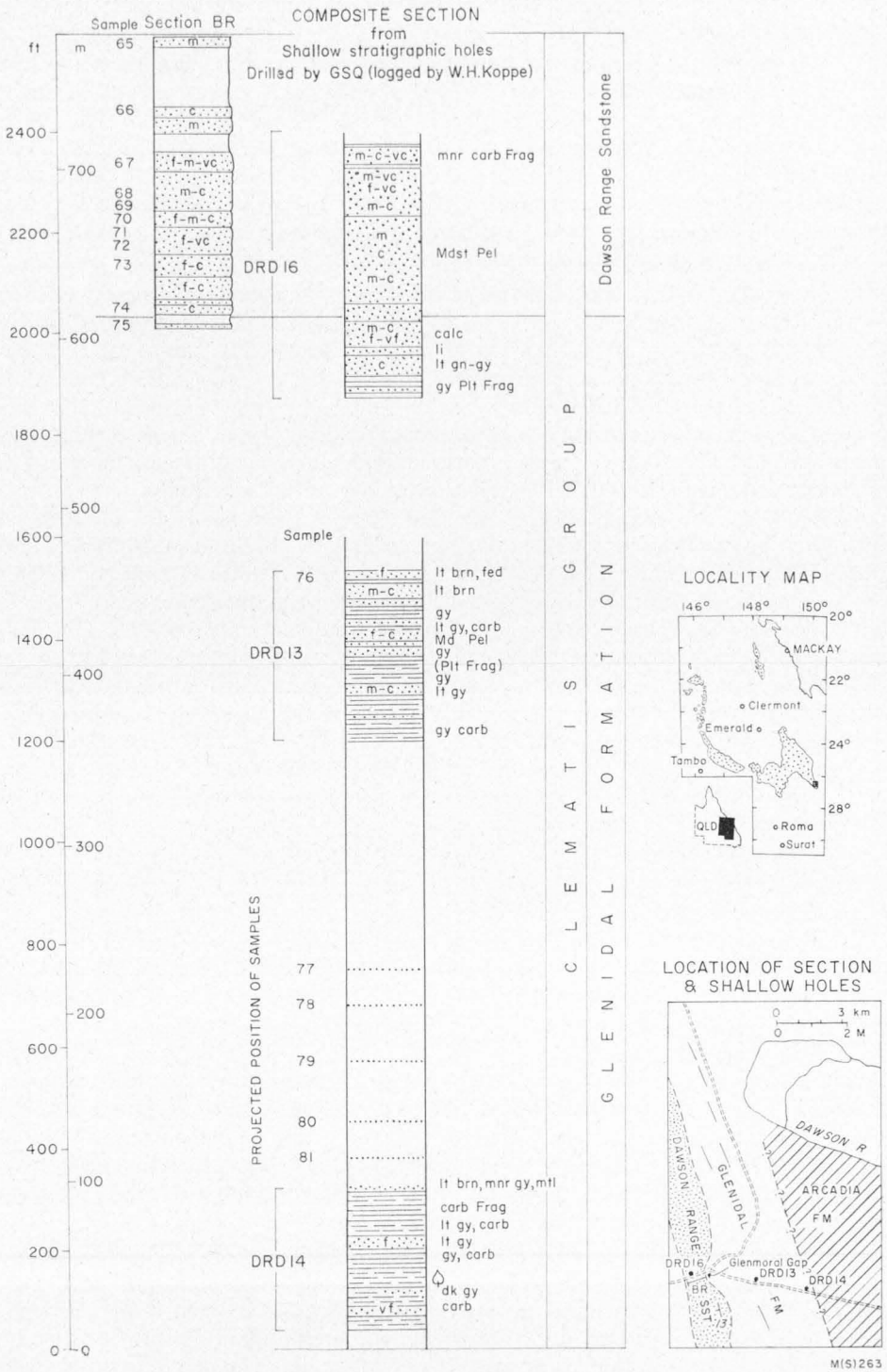


Fig. 33. Clematis Group, composite section in the southeastern area.

similar conglomerates are interbedded with the coal seams, the boundary is placed above the conglomerate.

The precise thickness of the Rewan Group is not known because of the lack of detailed structural information. The upper boundary is somewhere between the Geological Survey of Queensland holes DRD No. 14 and DRD No. 15, and is estimated to be 1000 m above the top of the coal measures. The stratigraphic levels of the holes are shown in Figure 32, and the calculated thicknesses are based on a limited number of dip measurements in the field. The results differ slightly from those shown by de Jersey (1970), but the discrepancies do not materially affect the conclusions regarding the stratigraphic sequence.

The sequence at the base of the group consists of light to dark grey medium to very coarse-grained labile sandstone (172B) interbedded with grey and brown mudstone containing scattered carbonaceous plant fragments. The sandstone contains rare intraformational conglomerate. Only thin beds of chocolate-brown mudstone are recorded in BMR Taroom No. 24, but higher in the sequence the proportion of chocolate-brown mudstone is about the same as that of interbedded grey mudstone and fine-grained green sandstone. Individual beds of chocolate-brown mudstone are relatively thin, and rarely exceed 2 m. In the upper part of the group, however, beds of chocolate-brown mudstone up to 20 m thick are interbedded with thick beds of fine to coarse-grained greenish grey sandstone (253C) and siltstone. With more stratigraphic drilling it may be possible to distinguish equivalents of the Sagittarius Sandstone and Arcadia Formation in the southeastern part of the basin. The Sagittarius Sandstone is carbonaceous and contains only thin beds of chocolate-brown mudstone, while the Arcadia Formation contains thick beds of chocolate-brown mudstone and is almost lacking in carbonaceous material. The boundary between the two units is about 200 m above the top of the coal measures, in about the same position as the appearance of de Jersey's (1970) *Densoisporites playfordi* assemblage and the base of Evans (1966a) unit Tr2a.

Glenidal Formation

A sequence equivalent to the Glenidal Formation lies with apparent structural conformity between the Rewan Group and the Dawson Range Sandstone. In the Cracow and Theodore areas, it forms low rounded hills and strike ridges with rare dip-slopes, but even on the hills and ridges the sequence is poorly exposed. Some sandstone and mudstone crop out on the Theodore-Glenmoral road about 2 km east of the Dawson Range, and also on the sides of small ridges running parallel to, and about 2 km from, the eastern side of the Dawson Range.

The sequence consists of mudstone interbedded with sandstone and minor siltstone. The proportion of sandstone increases upwards through the sequence. In DRD No. 14, near the base of the unit, the sand-shale ratio is about 0.14, but higher in the sequence, in DRD No. 13 (Fig. 33), the sand-shale ratio is about 0.57. The mudstone units with minor interbedded siltstone generally range from 12 to 25 m thick, and the sandstone beds are generally around 5 m thick, although one sandstone unit in DRD No. 13 is 25 m thick.

In the subsurface the mudstone ranges from light brown to light grey and contains scattered carbonaceous plant material, which in places forms thin coaly laminae. In DRD No. 13 there are also rare thin beds of mottled red-green mudstone and red-grey mudstone up to 1 m thick. In outcrop the mudstone is generally light brown and unlaminated; a hard green unlaminated mudstone with a subconchoidal fracture was observed in places.

TABLE 9. STRATIGRAPHIC SEQUENCE IN SOUTHEASTERN AREA

Unit	*Thickness* (m)	*Lithology*			*Definition of Base*	*Fossils*
		Sand/Shale	*Mudstone & Siltstone*	*Sandstone*		
Dawson Range Sandstone	200	1:0	Rare beds of thin grey mudstone	m-c; (712C) Becomes pebbly to conglomeratic southwards	Increase in framework quartz; change to sequence with little mudstone	Silicified fossil wood in conglomerate. Gradual microfloral change from Glenidal Formation
Glenidal Formation	600-730	1:3	Brown and grey mudstone with rare thin beds of mottled red-green mudstone	vf-m; (622B)	Change to sequence without thick red mudstone; change in arenite framework	Base corresponds with major microfloral change. Recycled Permian spores near top
Rewan Group	2000	1:1	Lower part: grey and brown mudstone; upper part: chocolate-brown	f-c; lower (172B), upper (253C)	Absence of coal seams; conglomerate marker in places	Boundary between upper and lower parts corresponds to first appearance of *Densoisporites playfordi*

In the subsurface the sandstone is generally light grey-brown to light grey, but is brown at the surface. It normally ranges from very fine to medium-grained, but thin beds of coarse pebbly sandstone have been noted in outcrop; the maximum size of the clasts is 1 cm. In the Cracow area the sandstone is labile (622B), and commonly contains abundant brown mud clasts. The sandstone outcrops are massive; cross-stratification is rare, but ripple lamination is present in some of the fine sandstone.

The lower boundary is taken where chocolate-brown mudstone gives way to grey or light brown mudstone. The exact position of the boundary in the Cracow area is not known because the sequence is not sufficiently well exposed. The thickness is estimated to be 600 to 730 m. The boundary as defined also corresponds with a sharp change in the composition of the arenite framework from a labile (253C) to a less labile (622B) sandstone.

Dawson Range Sandstone

The Dawson Range Sandstone, in contrast to underlying units, crops out strongly to form the Dawson Range, which extends northwards with only occasional breaks from the southeastern area to the Raby Creek area. The range has a steep eastern face surmounted by an almost continuous crest-line which stands about 250 m above the level of the lowlands to the east. To the west there are a number of dip-slopes or plateau-like extensions from the crest, which represent an exhumed Upper Triassic deeply weathered regolith from which the Jurassic cover rocks have only recently been stripped.

Most of the Dawson Range Sandstone is exposed in Glenmoral Gap (Fig. 33, Sect. BR) to the west of Theodore, where recent drilling has been carried out by the Geological Survey of Queensland. The formation is composed mainly of light brown to grey medium to coarse-grained sandstone containing scattered pebbles, up to 2 cm in diameter, and rounded mud clasts. The sandstone is generally cross-stratified, although horizontally laminated fine sandstone is present. The drilling records reveal the presence of beds of grey mudstone which are generally less than 15 cm thick, but which range up to 1 m.

The lower boundary is taken where the sequence changes from predominantly mudstone to predominantly sandstone. The boundary coincides roughly with a change from labile sandstone (622B) to sublabile sandstone (712C). At the upper boundary there is a change to a sequence containing a significant proportion of mudstone, and where the mudstone beds are over 1 m thick. The boundary coincides with a change to a sequence containing more labile sandstone (433C).

The formation can be traced northwards on the aerial photographs along the Dawson Range, but because of gaps in the range and changes in dip it is difficult to trace it as far as the Raby Creek area. It does, however, appear to be on strike with the lower part of the Expedition Sandstone. South of Glenmoral Gap the Dawson Range loses height and eventually fades out where the line of the range is intersected by scarps formed by the flat-lying Jurassic Precipice Sandstone. The number and thickness of conglomeratic bands in the sandstone increase to the south, and about 14 km south of the gap conglomerate beds up to 50 cm are interbedded with the sequence. The conglomerate consists of rounded cobbles and pebbles of volcanic rock and quartzite, and cobbles of silicified fossil wood derived from the Permian coal measures.

Sequences Farther West, on Margin of Galilee Basin

Mantuan Downs area

The Blackwater Group coal measures can be traced westwards from the south-western part of the Bowen Basin across the Springsure Shelf and into the Galilee Basin. At Tanderra homestead 90 km northwest of Mount Carnarvon, on the Springsure Shelf, Mollan et al. (1969) reported that the Rewan Group is absent, but that it reappears a few kilometres farther west, and has been mapped for many kilometres westwards. The sequence consists of brown or red-brown micaceous mudstone and siltstone interbedded with cross-stratified or laminated medium to fine micaceous sandstone (451B) with lustre-mottling. Beds of coarse to very coarse sandstone and brown spherulitic limestone have been recorded in places. The laminated sandstone commonly has a weak parting lineation. The sequence is estimated to be about 50 m thick near Mantuan Downs homestead, but the base is not exposed. It is overlain by a sequence mapped as Clematis Sandstone, but which can be correlated with the Expedition Sandstone. The sequence consists of 5 m of white very coarse-grained cross-stratified pebbly sandstone which grades in places into pebble conglomerate, overlain by thinly interbedded flaggy quartz-rich sandstone (811B) and minor lenses of ferruginous micaceous siltstone with desiccation cracks. The thickness of the Expedition Sandstone, from the base of the very coarse sandstone unit to the base of the Moolayember Formation, is estimated to be only 30 m.

Jericho and Lake Galilee area

In the Great Artesian Basin, the Triassic sequence to the west of the Bowen Basin has recently been traced along the eastern margin of the Galilee Basin. The geologists mapping the Great Artesian Basin have recognized the Clematis Sandstone and Moolayember Formation, and also the Dunda Beds (Vine, Jauncey, Casey, & Galloway, 1965) below the Clematis Sandstone. Farther north, Vine, Casey, & Johnson (1964) distinguished another Triassic unit beneath the Moolayember Formation which they named the Warang Sandstone.

The Dunda Beds of Vine et al. (1965) consist of a sequence of sandstone, 75 m thick, which rests conformably on the Rewan Group on the eastern edge of the Galilee Basin. The name was derived from Dunda Creek, a tributary of the Belyando River. In the type section, in an unnamed tributary of Dunda Creek in the Galilee Sheet area (lat. 22°27′S, long. 146°19′E), Vine et al. reported that the sandstone is lithic (361) to quartzose (721), fine-grained, and is interbedded with red, red-brown, white, and grey mudstone. According to White (1965) the plant fossils from the beds include *Thinnfeldia acuta, Taeniopteris spatula, Dicroidium odontopteroides, Sphenopteris* cf. *superba, Ginkgo antarctica, Araucarites* sp., *Cladophlebis australis,* and *Coniopteris delicatula.* Evans (1966c) recorded a Tr3 spore assemblage from the beds in the vicinity of Tambo, and discounted the suggestion by Exon, Galloway, Casey, & Kirkegaard (1966) that the Dunda Beds are a facies equivalent of the Rewan Formation. It now seems more likely that they are equivalents of the Glenidal Formation of the Bowen Basin.

The Dunda Beds are reported to be overlain disconformably by the Clematis Sandstone (Vine et al., 1965), which in this area is composed of quartzose sandstone with minor interbeds of grey-white and red mudstone and siltstone. At the base there is a conglomeratic sandstone, which grades in places into quartz-pebble conglomerate, and the unit is therefore correlated with the Expedition Sandstone.

The thickness of the beds in this part of the Galilee Basin ranges from 30 to 105 m. Plant fossils collected from the beds include *Cladophlebis australis, Ginkgo* cf. *magnifolia,* and *Dicroidium odontopteroides.*

North of latitude 20°S the Triassic sequence above the Upper Permian coal measures is known as the Warang Sandstone (Vine et al., 1964). The formation is composed of up to 250 m of 'poorly sorted kaolinitic quartz sandstone, commonly pebbly or gritty and with large-scale trough cross-bedding, and lenses of red and green siltstone grading to very fine-grained sandstone'. The upper parts are conglomeratic.

PETROGRAPHY

LUTITE

Nomenclature

In this Bulletin the term lutite is used to describe terrigenous clastic sedimentary rocks finer than 0.0625 mm, and it therefore includes rocks composed of silt and clay-size grains; siltstone is composed dominantly of silt-size grains (i.e. between 0.0625 and 0.004 mm); mudstone is a mixture of silt and clay-size grains; and shale is a fissile mudstone. The colour of the rocks is specified in terms of the Munsell system as presented in the Geological Society of America Rock Colour Chart (1963).

Much of the terminology employed in the description of the fabric of mudstone in thin section is based on a system developed primarily for the description of soil morphology, but extended to include the fabric of clastic sedimentary rocks (Brewer, 1964, p. 327). A comprehensive summary of Brewer's fabric nomenclatural scheme is not attempted here, and only an outline of his fundamental classification is given; for further details the reader is referred to the glossary of terms given by Stace et al. (1968).

The fabric of soil can be expressed in terms of three units of organization: peds, pedological features, and s-matrices. A ped is an individual natural soil aggregate consisting of a cluster of primary particles, separated from adjoining peds by surfaces of weakness, which are recognizable as natural voids or by the occurrence of cutans (Brewer, 1960). Peds were not recognized in any of the sedimentary rocks examined in thin section, possibly because all the work was carried out on small samples, and because original natural surfaces of weakness are difficult to identify in lithified sediment. Pedological features are recognizable units within soil material which can be distinguished from the enclosing material for reasons such as origin (deposition as an entity), differences in concentration of some fraction of the plasma, or differences in the arrangement of the constituents; for the purpose of the present study this includes shreds of carbonaceous material. The s-matrix of a soil is the material within the simplest peds, or the material composing apedal soil materials, in which the pedological features occur; it consists of plasma, skeleton grains, and voids that do not occur in any pedological features other than plasma separations. S-matrix differs from the 'matrix' of sedimentary rock nomenclature in that it includes skeleton grains (Brewer, 1964).

Rewan Group

A summary of petrographic observations on the lutites of the Rewan Group is presented in Table 10. Outcropping lutite within the Rewan Group includes:

TABLE 10. MAIN CHARACTERISTICS OF LUTITES OF REWAN GROUP AND GLENIDAL FORMATION

Unit	*Rock Type*	*Fabric*	*Notes on Mineral Phases*	*Remarks*
Rewan Group	Yellowish brown muddy siltstone and siltstone	Laminated and massive	Labile minerals present. No segregation of iron oxide; minor chlorite veins	Labile sediment; no signs of pedogenesis
	Red to brown mudstone	In outcrop massive but all samples have lamination; minor bioturbation	Laminae in places enhanced by segregation of iron oxide in finest fractions; only minor secondary movement of iron oxide	Lamination and lack of movement of clay and iron oxide indicate that they are not soils
	Yellowish green siltstone in thin layers within red to brown mudstone sequences	Finely laminated	Same sharp change from red to green clay minerals in both; only differences are grainsize and higher content of Fe_2O_3 in red variety	Green layers represent coarser sediments that did not originally contain Fe_2O_3 and finest clay fraction
		Non-laminated to mottled	Evidence for translocation of iron and clay	Pedogenic alteration of originally laminated sediment
Glenidal Formation (outcrop samples)	Greenish grey	Unistrial fabric		Fabric developed during sedimentation
	Brown	Asepic fabric	Abundance of fine-grained iron oxide	Original lamination probably obscured by iron oxide
	Reddish brown	Complex pedological fabric	Evidence of translocation of iron and clay	Not direct evidence of Triassic pedogenesis because sample taken from outcrop
Glenidal Formation (subsurface samples)	Grey mudstone	Complex pedological fabric, brown pedorelicts set in grey s-matrix	Translocation of clay	Soil fabric in upper part of profile
	Mottled red-green and grey mudstone	Complex pedological fabric	Major translocation and deposition of clay and iron in originally laminated sediment	Soil fabric
	Red mudstone	Faintly laminated and containing small rounded clay pellets	Minor translocation of clay and iron in sediment derived from erosion of soil	Previous soil dominated by nodular sesquioxides

(a) yellowish brown muddy siltstone and siltstone, which occur as relatively thick beds interbedded with sandstone; (b) red to brown mudstone, also in relatively thick beds; and (c) yellowish green siltstone in relatively thin layers within the red-brown mudstone.

(a) The yellowish brown (10YR 5/4) muddy siltstone and siltstone include both laminated and apparently massive rocks. The lamination is due to the presence of thin laminae of silt or very fine sand, or to the alignment of fine phyllosilicates, and in both cases the laminated rock has a weak unistrial skelsepic fabric. The massive variety has a weak skelsepic to intertexitic fabric. Skeleton grains include fresh plagioclase, epidote, apatite, and biotite. There are also detrital grains of iron oxide, but no secondary segregation of sesquioxides, except along rare joints. Where chlorite forms small veins it results in the development of a minor diagenetic crystic fabric.

(b) The variety of mudstone so typical of the Rewan Group, which is also found in the Glenidal Formation, ranges from dark reddish brown (10R 3/4) to dark greyish red (10R 3/2). The grainsize of the original sediment is difficult to determine. Pipette analyses of rock chips disintegrated by a sonic vibrator after immersion in distilled water suggest that much of the rock is composed of silt (Fig. 34), but disintegration is probably incomplete when there is a high proportion of amorphous iron oxide. In thin section the rocks appear to be silty mudstones.

Most of the red-brown mudstone appears to be massive in outcrop, but thin sections reveal the presence of fine lamination in all samples. In some samples the

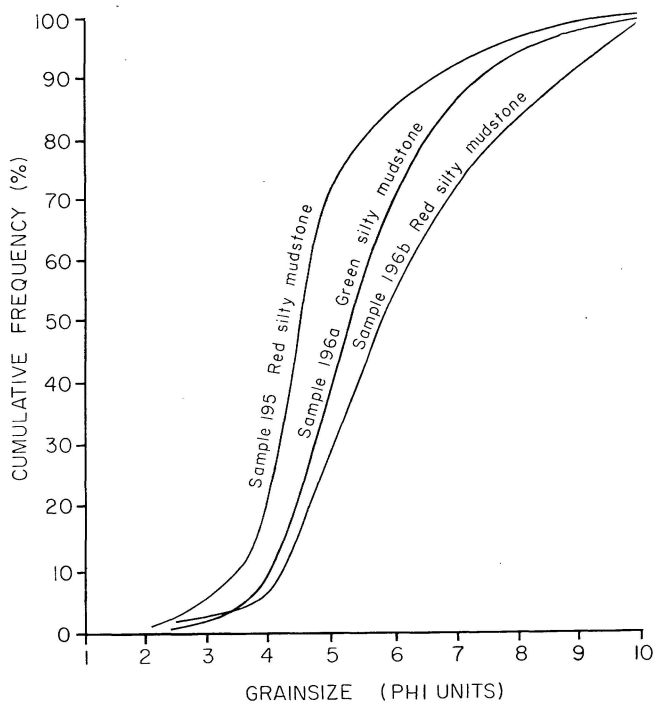


Fig. 34. Grainsize analysis of red and green lutite samples from the Rewan Group.

lamination is due to the alteration of fine and coarse layers composed of silt or very fine sand, and mud, but it is commonly enhanced by the segregation of sesquioxides, generally in the finer laminae (Fig. 35); the concentration is not always along layers of finer grainsize, and presumably reflects subtle changes in the type of sediment or current strength. The only evidence of movement of sesquioxides in the well laminated red-brown rocks is the replacement of faunal burrows, represented by short tubules 0.5 mm wide and 5 mm long, which cut across the bedding. In some of the finer mudstone with very few siltstone laminae a faint lamination is created by the alignment of small elongate wisps of clay. The sesquioxides, presumably hematite, are distributed evenly throughout the rock in two forms: (i) deep red nodules about 0.015 mm in diameter with diffuse borders; and (ii) amorphous 'pigmentation' of clay minerals. Despite the diffuse borders of the nodules and the fineness of the iron oxide, there is little evidence of the movement of iron oxide because concentrations are found only beneath rare discontinuous silt laminae and along small joints producing joint-plane ferrans. Some of the lamination is disrupted by bioturbation, but there is generally very little sign of pedogenesis. The skeleton grains include abundant quartz and chert, and a little fresh plagioclase in some samples.

(c) Some of the beds of yellowish green siltstone, which occur as relatively thin layers with the red-brown mudstone, grade into very fine sandstone, and others into green muddy siltstone. The siltstone is coarser than the red-brown mudstone and it may be finely laminated or non-laminated. In the well laminated rocks, the

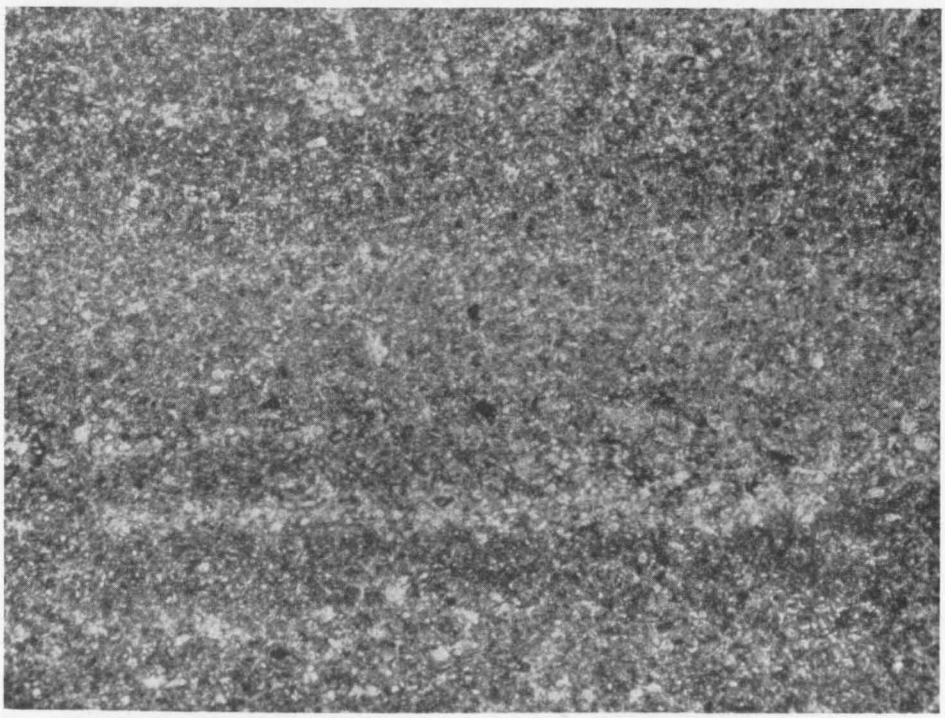


Fig. 35. Red mudstone of the Rewan Group showing distinct lamination. Plane polarized light, x 40.

change from red to green is generally quite sharp, and there is no sign of disruption of the laminae by depositional processes, or of the movement of iron oxide from one to the other. There are, however, signs of the movement of iron oxide within the red mudstone in which the thin silt laminae are bounded by ferrans. The composition of the clay minerals in the red and green layers is the same (Table 11), and pipette analysis suggests that the green is coarser than the red, although the difference is small (Fig. 23). The difference in colour is due to the presence of finely disseminated iron oxide in the red mudstone, and chemical analysis (Table 12) confirms that the red mudstone contains more ferric oxide than the green variety. Most of the iron in the green layers occurs in the mixed-layer clay, which is predominantly smectite. Thus it appears that in these laminated rocks considerably more iron oxide was deposited with the fine muddy sediment, which is now red, than with the slightly coarser silty sediment, which is now green.

There is a far more complex relationship in the non-laminated irregularly mottled green and red siltstone, which consists of abundant chert and quartz and minor heavy mineral grains and plagioclase set in a green skel-lattisepic plasma. Pedological features include: green skew-plane argillans; brown skew-plane argillans with a concentration of deeper brown pigmentation along one edge, grading into highly irregular and diffuse skew-plane ferrans; and isotubules, some filled with greyish green masepic plasma, and some with abundant skeleton grains. The internal fabric suggests that the mottling is caused by the movement of green clay along skew-planes and tubules, some of which were subsequently used by iron-rich solutions to deposit iron oxides along discontinuities caused by sharp changes in grain-size. It therefore appears that although the thin yellowish green layers interbedded with the red-brown mudstone sequences originally contained little iron oxide, subsequent pedogenesis has led to its introduction and the redistribution of some clay.

TABLE 11. CLAY MINERALS IN LUTITES

Unit	*Sample*	*Colour*	*Mica*	*Kaolinite*	*Mixed Layer Predominantly Smectite*	*Smectite*	*Mixed Layer Predominantly Mica*	*Chlorite*
Expedition Sandstone	189	grey	+	++	—	—	—	—
	191	grey	++	++	—	—	—	—
	203	grey	+	++	—	—	—	—
Glenidal Formation	187	grey	++	++	—	—	—	—
	292	green	+	++	—	—	—	—
	184	grey	+	—	++	—	—	—
	188	brown	++	+	—	—	—	—
	243	brown	+	++	—	—	—	+
	153	brown	+	+	—	+	+	—
	185	red	+	—	++	—	—	—
Rewan Group	180	brown	+	+	—	+	—	—
	194	green	+	+	+	—	—	—
	196	green	+	+	++	—	—	—
	197	green	+	+	+	—	—	—
	183	green	+	+	+	—	—	—
	195	red	+	+	+	—	—	—
	196	red	+	+	++	—	—	—
	198	red	+	+	+	—	—	—
	182	red	+	—	+	—	—	—
	183	red	+	—	+	—	—	—

TABLE 12. CHEMICAL ANALYSES OF LUTITES

Sample	182	212	180	195	194	196	196	197	198
Unit	ARCADIA FORMATION, NORTHERN AREA				ARCADIA FORMATION, SOUTHWESTERN AREA				
Colour	red	red	brown	red	red	red	green	green	red
SiO_2	61.0	62.7	63.0	56.5	60.4	56.0	60.5	66.2	60.4
Al_2O_3	16.5	16.4	16.3	16.5	16.9	16.5	15.9	16.0	16.0
Fe_2O_3	4.05	5.50	2.37	11.30	9.55	9.65	5.26	2.16	8.21
FeO	0.70		0.96	1.20		0.85	1.34	0.84	0.84
MgO	1.85	1.90	2.00	2.05	1.10	2.25	2.25	1.94	2.35
CaO	1.50	1.24	0.81	0.22	0.09	0.40	0.40	0.26	0.28
Na_2O	1.17	1.69	1.77	0.49	0.91	1.60	1.30	1.41	0.36
K_2O	3.00	3.50	2.65	3.15	3.30	1.95	1.95	3.00	3.15
TiO_2	0.73	0.64	0.67	0.85	0.85	0.70	0.75	0.74	0.65
P_2O_5	0.76	0.10	0.22	0.08	0.10	0.11	0.12	0.09	0.02
MnO	0.06	0.05	0.08	0.06	0.09	0.06	0.08	0.03	0.04
V_2O_5	0.02	0.01	0.03	0.03	0.20	0.05	0.05	0.03	0.04
Loss on ignition	7.95	6.80	8.10	7.80	6.95	9.60	9.30	6.90	7.80

Analyst: Aust. Mineral Development Laboratories. Direct reading emission spectroscopy except for FeO and Fe_2O_3.

Glenidal Formation

A summary of observation on the lutites of the Glenidal Formation is presented in Table 10.

Observations on outcrop material. In outcrop the mudstone of the Glenidal Formation ranges from greenish grey (5GY 6/1) to brown (5YR 4/4) and dark reddish brown (10R 3/4). In general there is little sign of post-depositional change in the greenish grey and brown well laminated varieties which contain carbonaceous plant material. The greenish grey mudstone generally has a strong unistrial fabric, probably initiated during deposition of the sediment. The asepic fabric in the brown mudstone is due to the abundance of brown fine-grained iron oxide, although laminae of silt and faunal burrows have been preserved.

On the other hand, the original lamination in the reddish brown mudstone sampled in the northern part of the basin has been completely destroyed by pedogenic processes. The mudstone consists of diffuse-bordered reddish brown orthic pedorelicts surrounded by a green s-matrix, which occupies channels, and which contains well defined channel argillans as well as moderately adhesive and diffuse sesquioxidic nodules and lithorelicts. The orthic pedorelicts consist of papules, skeleton grains of quartz, fragments of rocks, and feldspar, as well as lithorelicts, set in a ferruginous isotic plasma. There is little doubt that the complex fabric was produced by translocation of considerable amounts of clay and sesquioxides, but because these observations are based on surface samples there is no proof that the pedogenesis occurred in the Triassic.

Observations on subsurface material. The BMR Mount Coolon No. 7 hole in the northern part of the basin provided a core about 2 m long of mottled grey, red, and green mudstone. Six thin sections were cut in the core to determine the nature and origin of the apparent changes in lithology. The fabric analysis is presented in graphic form in Figure 36, and summarized in Table 13.

The grey mudstone (5GY 4/1) at the top of the core (33.57 m) has a porphyroskelic fabric with brown pedorelicts set in an s-matrix composed mainly of grey masepic plasma. The pedorelicts (Fig. 37) have diffuse irregular borders,

TABLE 13. FABRIC OF MUDSTONE IN GLENIDAL FORMATION

Depth (m)	*Main S-Matrix*	*Main Pedological Features*		
	Grey	*Skew-plane argillans*	*Embedded grain argillans*	*Brown pedorelicts*
	Skeleton grains: angular quartz silt; random distribution			*S-matrix:* angular quartz silt in masepic to skelsepic plasma (brown)
33.57	*Plasma fabric:* masepic			*Pedological features:* (1) void cutans now filled with s-matrix; (2) isotubules 0.2 mm in diameter; (3) sesquioxidic nodules—regular to irregular, average size 0.2 mm
		Orthic pedorelicts (yellow-brown phase)	*Skew-plane sesquans* (dark brown)	*Cutaus Sesquioxidic nodules*
	Skeleton grains: angular quartz silt			
33.76		*S-matrix:* Angular quartz silt in ma-skel insepic plasma	*S-matrix:* abundant skeletal grain in masepic plasma	
	Plasma fabric: vo-masepic and ma-vosepic (grey phase)	*Pedological features:* (1) voids—channels filled with s-matrix or calcite; (2) cutans—channel and embedded grain; (3) glaebules (i) papules, (ii) sesquioxidic nodules and concretions, (iii) inherited pedrorelicts (a) sesquioxidic nodules in brown masepic plasma	*Pedological features:* (1) small rare sesquioxidic nodules; (2) diffuse round pedorelicts (i) nodules, (ii) papules	

TABLE 13—*Continued*

	Yellowish green *Skeleton grains:* quartz silt	*Isotubules and striotubules* with very small shreds of carbonaceous material (grey phase)	*Skew-plane sesquans* associated with tubules (red phase); volumetrically dominant	*Granular sedimentary relicts*—yellow-brown and partly replaced by iron oxide	*Papules*
34.39	*Plasma fabric:* lattisepic			*S-matrix* *Pedological features:* (1) diffuse sesquioxidic nodules; (2) striotubules and isotubules	
	Faintly laminated				
35.00	*Skeleton grains:* abundant *Plasma fabric:* weakly strial, insepic	Diffuse *isotubules* filled with insepic plasma	Rare *orthic sesquioxidic concretions*	Rare *inherited sesquioxidic nodules*	
	Skeleton grains: very rare quartz silt	Abundant *sedimentary relicts* (clay pellets)	*Skew-plane sequans* (red phase)	*Grey-green isotubules*	*Striotubules*
35.46	*Plasma fabric:* lattisepic, in places insepic trending to strial	Very minor quartz silt in lattisepic to mosepic plasma		S-matrix: masepic to insepic plasma with abundant quartz silt *Pedological features:* carbonaceous material	
	Skeleton grains: moderately abundant quartz and chert	*Anastomosing tubules*		*Sesquioxidic concretions*	
35.76	*Plasma fabric:* lattisepic unistrial	*S-matrix:* inundulic plasma *Pedological features:* large skew-plane sesquans			

and are formed of sesquioxidic nodules, isotubules, and void cutans in a brown s-matrix. The grey s-matrix consists of translocated material filling interstices between the brown pedorelicts, and the diffuse nature of the border between the two phases indicates that the pedorelicts are orthic.

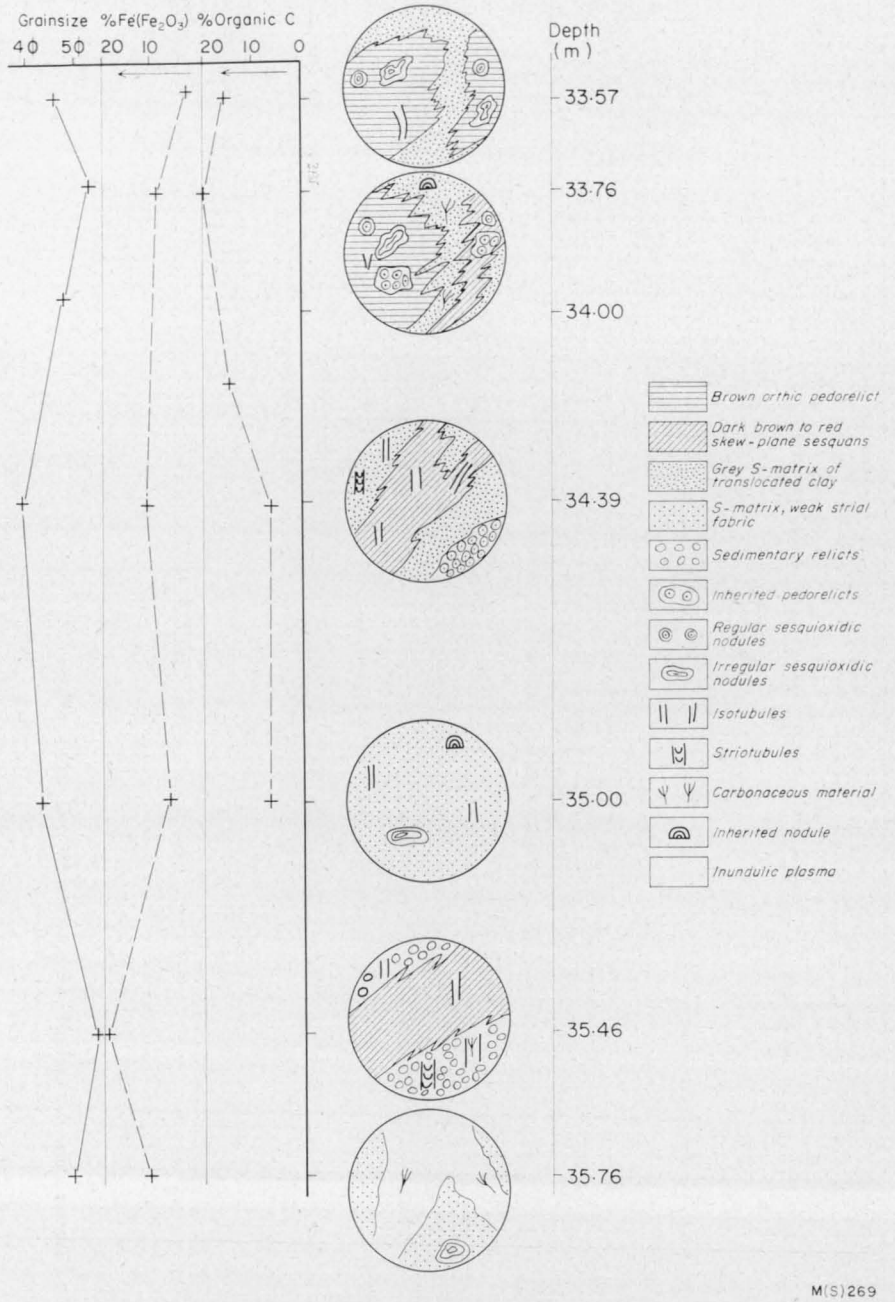


Fig. 36. Graphic log of fabric and compositional changes in Triassic soil profiles. Based on core from BMR Mount Coolon 7.

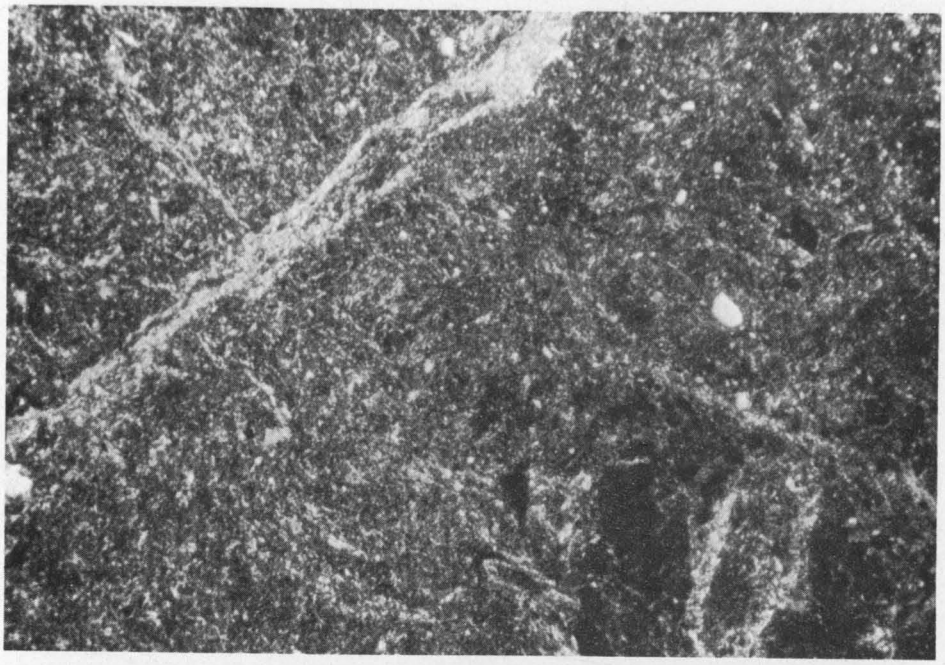


Fig. 37. Fabric of mudstone at 33.57 m in BMR Mount Coolon 7. On the left, the grey s-matrix with a masepic fabric is cut by a channel argillan (light grey diagonal zone). The darker area on the right consists of dark brown orthic pedorelicts embedded in a brown s-matrix. Crossed polarizers, x 40.

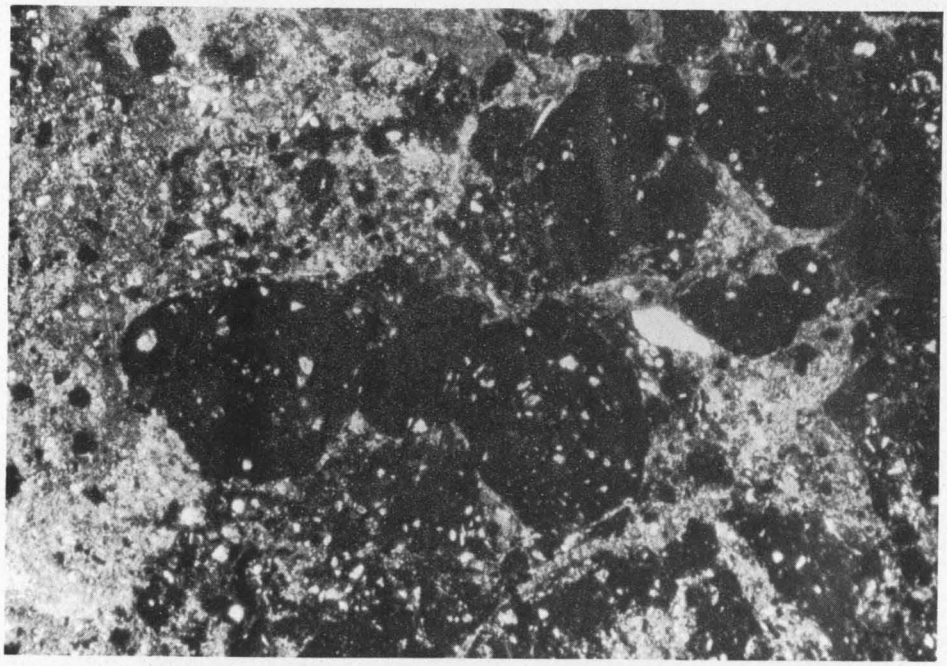


Fig. 38. Mudstone from 33.76 m in BMR Mount Coolon 7 showing inherited pedorelicts composed of aggregates of sesquioxidic nodules. Plane polarized light, x 40.

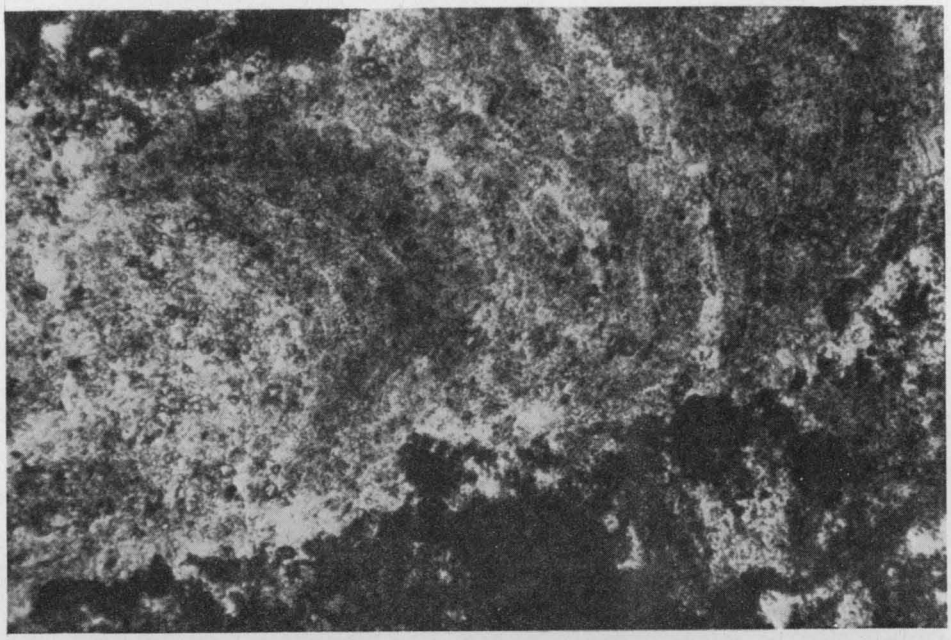


Fig. 39. A striotubule in mudstone of the Glenidal Formation. Sample from BMR Mount Coolon 7 at 33.76 m. Plane polarized light, x 125.

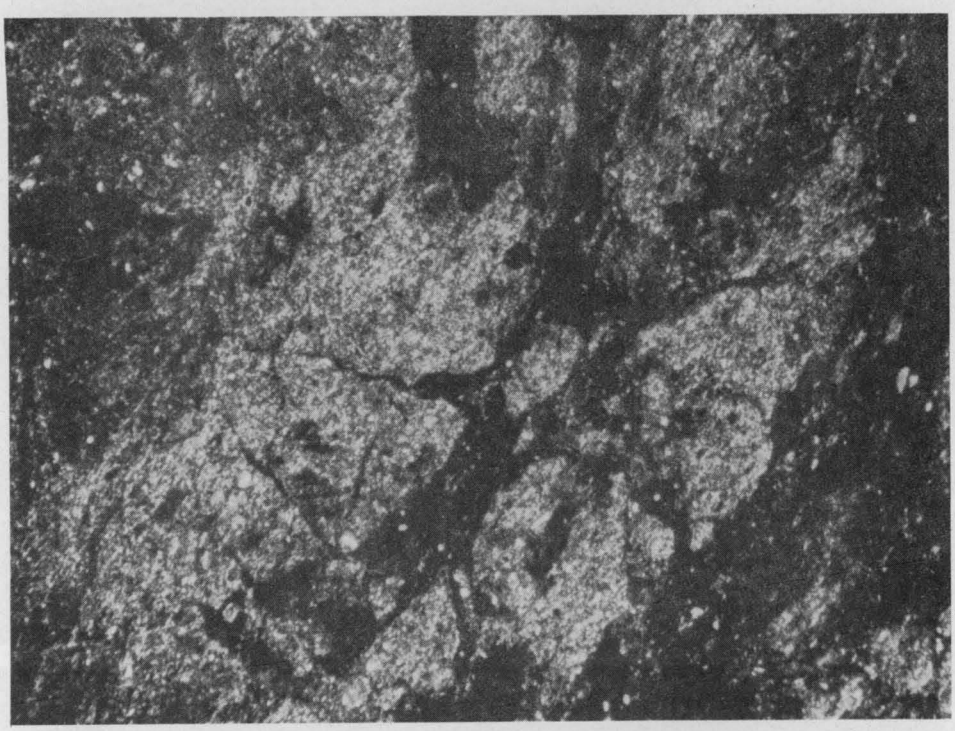


Fig. 40. At 34.39 m in Mount Coolon 7 the mudstone consists predominantly of red skew-plane sequans (dark areas) set in a yellowish green s-matrix (light grey) with a lattisepic fabric. Cross polarizers, x 40.

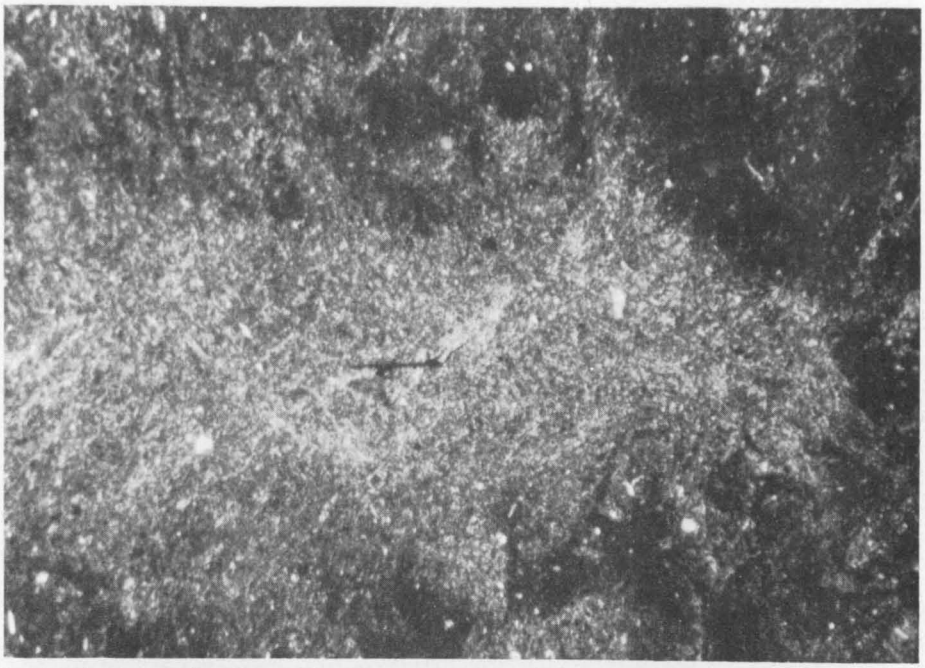


Fig. 41. An isotubule filled with yellow-green s-matrix with a lattisepic fabric; a shred of carbonaceous material is also present. The isotubule is surrounded by a diffuse skew-plane sesquan. Mudstone at 34.39 m in BMR Mount Colon 7. Crossed polarizers, x 40.

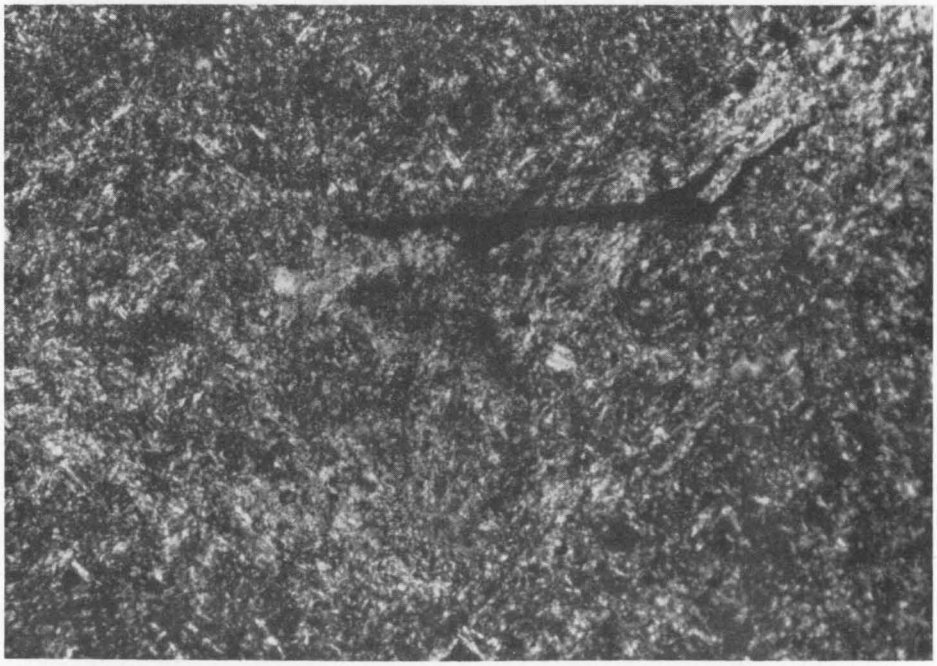


Fig. 42. Enlargement of part of isotubule in Figure 41 showing lattisepic fabric and carbonaceous fragment. Crossed polarizers, x 160.

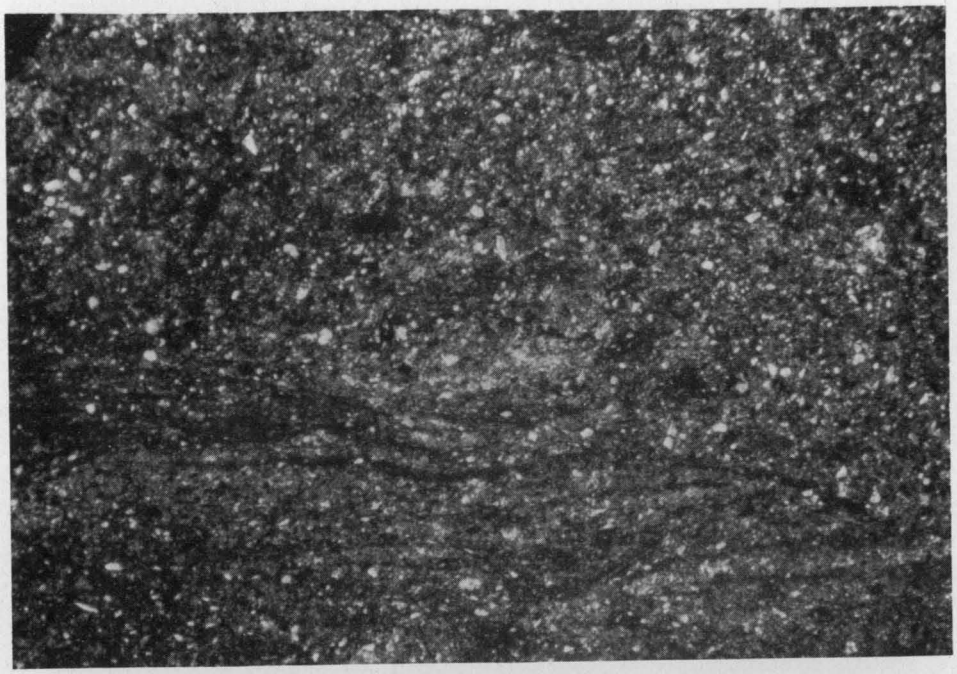


Fig. 43. Faint lamination in red mudstone at 35.00 m in BMR Mount Coolon 7. Crossed polarizers, x 40.

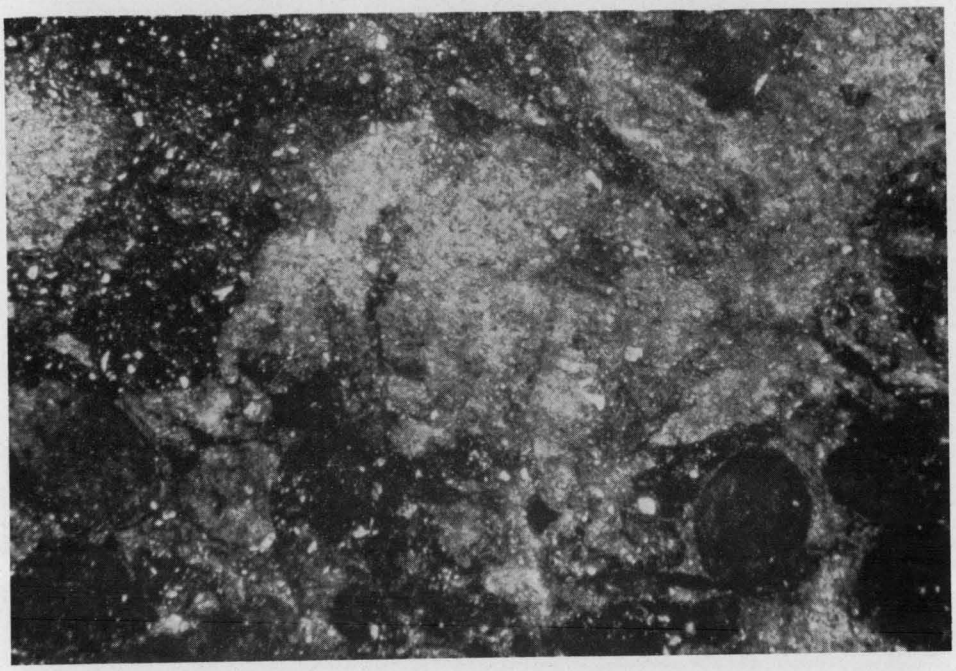


Fig. 44. Mudstone at 35.46 m in BMR Mount Coolon 7 characterized by diffuse red skew-plane sesquans and rounded sedimentary relicts. Plane polarized light, x 40.

A far more complex relationship is indicated by the fabric of the mottled mudstone 19 cm below the first sample (Fig. 38). Roughly the same fabric level is apparent with yellow-brown orthic pedorelicts embedded in a grey s-matrix, but other pedological features present are skew-plane sesquans, cutans, sesquioxidic nodules, and rare striotubules (Fig. 39). The orthic pedorelicts and skew-plane sesquans are themselves complex. The most important feature in the orthic pedorelicts is the presence of inherited pedorelicts composed of aggregates of sesquioxidic nodules and concretions in a brown masepic plasma. The orthic pedorelicts also have glaebules of sesquioxidic nodules and papules, which were presumably derived from the disintegration of the inherited pedorelicts in situ, or in the provenance area. The skew-plane sesquans, which consist essentially of anastomosing veins of dark red-brown s-matrix, also contain pedorelicts and sesquioxidic nodules, but not to the same extent as in the orthic pedorelict phase. The s-matrix is the dominant constituent of the sesquans; it differs from the grey s-matrix in that it contains an abundance of silt-size skeleton grains and ironstained plasma.

The grey s-matrix surrounding the orthic pedorelicts is a translocated phase like the grey s-matrix of the topmost sample. It occupies relatively broad channels in the originally granular parent material. The dark brown skew-plane sesquans were also formed by translocation of material, but this was secondary to the movement of the s-matrix, and from a very different source judging by the abundance of silt and iron oxides.

Skew-plane sesquans predominate in the section 63 cm below the second sample, but they are red rather than dark brown, and are composed mainly of red plasma (Fig. 40). The main yellowish green s-matrix with a lattisepic plasmic fabric also contains (a) numerous isotubules and striotubules filled with grey plasma and carbonaceous material; (b) yellow-brown granular rounded sedimentary relicts, which are partly replaced by iron oxide; and (c) scattered brown papules. The sedimentary relicts consist of multiple diffuse sesquioxidic nodules cut by isotubules and striotubules (Figs 41, 42). They appear to belong to the same generation of tubules filled with grey plasmic material as in the main yellow-green s-matrix.

The same type of tubules are almost the only pedological features to be seen in the faintly laminated and evenly coloured reddish mudstone (Fig. 43) 61 m below the third sample (35.00 m). Rare orthic sesquioxidic concretions and inherited sesquioxidic nodules are also present. The s-matrix at this level consists of numerous skeleton grains set in an insepic weakly strial brown plasma, which is apparently composed of clay pigmented with ferric oxide.

Within the next 46 cm down the sequence, however, there is a reversion to the complex fabric so prominent near the top of the first interval. The mudstone at this level (35.46 m) is strongly mottled red and yellow-green. The red colour is mainly due to the abundance of skew-plane sesquans and small rounded sedimentary relicts (clay pellets). The abundant granular clay pellet parent material (Fig. 44), which is surrounded by a little lattisepic to skel-insepic plasma, is cut by a number of isotubules and striotubules filled with grey-green masepic to insepic plasma, carbonaceous material, and abundant quartz silt. The tubules are commonly surrounded by sesquans. Either the iron-bearing solutions used the channels formed by the tubules, or the organic activity responsible for the formation of the tubules resulted in the precipitation of iron oxide. The clay pellets are slightly flattened spheres, averaging 0.5 mm in diameter, composed of clay and a little iron oxide. They contain very few skeleton grains.

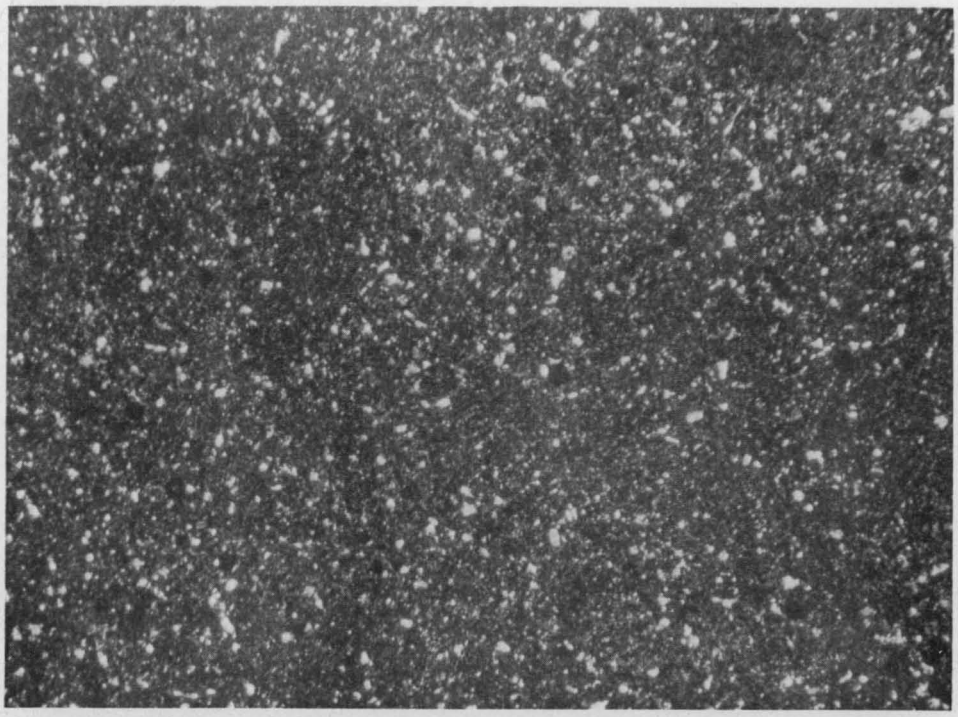


Fig. 45. Mudstone at 35.76 m in BMR Mount Coolon 7 with an inundulic plasmic fabric. Plane polarized light, x 40.

The pelletal parent material is not present 30 cm below this level, and the mottled red and green mudstone shows less pedogenic alteration. A faint sedimentary lamination is evident in part of the s-matrix. The yellow-brown lattisepic s-matrix with moderately abundant silt-size grains of quartz and chert is cut by large anastomosing tubules filled with grey inundulic plasma (Fig. 45). The inundulic fabric was formed by the concentration of amorphous iron oxides. Skew-plane sesquans are common, especially within the tubules.

From these observations, which are summarized in Figure 36, it is clear that the core is composed of a bedded sedimentary sequence. Lamination is faint, but reasonably clear in one sample, and faintly preserved in another. The changes in grainsize of the parent material confirm the bedded nature of the deposit. It is also clear that much of the lamination has been disrupted by movement of clay along channels created by organic activity, and through voids in the porous granular parent material. There is also some evidence of the movement of iron, generally after the movement of clay, along the same channelways, and also by diffusion through the s-matrix to form sesquioxidic concretions and nodules, or in particular micro-environments such as around tubules and grains.

As the sequence was originally stratified, it is difficult to recognize which changes in the present vertical profile were the result of post-depositional alteration, but there is little doubt that the sequence from unlaminated mudstone at the top of the core (33.57 m) to laminated mudstone 1.4 m below the top (35.00 m) represents a buried soil profile. There is another obvious change below this level, and the two samples described could be part of a second profile.

In the upper soil profile, in addition to the changes in lamination, there is moderate differentiation of the profile with depth. The fabric and grainsize analyses reveal a distinct concentration of grey translocated clay in the top two samples. From the 33.76-m level there is a decrease in the proportion of clay accompanied by a downwards decrease in the degree of plasmic orientation of the main s-matrix phase, from masepic at the top to insepic nearer the base. Brewer (1964, p. 339) has suggested that a masepic fabric can be produced by plastic flow, and thus the decrease in plasmic orientation probably reflects a decrease in the degree of translocation. The fabric analysis also suggests an independent increase downwards of mobilized iron oxide within the uppermost three samples, but not in the lowest or fourth sample (35.00 m), and chemical analysis (Table 12) confirms that there is a depletion of total iron in the topmost sample. Chemical analysis also shows a depletion of organic carbon below the level at 33.76 m (Table 12), and confirms the evidence from fabric analysis of the enrichment in organic matter at about this level by illuviation of clay containing shreds of plant material from above. Although the total proportion of organic carbon is lower than that normally found in modern soils, it is about the same as the amount recorded in buried soil profiles. The difference is probably due to degradation of organic matter with time under oxidizing conditions.

Insufficient data are available on the lower interval (35.00-35.76 m) to distinguish another buried profile, but the presence of highly complex 'fossil' soil material near the top (35.46 m), and of a zone characterized by a high concentration of amorphous iron oxide and faint relict bedding near the base, suggests that it is another soil profile. Furthermore, the upper sample, like the second topmost sample of the first profile, contains an abundance of carbonaceous material.

One of the most important facts to emerge from the examination of the core concerns the nature of the parent material on which the soil was formed. In its least altered form, as in the sample at 35.00 m, at least some of the parent material consisted of laminated silty mud, which probably contained iron oxide as an amorphous plasma. Higher in the profile, however, inherited pedorelicts consisting of sesquioxidic nodules and concretions are common, and it is not unlikely that these were derived from an earlier formed soil with a profile dominated by nodular sesquioxides, such as a lateritic podsolic (Stace et al., 1968, p. 345).

Expedition Sandstone

Rocks finer than very fine sand are rare in the Expedition Sandstone, and where present they generally consist of thin lenses of light grey or brown finely laminated siltstone or muddy siltstone. In thin section they have a strong unistrial fabric, but there is no indication of pedogenic alteration. The only exception is a red siltstone at the top of the formation in the southwestern area, in which there has been substantial movement of clay and iron oxide within vertical channels. The clay mineral assemblages in samples from both the southwestern and southeastern parts of the basin consist of mica and kaolinite (Table 11). The coarser silt-size grains consist of quartz and chert with rare feldspar.

Origin of Lutite Suites

Rewan Group

Despite differences in colour and areal distribution, the mudstones and siltstones of the Rewan Group vary little in mineralogical composition, except in the

proportion of hematite and quartz. The clay minerals consist of mica and kaolinite, together with a mixed-layer clay composed predominantly of smectite (Table 11), and in one case of smectite itself. The silt-size grains consist of stable minerals such as quartz and chert and grains of more labile minerals such as plagioclase, epidote, apatite, and biotite. By comparison with the minerals in the siltstone of the Expedition Sandstone, the Rewan Group is composed of much more labile minerals, similar to those in the sandstone with which it is interbedded, and it is therefore unlikely that these sediments were derived from a highly weathered source area.

The red mudstone contains more total iron and ferric oxide than the associated yellowish green and yellowish brown siltstones (Table 12). A similar relationship has been established for a number of redbed sequences by van Houten (1961), who has also shown that in any pair of samples from the same formation, the red contains more ferric oxide than the non-red. Jones (1965) has pointed out that the discrepancy could be accounted for by assuming reduction of the ferric iron in the non-redbeds and the subsequent removal in solution of the soluble ferrous iron. This is unlikely in the Rewan Group because each rock type is generally laminated, albeit only faintly in some localities, so post-depositional pedogenesis has not been substantial and there is no evidence of translocation of significant amounts of iron. There are a number of exceptions: (a) in the coarse non-laminated mottled siltstone there is strong evidence of illuviation and segregation of iron oxide; and (b) in the vicinity of small joints in the red mudstone sequences where recent leaching has resulted in the reduction and translocation of iron.

From the evidence in thin sections, the confirmatory X-ray diffractometer analysis of material finer than 2 microns, the main factor controlling the colour of the laminated red and green mudstone is the proportion of finely divided hematite. The proportion of hematite present is dependent on grainsize, with a marked concentration in the finest sediment. Robb (1949) maintained that the hematite pigment of some redbeds was derived from the alteration of biotite at the site of deposition, and Walker (1967) also concluded that the redbeds in the Pliocene-Recent deposits of the Sonoran Desert and the late Palaeozoic deposits of Colorado were formed by intrastratal alteration of iron-bearing detrital grains, particularly iron silicates such as hornblende and biotite. This process is unlikely to have been the cause of the pigmentation of the red mudstone in the Rewan Group, because there is no evidence of in situ production of iron oxide by the alteration of silicates. Furthermore, the sandstone interbedded with the red mudstone contains biotite, epidote, and other labile constituents that show no sign of replacement by iron oxide. Thus it is believed that the iron was transported as exceedingly fine, possibly colloidal, material, and that it was deposited with the clay fraction of the sediment. In the laminated mudstone and siltstone there is no evidence of the movement of iron after deposition of the sediment, and the differences in the concentration of hematite are due to differences in the composition of the sediment. The question of where the finely divided hematite is formed—in the source or the depositional area —still remains.

From thermodynamic calculations, Schmalz (1968) has demonstrated that theoretically hematite will only form in the presence of pure water, at relative humidities of less than 60 percent, and he concluded that except where it is present in the late members of an evaporite sequence, or where precipitated by organic agencies, hematite must be regarded as a detrital mineral formed by subaerial weathering. Langmuir (1971) states that precipitation from waters formed by the

oxidation and hydrolysis of ferrous iron minerals, which are substantially supersaturated with respect to hematite, generally produces a host of relatively unstable oxyhydroxide phases including amorphous material and fine-grained goethite. These form before hematite because of their relatively low nucleation energies, but hematite is eventually formed by long-term aging of the amorphous material, or by dehydration. Schmalz (1968) has demonstrated that it is theoretically unlikely that hematite will form below the water-table, and he postulated that redbeds are formed by a combination of two conditions: (a) a wet and preferably warm climate in which iron may be released from the parent material by chemical weathering; and (b) a dry climate in which the primary weathering products may be dehydrated. He went on to conclude that these conditions could be satisfied by a source area with markedly seasonal precipitation or, alternatively, by a combination of a humid source area and a relatively dry depositional area.

In order to test this interpretation, which is based primarily on thermodynamics and laboratory data, it is necessary to consider the nature of iron in modern soils. That markedly seasonal precipitation is required for the production of hematite in the source area is supported by Sherman (1952) who noted that limonite is the oxyhydroxide present in continuously wet Hawaiian soils. On the other hand Papadakis (1969) concluded from the work of Pedro (1964) that when soil is continuously wet no ferruginization takes place because the iron combines with silica and bases to form a trioctahedric ferromagnesian smectite. Papadakis (1969) has recognized three cases where iron oxides are produced in the soil profile by weathering agencies: (a) allitic weathering under aerobic conditions such as exist in tropical regions, where much ferric iron is released to form concretions and red coatings on soil grains (ferruginous soils); (b) siallitic weathering, where the soil dries out thoroughly from time to time and where it is reddened (rubified) by the production of fine red crystallites of dehydrated iron (cinnamonic soils); and (c) podsolic weathering in which, because the soil is rich in fulvic acids, it contains a brown mixture of finely flocculated iron and organic matter (brunisolic soils). Thus in the case of allitic and siallitic weathering dehydrated ferric oxides will accumulate in the soil and be available for transportation and deposition in the sedimentary basin. The erosion of brunisolic soils would presumably release a brown ferric oxide gel as reported from the alluvium of the lower Nile (van Houten, 1961, p. 110) or fine-grained goethite, both of which could be deposited with the clay fraction in the basin of deposition.

In the case of the Rewan Group, the source area was not subjected to allitic weathering, because the normal products of this process abound in 1:1 clays such as kaolinite, which is present but by no means predominant in the mudstone. Both podsolic and cinnamonic weathering produce 2:1 clays, but they differ in the way in which the iron and clay are distributed in the profile. Brunisolic soils are characterized by moderate to extreme profile differentiation, and in extreme cases iron pans are formed in an alluvial horizon (Papadakis, 1969, p. 14). On the other hand, the iron liberated by siallitic weathering is normally distributed throughout the profile in close association with clay, and the profile shows very little differentiation. One example of this type of profile is the Australian brown earth (Stace et al., 1968, p. 239). Erosion of this type of profile is considered to be the most likely source of the sediment which was transported and laid down to form the thick red mudstones of the Rewan Group.

Cinnamonic regions include areas with a Mediterranean climate (dry summer, subtropical) and arid areas where less iron is released and rubification is not as

intense. It is unlikely that the provenance of the red mudstone in the Rewan Group was an arid area, where there was a minimum of chemical weathering and physical removal of material, and it is much more likely that the provenance area had at least a moderate relief that enabled the soil to dry out thoroughly. It is therefore concluded that the source of the red mudstone in the Rewan Group, and indeed the rest of the sediment, was a well elevated region with a Mediterranean climate, in which rubification of soil material was common, and podsolization at a minimum. A summary of conclusions made from petrographic evidence is presented in Table 14.

Glenidal Formation

In terms of environmental analysis red and green mudstone is the most significant rock type in the Glenidal Formation, because the other types of mudstone and siltstone could have been deposited in a number of environments. The 'fossil' soil found in one of the cores from the northern part of the basin is characterized by moderate profile differentiation, which involved leaching of the uppermost organic-rich horizon and illuviation of clay and iron. The constant association of carbonaceous material and illuviated clay reflects the action of humic and fulvic acids during the development of the profile, which appears to be similar to the yellow, brown, or red podsolic soils of Stace et al. (1968, pp. 316-44). These soils are characterized by moderately differentiated profiles consisting of a bleached subsurface horizon overlying a zone richer in sesquioxides relative to those above and below; such soils are formed in humid temperature to subtropical climates.

The inherited pedorelicts within the 'fossil' soil must have been derived from a weathering profile in which nodular or pisolitic sesquioxides predominated. The formation of these structures requires a humid climate with a seasonal rainfall, and a fluctuating water-table, which results in the concentration of sesquioxides and the removal of bases and silica. In a tropical climate this induces allitic weathering and the production of kaolinitic clays. The composition of the clay minerals in the soil profile, however, is similar to that of surface samples, which consist of mica, kaolinite, and a mixed-layer clay with a swelling compound, presumably smectite. This assemblage is more akin to the clays reported in Australian lateritic podsolic soils (Stace et al., 1968, pp. 350-59), which are widely distributed in subhumid to humid areas all over Australia. It is therefore unlikely that the source area was subjected to strong allitic weathering, or that the sesquioxides were formed in a laterite. It is much more likely that in both the provenance area and at the depositional site podsolic weathering was predominant under the influence of a subhumid to humid temperate to subtropical climate.

Arenite

Classification

Much has been written on the classification and nomenclature of arenites, and yet there is still no generally accepted scheme. The basic problem is that insufficient data have been assembled and analysed in such a way as to reveal morphologically distinct groups which reflect genetic differences. New classifications introduced at this stage with a view to universal application tend to confuse the issue. Thus, neither a review of existing classifications nor the formulation of a radically new method of classification would serve any useful purpose with regard to the present study. Instead, the arenites of the Rewan and Clematis Groups have been grouped

TABLE 14. MAIN PETROGRAPHIC CHARACTERISTICS OF LUTITES

	Sagittarius Sandstone	*Arcadia Formation*	*Glenidal Formation*	*Expedition Sandstone*
Nature of surface cover in provenance area	Generally thin weathering crust—minimal soil cover—minor silicification of soil	Cinnamonic soils	Lateritic podsolic soils (fabric and mineral composition of subsurface samples)	Strongly leached mantle. (Kaolinite and mica only clay minerals)
Rate of erosion in provenance area	Very rapid (immature mineralogy composition)	Rapid (labile constituents), but rate of erosion did not outstrip soil formation)	Moderate (mixture of labile and stable minerals)	Probably slow (strong leaching over long period of time)
Rate of sedimentation	Very rapid (no development of soil profiles)	Rapid (minor soil profile development)	Moderate to slow (development of soil profiles)	
Climate in provenance area	Humid, temperate, possibly Mediterranean in part (thin redbeds)	Humid, temperate (Mediterranean)	Humid, temperate to sub-tropical	
Climate in depositional area			Subhumid to humid, temperate to sub-tropical	

into six broad categories on the basis of divisions on a QRF (quartz:rock fragment: feldspar) plot which reflect natural groups within the Triassic sequence.

The arenites of the Rewan and Clematis Groups are sandstones in the sense of Packham (1954) because they are characterized by cross-stratification and not graded bedding. Quartz, rock fragments, and feldspar have been selected as the basis for subdivision because (a) they are the basic components of the sandstone framework which forms the bulk of most types of sandstone; and (b) they are the most commonly used parameters for classification. Chert has been included with rock fragment because in many of the Triassic rocks the fragments of fine-grained volcanic rock are almost indistinguishable from chert, and indeed some of the indeterminate grains recorded as chert probably represent fragments of volcanic rock. Mica and heavy minerals have not been included in the framework for the purpose of calculation of the QRF plot. The choice of only three end members is open to some criticism because it ignores other important components, such as the type of feldspar present. The choice is in fact one of convenience until such time as analysis of a large number of sandstone samples indicates the ideal parameters necessary to define natural populations.

The QRF plot (Fig. 46), based on modal analyses of about 180 samples from both groups (Appendix 2), reveals a concentration of points within the 90 to 100 percent quartz field, and in particular on the zero percent feldspar line. These rocks are grouped together to form the quartz sandstone suite. Samples containing a little feldspar and over 90 percent quartz are grouped into the quartzose sandstone suite. The plot also reveals some concentration of points between 75 and 90 percent quartz, and samples of this type, which contain varying amounts of labile constituents, are regarded as sublabile sandstone. This nomenclature and classification is a modification of those of Packham (1954) and Crook (1960), who classified sandstone with less than 75 percent quartz as labile sandstone. The QRF plot (Fig. 46), however, reveals a basic subdivision into two main fields at about 53 percent quartz, so the suite of sandstones containing 53 to 75 percent quartz has been called semi-labile, and the suite with 0 to 53 percent quartz is described as lithic; a feldspatholithic suite could be recognized as well. It was also found that there is no gradation from the semi-labile suite into more lithic varieties with the same quartz content.

Description of Sandstone Suites

A summary of petrographic observations made on the sandstone suites is presented in Table 15.

Quartz sandstone suite

The quartz sandstone suite comprises moderately to poorly sorted sandstones ranging from fine to very coarse, and is characterized by the high content of framework quartz and the lack of feldspar. This type of sandstone is found only in the Clematis Group, particularly in the Glenidal Formation and the Expedition Sandstone in the southwestern area; it is also present in the Expedition Sandstone in the central and northern parts of the basin.

The quartz grains, which are the most common constituent of this type of sandstone, are predominantly angular to subangular, although some of the largest grains of coarse and very coarse sand-size are subrounded. In all areas, the majority

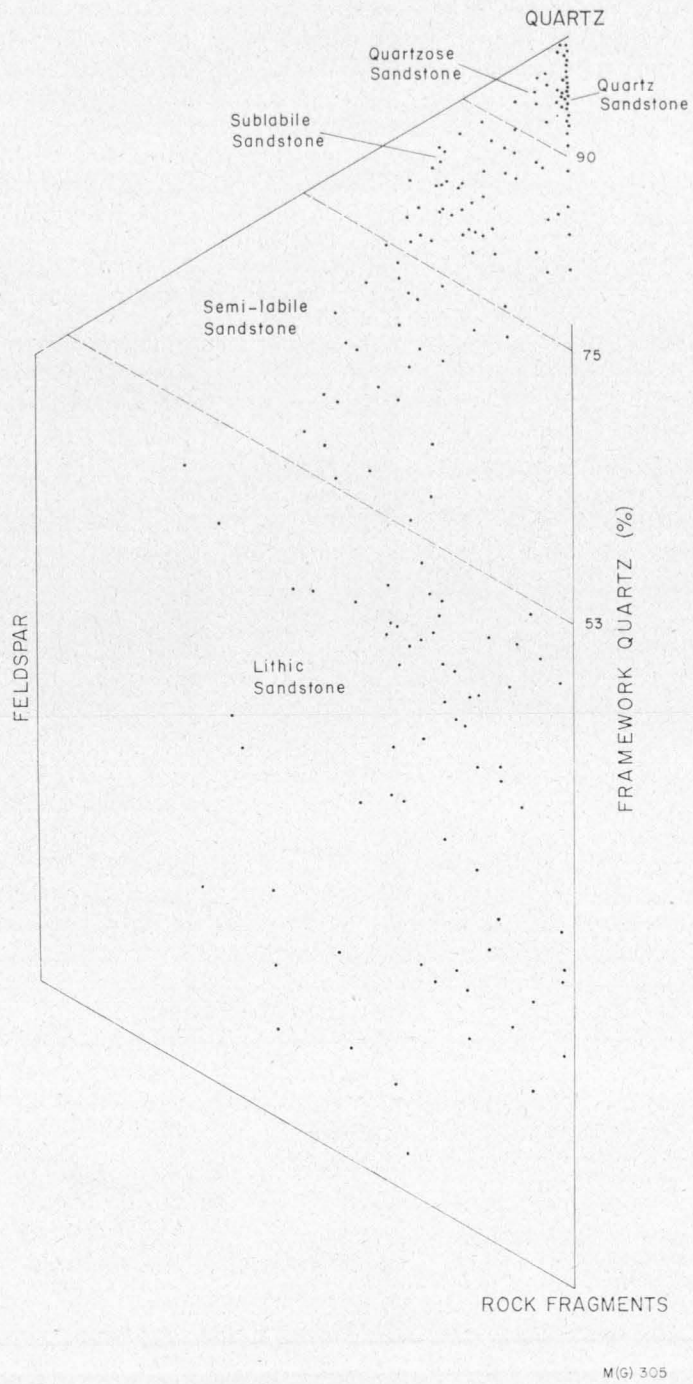


Fig. 46. Framework composition (QRF plot) of sandstones of the Rewan and Clematis Groups.

of the grains are monocrystalline and have an undulose extinction and moderately abundant vacuoles. The proportion of non-undulose monocrystalline and polycrystalline grains varies from sample to sample, but seldom exceeds about 20 percent of the total framework quartz. The components of most of the polycrystalline grains are equant, but grains with strongly elongate fabrics are present in the southwestern area. The medium to coarse sand-size polycrystalline grains generally have more than six components, which according to Blatt (1967) indicates derivation from a metamorphic rather than a plutonic source. The polycrystalline grains with a strongly elongate fabric, which are present in the southwestern part of the basin, and those with a bimodal size distribution of internal components, are also reasonably reliable metamorphic provenance indicators.

The sand-size lithic fragments that form up to a maximum of 10 percent of the framework are exclusively quartz-rich, and consist mainly of chert and some quartz-mica schist. Much of the chert is of indeterminate origin, and is composed of a mosaic of anhedral interlocking quartz crystals less than 10 microns in diameter. The fabric is generally equigranular, but markedly inequigranular fragments are common in the northern area. The faint flow-banding or lamination of the quartz in the northern area suggests a volcanic and minor low-grade metamorphic provenance. Fragments of schist, composed of intergrowths of quartz and mica, with varying degrees of elongation of the quartz crystals, are present in the southwestern area.

Large detrital flakes of mica are common in some of the sandstones of the quartz sandstone suite, but are absent in others. They generally consist of colourless muscovite or paragonite. Biotite is relatively uncommon, and when present is weathered.

The total proportion of matrix in the suite ranges from 4 to 24 percent, and averages 12 percent. The matrix commonly has a silasepic or weakly insepic plasmic fabric. The silasepic fabric is the result of deposition of fine-grained detrital material with the coarser framework grains, and little can be inferred from its presence. In some cases, however, there is a greater degree of plasma orientation and separation. In some of the coarse sandstone the pores are filled with matrix with a skel-insepic plasmic fabric or a bi-masepic fabric grading into a vosepic fabric. Some of the yellow-brown kaolinitic clay matrix in the southwestern part of the basin consists of channel argillans with a strong continuous orientation. The sepic fabrics are characteristic of those formed either by the swelling and shrinking of clay due to wetting and drying, as in the case of the bi-masepic and vosepic fabrics (Brewer, 1964), or by the illuviation of clay through channels formed by interconnected voids, as in the case of the strongly oriented channel cutans. These processes are characteristic of normal pedogenesis.

Kaolinite was found to be the most common clay mineral in the —2 micron fraction of three of the four samples analyzed (Table 16). Mica predominated in the fourth, and mixed-layer clays, predominantly mica, are present in all samples.

Quartz overgrowths on quartz grains are a common cementing phase in the quartz sandstone suite. The overgrowths consist of anhedral extensions of surfaces into voids or, more rarely, euhedral single crystals extending into voids. The overgrowths, which form up to 6 percent of the rock, are usually in optical continuity with the original grains, from which they can be distinguished by the paucity of inclusions. The age of the silicification is unknown. Stylolites are present in many of the well cemented sandstones, and silicification was presumably related to the

TABLE 15. MAIN PETROGRAPHIC CHARACTERISTICS OF SANDSTONE SUITES

	Quartz Sandstone Suite	*Quartzose Sandstone Suite*	*Sublabile Sandstone Suite*	*Semilabile Sandstone Suite*	*Labile Sandstone Suite*
Distribution	Clematis Group. Southwestern, central, and northern areas	Clematis Group. Northern and central areas. Subsurface samples from Glenhaughton No. 1	Clematis Group, Northern central, and southwestern areas	(a) Dawson Range Sandstone; (b) upper part of Sagittarius Sandstone in northern area; (c) minor occurrences in rest of Clematis Group	Rewan Group. All areas
Quartz	Angular to subangular, predominantly monocrystalline undulose	Angular to subangular, predominantly monocrystalline undulose	Angular to subangular, in places rounded. Monocrystalline undulose more common than polycrystalline	Angular to subangular, monocrystalline undulose	Angular to subangular, monocrystalline undulose dominant
Rock fragments	Exclusively quartz-rich, mainly chert, minor quartz-mica schist	Exclusively quartz-rich, mainly chert, minor quartz-mica schist	Chert, quartz-mica schist, microperthite, rare volcanic	Chert, some sedimentary and plutonic and volcanic	Mixture of volcanic, metamorphic, sedimentary, and plutonic rocks
Feldspar	—	Alkali feldspar subangular to round	Alkali feldspar, minor plagioclase	(a) Alkali feldspar replaced by halloysite; (b) alkali feldspar and plagioclase	Plagioclase, alkali feldspar
Heavy minerals	Tourmaline, zircon	Tourmaline, zircon	Epidote, tourmaline, zircon	Epidote	Epidote, zircon, tourmaline, garnet, apatite, magnetite, pyroxene
Mica	Muscovite or paragonite flakes	Muscovite	Muscovite, minor biotite	Muscovite? biotite rare	Biotite common, but weathered
Matrix	Mainly silasepic fabric developed during sedimentation, but some evidence of illuviated clay	Recrystallized clay; minor omnisepic cryptocrystalline	Complex fabrics; minor illuviation, some recrystallization	(a) Recrystallized clay; (b) some derivation of chloritic matrix	Complex clay matrix, no evidence of pedogenesis
Clay minerals	Kaolinite, mica, minor mixed layer predominantly mica	Mica, mixed layer predominantly mica, kaolinite, smectite	Kaolinite, mica, smectite, mixed layer predominantly smectite	(a) Kaolinite; mica, minor chlorite; (b) chlorite, smectite	Smectite with minor kaolinite, or mixed layer clays predominantly of smectite; chlorite, vermiculite
Cement	Quartz overgrowths, hematite, minor calcite	Quartz overgrowths, minor hematite	Quartz overgrowths, chalcedony, hematite common —illuviation and replacement fabrics; minor carbonate	(a) Siderite, halloysite, kaolinite; (b) hematite, quartz, calcite, chlorite	Chlorite, calcite

migration of silica away from points of high pressure at grain contacts to areas of low pressure, such as voids, particularly during compaction of the rocks. Some of the voids that are partly lined with silica overgrowths were subsequently filled with clay matrix.

Hematite or some form of hydrated iron oxide is a common constituent of the quartz sandstone suite, and may form up to 17 percent of the rock. The iron oxide occurs as irregular patches replacing the matrix and clay minerals, or as a simple filling in the voids. In at least one sample the hematite was deposited after silicification as it forms a coating on the secondary quartz.

A little calcite occurs as small anhedral intercalary crystals within the matrix in three samples. Poorly developed calcite crystals are common in many soil materials, but its origin and time of formation are unknown.

There is very little evidence of the provenance of the quartz in the quartz sandstone suite. The abundance of monocrystalline undulatory grains indicates that it is unlikely that they were mainly derived from sedimentary, volcanic, or hydrothermal sources. The type of rock fragments found in the northern part of the basin indicates that the small proportion of the detritus was derived from volcanic source rocks. A metamorphic provenance is suggested by type of quartz and rock fragments in all areas, particularly in the southwest. If the source rocks were metamorphic or igneous, the present mineral assemblage, which consists only of the most stable detrital grains and clays, belies the labile nature of the provenance. It is suggested therefore that the quartz sandstones were formed in an environment where the original detritus was subjected to strong chemical weathering in the source area or after the sediment was laid down. In the provenance area, the feldspars were altered to kaolinitic and micaceous clays, which are a characteristic component of the suite, and additional weathering took place during pedogenesis at the site of deposition.

Quartzose sandstone suite

The quartzose sandstone suite comprises sandstones containing over 90 percent framework quartz and a small proportion of feldspar (Fig. 47). This type of sandstone is confined to the Clematis Group in the northern and central areas. It is also present in the subsurface in the southwestern area (Core 2 of Marathon-Continental Glenhaughton No. 1), but not in surface samples. In most respects the suite is the same as the quartz sandstone suite. The quartz grains are predominantly monocrystalline and have undulose extinction; the rock fragments consist predominantly of chert with some quartz-mica schist. The matrix is slightly different, and generally consists of well crystallized clay minerals, and less commonly of cryptocrystalline clay with an omnisepic plasmic fabric. The clay matrix of the three samples examined (Table 16) consists of mixed-layer clays, predominantly mica, together with mica and kaolinite, and rare smectite. Quartz overgrowths and minor hematite are the only cementing phases in the northern and central areas, but sparry carbonate is present in the subsurface samples from the southwestern area.

The feldspar is exclusively orthoclase and microcline. The grains are subangular to round, and generally smaller than the average grainsize of the associated quartz. The grains are generally unaltered, except for the presence of cavities due to slight weathering (Folk, 1968). Some of the cavities are lined with a thin coating of clay. Isolated grains are partly replaced by fine disseminated phyllosilicate flakes, and some are almost entirely replaced by a fine interlocking mass of phyllo-

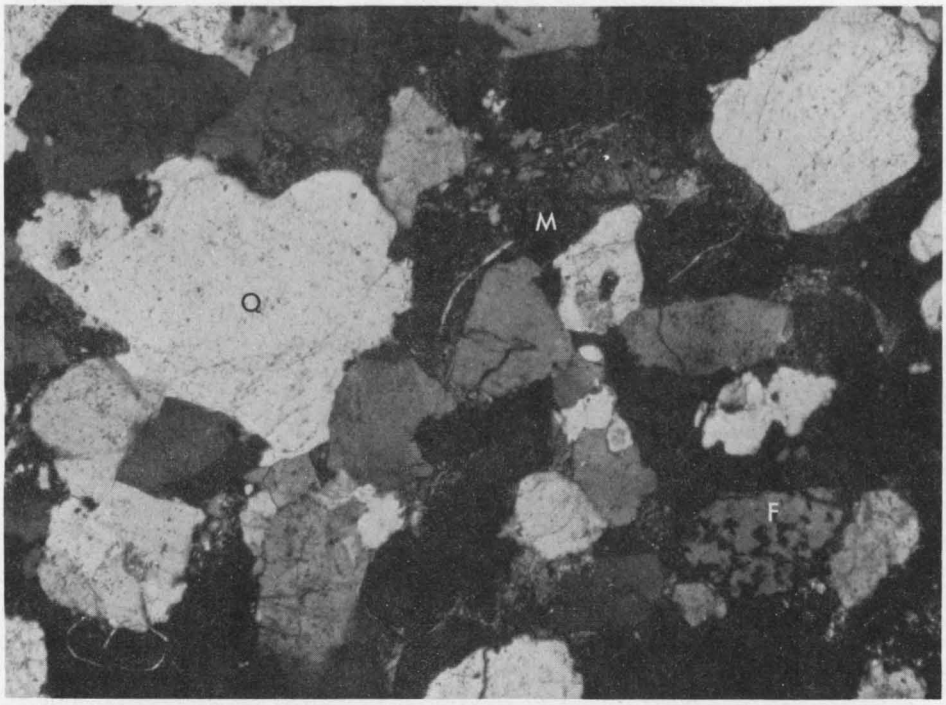


Fig. 47. Typical quartzose sandstone composed mainly of angular quartz (Q) with a moderate amount of overgrowth, and minor alkali feldspar (F) with cavernous weathering, cherty rock fragments, and a clayey matrix (M). Crossed polarizers, x 40.

silicates. These altered fragments are similar to grains of chert or pellets of clay, but the optical continuity of the original feldspar grains has been preserved. Because of their similarity, it is unlikely that the quartzose sandstone suite and the quartz sandstone suite differ radically in origin. The main differences are the presence in the quartzose sandstone of a small amount of alkali feldspar and the absence of post-depositional pedogenesis. The occurrence of feldspar does not indicate a difference in the type of provenance, but rather that a small amount of feldspar escaped destruction in the source and depositional areas.

Sublabile sandstone suite

Sublabile sandstones are found only in the Clematis Group in the northern, central, and southwestern areas. In the north, fine to coarse sublabile sandstones are present in both the Glenidal Formation and Expedition Sandstone; in the central and southwest fine to medium-grained sublabile sandstones are confined to the Glenidal Formation.

In spite of the increase in the proportion of rock fragments in the sublabile suite compared with the quartz sandstone and quartzose sandstone suites there is still little evidence on the provenance of the rock fragments. Quartz-mica schist is the only rock common to all fragments that can be identified, but microperthite and rare fragments of volcanic and sedimentary rocks can be recognized in the Glenidal Formation in the northern part of the basin.

TABLE 16. CLAY MINERALS IN SANDSTONE

Suite	*Sample No.*	*Mica*	*Kaolinite*	*Mixed Layer Mica Predominant*	*Smectite*	*Chlorite*	*Mixed Layer Smectite Predominant*	*Mixed Layer Undifferentiated*	*Vermiculite*
Quartz Sandstone	163	+	++	—	—	—	—	—	—
	177	+	++	—	—	—	—	—	—
	144	++	—	++	—	—	—	—	—
	115	—	++	+	—	—	—	—	—
Quartzose Sandstone	91	+++	—	—	—	—	—	—	—
	139	+	+	++	—	—	—	—	—
	153	+	+	+	+	—	—	—	—
Semilabile Sandstone	109	+	++	—	—	—	—	—	—
	66	+	++	—	—	—	—	—	—
	97	—	—	—	+++	—	—	—	—
	107	+	+	—	—	—	++	—	—
Sublabile Sandstone	73	+	++	—	—	—	—	—	—
	74	+	++	—	—	—	+	—	—
	68	+	++	—	—	—	—	—	—
	76	—	+	—	—	—	—	—	—
	148	—	+	—	—	—	—	++	—
Labile Sandstone	81	—	+	—	—	—	—	+	—
	21	+	+	—	+	—	—	—	—
	2	—	—	—	+++	—	—	—	—
	15	—	—	—	—	—	++	—	—
	12	—	—	—	—	—	—	++	—
	19	—	—	—	+++	—	—	—	—
	5	—	—	—	+++	—	—	—	—
	51	—	—	—	+++	—	—	—	—

+++ abundant; ++ common; + present; — minor.

As in the quartz sandstone and quartzose sandstone suites, the framework quartz grains are angular to subangular, except in the central area, where subrounded grains are common, and monocrystalline grains with undulose extinction predominate over polycrystalline grains.

There is evidence that the constituents forming the sublabile sandstone were subjected to less weathering than those on the quartzose sandstone suite. Unlike sandstone of the quartzose sandstone suite, the sublabile sandstone contains small quantities of weathered biotite, epidote, and plagioclase. Biotite occurs as large partly leached flakes, which commonly range from pale brown to colourless. Epidote occurs as detrital grains, or partly replaces feldspar grains, in the fine and medium-grained sandstone of the Glenidal Formation in the north and southwest. It is not present in either area in the quartzose sandstone of similar grainsize. As the epidote does not replace the matrix in the sublabile sandstone suite it is unlikely that the replacement of feldspar grains was diagenetic. Although the alkali feldspar grains are generally cloudy, the degree of alteration to clay minerals is small.

Of the three samples of clay from the sublabile sandstones analyzed each appears to have had a slightly different weathering history. One contains smectite

only; another contains a mixed-layer clay, predominantly smectite, with minor amounts of mica and kaolinite; the third contains kaolinite and minor mica. The clay of the matrix generally has a complex pattern, and the composition and fabric varies from void to void. Crystic fabrics, characteristic of crystallization in situ, are not uncommon, but samples containing a relatively homogeneous matrix with a sepic fabric are rare. In one sample of the Glenidal Formation from the south-western area there are signs of grain and void cutans within small patches with a silasepic fabric, but there is insufficient evidence to invoke pedogenesis. One sample from the same formation in the north, however, has a relatively homogeneous micaceous matrix with a masepic fabric and an intricate system of channel and grain argillans (Fig. 48); these fabrics can only have been formed by illuviation, although the time of formation is uncertain.

Silica is the most common cementing material; it occurs in the form of quartz overgrowths and, more rarely, as small voids filled with chalcedony. In a number of samples, however, hematite cementation has had a far greater effect on original fabric and mineral assemblage. In some of the hematite-rich laminated samples the distribution of the hematite is closely related to the grainsizes of the laminae, and it appears that it was deposited with the other detrital constituents. Nevertheless, there is considerable evidence of the mobility of hematite, as it is found not only as free grain and void ferrans, but also as a replacement of the matrix and in some cases of feldspar grains, rock fragments, and quartz. A small amount of carbonate cement is present in the only subsurface sample examined.

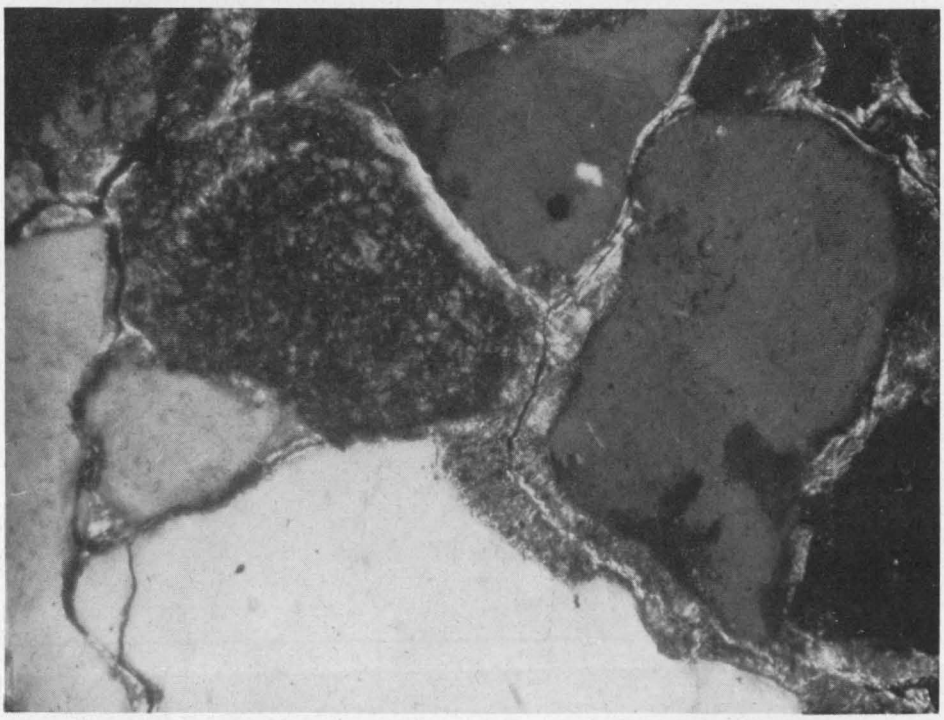


Fig. 48. Sandstone (sample 101) from the Glenidal Formation showing well developed grain and channel argillans. Northern area. Crossed polarizers, x 160.

Semi-labile sandstone suite

Semi-labile sandstones are found in the Dawson Range Sandstone and the upper part of the Sagittarius Sandstone in the northern area.

The samples of Dawson Range Sandstone form a distinctive group with rather special characteristics. Many of the outcrops in the southeast have been subjected to lateritization or some form of deep weathering during the Tertiary, and as a result the surface samples contain far more hematite than the subsurface material. The framework composition and matrix fabric and composition are, however, the same for both types of samples. The framework quartz, like that of the sandstones from other parts of the Clematis Group, is predominantly monocrystalline and has undulose extinction; the grains are generally angular, but there is a sprinkling of rounded, possibly multicyclic, grains. The scattered fragments of sedimentary rocks in the framework were derived from a sedimentary source, but most of the lithic grains consist of chert of indeterminate origin. The presence of grains of microperthite and the abundance of alkali feldspar, indicate the importance of acid plutonic source rocks. The fragments of fine-grained holocrystalline equigranular intermediate or basic rocks were derived from a volcanic source. A little muscovite and occasional grains of strongly leached biotite are present in some of the surface samples; in the subsurface samples the biotite is reasonably fresh.

The clay fraction in the Dawson Range Sandstone consists mainly of kaolinite, with some mica and a little chlorite or vermiculite. The kaolinite appears to fill pore spaces and to have a well developed crystic fabric containing small patches and veins of almost isotropic halloysite. In both surface and subsurface samples many of the large feldspar grains have been replaced by isotropic halloysite, and this type of replacement may have been involved in the 'cavernous' weathering seen in other samples from the Clematis Group. Ross & Kerr (1931, p. 143) have suggested that feldspar can be replaced in situ by halloysite which is subsequently replaced by well crystallized kaolinite. In places the halloysite forms cutans around framework grains embedded in kaolinite, but there is no evidence that pedogenic processes were involved in their formation. On the other hand, the formation of halloysite and kaolinite has been cited as evidence of moderately intense weathering (Loughnan, 1969, p. 93). The replacement of framework and matrix in subsurface samples by small quantities of siderite presumably indicates a change to a non-leaching environment after the weathering stage.

The second group of samples from the semi-labile sandstone suite comes from the upper part of the Sagittarius Sandstone in the northern part of the basin. They differ considerably from the Dawson Range Sandstone samples, and are almost identical with the samples from the rest of the Rewan Group, except that they contain more quartz.

The framework quartz grains are generally angular to subangular, and consist mainly of monocrystalline grains with undulose extinction. The rock fragments include metamorphic, igneous, and sedimentary types. Both alkali feldspar and plagioclase are common, and many of the grains are replaced by epidote, hematite, sericite, quartz, and calcite. The presence of numerous grains of detrital epidote indicates that the replacement of the feldspar by epidote relates to an earlier (pre-Triassic) period of metamorphism. The hematite is related to weathering in the source area because the replacement is restricted to individual grains and does not extend to other parts of the rock. The sericite is also related to weathering in the source of depositional areas. Replacement by quartz and calcite is diagenetic, and

the quartz commonly fills grain fractures caused by compaction. There is no replacement of feldspar by kaolinite or related minerals, and the main clay fraction of the matrix appears to be chlorite and smectite. At least some of the chlorite and smectite was formed by the alteration of ferromagnesian minerals, particularly biotite, which is common in these rocks. The formation of the chloritic matrix involved some movement of clays and the growth of crystals in voids; in places a vo-masepic plasmic fabric has been developed, and in others fibrous chlorite extends from void cutans into the centre of the void.

Lithic sandstone suite

The lithic sandstone suite is found only in the Rewan Group. The samples show a wide range of grainsize and degree of sorting, but all contain numerous lithic fragments in the framework. The suite includes rocks that would be classified as 'feldspatholithic' by Crook (1960).

The nature of the framework constituents in the lithic sandstone (Fig. 49) shows little variation stratigraphically or from area to area. The main difference is in the relative proportion of quartz, feldspar, and rock fragments. The overall character of the framework quartz grains does not differ even from that of the Clematis Group. The grains are generally monocrystalline and have undulose extinction; they are generally angular to subangular, in marked contrast to the subrounded and rounded lithic fragments. The composition of the lithic fragments

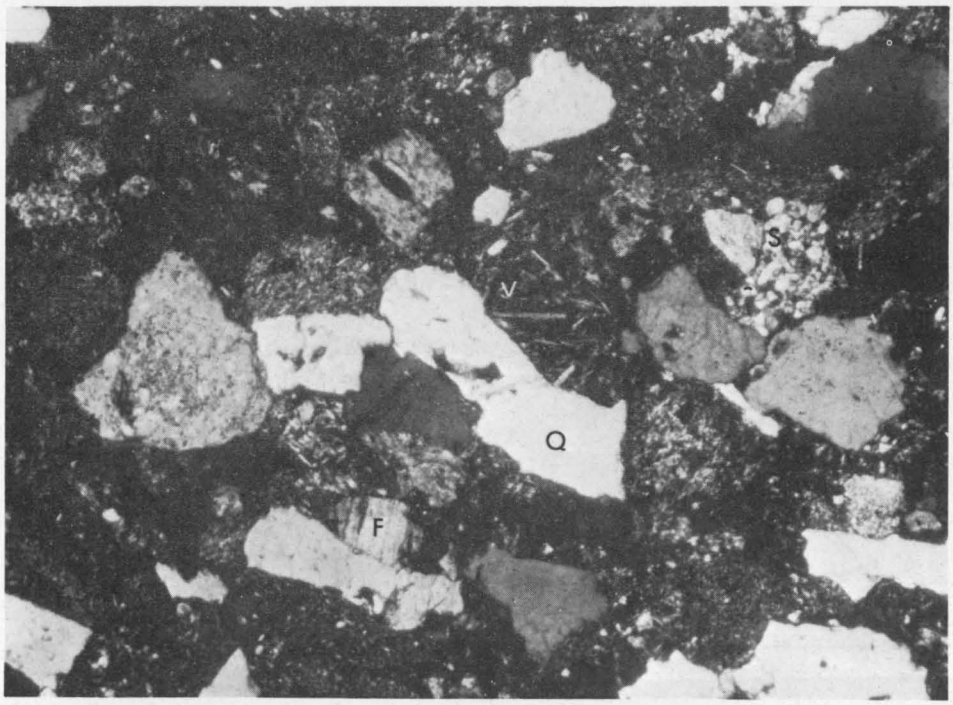


Fig. 49. Lithic sandstone (sample 84) with a framework of quartz (Q), feldspar (F), and fragments of volcanic (V) and sedimentary (S) rocks. Southeastern area. Crossed polarizers, x 40.

varies considerably, but a variety of rock types is invariably present. For example, in the northern part of the basin, outcrop samples contain fragments derived from volcanic, sedimentary, metamorphic, and plutonic source areas. The fragments of volcanic rocks, which are generally weathered and partly replaced by hematite, are of intermediate and acid composition. Many of the inequigranular fragments of slightly banded chert, which are so common in the suite, may also be of volcanic origin. The fragments of sedimentary rocks consist mainly of quartz-rich micaceous siltstone or fine sandstone, some of which have well rounded quartz grains. The fragments of metamorphic rocks include quartz-biotite schist and calc-silicate hornfels. The fragments identified as plutonic rocks are over 1.5 mm in diameter, and consist of coarse-grained equigranular intergrowths of quartz and feldspar, with or without mica. Angular and subangular grains of plagioclase and alkali feldspar are common constituents of the framework. Slight sericitization is common, particularly of the plagioclase, but most of the feldspar grains are not extensively weathered. In contrast, the numerous biotite flakes are almost invariably deeply weathered and in places leached.

In comparison with the sublabile sandstone and quartzose sandstone suites the lithic sandstones contain a wide variety of heavy minerals. Large grains of epidote are common in all parts of the basin. They appear to have been derived from both volcanic and metamorphic rocks, as small fragments of both, partly replaced by epidote, are also present. Small amounts of zircon, tourmaline, and garnet are commonly present, and small euhedral crystals of apatite are widely distributed. The apatite was probably derived from a volcanic source as euhedral grains are common in the sandstone in the underlying coal measures, which are particularly rich in volcanic detritus. Rounded grains of magnetite are concentrated along bedding planes in the upper part of the Rewan Group in the northern and southeastern areas and a little detrital pyroxene occurs in one sample from the southeast.

The matrix in the sandstones of the lithic suite is generally difficult to distinguish from chert and flakes of weathered biotite. In thin section kaolinite appears to be far less common than in the less labile sandstone, and X-ray diffractometer analysis of samples, mainly from the northern area, indicates that the clay consists of smectite with minor kaolinite, or mixed-layer clays composed predominantly of smectite. The samples, particularly those with mixed-layer clays, also contain minor chlorite or vermiculite.

The sandstone fabric provides little evidence of post-depositional pedogenesis. In most of the samples the matrix has no well defined consistent fabric. A weak silasepic or insepic fabric is the only sign of organization of the plasma, and the matrix probably represents fine material deposited with the framework constituents. In some samples, in which the clay matrix is relatively homogeneous throughout the thin section, there is still no direct evidence of pedogenesis. The subsurface samples of the lithic sandstone suite have a skelsepic plasmic fabric caused by compaction: the quartz grains have been embedded in the surface of mud clasts during compaction to form subcutanic plasma separations parallel to their surfaces. Some of the skeletal grains in a few surface samples are surrounded by cutan-like features, but the clay is recrystallized and there is no strong continuous orientation of clay parallel to the grain surface as found in normal pedological argillans. The remaining pore space is filled with secondary quartz or, in some samples, by chlorite fibres that extend outwards from the margin and fill the pore space completely. This type of clay could represent the original matrix that has crystallized during diagenesis, or alternatively a secondary matrix, or cement, formed by the

breakdown in situ of labile constituents such as biotite during weathering. It is difficult to explain the origin of the cutan-like features other than by the crystallization of illuviated clay, but in the absence of other evidence of pedogenesis no firm conclusions can be drawn. In the subsurface samples there is evidence of the generation of secondary chlorite during diagenesis, and it is possible that the cutan-like features in the surface samples also represent a diagenetic phase, although it is difficult to understand why the pore space was nowhere filled.

The most common cement in the lithic sandstone suite is calcite, and in places fine-grained sandstone grades into sandy marlstone. Both at the surface and subsurface, the carbonate cement occurs in the form of clear colourless sparry calcite, which is common throughout the basin, or brown micritic carbonate (electron probe analysis has shown that the calcite has a high iron content), as in the Sagittarius Sandstone in the central area. The sparry calcite cement occupies pore spaces and replaces framework grains. The brown micritic calcite consists either of silt-size and sand-size irregularly shaped pellets, some of which are fibrous (Fig. 50) and others structureless, or silt-size and sand-size pellets with a filamentous fabric (Fig. 51). The brown micrite was formed by the replacement of plant debris, or less probably, by secretions from algae. There is an unequivocal association of structureless brown micritic carbonate with sparry carbonate replacing shreds of carbonaceous material in at least one subsurface sample (Fig. 52), and the structureless and fibrous micritic pellets, which are commonly aligned along bedding planes, may represent the same type of carbonate separated from plant debris. According to Wolf (1965b) the original structure in micritic pellets formed by calcareous algae can be destroyed by diagenetic modification (grain diminution), so some of the structureless micrite may possibly be of algal origin. In the Sagittarius Sandstone, however, there are no other structures indicating derivation of carbonate by algal secretion. The filamentous micrite could be algal, as it is similar to the filamentous micrite figured by Wolf (1965a), but it is just as likely to be carbonaceous plant debris that has been completely replaced by carbonate while retaining some of the original fabric. A similar fabric is preserved in kaolinized stem fragments from the Sydney Basin (Balme & Brooks, 1953).

The only other cementing materials in the lithic sandstones are quartz and chalcedony. Quartz occurs mainly as overgrowths on quartz grains, but it also fills fractures caused by compaction of framework grains, particularly feldspar. Chalcedony has only been found in subsurface samples, in which it occupies small original voids or partly replaces the matrix.

There are two other features of the lithic sandstones in the Sagittarius Sandstone of the central and southwestern areas that are worthy of comment: firstly, the matrix occasionally contains kaolinitic ooliths; and secondly, the sandstone in places is so crowded with mud clasts, many of which are phosphatic, that it grades into intraformational conglomerate.

Ooliths have been found in two samples from the central area and in one from the southwest. They include solitary, composite, and encrusted ooliths (Fig. 53). The solitary ooliths are fairly uniform in size, with an average diameter of 0.1 mm, but the shape ranges from roughly circular to subtriangular, tabular, or irregular. Some of them are semicircular. The composite ooliths consist of two or more solitary individuals fused into a complex unit. The encrusted ooliths, some of which have been completely replaced by kaolinite, are partly developed solitary or composite forms adhering to the surface of quartz or rock fragments.

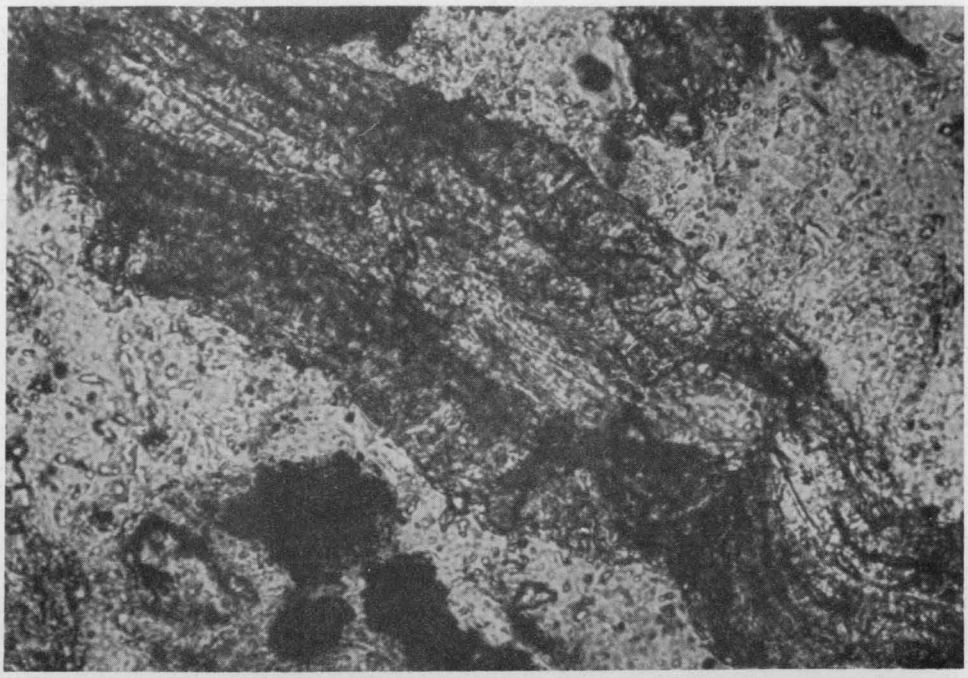


Fig. 50. Pellet from Sagittarius Sandstone composed of brown fibrous to micritic carbonate. Core at 120 m, BHP 2, Blackwater. Plane polarized light, x 125.

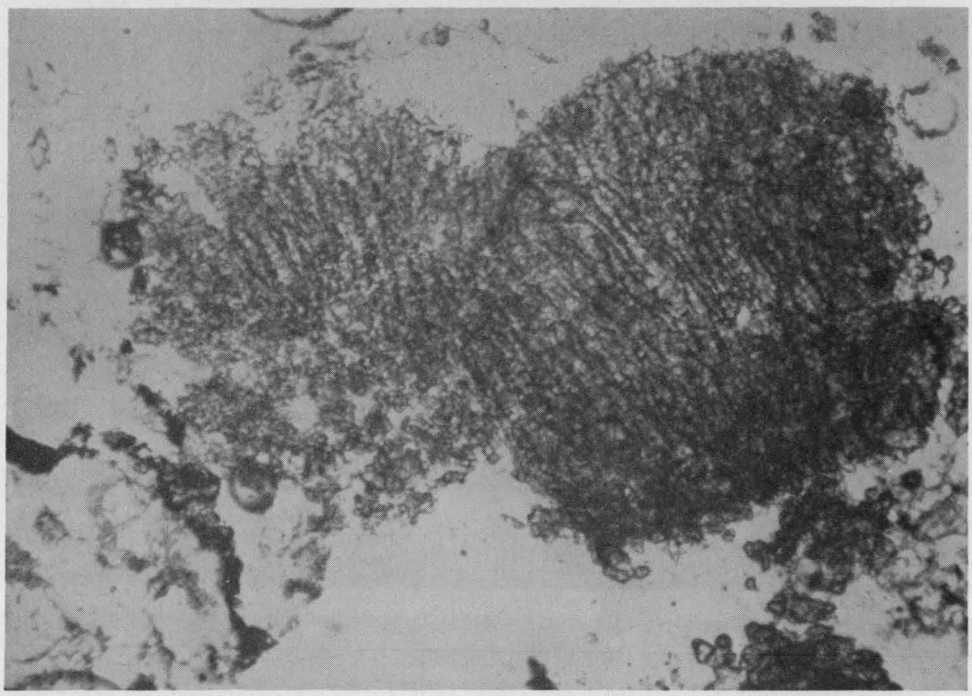


Fig. 51. Pellet from Sagittarius Sandstone composed of brown micritic carbonate with a filamentous fabric. Core at 196 m, BHP 2, Blackwater. Plane polarized light, x 125.

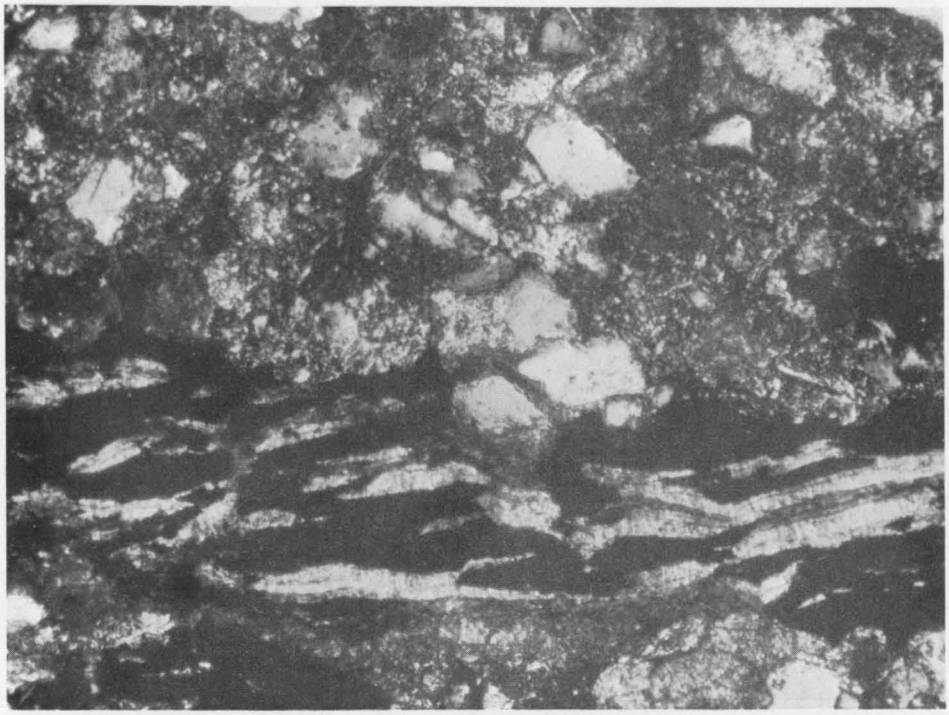


Fig. 52. Fine-grained sandstone in which sparry carbonate, probably siderite, partly replaces carbonaceous material and fills interstices between shreds. Core at 120 m, BHP 2, Blackwater. Crossed polarizers, x 160.

Many of the solitary ooliths consist of a core, roughly half the diameter of the oolith, composed of iron-rich calcite, iron oxide, or, more rarely, kaolinite. The shape of the core ranges from circular to irregular or tabular, but some of the cores are subtriangular, with slightly convex sides and rounded apices. Some of the rare dark brown cores of carbonate have a faint oolitic structure. The core of carbonate or iron oxide is commonly surrounded by a band, about 0.02 mm wide, of colourless kaolinite. The width of the kaolinite band is fairly consistent even in composite ooliths containing a number of nuclei. The kaolinite cores are surrounded by a shell of carbonate, with an outer rim, generally less than 0.005 mm wide, of iron oxide or brown carbonate, or a mixture of both. Many of the ooliths have been completely replaced by carbonate, but their original structure is revealed by the presence of dark brown rings. Some of the small round pellets of kaolinite, in which there is no sign of an oolitic fabric, are also surrounded by a dark brown iron-rich rim.

The composite ooliths may consist of two individuals sharing a common wall, or complex structures in which the shape of the original nucleus is highly irregular. They appear to grade into nodular aggregates of twisted vermicular kaolinite (Fig. 54), similar to the nodules illustrated by Carozzi (1960) and Schuller (1951), which grade in turn into aggregates of kaolinite partly replaced by brown carbonate. Although this type of kaolinite is not oolitic, the similarity in composition and fabric suggests that it is of similar origin.

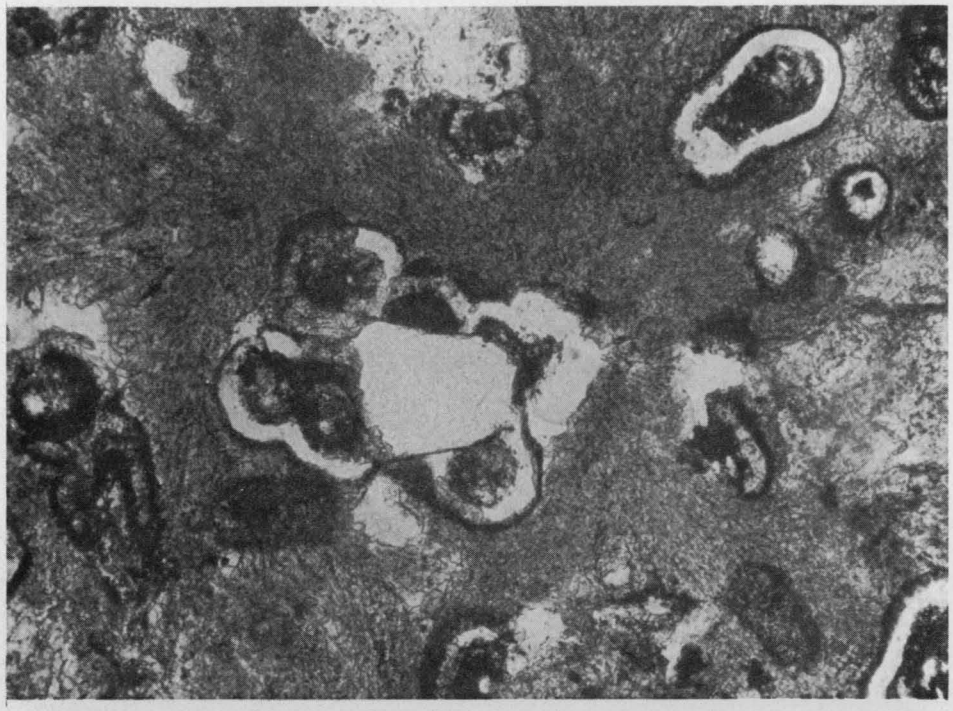


Fig. 53. Solitary and composite kaolinitic ooliths in Sagittarius Sandstone. Central area. Plane polarized light, x 160.

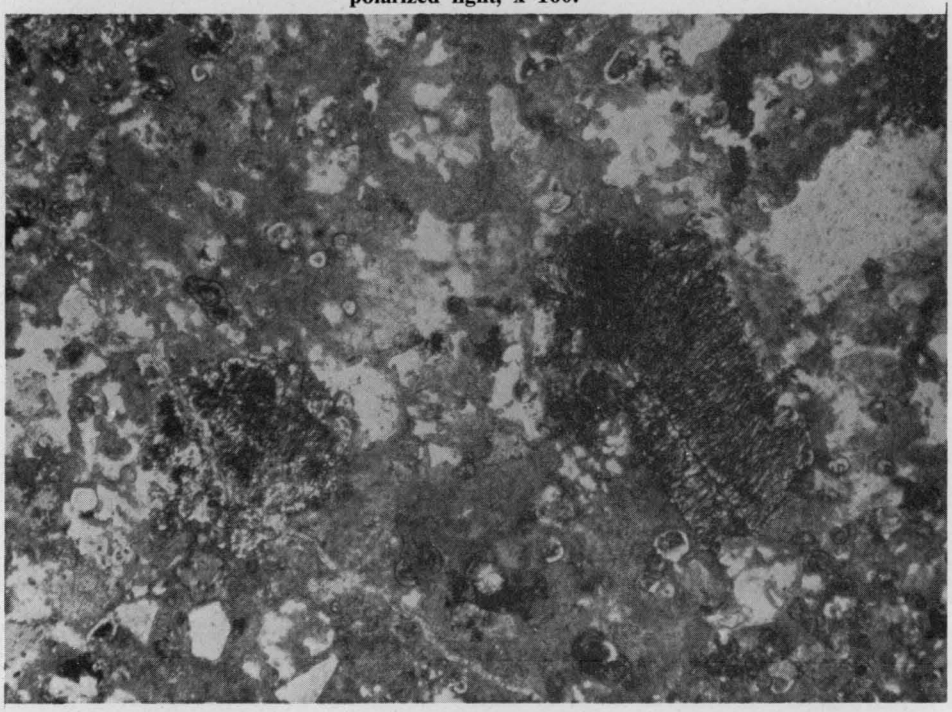


Fig. 54. Vermicular kaolinite pellets in Sagittarius Sandstone. Central area. Plane polarized light, x 40.

The presence of encrusted forms indicates that the ooliths were formed by a diagenetic process rather than by accretion in agitated water. The regularity of the solitary forms, however, could only be achieved in a soft sediment before lithification, probably during the early stages of compaction. It is believed that acid waters released from the underlying coal measures acted on the abundant volcanic detritus in the coal measures and Sagittarius Sandstone to produce kaolinite that crystallized around a variety of nuclei such as pyrite spheres (now spherical iron oxide cores) and spores (subtriangular cores). After the crystallization of the kaolinite much of the rock was replaced by carbonate, which was later recrystallized into a spherulitic fabric.

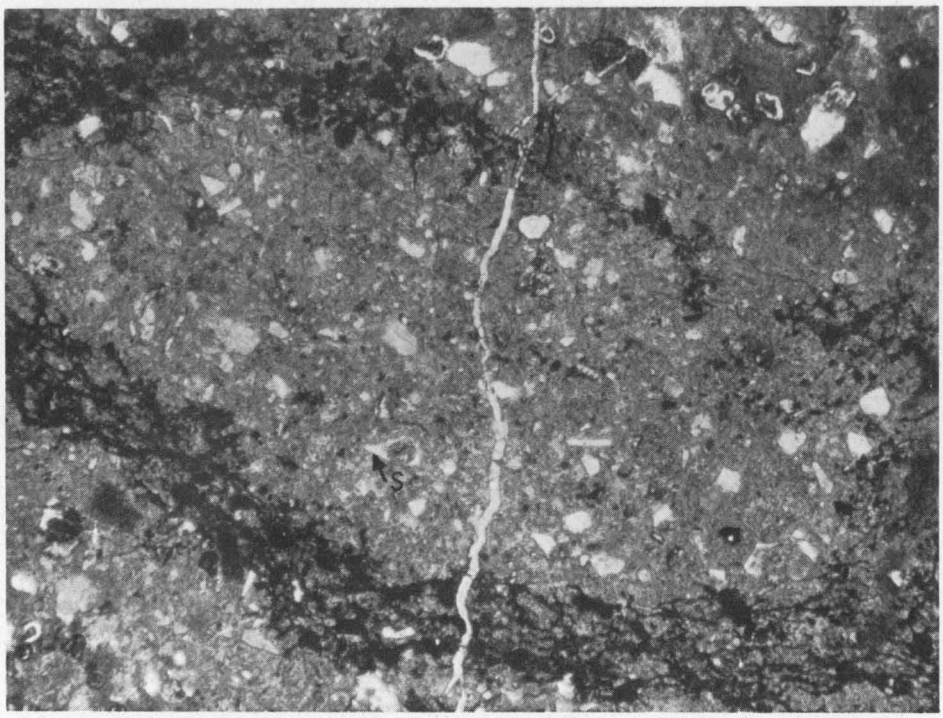


Fig. 55. Part of a phosphatic mud clast in the Sagittarius Sandstone. The clast has a diffuse sesquioxidic concretionary outer shell. The presence of shard-like fragments (e.g. S) suggests that some of the material is of volcanic origin. Central area. Plane polarized light, x 40.

The phosphatic mud clasts in the Sagittarius Sandstone (Fig. 55) have sharp to moderately diffuse borders according to the degree of replacement by carbonate cement. They consist of a microcrystalline, almost isotropic, plasma of collophane containing numerous angular grains of fine silt-size quartz and chert, mica and angular fragments of microcrystalline kaolinite. Some of the kaolinite fragments are shard-like. Narrow skew-plane sesquans extend into the centre of the nodule, where they join a diffuse irregular sesquioxidic concretion composed of numerous veins of iron oxide and embedded iron oxide nodules. The nodules also contain smooth-sided circular to irregularly shaped vugs, up to 1 mm in diameter, filled with recrystallized carbonate, skeleton grains, and complex kaolinite-carbonate

ooliths. Broad channels link the vugs with the conglomerate matrix. In addition to the phosphatic mud clasts the outcrop samples also contain clasts composed of oolitic kaolinite, which has been replaced by carbonate; these clasts also contain numerous fine grains of subangular quartz.

Phosphatic mud clasts have also been recorded near the base of the Sagittarius Sandstone in BHP No. 2. Some of the clasts have sharply defined borders and contain numerous extremely fine skeleton grains of quartz, mica, and possibly kaolin; others are composed of very fine grained-sandstone cemented with collophane and secondary carbonate, and have a framework of quartz, plagioclase, chert, and altered (kaolinized?) rock fragments. Although they have diffuse borders, the very fine sandstone nodules were not formed in situ because the framework constituents are much finer than those in the conglomerate matrix. This sandstone also contains clasts of slightly phosphatic carbonaceous siltstone, which has been almost completely replaced by carbonate and surrounded by a faint rim of reticulate iron oxide, and of brown mudstone with a strong unistrial plasmic fabric.

The mud clasts were formed by the erosion of partly consolidated mud deposits, some of which were composed mainly of kaolinite. The presence of occasional shard-like fragments replaced by kaolinite within the clasts suggests that the original kaolinitic mud was an altered volcanic ash. During diagenesis the kaolinite has been recrystallized and some of the kaolinitic clasts have been replaced by collophane. Post-depositional contraction and reorganization of the fabric during recrystallization is recorded by the presence of skew-planes and large voids within the clasts. The phosphate was probably derived from apatite in the volcanic ash, and was originally fixed within the clay. Kaolinite and other clays have a marked ability to fix phosphate ions (Haseman, Brown, & Whitt, 1950), and recrystallization of francolite in kaolinite ooliths has been recorded by Deans (1938). Alternatively, the phosphate was derived from apatite associated with the abundant detritus in the underlying coal measures, from which it was leached by acid groundwater during compaction.

Origin of Petrological Suites

The petrological suites were defined solely on the basis of the relative proportions of quartz, rock fragments, and feldspar, but each suite is also characterized by other mineral assemblages. For example, there is evidence of a progressive change in the clay mineral assemblages from one suite to the other (Table 16). At first sight these associated mineral assemblages appear to support the proposition that each suite represents some type of natural grouping. The justification for the grouping, however, varies appreciably. Although there are substantial differences between the two end members, the quartz sandstone and lithic sandstone suites, there is little difference between the quartz sandstone and the quartzose sandstone suites. The clay mineral assemblages also reveal a progressive change from one end member to the other. Thus, although natural petrological suites appear to exist within the Rewan and Clematis Groups, the most important feature is the progressive change in the mineral assemblages from one suite to the other, particularly in the proportion of labile constituents. The differences are presumably related to changes of provenance, the mechanism of transport, and the depositional environment or post-depositional changes.

Provenance factors

The framework of the sandstones is more directly related to provenance than the matrix or the cement, but the relationships are commonly obscured by changes that have taken place during and after the material was formed by erosion. The nature of the quartz grains has been used to infer provenance, but the principles involved are subject to considerable debate. A review of the early literature is provided by Blatt & Christie (1963). In all the sandstones in the Rewan and Clematis Groups monocrystalline grains of quartz with undulose extinction are predominant, but it is doubtful if this can be related to a specific provenance. According to the genetic classification of quartz grains introduced by Krynine (1946) and expanded by Folk (1968) the rocks do not appear to contain significant proportions of material from volcanic or hydrothermal sources. Volcanic quartz is characteristically euhedral and free of inclusions, and generally has non-undulatory extinction; vein quartz is characterized by the presence of numerous vacuoles.

No firm conclusions regarding provenance can be drawn from the predominance of monocrystalline over polycrystalline grains. Both varieties are released in abundance from granite, gneiss, and schist, but Blatt (1967) concluded that the polycrystalline grains are differentially destroyed during weathering and transport. Monocrystalline grains with undulatory extinction are also differentially destroyed compared with those with non-undulatory extinction (Blatt & Christie, 1963), and for this reason sandstone composed of recycled quartz grains contains a significantly higher proportion of non-undulatory monocrystalline quartz than less mature sandstone. Thus the abundance of undulatory quartz grains indicates that the quartz is unlikely to be multicyclic, and that it was not exclusively derived from a sedimentary terrain. This conclusion is supported by the angularity of the grains. By a process of elimination, then, the character of the quartz grains suggests that in general the predominant source of quartz was plutonic or metamorphic, or both.

It has been suggested that undulatory extinction can be imposed on quartz grains by post-lithification tectonic movements (Conolly, 1965, p. 133), but the samples from the Rewan and Clematis Groups do not come from strongly folded or faulted areas. It is interesting to note, however, that many of the grains share the same undulose strain shadow, and in some sections there is strong evidence that the feldspar grains were fractured during compaction. It is therefore possible that some of the strain effects in the quartz grains have been induced by compaction alone.

Of the framework constituents, rock fragments could be expected to provide the most direct link with the source areas, and in the Rewan and Clematis Groups there is apparently a progressive change in the provenance of the rock fragments from the lithic sandstone suite to the quartz sandstone suite. As in the case of quartz grains, however, there are a number of complications covering the provenance of the rock fragments. For example, there are certain limitations on the data available: interpretation is based on identifiable rock fragments, although all the sandstones contain a high proportion of grains, especially chert, of indeterminate origin; and the observations have been made on fine to coarse sand grains, so the detritus from rocks of coarse grainsize in the provenance area would not be identified.

The kind of rock fragments identified in each sample is recorded in the tables of modal analyses (Appendix 2) and the fragments recognized in each suite have been described on pages 84 to 94. In the labile sandstones the fragments consist of a mixture of volcanic, sedimentary, metamorphic, and plutonic rocks, but in the quartz sandstones they comprise only quartz-mica schist and chert, and occasional fragments of volcanic rock. Thus the change from the two end members not only involves a reduction in the number of rock fragments but also the progressive elimination of the less chemically stable types. Loughnan (1969, p. 75) and others have studied the chemical weathering of rocks under a variety of climatic conditions, but little is known of the relative stability of different types of rocks except in terms of the stability of the constituent minerals. The early work of Goldich (1938) has shown that the stability of minerals is to be related to Bowen's series for temperature of crystallization, and this has been broadly confirmed by subsequent studies (Pettijohn, 1941; Jackson & Sherman, 1953). Quartz and muscovite are generally more stable than feldspars and ferromagnesian minerals, and quartz-mica schist is more resistant to chemical erosion than volcanic rocks. Thus the changes in the type of rock fragments in the various types of sandstone in the Rewan and Clematis Groups can be explained by an increase in the intensity of chemical weathering.

The change in the feldspar content of the framework can also be attributed to increased chemical weathering. Goldich (1938, p. 34) has demonstrated that the relative stabilities of feldspars in a weathering profile varies inversely with their position in the Bowen reaction series; calcic plagioclase is the least and alkali feldspar the most stable. The lithic sandstone suite is characterized by the presence of relatively fresh feldspar, and the proportion of plagioclase commonly exceeds that of alkali feldspar. Plagioclase is subordinate to alkali feldspar in the sublabile sandstone suite, and is absent in the quartzose sandstone suite; the quartz sandstone suite contains no feldspar at all. Similarly, biotite, epidote, and apatite are less common in the quartzose and sublabile suites than in the more labile suites.

Much of the matrix in the sandstones of each suite is composed of clay minerals, the great majority of which strongly reflect the character of the source material rather than the depositional environment (van Houten, 1953; Weaver, 1958). The mineral composition of the detrital material is controlled by chemical weathering of the parent rock, which is mainly controlled by climate and tectonics (Strakhov, 1967, vol. 1, p. 4). Thus the clay mineral assemblages reflect the type of weathering in the provenance area, and not just the more restricted attribute of parent rock type, which is generally considered as part of the tectonic control.

The quartz sandstone suite is characterized by the presence of mica, kaolinite, and mixed-layer clays, with mica predominant, while the lithic sandstone suite contains abundant smectite and mixed-layer clays, with smectite predominant. In the lithic sandstone the range of rock fragments present indicates that they were derived from a variety of source rocks. In the source area chemical weathering was probably limited by climate and topography, and in the resulting non-leaching environment the parent minerals were incompletely broken down (Loughnan, 1969, p. 73). The quartz sandstone suite, which is characterized by the lack of feldspar and other labile constituents and by the presence of a mica-kaolinite assemblage, could be the product of more intense leaching, but there is no direct evidence that this took place in the source area. The clay mineral assemblages reflect the intensity of weathering in the source area.

Transportation factors

During transport the mineral composition of the clastic material changes as a result of differential destruction of weak grains, and differential grading according to grainsize (sorting); but it is unlikely that either of these processes could be responsible for the differences between the labile, sublabile, and quartzose sandstones in the Rewan and Clematis Groups. Previous studies of the destructive effects of transport on framework constituents were mainly made in relation to other grains of the same general nature. The studies of the differential destruction of polycrystalline quartz grains by Blatt & Christie (1963) have already been discussed. Pittman (1969) has demonstrated differential destruction of twinned plagioclase relative to untwinned plagioclase during transport, and Cameron & Blatt (1971) have demonstrated that fragments of schist are destroyed far sooner than fragments of volcanic rock within the same sand grade. The amount of feldspar was found to decrease rapidly downstream in high-gradient streams by Mackie (1896) and Plumley (1948). The rock fragments in sandstones of the Rewan and Clematis Groups are invariably more rounded than the monocrystalline quartz grains within the same rock, so it is assumed that they are less resistant to abrasion, and therefore to destruction, than monocrystalline quartz grains. The decrease in the proportions of both feldspar and rock fragments from the labile to the quartzose sandstones could represent an increase in the degree of mechanical destruction during transport. However, this is unlikely because: (a) the character of quartz grains does not change from one suite to another, and there is no increase in the more mechanically stable monocrystalline grains with non-undulose extinction; (b) there is no decrease in grainsize corresponding to the apparent increase in mechanical disintegration; and (c) it is the mechanically less stable schist fragments, and not the fragments of volcanic rock, that are concentrated in the mineralogically mature suites.

In some sequences it has been shown that the proportion of quartz rock fragments to feldspar varies with mean grainsize (Okada, 1971, p. 513), and thus if mechanical transport induces size-sorting, changes in the proportion of framework constituents might be expected. The samples examined range in grainsize from medium to very fine sand, but there is no well defined correlation between the proportion of framework constituents and grainsize (Fig. 56).

Post-depositional changes

Differences in the intensity of chemical weathering have been cited on page 88 to explain some of the differences in mineral content between the sandstone suites. Much of the alteration takes place in the source area, but the mineral composition can change significantly at the site of deposition as a result of chemical weathering and diagenesis. Most of the samples examined were collected from outcrops and they may have been subjected to chemical weathering in more recent times. In the case of Rewan and Clematis Groups some of the minerals have been altered after the rocks were deposited, but it is believed that most of the changes were due to chemical weathering in the source area.

The most direct evidence of weathering at the site of deposition is the presence of illuviation fabrics, which are rarely found in the sandstones. Some of the quartz sandstones and sublabile sandstone have illuviation fabrics, but the matrix is generally composed of a heterogeneous assortment of clay minerals and fine 'framework' constituents with a silasepic or weakly insepic fabric resulting from the

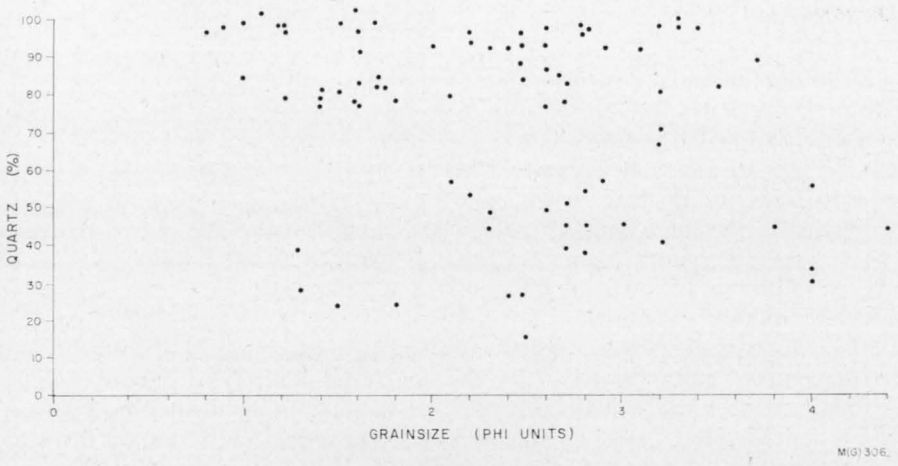


Fig. 56. Comparison of median grainsize with the amount of quartz in the framework of sandstones of the Rewan and Clematis Groups.

original sedimentation. The more pronounced sepic fabrics have been developed by compaction and diagenesis. The only other evidence of weathering in situ is the introduction of new mineral phases (in the redoxomorphic diagenetic stage of Dapples, 1967), such as hematite and limonite, which may partly replace the matrix and framework grains. Ferruginization undoubtedly occurred during the Tertiary at some localities, especially in the southwest, but even in this area, although some of the iron was introduced during weathering, there is evidence that some amorphous iron oxide was deposited with the clastic grains. In the same sample there is also evidence of minor remobilization of iron during Triassic weathering. The introduction of iron oxides, however, does little to alter the relative proportions of the framework constituents unless the labile components are replaced, and there is no evidence of this in the samples examined. Of greater significance is the replacement of feldspar in the Dawson Range Sandstone by halloysite, because this is found in subsurface samples and must therefore relate to Triassic weathering, and because alkali feldspars with a similar 'cavernous' texture are present in the sublabile sandstone and quartzose sandstone suites elsewhere. For this reason it is concluded that there has been some post-depositional weathering of alkali feldspar in an environment in which leaching was moderately intense.

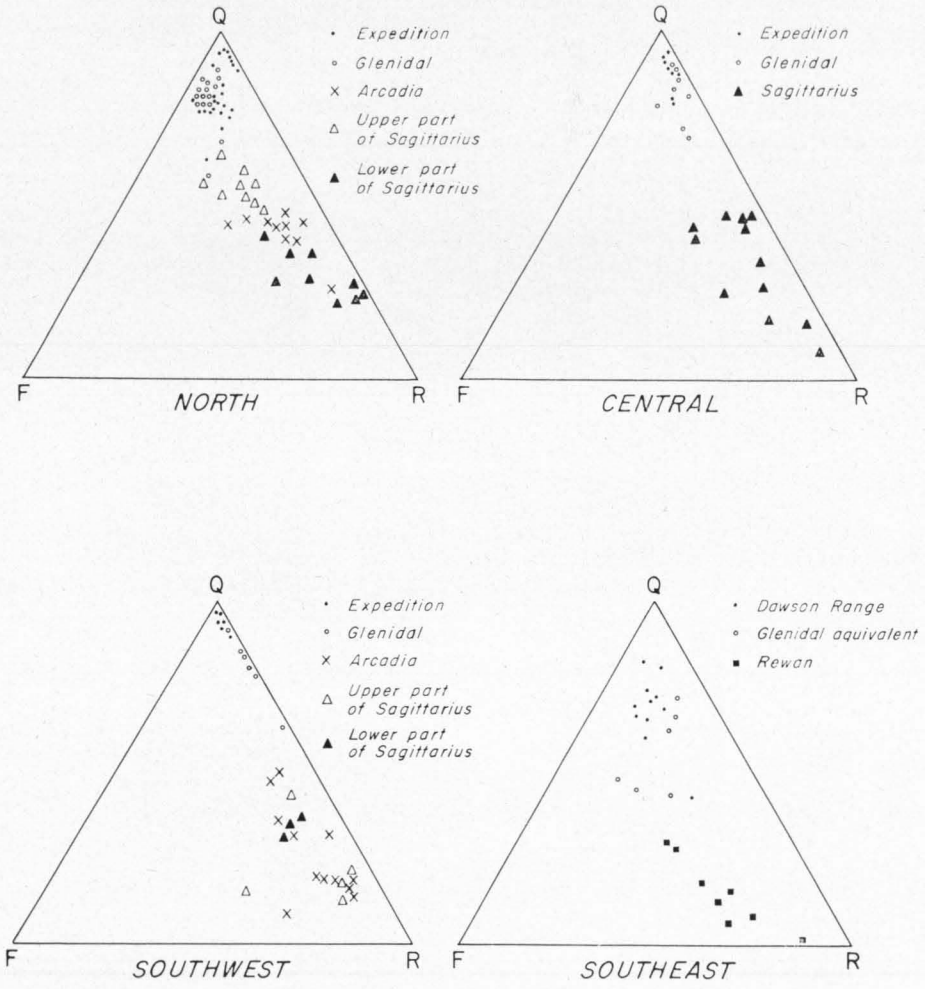
Post-weathering diagenetic mineral phases are present in all suites, but they had little effect on the relative proportions of framework grains. In the quartzose sandstone and sublabile sandstone suites quartz overgrowths are common, and some of the matrix may be replaced by a little chalcedony. In all suites, but especially in the quartz sandstones, there is evidence of the recrystallization of kaolinite, possibly after the deposition of secondary quartz.

According to Tripplehorn (1971) clay minerals may be recrystallized as a result of post-weathering diagenesis. Minor crystallization of calcite within pore spaces is common to all the sandstone suites, and in a few of the lithic sandstones some of the quartz, feldspar, and rock fragments have been replaced by calcite. In these rocks the relative proportions of framework constituents may have been altered by replacement by carbonate, but their prediagenetic framework composition would have been more labile than at present. The lithic sandstone and semi-labile

sandstone suites are also characterized by the presence of a diagenetic generation of colourless and green chlorite, which fills the pores and replaces the matrix and biotite. The chloritized fragments of volcanic rock represent an earlier period of diagenesis within the original volcanic rocks.

Stratigraphic Significance

Each of the stratigraphic units in the various parts of the basin is characterized by sandstone belonging to one, and sometimes two, related petrological suites; the relationship between the stratigraphic units and composition of the arenite framework is shown in Figure 57. In each part of the basin, the sandstone



M(G) 307

Fig. 57. Composition of the sandstone framework in units within the Rewan and Clematis Groups.

of the basal units is more labile than that of the upper units, and there is a general progression from lithic sandstone to quartz sandstone (Fig. 58). There are minor exceptions to the trend in the north, where the lower part of the Sagittarius Sandstone is less labile than the upper, and the upper part of the Expedition Sandstone is more labile than the lower. It should also be noted that fields covered by equivalent stratigraphic units in each part of the basin are not exactly the same. The sandstone throughout the sequence in the southwest contains less feldspar than the sequence in the southeast. The difference is more likely to be due to variations in the intensity of chemical weathering rather than to differences in the parent materials, because in both areas the clastic detritus was derived from a variety of rock types. This is well illustrated, for example, by the variety of rock fragments preserved in the framework of the sandstones from the Rewan Group.

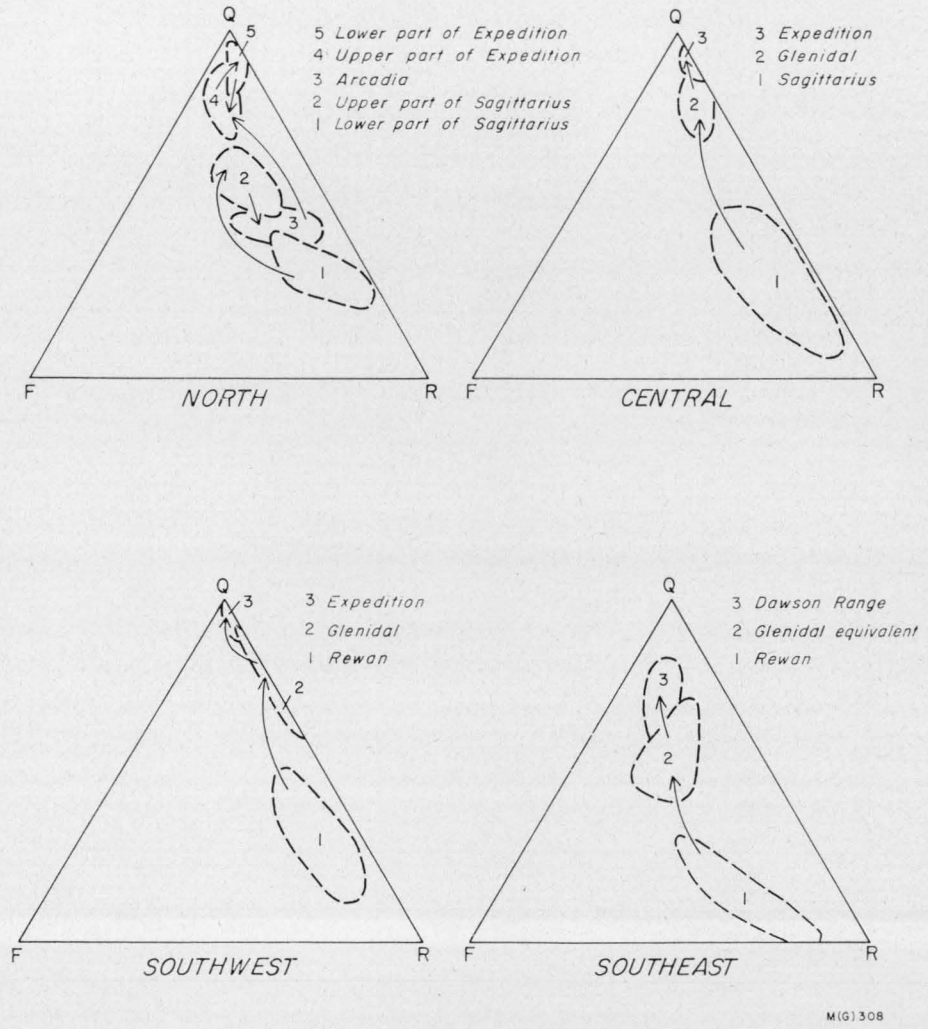


Fig. 58. Progressive changes in the composition of the sandstones in successively younger units of the Rewan and Clematis Groups.

ANALYSIS OF STRATIFICATION

Environmental Significance of Stratification

Until theoretical or empirical quantitative relationships have been established between bedding and hydraulic environments, and between hydraulic and physiographic environments, the most useful approach to the study of palaeoenvironments is vertical profile analysis as outlined by Visher (1965). The method is based on an application of Walther's Law, and relies on the fact that depositional sites are commonly composed of a number of laterally disposed facies (lithotopes), generally at slightly different elevations. Lateral shift of the lithotopes, owing for example to a change of base level, results in the progradation of laterally contiguous rock bodies (lithosomes) over one another, and the formation of a vertical accretion profile that reflects the original lateral disposition. Vertical profile analysis also depends on the assumption that the members of the profile represent laterally contiguous lithosomes, which implies that they are genetically related. If it can be shown that the members of a vertical sequence are laterally contiguous, then it follows they are genetically related; if there are insufficient outcrops to establish lateral continuity a genetic relationship can be established by proving that the sequence is repeated, and that the repetition is statistically not fortuitous.

The vertical profile of genetically related units is related to a specific physiographic environment of deposition. Although individual lithotopes are not restricted to one physiographic environment, it is axiomatic that every broad depositional environment is composed of a set of uniquely disposed lithotopes. It follows that the vertical profile produced by lateral movement of lithotopes is unique for each physiographic environment; but it must be emphasized that all the constituent lithosomes are required to characterize an environment. For example, the vertical profile established for point bar deposition can be related only to deposition in a meander bend of a unidirectional current system, and not necessarily to a fluvial environment. Meander bends are found in tidal estuaries as well as rivers situated well inland. Unfortunately, models of all depositional environments are not yet available and until they are vertical profiles cannot always be related to physiographic environment.

Classification of Sedimentation Units

In order to apply the methods of vertical profile analysis to the stratification of the Rewan and Clematis Groups, it was found necessary to modify systems of bedding classification. The classification must reflect environmentally significant changes in lithology, and must be based on easily observable and commonly preserved features. The two most obvious broad lithological features meeting these requirements are grainsize and stratification. The first major division is based on grainsize; all mudstone beds, whether laminated or massive, are included in the one category designated 'L'. Sandstone beds, however, are classified on the basis of stratification into massive, laminated, and cross-stratified groups. The massive beds (M) could in fact possess a latent stratification not visible to the field observer. Laminated sandstone beds (P) possess planar stratification parallel to the base of the bed. Cross-stratified beds are further subdivided.

Rapid advances have been made in recent years towards rationalization in the classification of cross-stratification, firstly by McKee & Weir (1953) and more recently by Allen (1963a), although even Allen's classification appears to have some disadvantages. Firstly, the selection of a 5-cm set-size boundary between two

populations of grouped cross-strata is presumably aimed at separating structures formed by ripples from those having their origin in the migration of dunes, but it does not allow for the possibility of naturally occurring progressions of size within the dune range which reflect changes in depositional environment. Secondly, the classification relies heavily on the shape of the lower bounding surface of the set or coset of cross-strata, which although of considerable genetic importance is seldom exposed. Thirdly, the same problem arises with regard to the nature of the lower surface, be it erosional, non-erosional, or transitional, and in the determination of the angular relationship between the cross-strata and the lower bounding surface.

Although data concerning the nature and shape of the lower bounding surface were collected where possible, the analysis of the cross-stratification presented here is based on only two features: (a) the manner of grouping of the cross-strata—solitary or grouped; and (b) the size of the sets of cross-strata. Solitary units (S) consist of a set of cross-strata which succeeds, and is succeeded vertically by, non-cross-stratified deposits, or by cross-stratified units of a different type. A cross-stratified unit is said to be grouped (G) if it comprises two or more vertically disposed sets of cross-strata. Three classes of group cross-stratified beds, based on the average size of the sets, are recognized. The limits chosen are: (a) less than 20 cm—Gc; (b) from 20 to 40 cm—Gb; and (c) greater than 40 cm—Ga. These values are arbitrary and do not necessarily reflect natural groups.

Recognition of Patterns of Sedimentation

Information regarding the nature of bedding in both the Rewan and Clematis Groups has been gathered from various parts of the basin where outcrop is sufficient. The information comes from: (a) *stratigraphic sections,* measured over a certain interval without reference to the lateral disposition of beds; and (b) measurements taken over a more restricted stratigraphic sequence where lateral relationships could be recorded in the form of *detailed graphic sections.* Two basic methods were adopted for detailed sections. Where planar vertical surfaces were exposed, polaroid photographs were taken and joined, and the trace of bedding planes and stratification marked on the photographs. Where photographs could not be taken, the exposed face was marked with a grid and the stratification recorded on squared paper.

In order to discern cycles of deposition, if present, first order Markov chain analysis as used by Gingerich (1969) was applied to sequences of vertically disposed beds in each section. Second and higher order Markov chain analysis such as that used by Doveton (1971) was not applied because of the small number of beds and the large number of categories.

Stratification in Rewan Group

The analysis of bedding transitions from seven localities in the Rewan Group (Table 17) strongly suggests the presence of at least one cyclic pattern (Fig. 59) consisting of a change from group cross-stratified sandstone beds to mudstone, in some cases by way of massive sandstone or sandstone beds with planar stratification. There is also an upwards decrease in set size and grainsize. Sandstone beds with Gc-type and P-type stratification are commonly finer than those with Ga-type. Patterns of this type are recorded over thick sequences such as in Section GA46 (Fig. 27) measured in the Arcadia Formation in the northern part of the basin. An example of one cycle is shown in Figure 26.

TABLE 17. BEDDING TRANSITIONS IN REWAN GROUP

(Localities GA10, 11, 26, 27, 34, 37, 46)

a. *Transition count matrix*

	Ga	Gb	Gc	L	M	P
Ga	0	3	9	9	3	2
Gb	2	0	2	15	2	0
Gc	1	0	0	9	0	1
L	20	13	1	0	1	2
M	0	1	0	4	0	1
P	0	0	0	0	4	0

b. *Independent trial matrix*

	Ga	Gb	Gc	L	M	P
Ga	0.0	0.27	0.14	0.47	0.08	0.05
Gb	0.31	0.0	0.13	0.44	0.07	0.05
Gc	0.28	0.22	0.0	0.39	0.05	0.04
L	0.38	0.31	0.16	0.0	0.08	0.06
M	0.26	0.21	0.11	0.38	0.0	0.04
P	0.26	0.21	0.11	0.36	0.06	0.0

c. *Probability transition count*

	Ga	Gb	Gc	L	M	P
Ga	0.0	0.11	0.35	0.35	0.11	0.08
Gb	0.10	0.0	0.10	0.71	0.10	0.0
Gc	0.09	0.0	0.0	0.82	0.0	0.9
L	0.54	0.35	0.03	0.0	0.03	0.05
M	0.0	0.17	0.0	0.67	0.0	0.17
P	0.0	0.0	0.0	1.0	0.0	0.0

d. *Resultant matrix*

	Ga	Gb	Gc	L	M	P
Ga	0.0	—0.16	0.21	—0.12	0.03	0.03
Gb	—0.21	0.0	—0.03	0.27	0.03	—0.05
Gc	—0.19	—0.22	0.0	0.43	—0.06	0.05
L	0.16	0.04	—0.13	0.0	—0.05	—0.01
M	—0.26	—0.04	—0.11	0.29	0.0	0.13
P	—0.26	—0.21	—0.11	0.64	—0.06	0.0

The group cross-stratified beds of the Rewan Group lie in a series of trough-shaped mildly erosional surfaces with a festoon pattern in cross-section (Fig. 60b). In longitudinal section the beds are arranged en echelon (Fig. 60c). Allen (1963b) related this type of stratification to the migration of large-scale asymmetric ripples (dunes). It is not possible to deduce details of the hydraulic environment from the morphological characteristics of the dune, but it has been shown that they form in the lower regime of flow (Simons, Richardson, & Nordin, 1965), at higher flow rates than small-scale ripples, and therefore in currents of greater transporting power. The upward decrease in the thickness of sets of cross-strata is a reflection of decreasing dune size, but because of the number of variables affecting the size and shape of bed forms it is not possible to specify the cause of this change. One of the most important factors controlling dune amplitude is depth of flow (Simons et al., 1965), because it limits the ultimate size of the bed features, but other factors include fall velocity and sorting of the bed material. The average height of dunes in moderately well sorted sand is less than in poorly sorted sand for the same depth

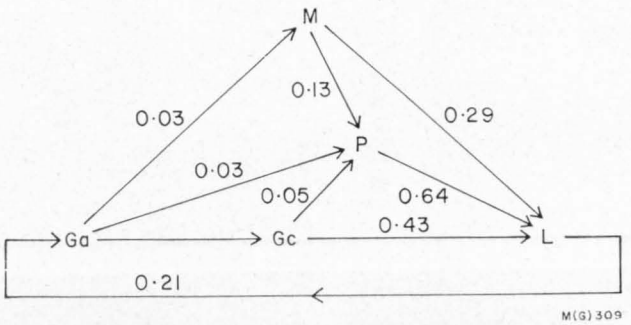


Fig. 59. Summary of cyclic pattern in the Rewan Group. (Based on Table 17d).



a



b



c

Fig. 60. Arcadia Formation (Sect. GA10) in the Dawson River near Theodore, southwestern area. (a) Original outcrop; (b) bedding planes in cross-section of sandstone (picked out with white paint); (c) bedding planes in longitudinal section (picked out in white paint).

and slope conditions. However, in beds such as F and G of Section GA11 (Figs 61, 62), which represent Ga and Gc respectively, there is little change in sorting (Fig. 63) despite the change in the size of the original dune. In changes of this nature the controlling factor has been a decrease in the depth of water, and the corresponding reduction in transportation power of the stream. A similar change is also indicated by the overall decrease in grainsize.

Planar stratification of sandstone beds has been attributed to deposition in the upper flow regime (Simons, Richardson, & Albertson, 1961), and the change from Ga or Gc to P could be interpreted as a change from lower to upper regimes of flow. It is shown in Appendix 1, however, that the planar-stratified sandstone of the Rewan Group was laid down in the lower flow regime, and there is therefore no indication of increasing stream transportation power. Moss (1968) has noted that the formation of ripples and dunes is favoured by stability of current direction as a result of features such as flume walls and river bands. The change to planar strati-

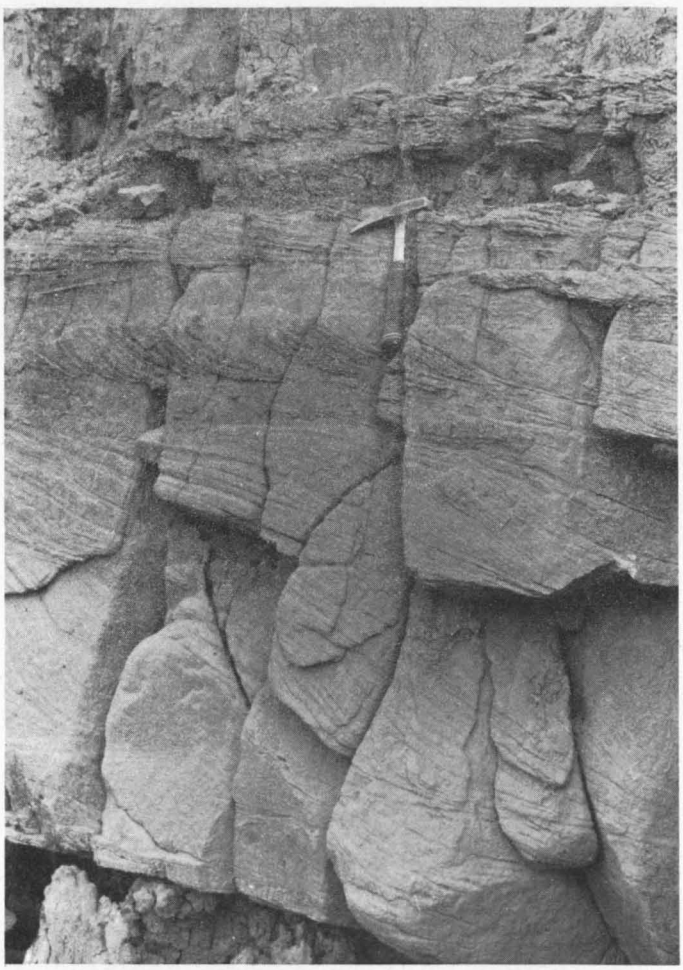


Fig. 61. Cross-stratified sandstone of the Arcadia Formation showing upward decrease in set size. Southwestern area.

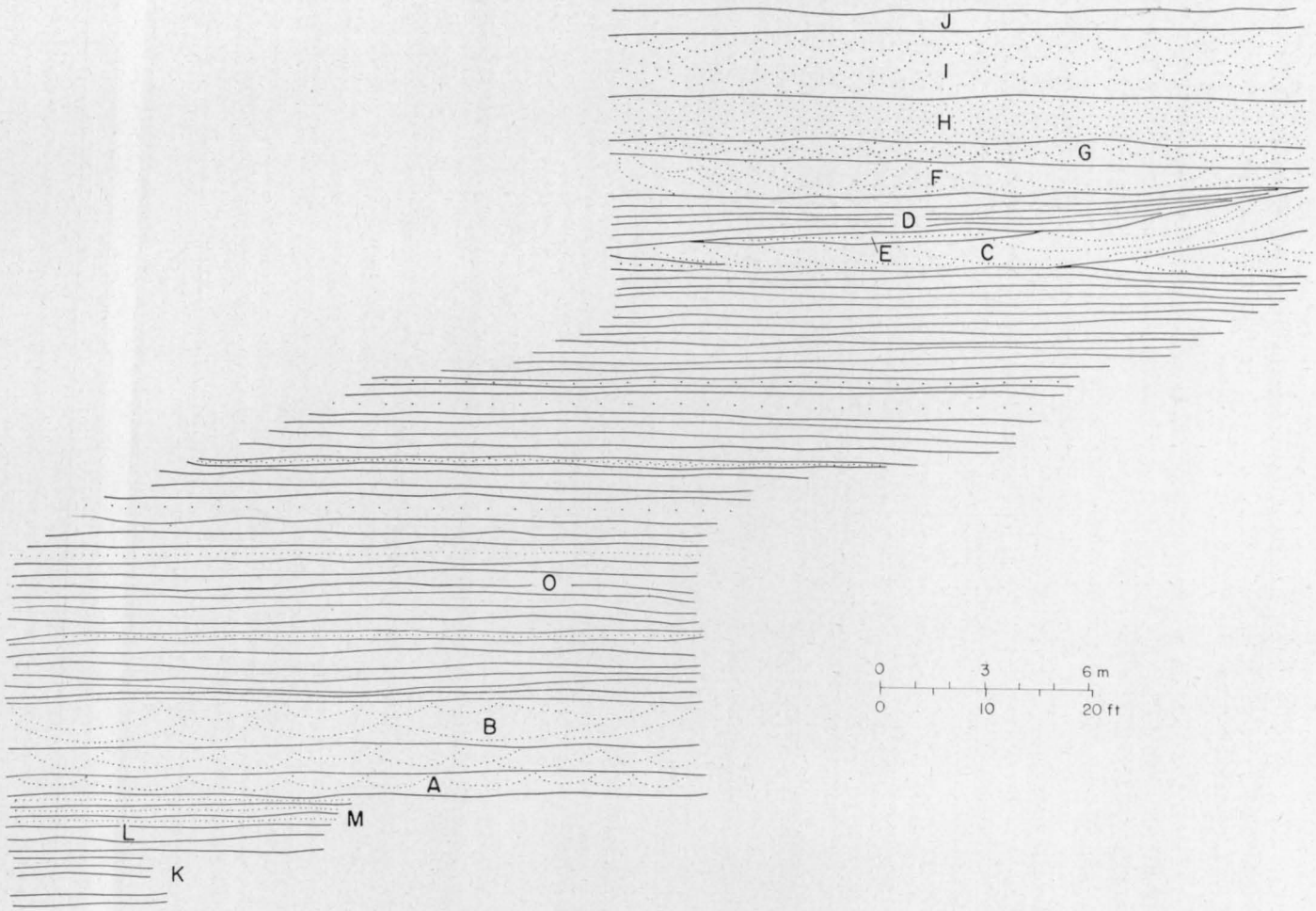


Fig. 62. Stratification in the Arcadia Formation in Section GA11, southwestern area.

fication in the Rewan Group, therefore, probably represents a change in physiographic environment such as from channel to flood plain.

Thus the changes in stratification and grainsize in the Rewan Group suggest that the cyclic pattern of sedimentation reflects the successive progradation of lithofacies arranged in decreasing order of the energy of the depositional current. With minor modification, this pattern can be compared with that proposed by Visher (1965) for sedimentation in a meandering stream. In the cycles of the Rewan Group there is no clearly marked basal unit containing poorly sorted coarse detritus, which appears in Visher's model presumably because studies such as those by Happ,

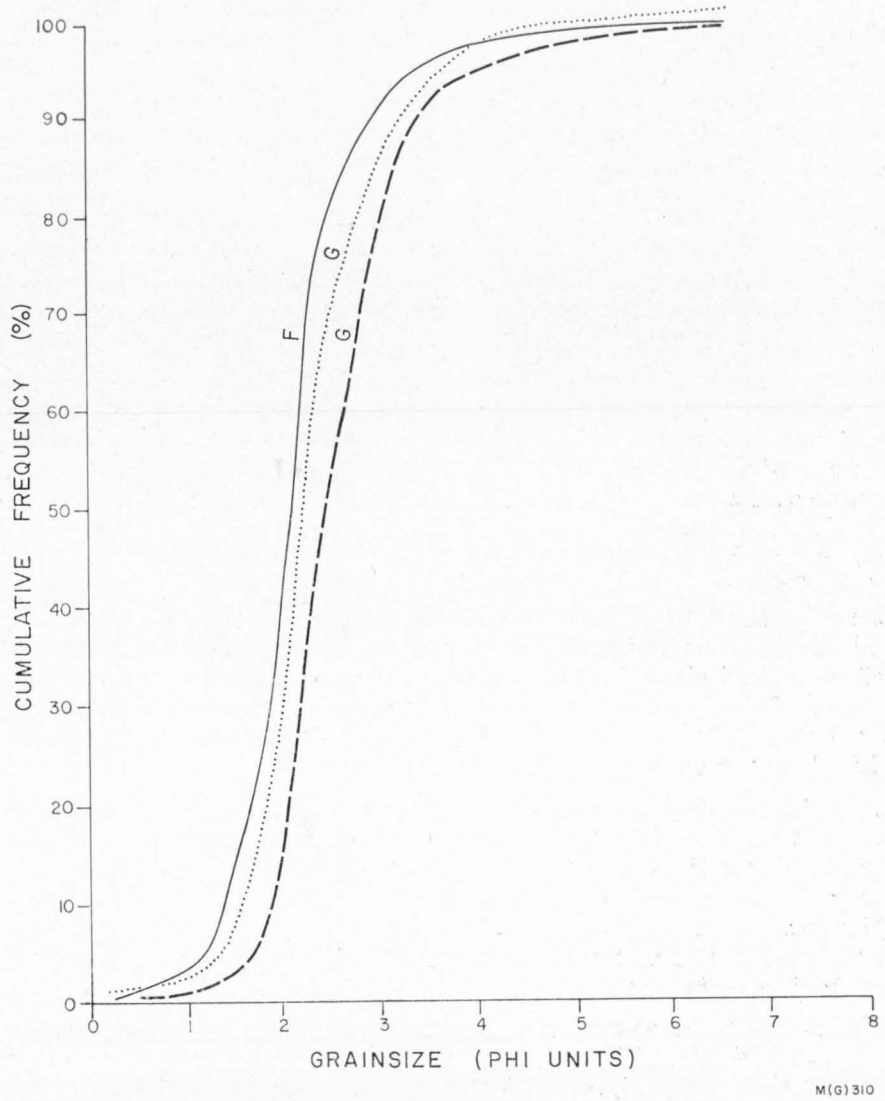


Fig. 63. Cumulative frequency curves of grainsize distribution of two samples from Bed G and one from Bed F in Section GA11 (Fig. 62) showing the similarity of grainsize and sorting despite a change in the size of set of cross-strata.

Rittenhouse, & Dobson (1940) and Allen (1965) describe channel lag deposits, typically gravels, deposited on an erosion surface at the base of the fluvial sequence. If the stream were not transporting gravel, the channel deposits would presumably be the coarsest sediment available, but the stratification of such deposits has not been described in studies of modern streams. The coarsest sediment in the Rewan Group, generally category Ga, does occur at the base of cycles in the northern part of the basin, but is not always underlain by a well defined surface of erosion.

The group cross-stratified sandstone of the Rewan Group has the characteristics of the 'cross-stratified sand zone' that constitutes the bulk of the point bar. Visher's model does not indicate any upward decrease in the size of cross-stratification, but this has been recorded by McDowell (1960) in the point bar sands of the Old River in Louisiana, and by Bluck (1971) in the sands of the supra-bar platform of a meandering mixed-load stream in Scotland.

Horizontally stratified beds have been described in point-bar sediments in the Rio Grande by Harms & Farnstock (1965), although there was no distinct distribution pattern. In the Rewan Group, they are generally found above the zone of cross-stratified sandstone, which is in agreement with Visher's model. It has already been suggested that the change from cross-stratified to planar stratified sandstone probably represents a change in physiographic environment, such as from channel to flood plain, and it is possible that horizontal stratification is formed in levées, in which the only sedimentary structures recorded are lamination and small-scale stratification (Allen, 1965, p. 146).

Rocks in category 'L' include lenses of mudstone within sequences composed mainly of sandstone, and thick sequences consisting mainly of mudstone. The thin lenses of mudstone were deposited in hollows in the bed of the stream channel, and are not part of the main point-bar cycle. In places, the relatively thick and more extensive sequences of mudstone contain thin lenses of fine sandstone with a faint small-scale cross-lamination; this type of sequence is the closest approach to the 'zone of climbing ripples' found in the cycles of the Rewan Group. If Visher's model for fluvial sedimentation is applicable, the apparent lack of the climbing ripple structure could be due to poor preservation. The thick sequences of fine-grained, and in places laminated, mudstone in the Rewan Group were presumably deposited on flood plains from slowly moving currents or from suspension after flow ceased. The thin, rare, persistent beds of green siltstone interbedded with the thick red mudstone sequences represent the coarsest fraction of the suspended load laid down immediately after each major flood receded.

Applying the fluvial meandering stream model to the Rewan Group it can be seen that Section GA34 (Fig. 64) represents a point-bar deposit. The basal sandstone beds (D, B, F, G, H) with Ga-type stratification were laid down in the deeper part of the channel incised into earlier formed vertical accretion deposits; Bed N represents a plugged channel at the neck of the meander loop, Bed K was deposited on the upper part of the point bar or in levées, and Bed L is the basal part of the flood-plain deposits.

The fluvial model proposed by Visher does not apply to the other type of cyclic sequence developed in the Rewan Group, which consists of an alternation of types Gb and L (Fig. 24, Sect. GA37). This association is found mainly in one section at the top of the group in the northern part of the basin, where thick sequences of mudstone are interbedded with beds of group cross-stratified sandstone with no evidence of fining upwards or any decrease upwards in set size, except

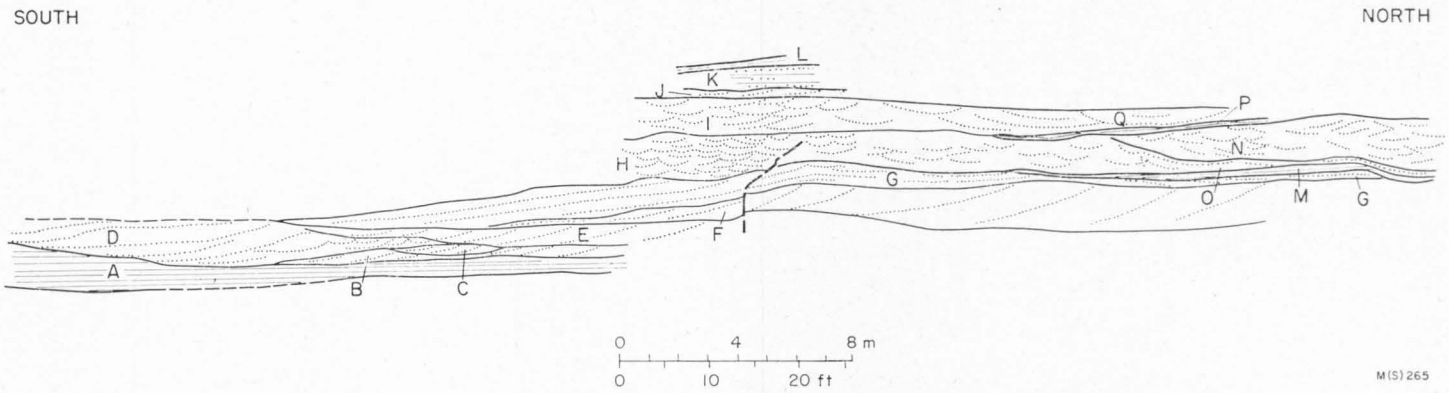


Fig. 64. Stratification in the Sagittarius Sandstone in Section GA34, northern area. The section probably represents a point bar sequence resting on an erosion surface (A-D), with a small secondary channel (N) at the northern end.

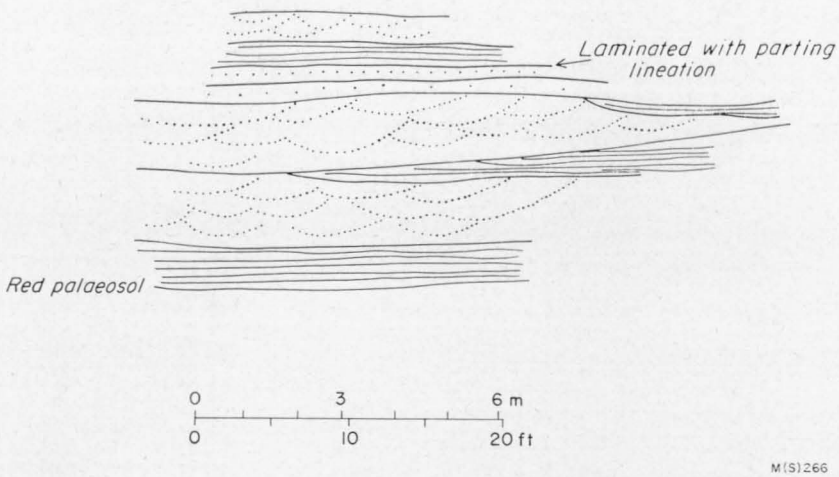


Fig. 65. Stratification in the Arcadia Formation in Section GA37-1, northern area.

in the case of the small detailed Section GA37-1 (Fig. 65). Taken by itself Section GA37-1 conforms to the fluvial model, and the included mudstone has been subjected to minor pedogenic alteration. Because of this and because of the similarity of rocks of the Gb-L association to the rest of the group there appears no reason to suggest anything other than a continental environment of deposition for the Gb-L association. The abundance of mudstone and the lack of coarse-grained sandstone is presumably due to the presence of a greater proportion of suspended-load sediment than in the streams responsible for the deposition of other parts of the group, and the most likely type of stream pattern under these conditions is a system of anastomosing channels (Schumm, 1968). This would explain the absence of point-bar profiles, which would not be developed in a system lacking meanders.

Stratification in Clematis Group

On the basis of stratification the sequences in the Clematis Group can be divided into three types: (a) the Glenidal Formation in the north, and the Expedition Sandstone in the southeast, centre, and southwest; (b) the Glenidal Formation in the southwest; and (c) the Expedition Sandstone in the north. The first type is characterized by a mixture of solitary and group cross-stratified beds, and beds with horizontal stratification. Analysis of bedding transitions (Table 18) from nine localities with stratification of this type suggests the presence of the cyclic sequence illustrated in Figure 66. Section GA05 (Figs 67, 68) is a simple example

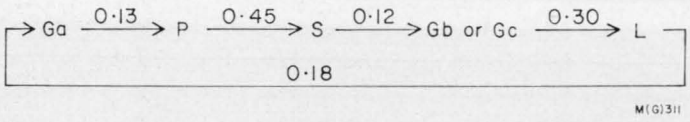


Fig. 66. Cyclic pattern suggested by results of analysis in Table 18.

TABLE 18. BEDDING TRANSITIONS IN CLEMATIS GROUP

(Localities GA4, 5, 6, 9, 14, 36, 45, 54, 73)

a. *Transition count matrix*

	Ga	Gb	Gc	L	M	P	S	E
Ga	0	5	5	3	1	7	1	4
Gb	2	0	0	3	0	0	1	2
Gc	1	0	0	5	2	1	4	3
L	4	0	1	0	1	1	2	1
M	4	0	2	0	0	0	2	0
P	0	1	1	1	1	0	10	1
S	2	6	5	3	2	2	0	5
E	4	0	3	0	3	3	6	0

b. *Independent trial matrix*

	Ga	Gb	Gc	L	M	P	S	E
Ga	0.0	0.08	0.15	0.09	0.17	0.14	0.33	0.19
Gb	0.22	0.0	0.13	0.08	0.07	0.13	0.21	0.16
Gc	0.23	0.07	0.0	0.09	0.07	0.14	0.23	0.18
L	0.22	0.07	0.14	0.0	0.07	0.13	0.21	0.16
M	0.22	0.07	0.13	0.08	0.0	0.13	0.21	0.16
P	0.23	0.07	0.14	0.09	0.07	0.0	0.22	0.17
S	0.26	0.08	0.15	0.10	0.08	0.15	0.0	0.19
E	0.24	0.07	0.15	0.09	0.07	0.14	0.23	0.0

c. *Probability transition count*

	Ga	Gb	Gc	L	M	P	S	E
Ga	0.0	0.19	0.19	0.12	0.04	0.27	0.04	0.15
Gb	0.25	0.0	0.00	0.38	0.0	0.00	0.13	0.25
Gc	0.06	0.0	0.0	0.31	0.13	0.06	0.25	0.19
L	0.40	0.0	0.01	0.0	0.01	0.01	0.02	0.01
M	0.50	0.0	0.25	0.0	0.0	0.0	0.25	0.0
P	0.0	0.07	0.07	0.07	0.07	0.0	0.67	0.07
S	0.08	0.24	0.20	0.12	0.08	0.08	0.0	0.20
E	0.21	0.0	0.16	0.0	0.16	0.16	0.32	0.0

d. *Resultant matrix*

	Ga	Gb	Gc	L	M	P	S	E
Ga	0.0	0.07	0.04	0.03	—0.13	0.13	—0.19	—0.04
Gb	0.03	0.0	—0.13	0.30	—0.07	—0.13	0.0	0.09
Gc	—0.17	—0.07	0.0	0.22	0.06	—0.08	0.02	0.01
L	0.18	0.0	—0.13	0.0	—0.06	—0.12	—0.19	—0.15
M	0.23	—0.07	0.12	—0.08	0.0	—0.13	0.04	—0.16
P	—0.23	0.0	—0.07	0.02	0.0	0.0	0.45	—0.10
S	—0.18	0.12	0.09	0.02	0.0	—0.07	0.0	0.01
E	—0.03	—0.07	0.01	—0.09	0.09	0.02	0.09	0.0

of a sequence similar to the ideal pattern, except that no planar-stratified sandstone exists between the solitary unit (A) and the large-scale group cross-stratified unit (Beds M to C). For the purposes of classification type Ga commonly includes thin lenses up to 30 cm thick of siltstone and muddy siltstone, interbedded with grey very coarse sandstone or, in places, granule conglomerate. The association of coarse sand or gravel with silt is the result of deposition of the finer material in an erosion hollow (a *dead slough* of Wolman & Brush, 1961). Surfaces of marked erosion (E) were treated as a bedding type in the analysis, but neither these nor massive beds (M) form part of the cyclic pattern.

Most of the basal sandstone beds with Ga-type stratification were formed as a result of migration of dunes in a unidirectional current flow; the dune form is seldom preserved, but it can be seen in Bed G of Section GA05 (Fig. 67) where it has been protected from subsequent erosion by the overlying mud drape.

The repeated superposition of planar-stratified mudstone beds and solitary cross-stratified beds reflects a genetic link as shown by the lateral relationships in detailed sections. The solitary cross-stratified units were laid down in microdeltas, such as the one illustrated in Section GA73 (Fig. 69) where Beds Q and C have been developed by accretion of sand laminae on an avalanche face of a solitary bank. At the inflection caused by the irregularity of the basal surface at Beds K and J, Bed C changes from a solitary cross-stratified unit to a horizontally stratified group of bottom-set beds. The elongation function analysis (Appendix 1) provides further evidence that the solitary cross-stratified units of the Clematis Group represent solitary banks and not dune fields. The solitary banks, the size of which ranges from 1 to 7 m, were formed at topographic discontinuities, such as that shown in Figure 70, or on level surfaces where there was a rapid shift of base level (see Jopling, 1966). Rare solitary banks were also formed as a result of en-echelon superposition of successive dune fields now recorded in places as double cross-stratification (Fig. 71). As a result of this process the gradient of the lee slope is increased to the point where sand moves down the surface under gravity and without the formation of dunes.

The genetic relationship between solitary cross-stratified units and the overlying group cross-stratified units is illustrated in Section GA54 (Fig. 72). Beds D and I represent a solitary cross-stratified unit formed by the accumulation of sand in a microdelta. The group cross-stratified beds lie in a number of troughs in the upper surface of the microdelta. In places individual bedding planes can be traced from the group cross-stratified beds into the solitary unit (from E to I in Fig. 72). The zone of group cross-stratified units extends over the lee face of the solitary unit, and can be interpreted only as dunes (asymmetric ripples) that were formed on the upper surface of a microdelta, which they eventually over-ran. Bed J in the same section changes laterally from a solitary unit into a group cross-stratified unit, presumably by the same process. In this section the bottom-set deposit (Bed C) shows a reverse facing that was possibly developed in the zone of back-flow that exists in advance of a microdelta (Jopling, 1963).

Although there is a change from group cross-stratified sandstone at the base to siltstone or muddy siltstone at the top, the cyclic pattern in the Clematis Group is clearly not the normal fining-upwards cycle of a meandering stream. The pattern is, however, similar to that described by McGowen & Garner (1970) in coarse-grained point bars formed in bed-load streams in which the channel morphology lies somewhere between braided and meandering. The lower part of the cycle (Ga),

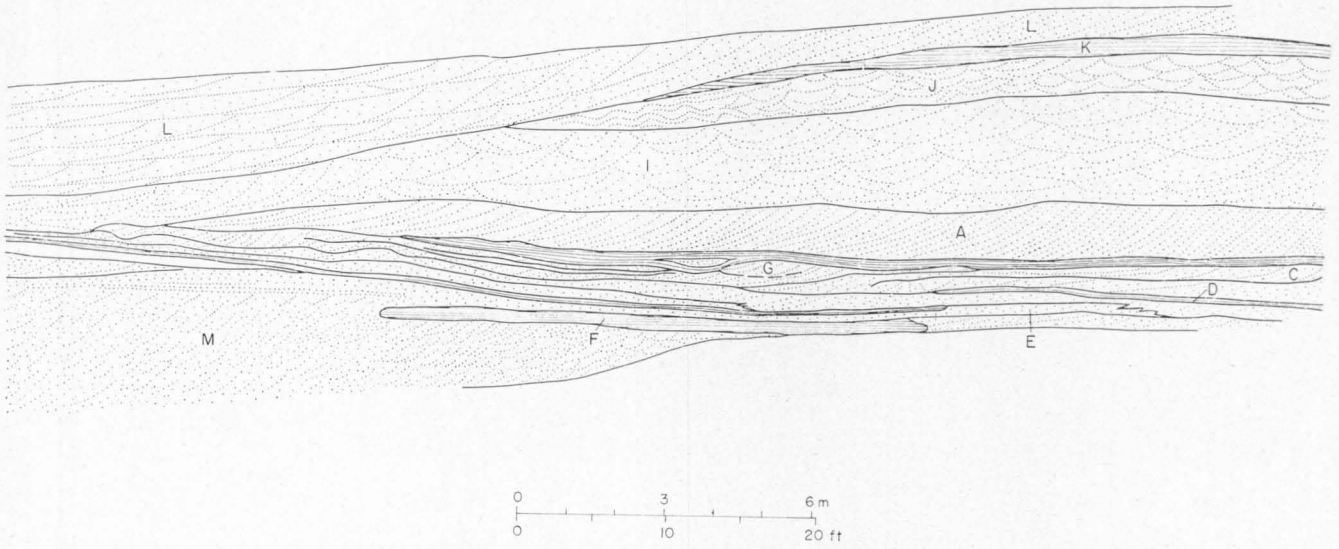


Fig. 67. Stratification in the Expedition Sandstone in Section GA05 (Spring Creek), southwestern area.

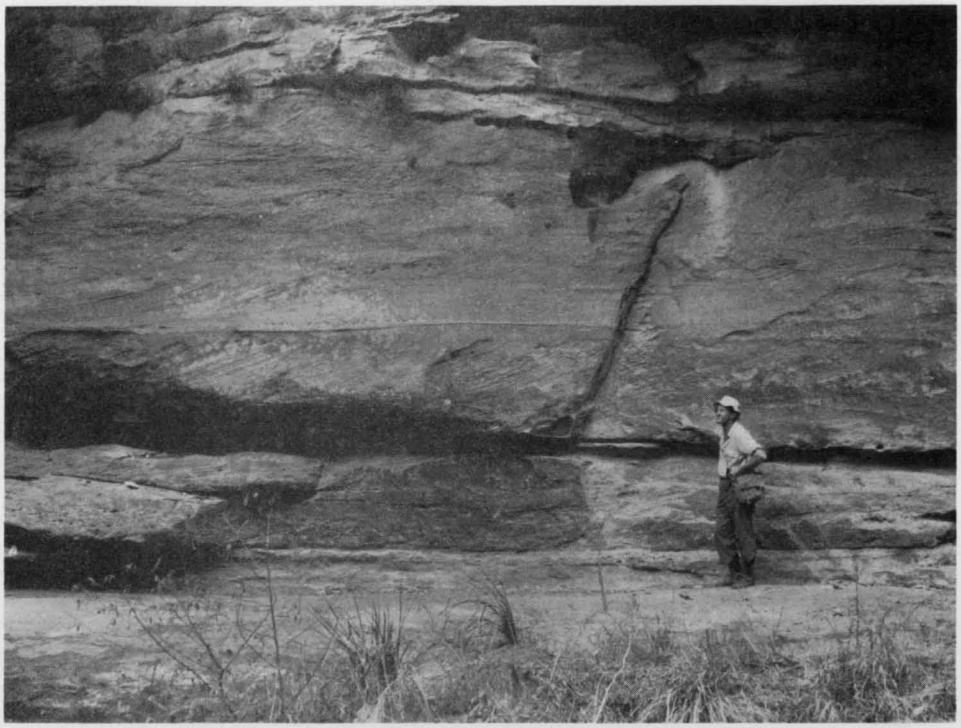


Fig. 68. Section GA05 (see Fig. 67) in the Expedition Sandstone, southwestern area. The large solitary cross-stratified unit at head level is overlain by a zone of group cross-stratified units.

consisting of group cross-stratified sandstone and minor lenses of gravel and silt, corresponds to the deposits laid down in a scour pool or lowest part of the lower bar platform. The solitary cross-stratified beds represent chute bars developed during floods by the passage of bed-load sediment through chutes cut into the upper part of the point bar. The group cross-stratified beds at the top of the sequence (Gb and Gc) were laid down on the uppermost part of the supra-platform bar and on the flood plain where beds of siltstone (L) were also deposited from time to time.

The second type of sequence based on stratification is that of the Glenidal Formation in the southwest, which is characterized by the abundance of thinly bedded group cross-stratified sandstone and sandstone with planar stratification. The unit also contains interbedded siltstone and mudstone, but no cyclic pattern has been recognized in the arrangement of beds.

The sequences dominated by sandstone consist of group cross-stratified sandstone (Gb and Gc), with lenses of siltstone and very coarse sandstone, interbedded with thick sandstone units with planar stratification. The planar stratification usually extends for considerable distances along strike with minor gentle undulations in places. The lenses of siltstone and very coarse sandstone were probably deposited in isolated pools or shallow channels in the surface of the group cross-stratified sandstone. The sequences dominated by sandstone were laid down mainly within the lower flow regime. The group cross-stratified beds represent deposits of ripples and dunes, and it can be shown by elongation function analysis (Appendix 1)

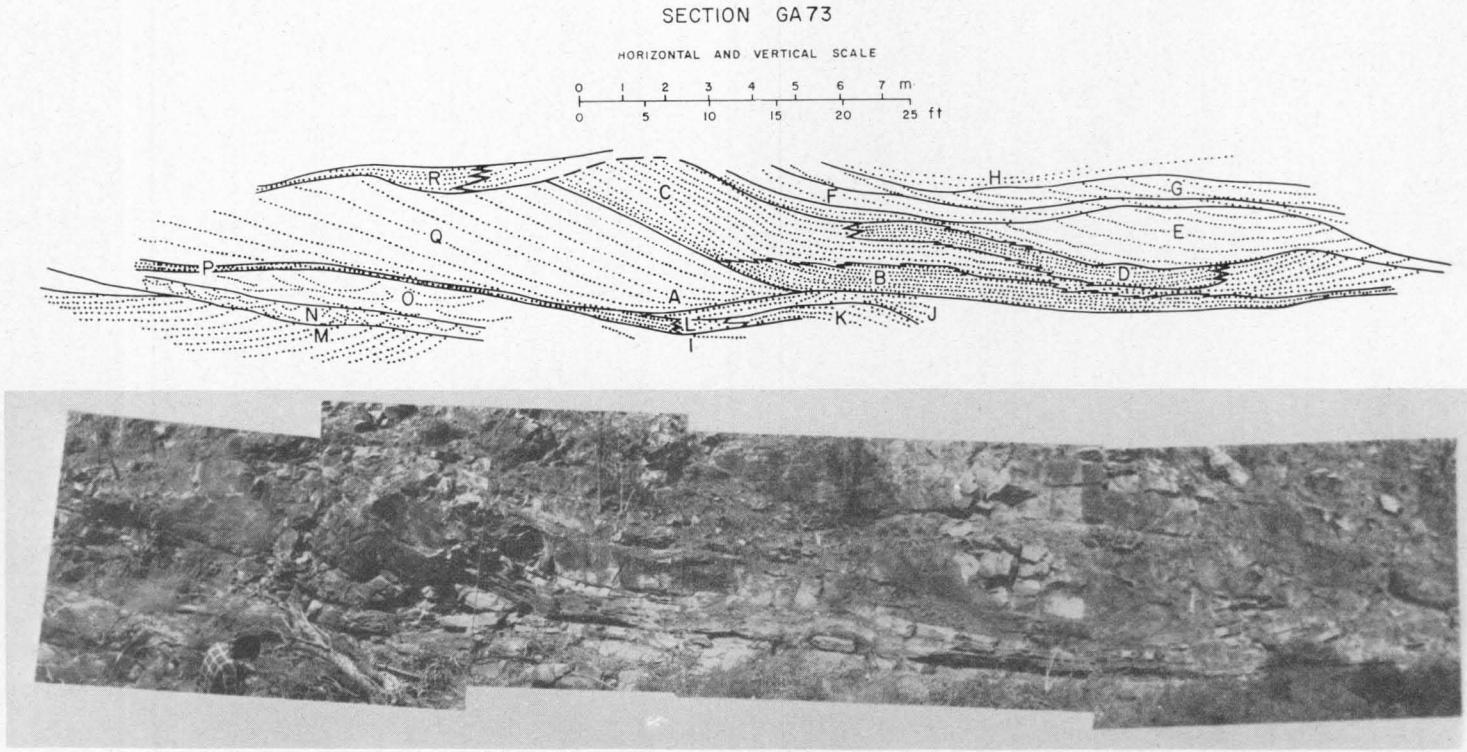


Fig. 69. Stratification within a microdelta in the Expedition Sandstone. Expedition Range, near the Dawson Highway.

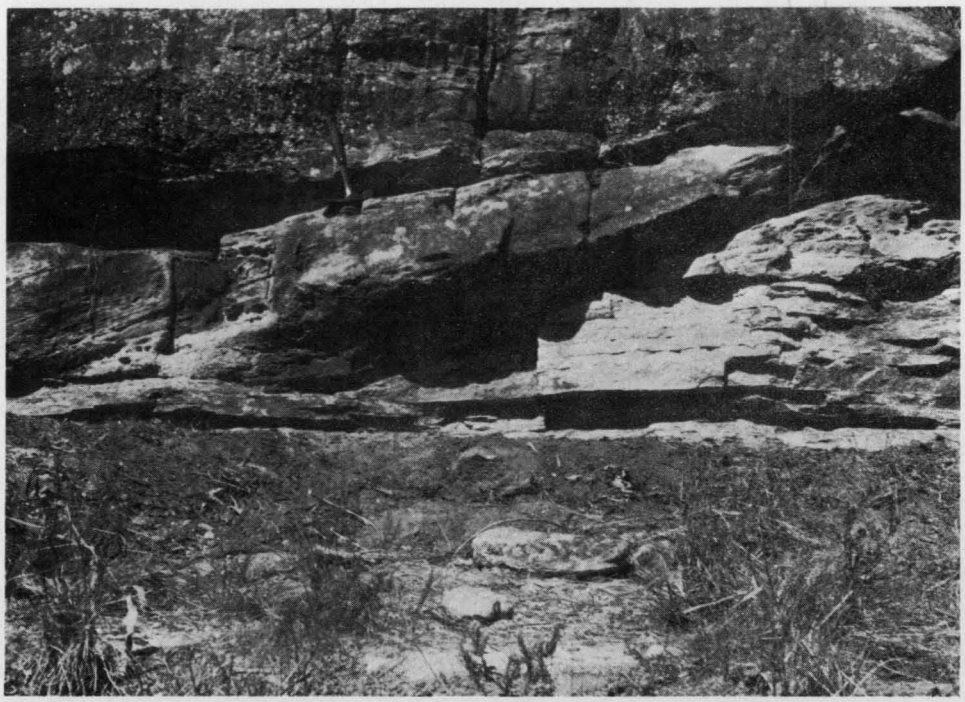


Fig. 70. Expedition Sandstone showing solitary cross-stratified sandstone unit in small erosion hollow cut in planar-stratified sandstone. Southwestern area, near Serocold homestead.

that sandstone with horizontal stratification was also formed within the lower regime of flow. Thus, as in the case of the Rewan Group, the change from group cross-stratified to planar-stratified sandstone reflects a change from laterally confined to unconfined flow. The concept is supported by the relatively great lateral extent of the planar-stratified units, which suggests that the sand was laid down over large relatively flat areas, such as flood plains. The deposition of sand deposits of this type on flood plains is not known, and McKee, Crosby, & Berryhill (1967) found that horizontally stratified sand constituted almost all the sediment deposited on the flood plain of Bijou Creek in Colorado during a recent flood. There is also evidence that parts of the flood plain were covered by shallow lakes. Oscillation ripple marks due to wave motion are preserved in some of the fine sandstone beds which also contain convex hypo-relief nesting tracks grouped in patches about 10 cm in diameter (Fig. 19b). Other sandstone beds contain vertical burrows which were subsequently lined with iron oxide and filled with sand (Fig. 19a). The preservation of these organic structures indicates a relatively quiet environment, and rapid burial with suspended load or bed load transported by very weak currents. The presence of moulds of desiccation cracks in clayey sandstone with planar stratification attest to periods of subaerial exposure and the transient nature of standing bodies of water.

The third type of sequence, based on stratification, within the Clematis Group is that of the Expedition Sandstone in the north: there are no beds of horizontally stratified sandstone, few lenses of mudstone and siltstone, and fewer solitary

cross-stratified beds. In addition, there is no readily distinguished cyclic pattern in the arrangement of group cross-stratified units.

The stratification is mainly the result of the migration of dunes in the lower flow regime, and is quite different to that produced by mixed-load meandering streams in which much of the Rewan Group was laid down. Conditions were also quite different from the meandering bed-load streams in which the Expedition Sandstone was deposited in other parts of the basin. The only alternative within the fluvial domain is that of a braided stream, which is generally dominated by bed-load (Schumm, 1968); no satisfactory braided stream models are available for comparison.

A model has been provided by Williams & Rust (1969) in their description of a braided stream in the Yukon, but it has two disadvantages. Firstly, the channel described was being actively degraded, so the present-day bedforms cannot be related to those in an aggrading braided channel. Secondly, the sediment being transported by the stream ranged from gravel to silty clay, so that it is difficult to compare the model with the sandstone sequences in the Clematis Group, particularly as the model is based on vertical grainsize differentiation. The model proposes

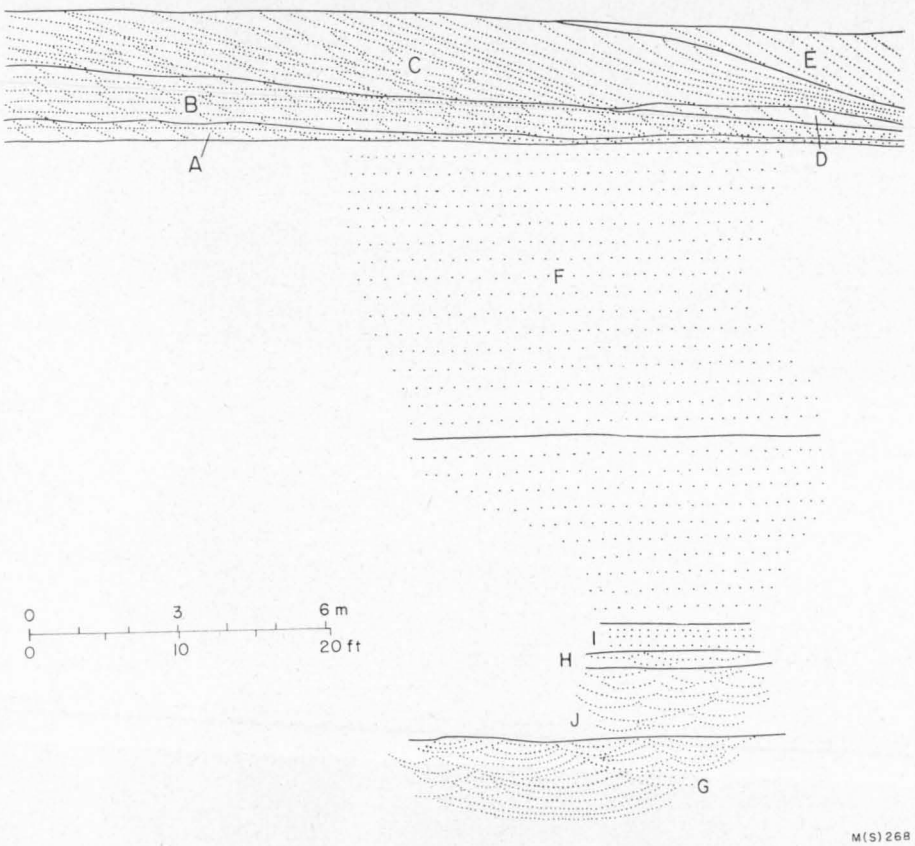


Fig. 71. Stratification in the Expedition Sandstone in Section GA55, central area. Beds B and C are doubly cross-stratified.

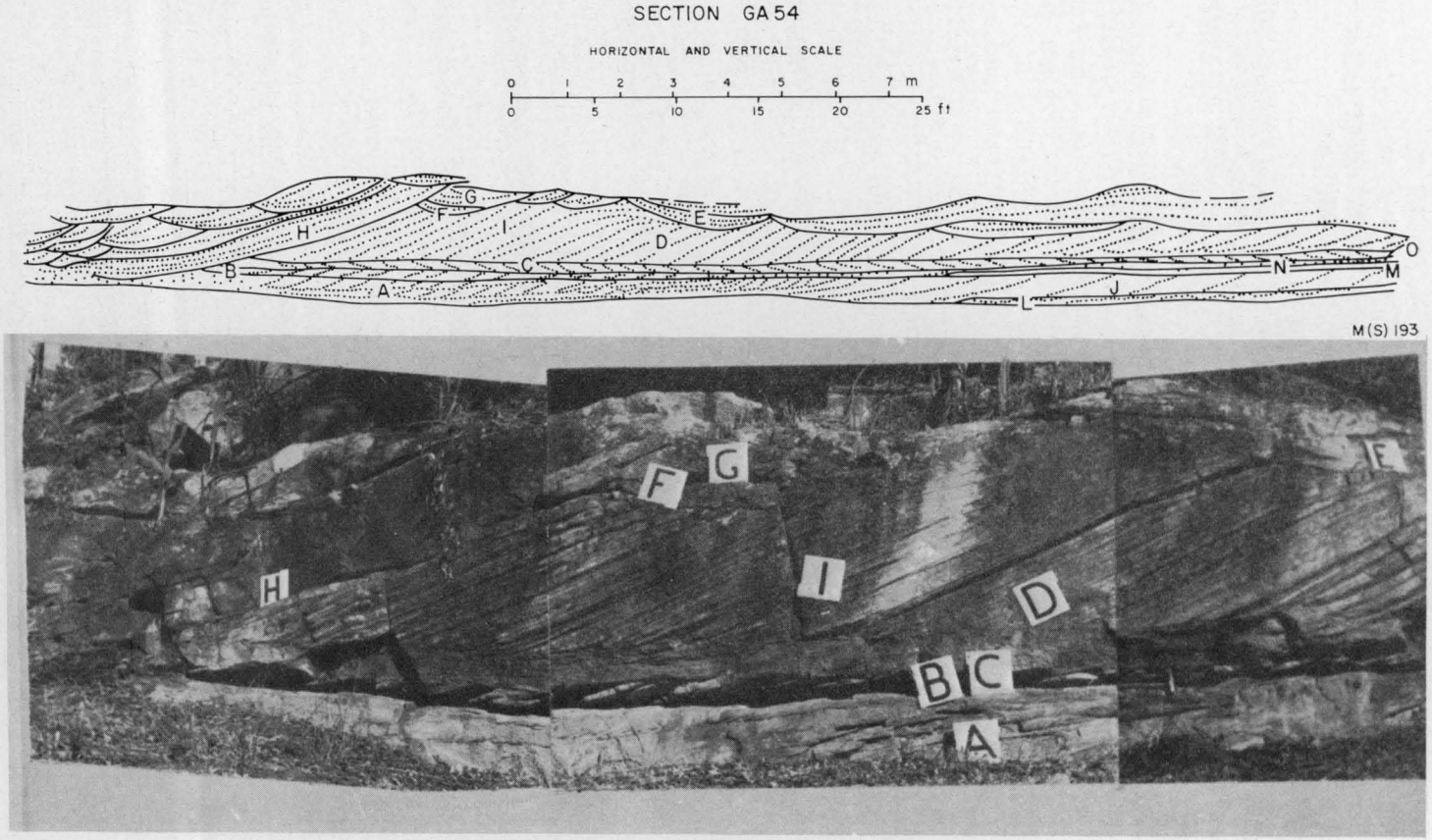


Fig. 72. Expedition Sandstone showing solitary cross-stratified sandstone unit (D & I) overlain by a group cross-stratified unit (E, F, & G). The sequence was formed by the progradation of dunes over the avalanche face of a microdelta. Raby Creek area.

progradation of interbedded sand and silt or sand over gravel deposited in the lower part of the channel, followed by progradation of interbedded silty clay over the interbedded sand and silt. The result is essentially a fining-upwards sequence. Coleman (1969) has described the braided river system of the Brahmaputra, but the description does not include a sedimentation model for braided streams. In fact Coleman considers that detailed characterization of braided stream deposits would be misleading and unrealistic because of their complexity. By combining the results of the few studies that have been made of sedimentation in braided channels, however, it is possible to obtain some indication of the nature of stratification to be expected under these conditions.

Cross-stratification is the most common sedimentary structure recorded in modern braided streams, but it is difficult to generalize on the type of cross-stratification commonly developed because of the multiplicity of nomenclatures and classifications used. Abundant small-scale cross-stratification (less than 5 cm high) has been reported by Williams & Rust (1969), who relate it to the great variety of ripple marks found in fine sand and silt in stream channels. Coleman (1969) also reports an abundance of small-scale cross-stratification, although he includes structures from a few centimetres to over a metre. In particular, he noted that ripple-drift cross-lamination is very common; he attributes this to the advance of small-scale ripples over one another where an 'over-abundance of sediment leads to constant sand fallout during the migration of bedforms'. Small-scale cross-stratification was also found in the upper part of megaripples, and Coleman postulated progradation of small ripples over the larger bedforms in such a way as to retain the original wave form. Doeglas (1962) records small-scale cross-stratification in medium-grained sand of braided tributaries of the Rhone, and it is also recorded by Sarkar & Basumallick (1968) from a channel island in the Barakar River.

So called 'large-scale' cross-stratification is recorded by Coleman (1969) as the internal stratification of large bedforms such as dunes and sandwaves, ranging from 7 to 18 m in height. The cross-stratification forms sets up to 2 m thick and cosets up to 6 m thick. Williams & Rust (1969) have also recorded abundant large-scale cross-stratification in trough-shaped and tabular sets, but they related the structure to the movement of 'bar-avalanche face topography'. Ore (1964) in his review of braided stream deposition, found that although braided stream deposits are characterized by foreset, bed roughness, and trough-fill cross-stratification, foreset cross-stratification is the most common of the three. Ore's studies, like those of Williams & Rust (1969), were based on degradational systems, where transverse bars are much more likely to form because the initiation of microdeltas is aided by erosional events.

Horizontal stratification of sand-size material is not often recorded in the deposits of braided streams. Ore (1964) has postulated deposition of the coarser elements of the bed-load and the subsequent trapping of the finer material to form horizontally stratified longitudinal bars, but he has pointed out that this type of deposit commonly appears to be unbedded, or alternatively that as the proportion of fine-grained material increases, foreset lamination develops on the downstream end of the bar. Coleman (1969) has reported that horizontally stratified sand is present in channels, and he suggests that it was deposited from rapidly migrating and aggrading trains of exceedingly small bedforms. Presumably this would take place in the lower flow stage. Doeglas (1962) recorded rare horizontal stratification of gravel and fine sand through vertical accretion on tops of sand bars.

Very few other sedimentary structures have been reported in descriptions of braided streams. Coleman (1969) has emphasized the abundance of contorted laminae, both in banks, where it is associated with bank collapse, and in the channels, which contain overturned foresets, flow rolls, and convoluted lamination. Coleman also noted the occurrence of thin sequences comprising, from bottom to top, parallel laminations, ripple-drift cross-laminations, contorted laminations, sharp erosional contacts, and horizontally laminated fine sands. This sequence was interpreted as representing increasing current strength, and was also found in point-bar deposits of the Mississippi (Coleman & Gagliano, 1965). Williams & Rust (1969) have noted the abundance of current crescents downstream from pebbles in stream channels, and silt volcanoes on the slopes between bars and channels. Neither of these structures can be regarded as diagnostic of the braided stream environment.

The stratification preserved in the Expedition Sandstone in the northern part of the basin could have originated in a braided stream environment, but there is no conclusive evidence for this based on stratification alone. The group cross-stratification, which is so common in the formation, was formed as a result of the migration of ripples, dunes, and sand waves, which is the predominant process of sedimentation in braided streams. The stratification in the Expedition Sandstone in the northern area is similar to the illustrations given by Coleman (1969) of the internal stratification in sand waves. Even if exactly the same, it is not diagnostic of a braided stream. Contorted laminae and overturned cross-stratification, similar to structures described by Coleman, are present in the Expedition Sandstone on the Redcliffe Tableland, but they are by no means common, and again, as Coleman has pointed out, they are not diagnostic of braided channels. Thus, although they are not diagnostic, the structures present are those of braided channels, and furthermore the scarcity of other sedimentary structures, including horizontal stratification, and the absence of flood-plain deposits provides negative evidence in support of the comparison.

Comparison with Sequences of Non-fluvial Environments

Rewan Group

It has been shown that the most of the sedimentary rocks in the Rewan Group were laid down in a meandering mixed-load fluvial system. However, Land & Hoyt (1966) have pointed out that the deposits in a meandering estuary are almost identical with those of its fluvial counterpart, and that the estuarine deposits can only be distinguished by the effects produced by reversals of current flow, and by the presence of a marine fauna. Much of the Rewan Group contains no fossils at all, so the absence of a marine fauna is inconclusive. The reversing tidal flow in a meandering estuary is reported to produce orientation roses in cross-strata, with unequal maxima diametrically opposed and with very little dispersion. Unimodal distributions are common in the Rewan Group (Fig. 73), and where the distribution is bimodal the second mode is never diametrically opposed to the first, so it seems unlikely that the beds were deposited in an area subjected to reversing current flow. Furthermore, as in the case of the Expedition Sandstone, there is no evidence of coastal or shoreline deposits, such as those laid down in a beach environment. Thus, although on the evidence of stratification alone the possibility of deposition in a tidal estuary cannot be ruled out, it does appear to be unlikely.

Expedition Sandstone

It has been shown that the cyclic sequences within certain parts of the Expedition Sandstone are similar to the type of vertical profile found in a meandering bed-load stream. In the northern part of the basin, however, no pattern of sedimentation has been recognized, and the environmental interpretation is based mainly on the presence or absence of certain types of stratification. The beds are believed to have been laid down in a braided stream environment, but many modern studies have emphasized that sand bodies with high-angle cross-stratification can be deposited in a shallow marine environment as a result of the action of longshore

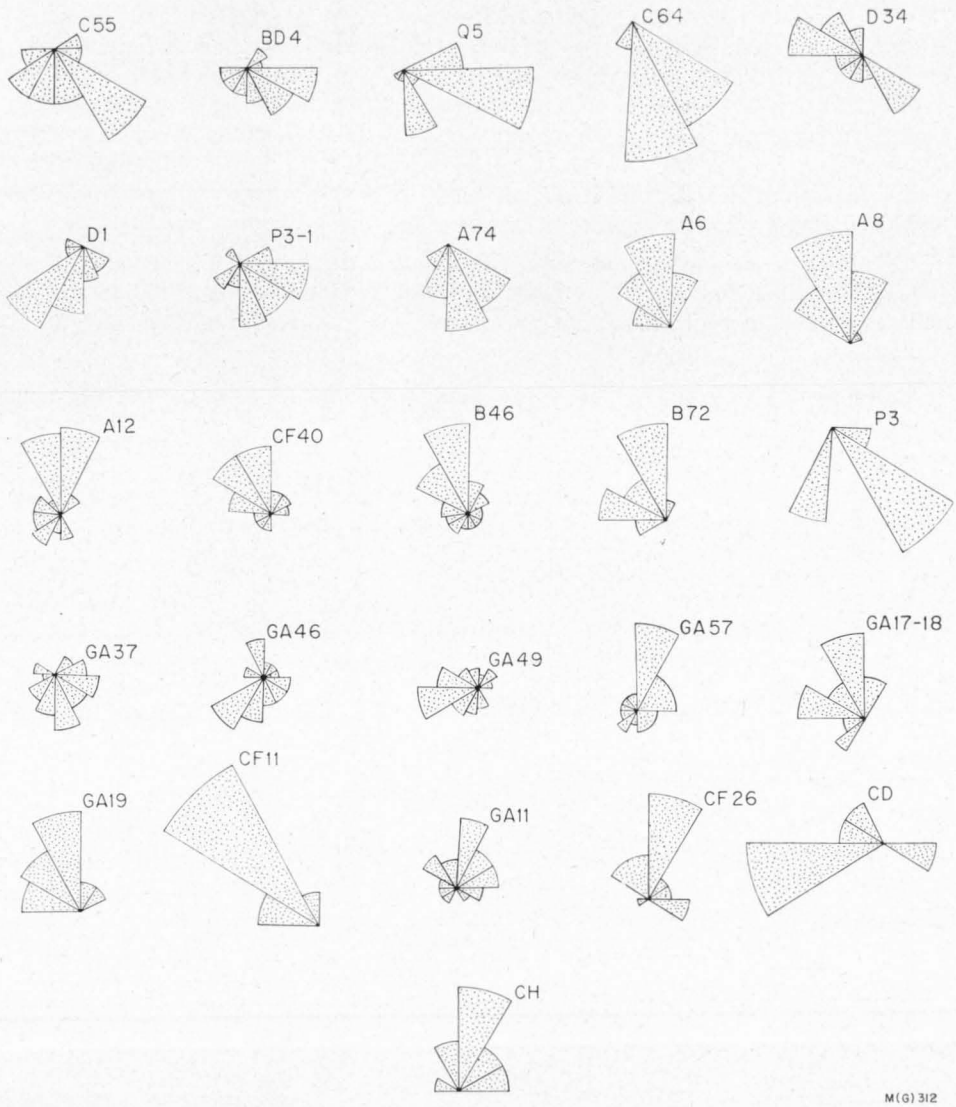


Fig. 73. Azimuthal distribution of cross-stratification in the Rewan Group.

and tidal currents. In all cases the cross-stratification is the result of migration of bed roughness structures, ripples, dunes, and sand-waves, which presumably differ little from those found in channels of a large braided stream. Thus on the basis of stratification of sandstone alone it is impossible to differentiate between these continental and marine environments. Consideration of the associated facies, however, indicates that it is most unlikely that any part of the Expedition Sandstone was deposited in a marine environment.

The most common sites of accumulation of sand with high-angle cross-stratification in a shallow marine environment are within barrier island complexes, tidal estuaries, and tidal deltas. Sedimentation within the barrier complex has been discussed by Bernard & Le Blanc (1965) and Scott, Hayes, Andrews, & Behrens (1964), and a model was proposed by Davies, Etheridge, & Berg (1971). High-angle cross-stratified sand is deposited only in tidal channels within the upper shoreface-beach environment, and in an aeolian environment. The Expedition Sandstone is too coarse to have been deposited in an aeolian environment. It could possibly have been deposited in tidal estuaries, but there are no indications in the Expedition Sandstone, or in the formations above or below, of the lower shoreface facies, which consists of interlaminated silt and clay, or of the middle shoreface facies of burrowed and unstratified sand; nor is there any sign of beach deposits.

High-angle cross-stratified sand can be deposited by tidal currents; Klein (1970) described the depositional and dispersal dynamics of intertidal sand bars, and listed 13 diagnostic characteristics of tidal sand bars. Some of these cannot be

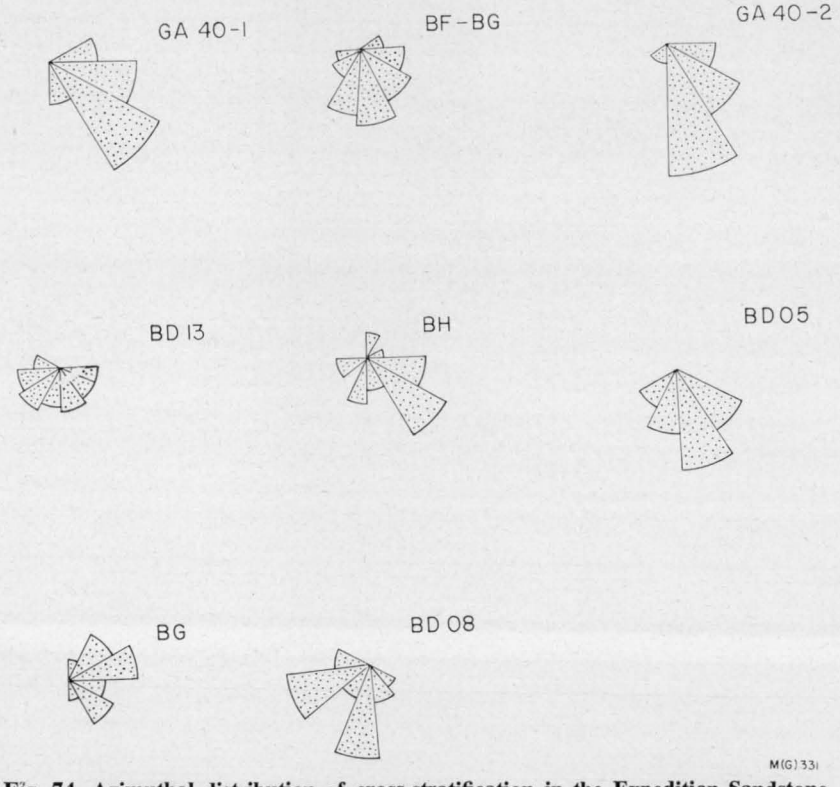


Fig. 74. Azimuthal distribution of cross-stratification in the Expedition Sandstone.

checked in the outcrops of the Expedition Sandstone. Of the remainder, three can be related to features observed in the formation, and about six cannot be related. Sharp erosional boundaries between sets of cross-strata, which Klein relates to constructional and destructional phases of tidal currents or stream erosion, are present. In most localities there is a unimodal direction of orientation of cross-stratification (Fig. 74); in the tidal environment this is produced by the domination of either flood or ebb tidal currents. There is a complex organization of sets of cross-strata in the Expedition Sandstone, which in the tidal environment is produced by the deposition of sand in sand waves, accompanied by the migration of the dunes upslope. However, rounded upper set boundaries have not been observed in the Expedition Sandstone, and a unimodal distribution of the dip of the cross-stratification is indicated by the dips (Fig. 75) in most localities. Four of the criteria of Klein (1970) relate to the shape and orientation of ripples; no ripple marks are preserved in the Expedition Sandstone and small-scale cross-stratification which would have been produced by the migration of ripple marks is rare. All the criteria which do apply (sharp erosional set boundaries, unimodal direction of cross-stratification, and arrangement of sets in sand waves) can be expected in a braided stream environment.

Orientation of Cross-Stratification

In the palaeocurrent map of part of the basin presented by Olgers et al. (1966) the palaeocurrents for the Clematis Group are shown as flowing eastwards across the western limb of the Mimosa Syncline and swinging south on the eastern limb. No attempt was made to analyse parts of the group separately and the

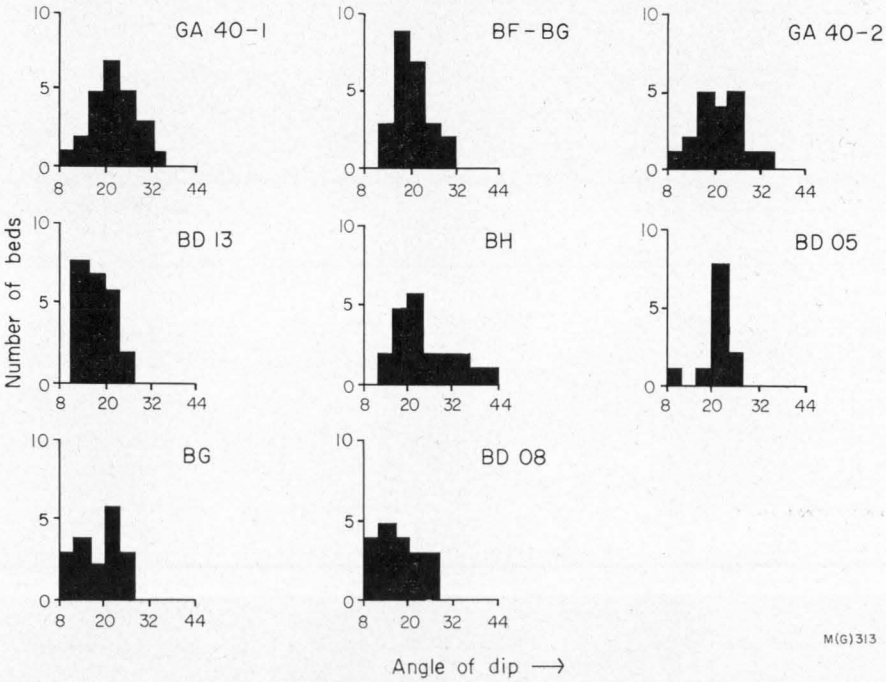


Fig. 75. Histogram of dip angle of cross-strata.

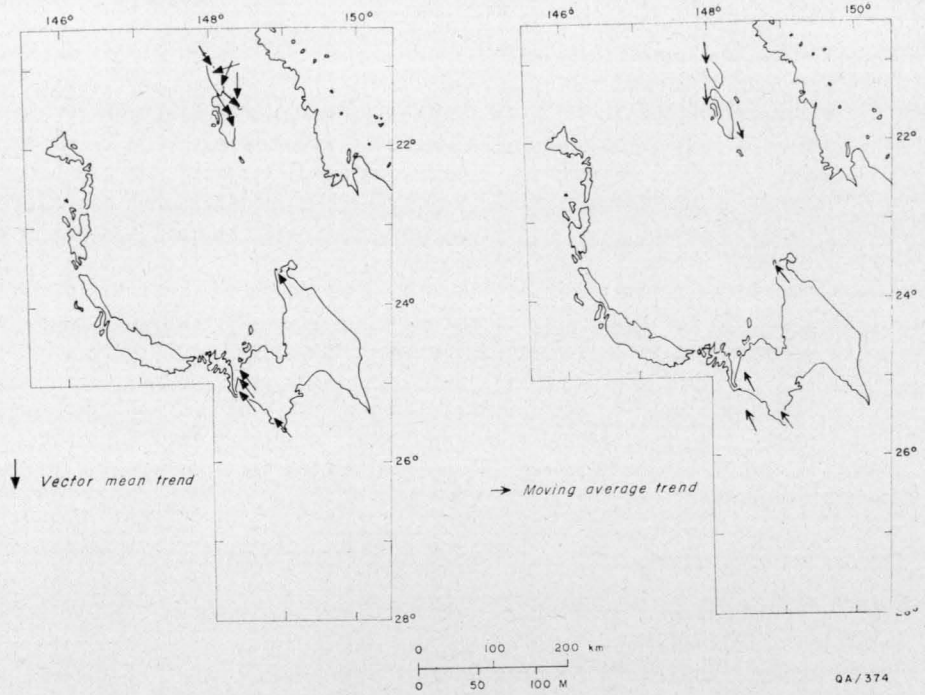


Fig. 76. Orientation of cross-stratification in the Sagittarius Sandstone.

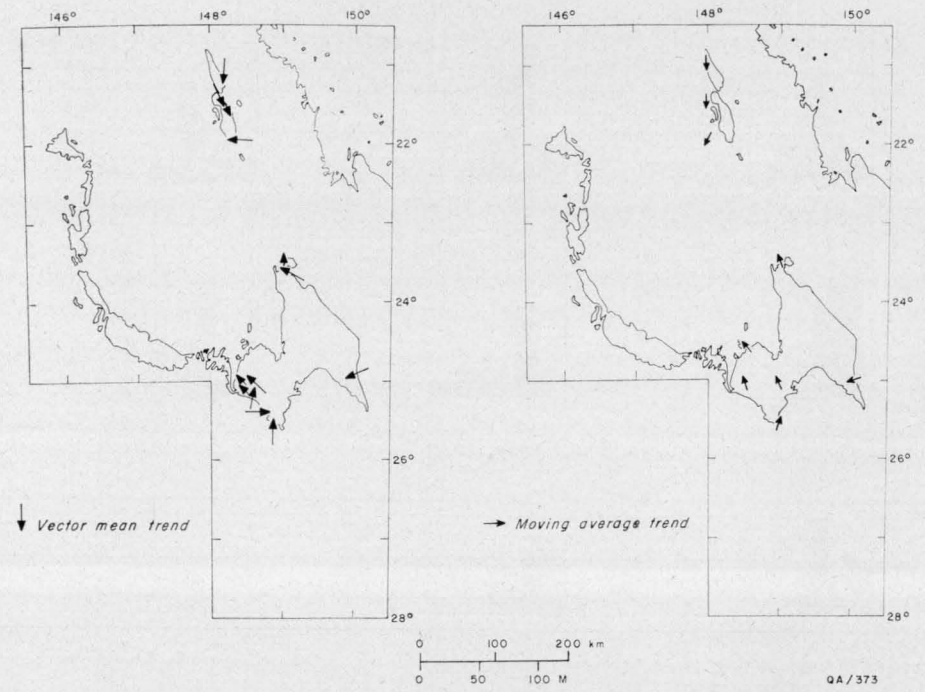


Fig. 77. Orientation of cross-stratification in the Arcadia Formation.

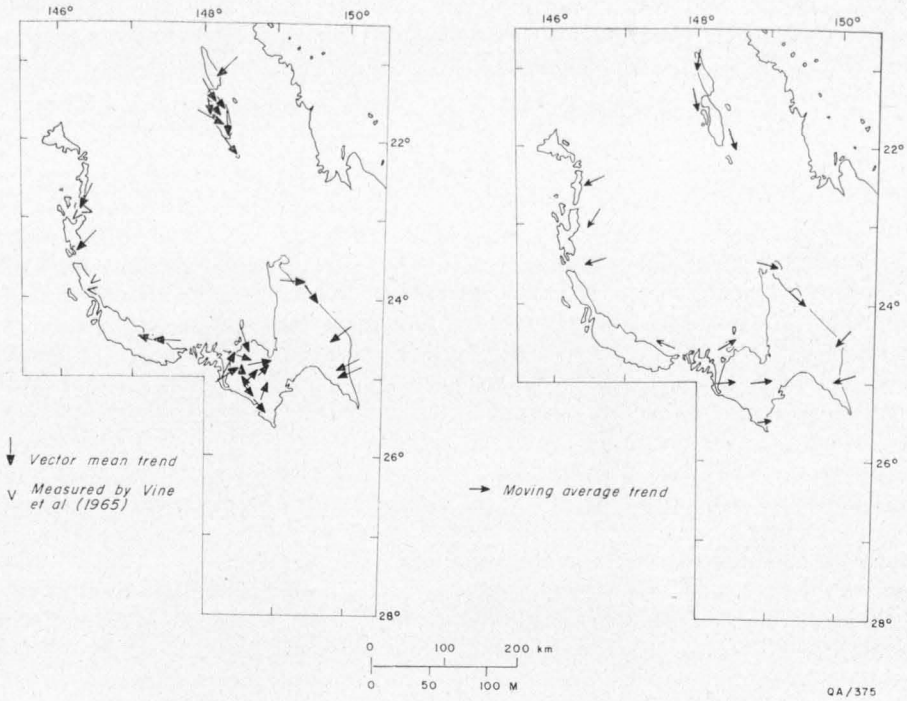


Fig. 78. Orientation of cross-stratification in the Glenidal Formation.

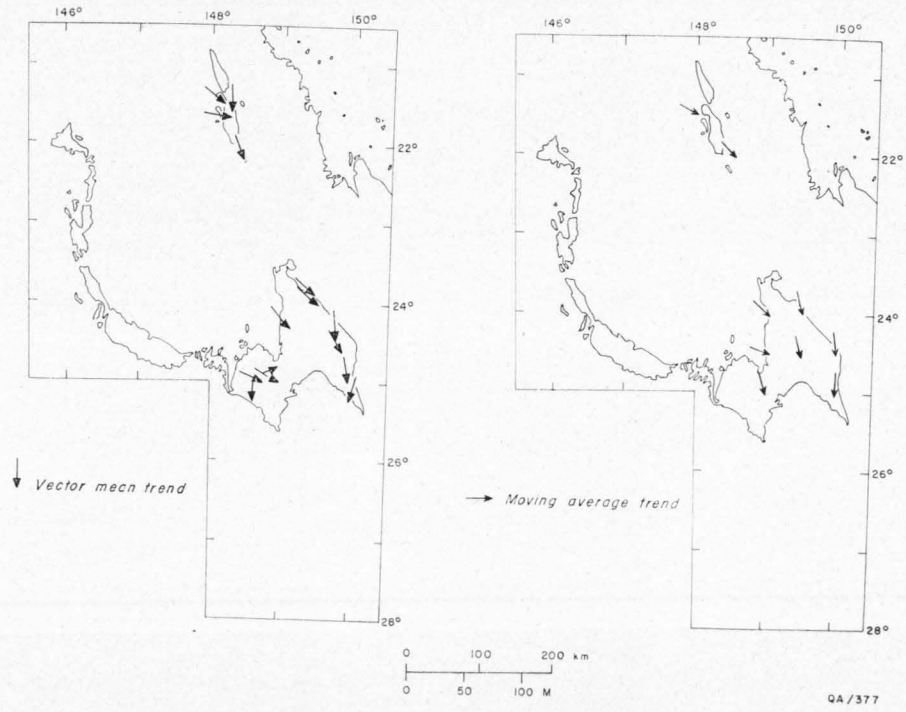


Fig. 79. Orientation of cross-stratification in the lower part of the Expedition Sandstone.

stratigraphic position of the measurements was not recorded. The aim of the present study was to detect changes in the direction of the palaeocurrents within each unit over the whole basin, and between units in each area.

Regional Trends of Palaeocurrents

During the deposition of the Sagittarius Sandstone the palaeocurrents (Fig. 76) were directed towards the central part of the basin from the north and southwest; in the overlying Arcadia Formation they were directed in much the same way (Fig. 77), although there is also evidence of a flow towards the west in the southeast. The combined results (Fig. 81a) show that the Rewan Group was derived from three separate source areas to the south, east, and north. The currents flowed towards the central area, but because of the lack of outcrop it is not certain whether they were ultimately directed to the west or east, if indeed there was any flow away from the centre. The westerly trend in the southwest, and near Bluff to the north of the Dawson Range, suggests that a westerly flow is the most likely. This pattern is not unlike the indicated directions of flow in the underlying coal measures (Fig. 4), except that they were directed more towards the north in the southeast and more westerly in the southwest. The basic pattern of flow towards the central area, and thence probably westwards, is the same. The interpretation of the direction of transport in the Permian and Triassic sediments are complicated by the folding of the sequence and the compression of the basin in an east-west direction by folding and faulting. Folding is so intense in the central area that it is

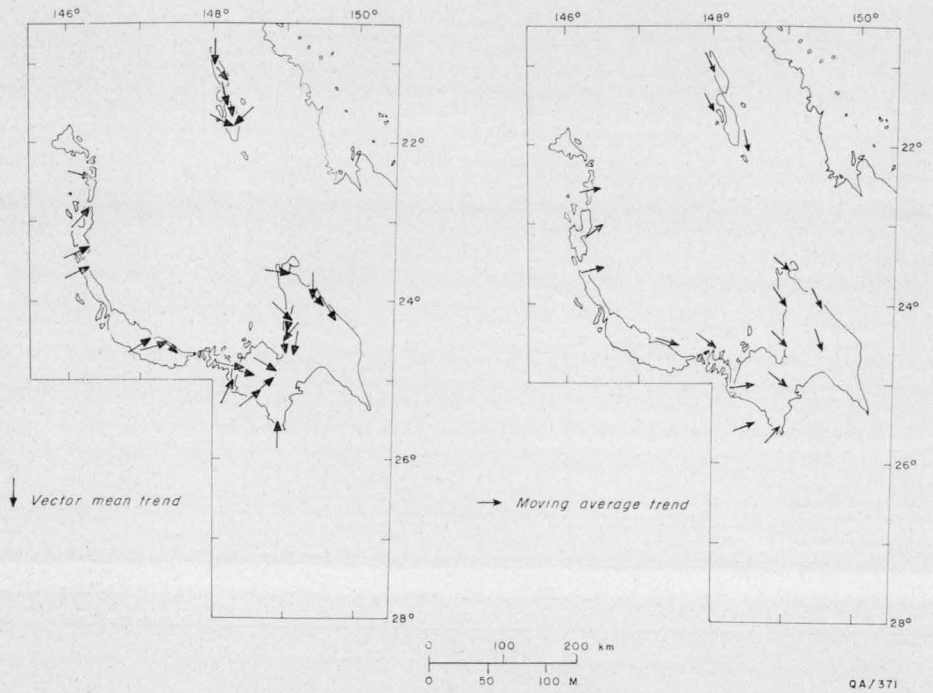


Fig. 80. Orientation of cross-stratification in the upper part of the Expedition Sandstone.

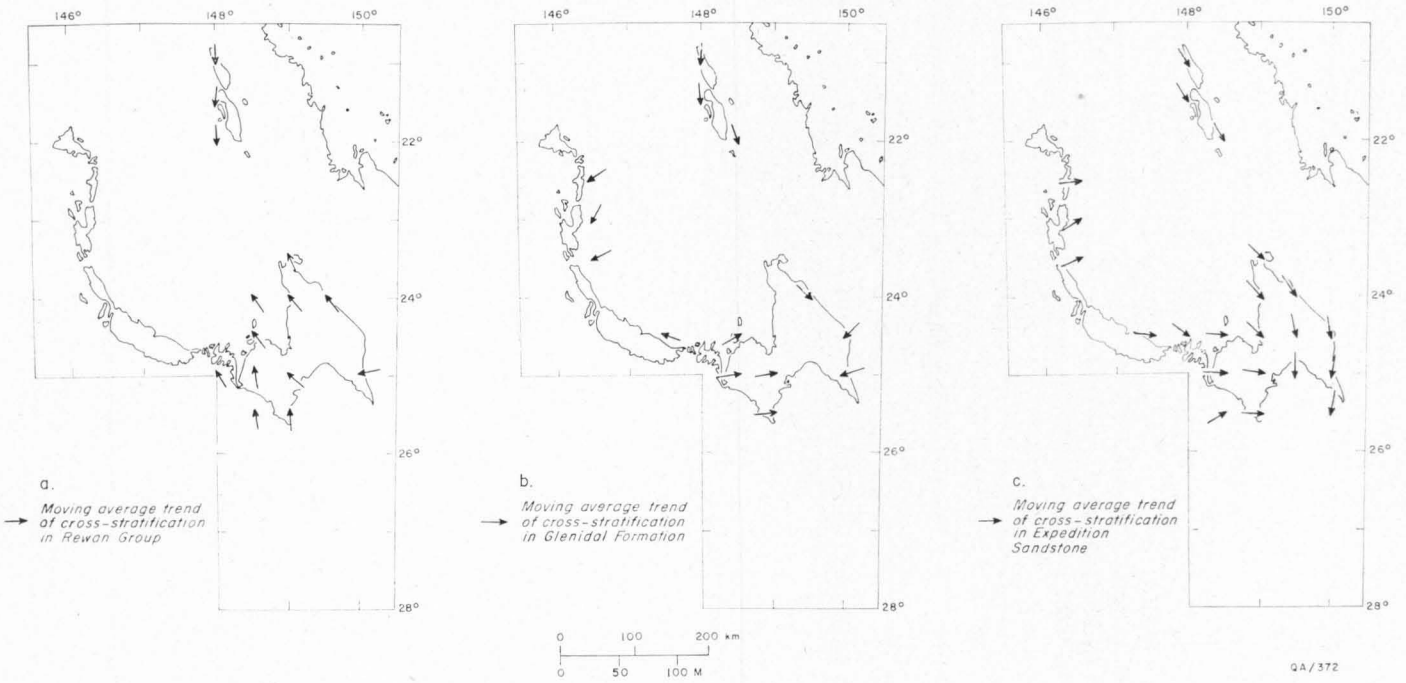


Fig. 81. Summary of cross-stratification trends in the Rewan and Clematis Groups.

impossible to reconstruct the original slope of the basin. The trends of cross-stratification on the eastern side of the basin can be regarded as applicable to the sediments originally laid down farther east. The prevailing currents during the deposition of the Glenidal Formation (Fig. 78) continued to flow south in the northern part of the basin, and to the west in the southeast, but elsewhere there appear to have been radical changes in direction compared with those in the underlying units. In the southwest, the currents were directed to the east instead of towards the northwest, and the same change can be seen in the central part of the basin. Despite the easterly flow in the southwest, the palaeocurrents farther west at Mantuan Downs were to the west. Confirmation of this trend is found in the Dunda Beds, which are equivalent to the Glenidal Formation on the eastern margin of the Galilee Basin, where cross-stratification indicates a southwesterly flow. If the Glenidal Formation and the Dunda Beds are coeval, it appears that there was a dividing range between the two basins in the vicinity of longitude 148°E at this time. This appears to be confirmed by the absence of the Rewan Group in the area between Mantuan Downs and the southwestern part of the Bowen Basin, which was presumably being eroded at this time.

The lower part of the Expedition Sandstone is present only in the Bowen Basin. The currents responsible for the distribution of the sediment (Fig. 79) were directed essentially in the same directions as in the underlying Glenidal Formation. In the north there appears to be a slight swing to the east, but this is not regarded as significant. In the south there is a slight change to a more southerly direction on

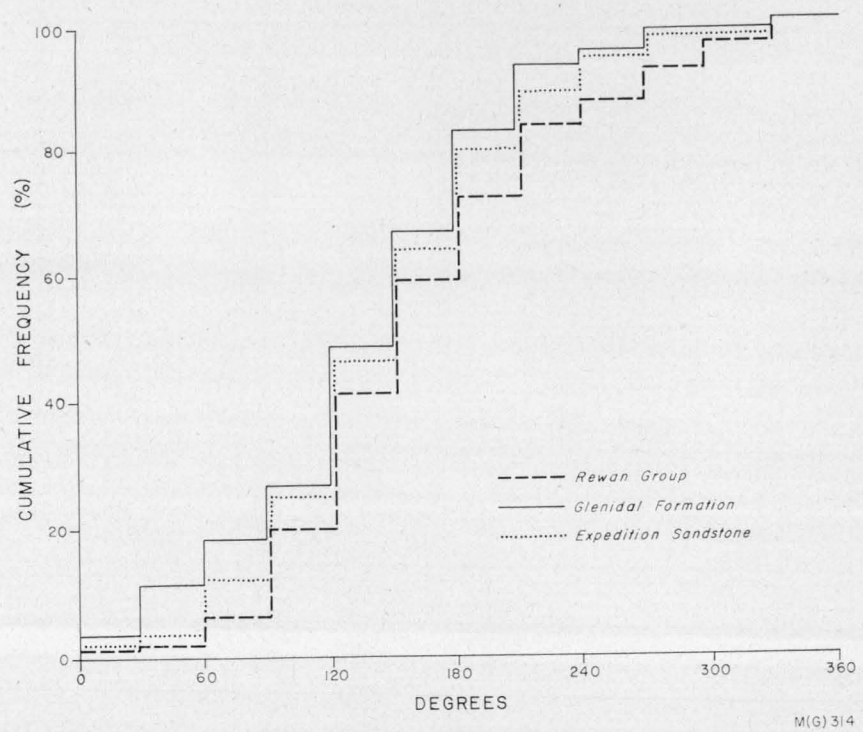


Fig. 82. Cumulative frequency histogram for azimuths of cross-stratification in units in the northern area.

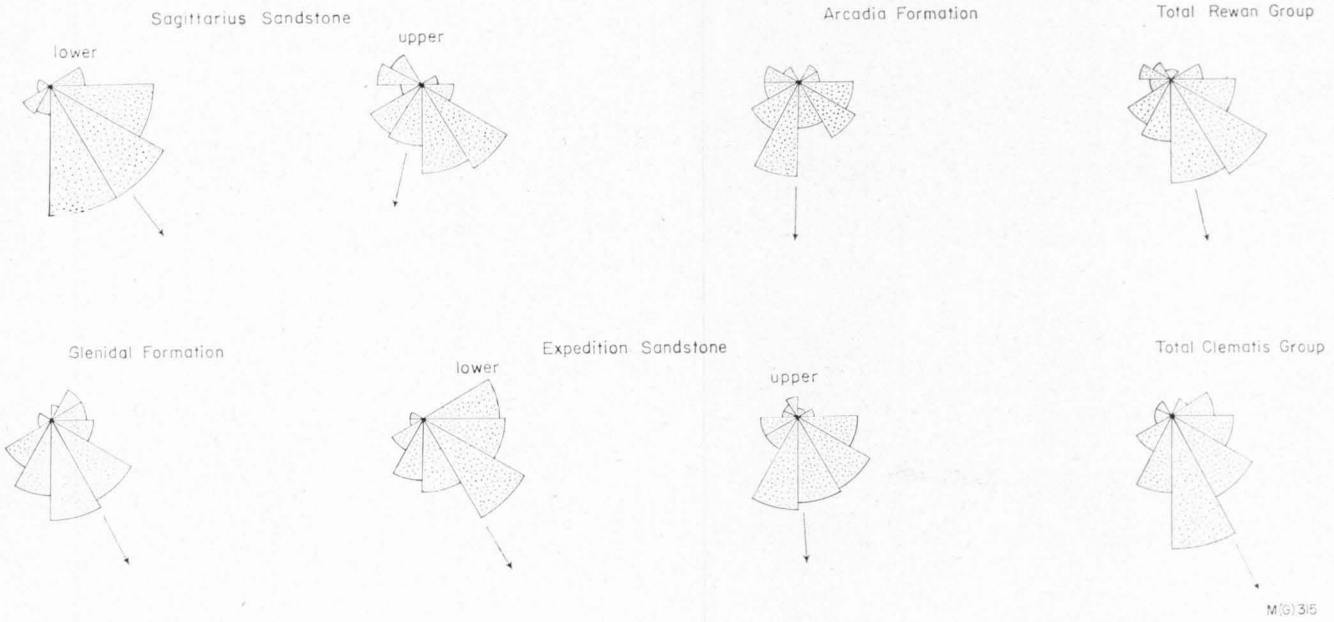


Fig. 83. Azimuthal distribution and vector means of cross-stratification in units in the northern area.

both sides of the basin, although material was probably still being derived from both the east and west. The upper part of the Expedition Sandstone can be recognized on the eastern margin of the Galilee Basin, and in all but the southeastern part of the Bowen Basin. The palaeocurrents were directed eastwards from the Galilee Basin and southwards from the northern margin of the Bowen Basin (Fig. 80). The main flow in the southern part of the exposed basin was towards the southeast across the western limb of what is now the Mimosa Syncline.

One of the most important facts to emerge from the analysis of palaeocurrents in the basin is that the direction of sediment transport in the north varied little throughout the deposition of the Rewan and Clematis Groups (Fig. 81). This can be demonstrated by application of the Kolmogorov-Smirnov test as described by High & Picard (1971). The maximum difference between cumulative frequency curves for the Rewan Group, Glenidal Formation, and Expedition Sandstone can be graphically calculated from Figure 82. Each represents the mean curve derived from a number of localities in each unit, calculated by taking the mean percentage frequency of occurrences with each 30° segment. To give equal weight to the three main divisions of the Rewan Group in the northern part of the basin, the results from four localities from each unit were used. Nine localities were included for the Glenidal Formation, and ten for the Expedition Sandstone.

The maximum difference between the curves for the Rewan Group and Glenidal Formation (d_n) is 11.0°. The minimum expected difference assuming that each curve is drawn from a different population (null hypothesis) is calculated from the formula $d_{0.05} = 136 \sqrt{1/n_1 + 1/n_2}$, where n_1 and n_2 are the number of measurements for each curve, and the subscript of d represents the probability of error. In this case $d_{0.05}$ is equal to 58.5, which is greater than the maximum observed difference between the two curves and therefore suggests that the two samples are drawn from the same population. In a similar test comparing the Glenidal Formation with the Expedition Sandstone in the northern part of the basin, $d_n = 6.6$ and $d_{0.05} = 58.2$, and it is again concluded that the directions of sediment transport are the same. The similarity of direction is also illustrated graphically in Figure 83.

Variability of Azimuthal Distribution

No simple pattern emerges from a study of the standard deviation of cross-stratification for each unit. Application of Students 't' test to means calculated for sets of standard deviation from various units has revealed that there is no significant difference of means for any two units at the 95 percent confidence limit, except in the case of the Rewan and Clematis Groups in the northern part of the basin. The mean standard deviation in the Rewan Group in the northern area is significantly higher (61°) than those of the Glenidal Formation (46°) or Expedition Sandstone (49°).

Variation in the orientation of cross-stratification can be used to determine stream gradients in a fluvial regime, and to distinguish between marine, fluvial, and aeolian environments of deposition. Potter & Pettijohn (1963) cite the work of Hamblyn (1958), who found that the standard deviation in several modern streams ranged from 20° to 83° depending on the degree of meandering, which is presumably related to gradient. If the sediments of the Rewan and Clematis Groups in the northern part of the basin are fluvial the decrease in dispersion of the direction of cross-stratification could be related to increasing gradient.

The use of this method to distinguish between marine, non-marine, and aeolian environments is beset with a number of difficulties (see Potter & Pettijohn, 1963). The method of measurement and the total area considered vary from study to study, so that it is impossible to make direct comparisons of standard deviation or variance. The dispersion of the direction of cross-stratification in marine sequences is generally greater than in fluvial and aeolian sequences, but more data are required to confirm this trend. At this stage, therefore, the variability of the cross-stratification in the Clematis and Rewan Groups cannot be used to define the environment of deposition.

INTEGRATION OF RESULTS

Controls of Sedimentation

Few attempts have been made to explain the causes of the changes from coal measures to sediments of the Rewan Group, or from the Rewan to the Clematis Groups. Whitehouse (1955) suggested that the Clematis Group and other similar Mesozoic units in Queensland were laid down in a fluvial environment with heavy seasonal runoff, in contrast to the conditions leading to the formation of certain calcareous units such as the overlying Moolayember Formation, which was laid down under quieter conditions accompanied by the accumulation of swamp soils. With regard to the change from the Rewan Group to the Clematis Group, Malone, Olgers, & Kirkegaard (1969) postulated that it resulted from: (a) a change in provenance which reduced the supply of volcanic detritus and increased the supply of quartz, and (b) a change in depositional environment from rapid subsidence and sedimentation (Rewan Group) to a slower rate of subsidence and sedimentation, which resulted in greater reworking and the deposition of more mature sediments (Clematis Group). However, there is insufficient evidence to substantiate these changes in provenance or environment of deposition.

Sedimentation in the Sydney Basin, 1100 km to the south of the Bowen Basin, produced a remarkably similar sequence, and the theories of sedimentation postulated for the Sydney Basin have to be considered in formulating a theory for deposition for the Triassic rocks in the Bowen Basin.

In his interpretation of the sedimentation of the Narrabeen Group and Hawkesbury Sandstone, McElroy (1969) postulated a subtle climatic change as the cause of the end of the deposition of the coal measures, but he also mentioned the possibility of mild tectonic influences in certain parts of the basin. McElroy envisaged deposition of the Narrabeen Group on a vast deltaic plain, with areas of piedmont deposition, traversed by one or more major river systems. With regard to the interpretation of the redbeds of the Narrabeen Group, McElroy referred to the work of Loughnan, Koko, & Bayliss (1964) and noted (a) the difficulty in ascribing any single origin to all the redbeds; (b) that the Bald Hill Claystone (part of the Clifton Sub-group) has all the attributes of a re-sorted laterite; and (c) alternating wet and dry conditions were postulated as the climate most conducive to the formation of redbeds in this area. McElroy considered that the overlying Hawkesbury Sandstone was laid down in a fluvial environment, and that the change in composition was related to increasing maturity of the sediments rather than to a change in provenance.

Conolly (1968) has rejected the fluvial origin of the Hawkesbury Sandstone, and has suggested that it was deposited in a tidal delta system which prograded

over the distributory and fluvial facies of the Narrabeen Group. He considers that the redbeds were laid down mainly as interdistributory silt and clay, which was oxidized by marine waters.

Because of the similarity of the Permo-Triassic rocks in the Sydney Basin to those of the Bowen Basin, it was necessary during the present study to consider the possibility that the Rewan Group is not continental, but that it was deposited in a marine, possibly deltaic environment, and that the Clematis Group represents the deposits of tidal delta systems which prograded over the sediments of the Rewan Group.

In the following section the influence of environment of deposition and provenance are assessed as controls of sedimentation in the development of the Permo-Triassic sequence of the Bowen Basin.

Depositional Environments—Stratigraphic and Tectonic Implications

Blackwater Group

The Blackwater Group is generally considered to have been laid down in a continental environment. The presence of fossil stumps standing in their growth position clearly indicates a continental environment for at least part of the Fort Cooper Coal Measures, but in other parts of the group the only evidence is the abundance of fossil plant material and the absence of marine fossils. The Fair Hill Formation is underlain by the Back Creek Group, which contains abundant marine fossils, and although it is presumed that the Fair Hill Formation is continental, the only supporting evidence is the abundance of large transported fossil logs. On the basis of this assumption, the Fair Hill Formation represents the first sediments to be deposited on a newly emergent land surface in the wake of a marine regression towards the south or southeast. Parts of the formation are facies equivalents of shallow marine regressive units in the northern part of the basin (Milligan, 1971, p. 77).

The marked changes in sedimentary structures and lithology in the Burngrove Formation must reflect some type of environmental change, and the palaeocurrent data suggest a change to a poorly drained, possibly endoreic, basin. The bedding characteristics indicate deposition in still or nearly still water, presumably lakes, and the presence of exceedingly well preserved delicate leaf impressions suggests that the material was not transported far from the shore. The occurrence of rare layers of mud clasts indicates occasional periods of desiccation, and the possible amphibian trails are not inconsistent with this interpretation. The abundance of very fine-grained volcanic material and the absence of coarse epiclastic detritus in the Burngrove Formation can be explained by the suitability of the lacustrine environment for the accumulation of this material without the addition of coarse epiclastic detritus: no specific period of volcanism within the Late Permian in areas adjacent to the basin is therefore suggested. The extent of the lakes formed at this time cannot be estimated from the data available. The equivalents of the Burngrove Formation on the eastern side of the basin contain laminated fine rocks indicative of a lacustrine facies, but they also contain conglomerate and coarse sandstone. It is therefore possible that the lakes, induced by poor drainage, persisted longer in the central part of the basin than in the east.

The transitional boundary between the Burngrove Formation and the Rangal Coal Measures indicates a gradual but relatively slight change in the environment.

The presence of a fining-upwards cycle consistent with models for a meandering stream has been noted by Burgis (1973). Furthermore, the structures in the interseam sediments suggest that they were deposited in flood-plain lakes formed by differential compaction of thick peat deposits. Swaine (1971, p. 43) has suggested that the high boron content of the coals from the Baralaba Coal Measures near Theodore indicates a marine influence; similar values were found in certain coals in the Sydney Basin where there is independent evidence of a marine influence. In other parts of the Bowen Basin, the low boron content of the Rangal Coal Measures and their equivalents suggests a freshwater environment of deposition.

Although both the Rangal Coal Measures and Burngrove Formation were laid down in lakes, there were important differences in the rate of accumulation of vegetal material, which was largely controlled by the rate of subsidence. The development of thick peat deposits is favoured by rapid subsidence, but if the rate is excessive the depth of water is too great for plants, and lacustrine conditions are established. It has already been suggested that lacustrine conditions persisted longer in the central part of the basin than on the eastern margin. The Rangal Coal Measures are therefore considered to be a paludal and fluvial facies which is partly equivalent to the Burngrove Formation; they were laid down initially on the margins of the basin and migrated towards the centre with time to replace the lacustrine facies of the Burngrove Formation.

Rewan and Clematis Groups

The Rewan and Clematis Groups were also deposited in continental environments. The vertical profiles recognized in both groups can be correlated with known fluvial profiles, but not with profiles from shallow marine environments, and the red mudstone of the Glenidal Formation in the northern part of the basin undoubtedly represents a palaeosol; in places both the mudstone and sandstone of the Arcadia Formation and Expedition Sandstone contain fabrics which have been modified by pedogenic processes. Finally, the only fossils found in the sequence, conchostracans, reptiles, labyrinthodonts, and plants, are of continental origin.

The stratification in the Sagittarius Sandstone indicates that it was deposited in a meandering mixed-load river system, which flowed in much the same direction as that in the underlying coal measures. There is no evidence of a significant disconformity between the coal measures and the Sagittarius Sandstone, but it is not clear from palynological evidence (de Jersey, 1970, p. 24) whether there was an ecological rather than an evolutionary control of the microfloral assemblages. It is therefore possible that the boundary between the two is diachronous, and that they are at least partly coeval. The Sagittarius Sandstone is therefore considered to have been laid down in a transitional zone between the paludal environment of the coal measures and a well drained fluvial upland. With the contraction of the paludal environment towards the centre of the basin, the basal sediments of the Sagittarius Sandstone were also laid down in the centre of the basin.

The analysis of stratification in the Arcadia Formation has shown that repeated patterns of sedimentation can be recognized in all parts of the basin. The most common cycle consists of a fining-upwards sequence, but there is also a second cycle composed of alternating group cross-stratified fine or medium-grained sandstone and mudstone. The fining-upwards sequence represents changes in the

hydraulic regime as a result of a decrease in current velocity or depth of water, and comparison with Visher's (1965) model suggests deposition in a meandering mixed-load stream. The second type of cycle in the Arcadia Formation is also considered to be fluvial, although there is generally a less marked vertical differentiation than in the fining-upwards sequence. The beds of the second cycle were probably laid down in an anastomosing stream system dominated by suspended-load deposition. The sediments deposited on the flood plains in both the meandering and anastomosing systems were buried moderately rapidly before soil profiles could be developed, with a minimum opportunity for bioturbation and translocation of clay and iron. Thus the rate of subsidence probably only slightly exceeded the rate of supply of sediment at all times, and the gradients in the drainage basin were low. As the sediments of the Arcadia Formation spread away from the margins of the basin they gradually replaced the sediments of the Sagittarius Sandstone without a major disruption of the drainage system. The ecological changes within the basin hinge on the decreased rate of subsidence relative to the rate of sedimentation, which resulted in higher stream gradients, lower water-tables, and desiccation between periodic floods.

At the initiation of sedimentation leading to the deposition of the Glenidal Formation the regional drainage system was reorganized as a result of a decrease in the rate of subsidence of the basin relative to the rate of supply of sediment along the western and northern margins. In the southwest there was a radical change in the direction of the currents from northwest to east, and in places the type of flood-plain sediment laid down changed from mud to sand. The disruption of the regional slope in this area was responsible for the formation of shortlived local base levels and the deposition of minor lacustrine and semi-paludal beds. At this time the southwestern area was separated from the Galilee Basin by a ridge along the line of the Anakie Inlier.

In the northern part of the basin, the basal part of the Glenidal Formation was laid down without any change in the direction of the dispersal system. The relative decrease in the rate of subsidence created an environment in which soil profiles were developed on the fine flood-plain material laid down by the meandering bed-load streams. Much of the finest suspended load was carried farther south and laid down, together with fine sediment from the west, in the southeastern part of the basin, which continued to subside faster than the sediment was supplied.

With a further decrease in the rate of subsidence in the basin, and the continued supply of material from the northwest, and possibly from the northeast, coarse sediment accumulated at the margins of the basin and gradually spread southwards behind the sediments of the Glenidal Formation. The steeper stream gradients, resulting from the disparity between the rates of sediment supply and subsidence, promoted the development of braided stream channels in the northern part of the basin; elsewhere, meandering channels, characterized by bed-load deposition and by chute bars on the upper part of point bars, were formed.

Erosion of the divide along the line of the Anakie Inlier eventually led to the redirection of the drainage in the eastern part of the Galilee Basin. In the last stage of weathering of the divide very coarse and quartz-rich gravel accumulated on the western side of the Bowen Basin. At about this time, renewed uplift in the southeastern provenance areas resulted in the deposition of petromictic conglomerate (lowest part of the Moolayember Formation) in the southeastern part of the basin.

Provenance—the Significance of Mineralogical Changes

Determination of the provenance of the Late Permian rocks is facilitated by the abundance of petromictic conglomerate and lithic sandstone. In the sand-size and gravel-size detritus fragments of volcanic rock are predominant in all parts of the basin, especially in the southeast, where they consist exclusively of volcanic rocks. Elsewhere, fragments of sedimentary and metamorphic rocks can be recognized. The labile nature of the sediments indicates a minimum of chemical weathering relative to mechanical weathering in the source area, and a copious supply of coarse detritus to the rapidly subsiding basin.

Strakhov (1967, vol. 1, p. 4) in his discussion of the relative importance of mechanical and chemical weathering has stressed the importance of climate and relief. During the Late Permian there is little direct evidence of the type of climate in the source areas of the Bowen Basin. Rigby (1971, p. 27) favoured a cool temperate climate in the basin of deposition because of the restricted number of plant species present, and because of the presence of thick coal seams which must have been formed under conditions inhibiting bacterial decay; in addition he postulated a marked seasonal variation because of the strongly defined growth rings in the silicified wood associated with the coal measures. Gould (1972, p. 32) considered that severe winters were unlikely because of the presence of the tree-fern *Palaeosmunda*. Palaeomagnetic reconstructions (McElhinny, 1969, p. 62) support the palaeobotanical evidence which suggests that the Bowen Basin in Permian time was situated in a zone with a cool temperate climate. In the Sydney Basin fossil insects indicate a temperate climate at this time (Riek, 1972, p. 76), and in the marine deposits there are no indications of warm water faunas (Dickins, 1972, p. 19).

Strakhov (1967, vol. 1, p. 7) has pointed out that chemical weathering is most intense in areas of tropical forest and in the podsoltaiga zone of the temperate regions. The importance of chemical weathering in colder climates has been recently documented by Reynolds & Johnson (1972). The predominance of mechanical weathering in Late Permian time in the Bowen Basin must have been the result of the erosion of a mountainous area. The mountainous regions came into existence during the Late Permian orogenic movements, which were responsible for the emplacement of numerous intrusives along the Connors and Auburn Arches (Dickins & Malone, 1973), the extrusion of volcanics of the shoshonite association, the Late Permian marine regression, and the creation of a rapidly subsiding intermontane basin. The recycled Permian spores in the Rewan Group attest to the erosion of recently uplifted sedimentary sequences.

The petrographic studies of the Triassic arenites show that there was a marked progressive decrease in the relative abundance of labile minerals and rock fragments with time in all parts of the basin, and that this was related to an increase in the intensity of weathering in the source areas rather than to changes in provenance. This is clearly demonstrated by the progressive increase in maturity of the sediment even in the northern part of the basin, where palaeocurrent studies strongly suggest that the provenance areas did not change. The basinwide similarity in composition of the sediments of the Rewan Group, which were derived from many different source areas, confirms that the products of erosion do not depend primarily on the type of rocks in the source area. However, the type of rocks in the source area did have a minor effect on the nature of the sediment deposited in the southeast. At all times the sand laid down in this area was more labile than the sand deposited in

other parts of the basin, owing to the presence of an exclusively volcanic provenance immediately to the east.

Despite the progressive increase in intensity of weathering in the source area there is no evidence of substantial changes of climate in the depositional basin during this time. The modern representatives of the conchostracans found in the Sagittarius Sandstone live in shallow pools of inland basins with a warm temperate climate (Kobayashi, 1954), although cold water forms are known. The presence of a palaeosol in the Glenidal Formation, similar to a present-day grey-brown podsolic soil, indicates a humid temperate, or possibly subtropical, climate. In addition the presence of plant fossils in the Glenidal Formation and the absence of evaporites suggest humid, not arid, conditions.

The petrographic evidence suggests siallitic and podsolic weathering of the source areas under humid temperate conditions during the deposition of the Rewan Group and Glenidal Formation. The abundance of quartz in the Expedition Sandstone, and the absence of gibbsite and boehmite, rule out the possibility of allitic weathering, although in the Dawson Range Sandstone the feldspar is occasionally replaced by halloysite. It is therefore more likely that the progressive increase in intensity of weathering is related to factors other than climate, such as relief and time available for the alteration of the source rocks before and after erosion.

Schumm (1963) pointed out that modern rates of orogenic uplift are much greater than the average maximum rate of denudation. Assuming that this principle can be applied to the Bowen Basin the mountainous regions around the basin, which were uplifted rapidly in the Late Permian, were gradually eroded over a much longer period during the Triassic. Ahnert (1970) has postulated that the relief of a mountain region, after allowing for isostatic compensation, is reduced to 10 percent of its initial value over 18.5 m.y. in a mid-latitude drainage basin. He also postulates that the mean denudation rate in such areas is directly proportional to the mean relief. Thus the nature of the epiclastic detritus derived from a mountain region in a humid temperate climate will progressively change because more and more time is available for weathering of the parent rocks, and because the material is derived from vertically disposed climatic zones. In the Permo-Triassic sequence of the Bowen Basin, the change from the type of sediment forming the coal measures to that in the Rewan Group, especially the Arcadia Formation, represents a change from the erosion of lithosols to the erosion of cinnamonic soils with minimal profile development. The change to the type of sediment in the Glenidal Formation could be related to a marked reduction in relief, so that changes in local climate could result in changes in vegetation from, say, conifers to latifoliates. This is reflected in the microfloral change recognized by de Jersey (1970, p. 23) at the boundary between the Arcadia and Glenidal Formations. The lithological differences between the Glenidal Formation and the Expedition Sandstone reflect an increase in the intensity of podsolic weathering in the source areas, the increase being related to the longer duration of weathering of the landscape before erosion.

The same general trend as that distinguished in the arenites of the Bowen Basin succession (Fig. 58) has been found in other basins with similar climatic and tectonic regimes (Strakhov, 1967, vol. 2, p. 390: Shutov, 1967, p. 603). The changes in the lutite assemblages fit into the same type of pattern. The evolution of the Permo-Triassic sediments is therefore seen as the result of humid temperate lithogenesis within an exogeosynclinal intermontane basin.

Conclusions

As a result of the examination of outcrops in the northern half of the Bowen Basin, and the measurement of a number of stratigraphic sections of the Rewan and Clematis Groups, it is possible to erect a stratigraphic framework which allows both the grouping and differentiation of lithogenetically related units within the sequence. In the new framework a distinction is made between the Glenidal Formation and the overlying Expedition Sandstone, but they are also combined to form the Clematis Group; the framework also distinguishes between the Sagittarius Sandstone and the Arcadia Formation, but at the same time recognizes the lithogenetic affinity between them by placing them in the Rewan Group. As a result of a review of the palynological evidence, and by studying the palaeocurrents, it is concluded that the lithogenetically related units are at least partly facies equivalents.

The classification of group cross-stratification, based partly on size of set, has been found to be useful, and elongation function studies can also be applied to identify sequences laid down by unidirectional currents with increasing and decreasing transportation power. Applications of vertical profile analysis has shown that the sediments of both the Rewan and Clematis Groups were deposited in fluvial environments. Fining-upwards sequences laid down in meandering streams are present in the Rewan Group, and a second type of cyclic sequence within the group can be explained by deposition in an anastomosing channel system. The stratification in the Expedition Sandstone can be explained in terms of a recently defined fluvial model for bed-load meandering channels, although braided channels were probably predominant in the northern part of the basin.

The regional palaeocurrent trends suggest the existence of an internal drainage basin during the deposition of the coal measures and the overlying Rewan Group. This system was disrupted when deposition of the Glenidal Formation began and the rate of supply of sediment exceeded the rate of subsidence. The main drainage then flowed south through the basin, with subordinate drainage from the western and eastern margins.

The Permo-Triassic succession shows a progressive change from labile to a mature composition, and there is a corresponding change in the fabric of the sediments from those showing little evidence of weathering to those showing profound pedological changes, in both the depositional and provenance areas.

An understanding of the nature and origin of all redbeds cannot be derived from the investigation of one occurrence, but the present study does make some contribution to the solution of the general problem. Firstly, it has been shown that the climate of both the source areas and the basin of deposition was temperate and not tropical or subtropical, as is commonly held to be necessary. In addition, the climatic conditions were, for the most part, humid and not arid, although a Mediterranean mountain climate is invoked to allow rubification of the soil. Secondly, in the case of the red mudstone of the Arcadia Formation, the pigment is hematite, mainly less than 2 microns in diameter, produced by siallitic weathering in the source area, and transported with clays to the depositional site. Thirdly, some of the red mudstone has been produced by podsolic weathering in a humid temperate climate with the development of brunisolic and lateritic podsolic soils in the source area. The soils were then eroded and the iron transported as hematitic pedorelicts and probably as brown ferric oxide gel to the depositional site, where pedogenic processes, dehydration by aging, and lithification led to the development of mottled red and green rocks.

Little can be gained by comparing the effects of tectonic control versus climatic control within a sedimentary basin, because the sediments are the product of the interaction of both. During the Permo-Triassic sedimentation in the Bowen Basin the regional climate was similar to that obtaining in the cool temperate zones of the present day; the main tectonic control was by late-stage uplift within an exo-geosyncline. The net result was an intermontane basin with a humid temperate climate. Sedimentation in the basin was controlled by the effects of the progressive decrease in relief and associated changes of local climate, vegetation, and rate of denudation, and by the relative rate of subsidence of the basin.

ACKNOWLEDGMENTS

This study was carried out during and after the tenure of an Australian Public Service Post-graduate Scholarship, and the results were submitted as a Ph.D. thesis to the Australian National University. I am particularly indebted to Drs K. A. W. Crook and C. E. B. Conybeare for their supervision of the work and invaluable criticism of the original draft. Drs C. T. McElroy, C. F. K. Diessel, and C. D. Williams also read the original draft and provided most useful comments. I would like to thank Drs P. H. Walker and A. J. Moss of CSIRO for discussions on soil genesis and elongation analysis, and for the organic carbon analyses.

I am also grateful to Dr I. K. Crain and Mrs L. Crain for their preparation of the computer programs GRAINS and TAPECARD, and Dr S. Henley for his assistance in modifying various programs. Mr R. N. England kindly performed the electron microprobe analyses, and Mr G. Berryman prepared diffractograms of the clay minerals and iron oxides.

Finally, I would like to express my appreciation of the technical assistance provided by Mr T. K. Zapasnik, who prepared most of the samples for petrographic, X-ray, and fabric analysis, and who helped with the measurement of many of the stratigraphic sections.

REFERENCES

ANHERT, F., 1970—Functional relationships between denudation, relief and uplift in large mid-latitude drainage basins. *Am. J. Sci.*, 268(3), 243-63.

ALLEN, J. R. L., 1963a—The classification of cross-stratified units, with notes on their origin. *Sedimentology*, 2, 93-114.

ALLEN, J. R. L., 1963b—Asymmetrical ripple marks and the origin of water-laid cosets of cross-strata. *Lpool Manc. geol. J.*, 3(2), 187-236.

ALLEN, J. R. L., 1965—A review of the origin and characteristics of Recent alluvial sediments. *Sedimentology*, 5, 89-191.

ARMAN, M., 1965—Petrographic notes on Bowen Basin shallow holes drilled in 1963. *Bur. Miner. Resour. Aust. Rec.* 1964/92 (unpubl.).

BALME, B. E., & BROOKS, J. D., 1953—Kaolinite petrifications in a New South Wales Permian coal seam. *Aust. J. Sci.*, 16(2), 65.

BARTHOLOMAI, A., & HOWIE, A., 1970—Vertebrate fauna from the Lower Trias of Australia. *Nature*, 225(5237), 1063.

BASTIAN, L. V., 1965a—Petrographic notes on the Rewan Formation, southern Bowen Basin. *Bur. Miner. Resour. Aust. Rec.* 1965/260 (unpubl.).

BASTIAN, L. V., 1965b—Petrographic notes on the Clematis Sandstone and Moolayember Formation, Bowen Basin, Queensland. *Ibid.*, 1965/240 (unpubl.).

BERNARD, H. A., & LE BLANC, R. S., 1965—Resumé of Quaternary geology of northwestern Gulf of Mexico province; *in* THE QUATERNARY OF THE UNITED STATES. *Princeton, N.J., Princeton Univ. Press.*

BLATT, H., 1967—Original characteristics of clastic quartz grains. *J. sediment. Petrol.*, 37, 401-24.

BLATT, H., & CHRISTIE, J. M., 1963—Undulatory extinction in quartz of igneous and metamorphic rocks and its significance in provenance studies of sedimentary rocks. *J. sediment. Petrol.*, 33, 559-79.

BLUCK, B. J., 1971—Sedimentation in the meandering River Endrick. *Scott. J. Geol.*, 7(2), 93-138.

BREWER, R., 1960—Cutans: their definition, recognition, and classification. *J. Soil Sci.*, 11, 280-92.

BREWER, R., 1964—FABRIC AND MINERAL ANALYSIS OF SOILS. *N.Y., Wiley.*

BROWN, D. A., CAMPBELL, K. S. W., & CROOK, K. A. W., 1968—THE GEOLOGICAL EVOLUTION OF AUSTRALIA AND NEW ZEALAND. *Oxford, Pergamon.*

BURGIS, W. A., 1973—Environmental significance of folds in the Rangal Coal Measures at Blackwater, Queensland. *Bur. Miner. Resour. Aust. Rec.* 1973/39 (unpubl.).

CAROZZI, A. V., 1960—MICROSCOPIC SEDIMENTARY PETROGRAPHY. *N.Y., Wiley.*

CAMERON, K. L., & BLATT, H., 1971—Durabilities of sand sized schist and 'volcanic' rock fragments during fluvial transport, Elk Creek, Black Hills, South Dakota. *J. sediment. Petrol.*, 41(2), 565-76.

COLEMAN, J. M., 1969—Brahmaputra River: channel processes and sedimentation. *Sediment. Geol.*, 3(2-3), 131-237.

COLEMAN, J. M., & GAGLIANO, S. M., 1965—Sedimentary structures: Mississippi River deltaic plain; *in* MIDDLETON, G. V. (Ed.): Sedimentary structures and their hydrodynamic interpretation. *Soc. econ. Paleont. Miner. spec. Publ.* 12, 133-48.

CONOLLY, J. R., 1965—The occurrence of polycrystallinity and undulatory extinction in quartz in sandstone. *J. sediment. Petrol.*, 35(1), 116-35.

CONOLLY, J. R., 1968—Models for Triassic deposition in the Sydney Basin. *Geol. Soc. Aust. spec. Publ.* 2, 209-23.

CROOK, K. A. W., 1960—Classification of arenites. *Am. J. Sci.*, 258, 419-28.

CSIRO [Commonwealth Scientific and Industrial Research Organization], 1967—Lands of the Isaac-Comet area, Queensland. *CSIRO Land Res. Ser.* 19.

CSIRO, 1968—Lands of the Dawson-Fitzroy area, Queensland. *Ibid.*, 21.

DAPPLES, E. C., 1967—Diagenesis of sandstones; *in* LARSEN, G., & CHILLINGAR, G. V., DIAGENESIS IN SEDIMENTS. *Amsterdam, Elsevier*, 91-125.

DAVID, T. W. E. (Ed. BROWNE, W. R.), 1950—THE GEOLOGY OF THE COMMONWEALTH OF AUSTRALIA. *London, Arnold.*

DAVIS, A. (Ed.), 1971—Proceedings of the Second Bowen Basin Symposium. *Geol. Surv. Qld Rep.* 62, 144.

DAVIES, D. K., ETHERIDGE, F. G., & BERG, R. R., 1971—Recognition of barrier environments. *Bull. Am. Ass. Petrol. Geol.*, 55(4), 550-65.

DEANS, T., 1938—Francolite from sedimentary ironstones of the coal measures. *Miner. Mag.*, 25, 135.

DEAR, J. F., MCKELLAR, R. G., & TUCKER, R. M., 1971—Geology of the Monto 1:250 000 Sheet area. *Geol. Surv. Qld Rep.* 46.

DE JERSEY, N. J., 1968—Triassic spores and pollen grains from the Clematis Sandstone. *Geol. Surv. Qld Publ.* 338.

DE JERSEY, N. J., 1970—Early miospores from the Rewan Formation. *Ibid.*, 345.

DENMEAD, A. K., 1930—Rewan-Clematis Gorge-Christmas Creek-Consuelo traverse. *Qld Govt Min. J.*, 31, 155-6.

DEPARTMENT OF NATIONAL DEVELOPMENT, 1967—Fitzroy Region, Queensland: Soils. *Dep. Nat. Dev. Resour. Ser.*

DERRINGTON, S. S., 1957—AAO No. 7 (Arcadia) well completion report (unpubl.). *Mines Administration Pty Ltd.*

DERRINGTON, S. S., 1962—The tectonic framework of the Bowen Basin. *APEA, 1961 Conf. Pap.*, 18-21.

DERRINGTON, S. S., & MORGAN, K. H., 1960—Southeastern and south-central Bowen Basin; *in* HILL & DENMEAD (Eds), 204-12.

DICKINS, J. M., 1972—Climates of the Permian in Australia, palaeontological evidence. *44th ANZAAS Cong., Sydney, Sect. 3, Geology, Abstr.*, 18-19.

DICKINS, J. M., & MALONE, E. J., 1973—Geology of the Bowen Basin, Queensland. *Bur. Miner. Resour. Aust. Bull.* 130.

DICKINS, J. M., MALONE, E. J., & JENSEN, A. R., 1964—Subdivision and correlation of the Permian Middle Bowen Beds, Queensland. *Bur. Miner. Resour. Aust. Rep.* 70.

DOEGLAS, D. J., 1962—The structure of sedimentary deposits of braided rivers. *Sedimentology*, 1(3), 167-90.

DOVETON, J. H., 1971—An application of Markov chain analysis to the Ayrshire Coal Measures succession. *Scott. J. Geol.*, 7(1), 11-27.

DURRAND, D., & GREENWOOD, J. A., 1958—Modifications of the Rayleigh test for uniformity in analysis of two-dimensional orientation data. *J. Geol.*, 66, 229-38.

EVANS, P. R., 1962—Microfossils associated with the 'Bundamba Group' of the Surat Basin, Queensland. *Bur. Miner. Resour. Aust. Rec.* 1962/115 (unpubl.).

EVANS, P. R., 1963a—Palynological appendix *in* MYERS, N. L., 1963—Planet Oil Warrinilla North No. 1, well completion report (unpubl.).

EVANS, P. R., 1963b—Spore preservation in the Bowen Basin. *Bur. Miner. Resour. Aust. Rec.* 1963/100 (unpubl.).

EVANS, P. R., 1964—Some palynological observations on the Mesozoic of the Baralaba, Monto, Taroom and Mundubbera 1:250 000 Sheet areas, Bowen-Surat Basin. *Ibid.*, 1964/91 (unpubl.).

EVANS, P. R., 1966a—Mesozoic stratigraphic palynology in Australia. *Aust. Oil Gas J.*, 12(6), 58-63.

EVANS, P. R., 1966b—Contributions to the palynology of the Permian and Triassic of the Bowen Basin. *Bur. Miner. Resour. Aust. Rec.* 1966/134 (unpubl.).

EVANS, P. R., 1966c—Palynological studies in the Longreach, Jericho, Galilee, Tambo, Eddystone, and Taroom 1:250 000 Sheet areas, Queensland. *Ibid.*, 1966/61 (unpubl.).

EXON, N. F., GALLOWAY, M. C., CASEY, D. J., & KIRKEGAARD, A. G., 1966—The geology of the Tambo, Augathella and Blackall 1:250 000 Sheet areas, Queensland. *Bur. Miner. Resour. Aust. Rec.* 1966/89 (unpubl.).

FOLK, R. L., 1968—PETROLOGY OF SEDIMENTARY ROCKS. *Austin, Hemphills.*

GINGERICH, P. D., 1969—Markov analysis of cyclic alluvial sediments. *J. sediment. Petrol.*, 39(1), 330-32.

GOLDICH, S. S., 1938—A study in rock weathering. *J. Geol.*, 46, 17-58.

GOULD, R. E., 1972—Some palaeobotanical evidence on the Upper Permian climate of the Bowen Basin, Queensland. *44th ANZAAS Cong., Sect. 3, Geology, Abst.*, 32.

HAMBLYN, W. K., 1958—Cambrian sandstones of northern Michigan. *Geol. Surv. Michigan Publ.* 51.

HAPP, S. C., RITTENHOUSE, G., & DOBSON, G. C., 1940—Some aspects of accelerated stream and valley sedimentation. *U.S. Dep. Agr. tech. Bull.* 695, 1-34.

HARMS, J. C., & FARNSTOCK, R. K., 1965—Stratification, bedforms and flow phenomena; *in* MIDDLETON, G. V.: Primary sedimentary structures and their hydrodynamic interpretation. *Soc. econ. Paleont. Miner. spec. Publ.* 12, 84-115.

HASEMAN, J. F., BROWN, E. H., & WHITT, C. D., 1950—Some reaction of phosphate with clays and hydrous oxides of iron and aluminium. *Soil Sci.*, 70, 257-71.

HIGH, L. R., JNR, & PICARD, M. D., 1971—Mathematical treatment of orientation data *in* CARVER, R. E., 1971: PROCEDURES IN SEDIMENTARY PETROLOGY. *N.Y., Wiley-Interscience,* 21-45.

HILL, D., 1957—Explanatory notes on Springsure 4-mile Geological Sheet. *Bur. Miner. Resour. Aust. Note Ser.* 5.

HILL, D., & DENMEAD, A. K. (Eds), 1960—The geology of Queensland. *J. geol. Soc. Aust.,* 7.

ISBELL. R. F., 1955—The geology of the northern section of the Bowen Basin. *Pap. Univ. Qld Dep. Geol.,* 4(11).

JACK, R. L., & ETHERIDGE, R., JNR, 1892—The geology and palaeontology of Queensland and New Guinea. *Geol. Surv. Qld Publ.* 92.

JAKES, P., & SMITH, I. E., 1970—High potassium calc-alkaline rocks from Cape Nelson, Eastern Papua. *Contrib. Miner. Petrol.,* 28, 259-71.

JACKSON, M. L., & SHERMAN, G. D., 1953—Chemical weathering of minerals in soils. *Adv. Agron.,* 5, 219-318.

JENSEN, A. R., 1968—Upper Permian and Lower Triassic sedimentation in part of the Bowen Basin, Queensland. *Bur. Miner. Resour. Aust. Rec.* 1968/55 (unpubl.).

JENSEN, A. R., 1971—Regional aspects of the Upper Permian regression in the northern part of the Bowen Basin; *in* Proc. 2nd Bowen Basin Symp. *Geol. Surv. Qld Publ.* 62, 7-20.

JENSEN, A. R., & ARMAN, M., 1966—Notes on some Upper Permian and Lower Triassic units of the Bowen Basin, Queensland. *Bur. Miner. Resour. Aust. Rec.* 1966/21 (unpubl.).

JENSEN, A. R., GREGORY, C. M., & FORBES, V. R., 1964—The geology of the Taroom 1:250 000 Sheet area and of the western third of the Mundubbera 1:250 000 Sheet area, Queensland. *Bur. Miner. Resour. Aust. Rec.* 1964/61 (unpubl.).

JENSEN, H. I., 1926—Geological reconnaissance between Roma, Tambo, Springsure and Taroom. *Geol. Surv. Qld Publ.* 277.

JONES, B. G., 1970—A computer programme for analysing directional data designed for use on a CDC 3600. *Bur. Miner. Resour. Aust. Rec.* 1970/67 (unpubl.).

JONES, G. P., 1965—Red beds in northeastern Nigeria. *Sedimentology,* 5, 235-47.

JOPLIN, G. A., 1968—A PETROGRAPHY OF AUSTRALIAN IGNEOUS ROCKS. *Sydney, Angus & Robertson.*

JOPLING, A. V., 1963—Hydraulic studies on the origin of bedding. *Sedimentology,* 2, 115-21.

JOPLING, A. V., 1966—Some applications of theory and experiment to the study of bedding genesis. *Ibid.,* 7, 71-102.

KING, D., & JENSEN, A. R., 1966—Fused coal measures in the Bowen Basin. *Qld Govt Min. J.,* 67, 560-61.

KLEIN, G. DE V., 1970—Depositional and dispersal dynamics of intertidal sand bars. *J. sediment. Petrol.,* 40(4), 1095-127.

KOBAYASHI, T., 1954—Fossil estherians and allied fossils. *J. Fac. Sci. Tokyo Univ., Ser. II,* 9(1).

KRYNINE, P. D., 1946—Microscopic morphology of quartz types. *Geol. Paleont. Miner. Petrol.,* 3, 2a. Comissoa.

LAND, L. S., & HOYT, J. H., 1966—Sedimentation in a meandering estuary. *Sedimentology,* 6(3), 191-207.

LANGMUIR, D., 1971—Particle size effect on the reaction of goethite = ilmenite + water. *Am. J. Sci.,* 271, 147-56.

LASSAK, E. V., & GOLDING, H. G., 1967—Phosphate bands in Narrabeen sediments. *Aust. J. Sci.,* 29(7), 223.

LOUGHNAN, F. C., 1969—CHEMICAL WEATHERING OF THE SILICATE MINERALS. *N.Y., Elsevier.*

LOUGHNAN, F. C., KOKO, M., & BAYLISS, P., 1964—The red beds of the Triassic Narrabeen Group. *J. geol. Soc. Aust.,* 11(1), 65-77.

MACKIE, W., 1896—The sands and sandstones of eastern Moray. *Trans. Edinb. geol. Soc.,* 7, 148-72.

MCDOWELL, J. P., 1960—Cross-bedding formed by sand waves in Mississippi River point bar deposits. *Bull. geol. Soc. Am.,* 71, 1925 (Abstr.).

MCELHINNY, M. W., 1969—The palaeomagnetism of the Permian of southeast Australia and its significance regarding the problem of intercontinental correlation. *Geol. Soc. Aust. spec. Publ.* 2, 61-7.

MCELROY, C. T., 1969—Narrabeen Group sedimentation; *in* PACKHAM, G. H. (Ed.): The geology of New South Wales. *J. geol. Soc. Aust.,* 16(1), 439-43.

MCGOWEN, J. H., & GARNER, L. E., 1970—Physiographic features and stratification types of coarse-grained point bars: modern and ancient examples. *Sedimentology,* 14(1-2), 77-113.

McKee, E. D., & Weir, G. W., 1953—Terminology for stratification and cross-stratification in sedimentary rocks. *Bull. geol. Soc. Am.*, 64, 381-90.

Malone, E. J., 1964—Depositional evolution of the Bowen Basin. *J. geol. Soc. Aust.*, 11(2), 263-82.

Malone, E. J., Corbett, D. W. P., & Jensen, A. R., 1964—Geology of the Mount Coolon 1:250 000 Sheet area. *Bur. Miner. Resour. Aust. Rep.* 64.

Malone, E. J., Olgers, F., & Kirkegaard, A. G., 1969—The geology of the Duaringa and Saint Lawrence 1:250 000 Sheet areas, Queensland. *Bur. Miner. Resour. Aust. Rep.* 121.

Milligan, E. N., 1971—Geology and correlation in the German Creek Coal Measures; *in* Proc. 2nd Bowen Basin Symp. *Geol. Surv. Qld Publ.* 62, 77-85.

MINAD [Mines Administration Pty Ltd], 1959—New names in Queensland stratigraphy. *Aust. Oil Gas J.*, 5(8), 27-35.

Mollan, R. G., Dickins, J. M., Exon, N. F., & Kirkegaard, A. G., 1969—Geology of the Springsure 1:250 000 Sheet area, Queensland. *Bur. Miner. Resour. Aust. Rep.* 123.

Mollan, R. G., Forbes, V. R., Jensen, A. R., Exon, N. F., & Gregory, C. M., 1972—Geology of the Eddystone, Taroom, and western part of the Mundubbera Sheet areas, Queensland. *Bur. Miner. Resour. Aust. Rep.* 142.

Moss, A. J., 1968—Bed-load deposits of shallow unidirectional currents. *Ph.D. Thesis, Aust. Nat. Univ.* (unpubl.).

Okada, Hakuyu, 1971—Classification of sandstones: analysis and proposal. *J. Geol.*, 79(5), 509-25.

Olgers, F., 1973—Geology of the Drummond basin, Queensland. *Bur. Miner. Resour. Aust. Bull.* 132.

Olgers, F., Webb, A. W., Smit, J. A. J., & Coxhead, B. A., 1966—The geology of the Baralaba 1:250 000 Sheet area, Queensland. *Bur. Miner. Resour. Aust. Rep.* 102.

Ore, H. T., 1964—Some criteria for recognition of braided stream deposits. *Contrib. Geol. (Wyoming U.)*, 3, 1-14.

Packham, G. H., 1954—Sedimentary structures as an important factor in the classification of sandstones. *Am. J. Sci.*, 252, 466-76.

Papadakis, J., 1969—soils of the world. *Amsterdam, Elsevier.*

Pedro, G., 1964—contribution a l'etude experimentale de l'alteration geochimique des roches cristallines. *Paris, Inst. nat. Rech. agron.*

Pettijohn, F. J., 1941—Persistence of heavy minerals and geological age. *J. Geol.*, 49, 610-25.

Pettijohn, F. J., 1957—sedimentary rocks. *N.Y., Harper,* 2nd Ed.

Pittman, E. D., 1969—Destruction of plagioclase twins by stream transport. *J. sediment. Petrol.*, 39(4), 1432-37.

Plumley, W. J., 1948—Black Hills terrace gravels: a study in sediment transport. *J. Geol.*, 56, 526-77.

Potter, P. E., & Pettijohn, F. J., 1963—paleocurrents and basin analysis. *Berlin, Springer.*

Reeves, F., 1947—Geology of the Roma district, Queensland. *Bull. Am. Ass. Petrol. Geol.*, 31(8), 1341-71.

Reid, J. H., 1924-25—Geology of the Bowen River coalfield. *Qld Govt Min. J.*, 25, 399-411, and 26, 4-11.

Reid, J. H., 1928—The Isaacs River Permo-Carboniferous coal basin. *Ibid.*, 29, 192-97, 236-41, 282-5.

Reid, J. H., 1930—Geology of the Springsure district. *Ibid.*, 31, 87-98, 149-55.

Reid, J. H., 1944—Dawson coalfield, Baralaba. *Ibid.*, 45, 204-5.

Reid, J. H., 1945—The Dawson River area. *Ibid.*, 46, 296-9.

Reid, J. H., 1946—Geological reconnaissance of the Nebo district. *Ibid.*, 47, 10.

Reik, E. F., 1972—Ecological inference from the Australian Permian insects. *44th ANZAAS Cong. Sydney, Sect. 3, Geology, Abstr.* 76.

Reynolds, R. C., Jnr, & Johnson, N. M., 1972—Chemical weathering in the temperate glacial environment of the Northern Cascade Mountains. *Geochim. cosmochim. Acta,* 36, 537-54.

Rigby, J. F., 1971—Some palaeobotanical observations concerning the Bowen Basin; *in* Proc. 2nd Bowen Basin Symp. *Geol. Surv. Qld Publ.* 62, 21-8.

Robb, G. L., 1949—Red bed coloration. *J. sediment. Petrol.*, 19, 99-103.

Roddick, S. L., 1971—A petrographic examination of samples from five holes in the Lower Triassic, Bowen Basin, Queensland. *Bur. Miner. Resour. Aust. Rec.* 1971/81 (unpubl.).

Ross, C. S., & Kerr, P. F., 1931—Halloysite and allophane. *U.S. geol. Surv. prof. Pap.* 185G, 135-48.

Sarkar, S. K., & Basumallick, S., 1968—Morphology, structure, and evolution of a channel island in the Baraka River, Baraka, West Bengal. *J. sediment. Petrol.*, 38(3), 747-54.

SCHMALZ, R. F., 1968—Formation of red beds in modern and ancient deserts; discussion. *Bull. geol. Soc. Am.*, 70(2), 277-80.

SCHULLER, A., 1951—Zur Nomenklatur und Genese der Tonsteine. *Neues Jb. Miner. Monatsh.*, 5, 97-109.

SCHUMM, S. A., 1963—The disparity between present rates of denudation and orogeny. *U.S. geol. Surv. prof. Pap.* 454H.

SCHUMM, S. A., 1968—Speculations concerning the paleohydrologic controls of terrestrial sedimentation. *Bull. geol. Soc. Am.*, 79, 1573-88.

SCOTT, A., HAYES, M. D., ANDREWS, P. B., & BEHRENS, E. W., 1964—Depositional environment; south-central Texas Coast. *Gulf Coast Ass. geol. Soc. Guide Book.*

SHUTOV, V. D., 1967—Classification of sandstones. *Lith. Miner. Resour.*, 5, 596-611.

SHERMAN, G. D., 1952—The genesis and morphology of the alumina-rich laterite clays; *in* CLAY AND LATERITE GENESIS. *Amer. Inst. Min. Metall.*, 154-61.

SIMONS, D. B., RICHARDSON, E. V., & ALBERTSON, M. L., 1961—Flume studies using medium sand (0.45 mm). *Wat. Supply Irrig. Pap. Wash.*, 1498A, 76.

SIMONS, D. B., RICHARDSON, E. V., & NORDIN, C. F. JNR, 1965—Sedimentary structure generated by flow in alluvial channels; *in* MIDDLETON, G. V. (Ed.): Primary sedimentary structures and their hydrodynamic interpretation. *Soc. econ. Paleont. Miner. spec. Publ.* 12, 34-52.

STAGE, H. C. T., HUBBLE, G. D., BREWER, R., NORTHCOTE, K. H., SLEEMAN, J. R., MULCAHY, M. J., & HALLSWORTH, E. G., 1968—A HANDBOOK OF AUSTRALIAN SOILS. *Glendide, S.A., Rellim.*

STAINES, H. R. E., 1972—Blackwater coalfield—correlation of seams in the Rangal Coal Measures, Mackenzie River to Sirius Creek. *Geol. Surv. Qld Rep.* 70.

STRAKHOV, N. M., 1967—PRINCIPLES OF LITHOGENESIS. *London, Oliver & Boyd,* 3 vols.

SWAINE, D. J., 1971—Boron in coals of the Bowen Basin as an environmental indicator; *in* Proc. 2nd Bowen Basin Symp. *Geol. Surv. Qld Publ.* 62, 41-8.

TRAVES, D. M., 1966—Petroleum in the Roma-Springsure area. *8th Cwealth Min. metall. Cong.*, 5, 147-56.

TRIPPLEHORN, D. M., 1971—'Weathering of the Sioux Quartzite near Ulm, Minnesota, as related to Cretaceous climates' by G. S. Austin—a discussion. *J. sediment. Petrol.*, 41(2), 603-5.

VAN HOUTEN, F. B., 1953—Clay minerals in sedimentary rocks and derived soils. *Amer. J. Sci.*, 251, 61-82.

VAN HOUTEN, F. B., 1961—Climatic significance of red beds; *in* NAIRN, A. E. M. (Ed.): DESCRIPTIVE PALEOCLIMATOLOGY 89-139. *N.Y., Interscience.*

VEEVERS, J. J., RANDAL, M. A., MOLLAN, R. G., & PATEN, R. J., 1964—The geology of the Clermont 1:250 000 Sheet area, Queensland. *Bur. Miner. Resour. Aust. Rep.* 66.

VINE, R. R., CASEY, D. J., & JOHNSON, N., 1964—Progress report, 1963, on the geology of part of the northeastern Eromanga Basin, Queensland. *Bur. Miner. Resour. Aust. Rec.* 1965/244 (unpubl.).

VINE, R. R., JAUNCEY, W., CASEY, D. J., & GALLOWAY, M. C., 1965—Longreach-Jericho-Lake Buchanan area. *Bur. Miner. Resour. Aust. Rec.* 1965/245 (unpubl.).

VISHER, G. S., 1965—Use of vertical profile in environmental reconstruction. *Bull. Am. Ass. Petrol. Geol.*, 19, 41-61.

VOISEY, A. H., 1959—Australian geosynclines. *Aust. J. Sci.*, 22, 188.

WALKER, T. R., 1967—Formation of red beds in modern and ancient deserts. *Bull. geol. Soc. Am.*, 78(3), 353-68.

WARREN, ANNE, 1972—Queensland trace fossils pose a 230 million years old problem. *Aust. nat. Hist., March* 1972, 160-62.

WARREN, R. G., 1972—A commentary on the metallogenic map of Australia and Papua New Guinea. *Bur. Miner. Resour. Aust. Bull.* 145.

WEAVER, C. E., 1958—Geologic interpretation of argillaceous sediments. *Bull. Am. Ass. Petrol. Geol.*, 42, 254-71.

WHITE, M. E., 1965—Report on 1964 plant fossil collections. *Bur. Miner. Resour. Rec.* 1965/101 (unpubl.).

WHITEHOUSE, F. W., 1955—The geology of the Queensland portion of the Great Artesian Basin. Appendix G *in* Artesian Water Supplies in Queensland. *Dep. Co-ord. Gen. Pub. Works, Qld parl. Pap.* 456.

WILLIAMS, H., TURNER, F. J., & GILBERT, C. M., 1955—PETROGRAPHY—AN INTRODUCTION TO THE STUDY OF ROCKS IN THIN SECTION. *San Francisco, Freeman.*

WILLIAMS, P. F., & RUST, B. R., 1969—The sedimentology of a braided river. *J. sediment. Petrol.*, 39(2), 649-79.
WOLF, K. H., 1965a—Gradational sedimentary products of calcareous algae. *Sedimentology*, 5, 1-37.
WOLF, K. H., 1965b—Grain diminution of algal colonies to micrite. *J. sediment. Petrol.*, 35(2), 420-7.
WOLMAN, M. G., & BRUSH, L. M., 1961—Factors controlling the size and shape of stream channels in coarse noncohesive sands. *U.S. geol. Surv. prof. Pap.* 282G.
WOOLLEY, J. B., 1944—Geological report on Arcadia. *Shell (Qld) Devel. Pty Ltd, geol. Rep.* 12 (unpubl.).

APPENDIX 1
ELONGATION FUNCTION ANALYSIS

Although it is rarely possible to determine the specific physiographic domain in which particular sands were deposited, certain conclusions can be drawn about the operative hydrodynamic conditions. Although the current velocity and depth of water cannot be specified, sequences laid down by unidirectional currents of increasing or decreasing transporting power can be recognized. Recognition of the flow regime in which structures are formed is of fundamental importance. For example, some types of cross-stratification result from the formation of ripples and dunes which are indicative of the lower flow regime. The interpretation of planar stratification, a structure found in both the Rewan and Clematis Groups, is, however, not as simple. Flume studies (Simon et al., 1961) have shown that plane beds are established in medium sand in the lower part of the upper flow regime, and it is also known that plane beds and not ripples are, in some cases, established in the lower flow regime in coarse sand (Allen, 1970, fig. 13). Furthermore, Moss (1968, p. 35) has observed plane beds in medium-grained and finer sands within the lower flow regime. Part of the purpose of this study has therefore been to determine the flow stage operative during the formation of horizontally stratified beds in the Rewan and Clematis Groups by the application of elongation function analysis.

It has been shown that at least some of the cross-stratification was formed by the migration of solitary transverse bars or microdeltas. A second part of the application of elongation function analysis has therefore been directed towards the determination of the mechanism responsible for the formation of solitary cross-stratified units.

Theoretical Basis

Moss (1962, 1963) investigated the size-shape relationships of clastic sediments by measuring the size of a number of grains from single laminae. The basic measurements used were: length (p), breadth (q), and depth (r). Plots of p against p/q (elongation function curves) suggested that water-laid sandy and pebbly deposits consist of mixtures of up to three distinct particle populations designated A, B, and C. In terms of the physical constitution of the sediment, grains of population A form the framework and are always present, whereas interstitial grains of population B may not be present. Population C consists of grains larger than those of A, which roll over or are embedded in the surface formed by population A grains.

The shape of the elongation function curves depends on the presence and nature of the three populations. The curve for sediments composed entirely of population A (e.g. beach sands) is linear. For normal deposits of unidirectional currents it is much more complex, but by assuming a linear population A component, Moss (1972) distinguished two separate curves for populations B and C, and demonstrated that bed-load sediments deposited in the lower flow regime can be differentiated from those of the upper flow regime by the shape of the composite curve.

Method

For the construction of elongation function curves it is only necessary to measure two dimensions of a number of grains taken from a single depositional lamina. The samples from the Rewan and Clematis Groups were disintegrated by boiling in a weak detergent solution followed by irradiation in an ultrasonic bath. It was found that many clay-cemented samples could be disintegrated with little or no alteration of the original grain shapes.

In his early work Moss (1962) measured sand grains with an eyepiece micrometer fitted to a microscope. The sand grains to be measured were placed in a flat-bottomed glass dish. The position of the point that would be the centre of gravity of the two dimensional image was estimated, and the longest and shortest distances across the grain were measured. Later (Moss, 1968) the measurements were made on a projection head fitted to the microscope, and the image measured with a scale. Using this method about 1000 grains per day can be measured. The elongation function curve was constructed by computing the mean elongation function (p/q) for groups of measurements of p. Moss (1962, 1968) fitted the curves by eye, because he held that there was no justification for fitting a statistically based curve to the data. The number of grains measured varied between 400 and 6000, and averaged 1000.

One of the disadvantages of this method of analysis is the considerable time required to measure the grains and to make calculations for the construction of the curves, so a method was devised to reduce the time required for both the measurements and calculations. After disaggregation of the rock, the sand grains were placed on a glass slide under the stage of a Nikon Profile Projector. Contact prints of the image produced on a ground-glass screen, 31 cm in diameter, were then prepared using a low-cost automatic developing and printing machine. The whole process to this stage takes less than 10 minutes.

The elongation function measurements were made on the photographs using a Zeiss TGZ3 particle-size analyser. The TGZ3 produces a circle of light which can be varied over two ranges of scale (4.82-9.24 mm and 14.46-27.71 mm) and the diameter selected is recorded on one of a series of 48 telephone counters. The diameter of the circle of light increases as either a linear or an exponential function in both ranges. The exponential increase allows the same relative precision at small and large diameters. The counters record individually or as a group above the selected diameter to enable cumulative addition.

The analyser was connected to a paper punch which recorded the serial number of the counter triggered by each measurement. The program TAPECARD was used to prepare computer cards listing pairs of counter readings (p and q) as recorded on the tape. The serial number of each counter represents a diameter, the size of which depends upon the magnification of the photograph, and the type of measurement facility selected on the particle-size analyser (exponential or linear increase in circle diameter, and small or large range of diameters). Each serial number was converted to a grain diameter by the program GRAINS, which also calculates the elongation function for each grain measured, and takes the means on two dimensional co-ordinates. The elongation function curve can then be fitted by eye.

The method adopted involved the measurement of the diameter of the smallest circle enclosing the grain outline (circumscribed) and of the largest circle fitting with the grain outline (inscribed). These measurements do not correspond to those of Moss (1962, 1968) but, except in the case of 'banana-shaped' grains, the difference is negligible. The method has the advantage that the precision of the measurement does not rely on an ability to estimate the centre of gravity of the grain image, and the circles can be fitted rapidly with the particle-size analyser. With practice, about 400 grains (800 measurements) can be measured per hour.

In general it was found preferable to use the linear opening range on the particle-size analyser for two reasons: first, with an exponential increase an unduly large range of diameters is grouped within one counter unit at the upper end of the scale (i.e. from counters 14 to 48); secondly, it is not possible to construct a meaningful scatter plot with differing ranges of 'p' values as recorded on the counters. Using a linear opening range and counters 14 to 48 the maximum measurement error is 6.4 percent. On the other hand, if the grains are small and the magnification is such that counters 1 to 14 must be used, an exponential increase is preferable. The maximum error in that case is 7.2 percent.

Results

The samples used for elongation function analysis are listed in Table A, and the resultant elongation function curves are shown in Figures A1 to A15. In each of the figures the points represent the means for groups of either 30 or 90 measurements, and the bar represents one standard deviation about the mean.

In the first part of the study, three samples from the lower flow regime measured by Moss (1968) were re-measured, using the method described in the previous section. The resultant curves are not precisely the same as those derived by Moss, but they are sufficiently close to show that the new method is satisfactory. The result for sample 1189 (Fig. A1) suggests greater elongation for grains around 0.2 mm than suggested by Moss, but the curve is approximately the same shape and could not be mistaken for those derived for samples deposited in the upper flow regime. In the case of sample A44 from the dune stage of the lower flow regime (Fig. A2), the two curves are the same shape, but the elongation function curve derived by the new method is slightly displaced toward the lower values. The curve for sample 1175 (Fig. A3) derived by Moss (1968) extends over a range greater than the one in the present study, but the results are similar in the range common to both curves. There is a strong suggestion in the newer curve of a bimodality at the finer end of the sediment, and two curves can be constructed to represent two grain populations, A and B. Thus it is possible that this method is capable of providing a slightly clearer picture of the fabric in the finer grainsize range than has hitherto been possible. The scatter plot of the same sample (Fig. A4) reveals a tendency towards bimodality, but the overlap of the two postulated curves is not sufficiently great to confirm that they exist independently.

TABLE A. SAMPLES USED IN ELONGATION FUNCTION ANALYSIS

Sample	*Structure*	*Stratigraphic Unit*	*No. of Grains*	*Linear* (L) *Exponential* (E)
1189	Samples provided by Dr A. J. Moss—		1030	L
A44	unconsolidated sand deposited in the lower		921	L
1175	flow regime		1298	L
220	Planar stratification, parting lineation	Rewan Group	1980	E
218	Planar stratification, parting lineation	Rewan Group	2248	E
204	Planar stratification, parting lineation	Rewan Group	1532	E
204	Planar stratification, parting lineation	Rewan Group	2070	E
219	Planar stratification	Glenidal Formation	1630	E
252	Planar stratification	Glenidal Formation	1542	E
213	Rib-and-furrow marks	Rewan Group	1712	E
215	Planar stratification	Expedition Sandstone	1022	L
253	Planar stratification	Expedition Sandstone	1049	E
214	Solitary cross-stratification	Expedition Sandstone	1291	L
217	Solitary cross-stratification	Expedition Sandstone	1176	L

The curves derived from the measurement of two of three planar stratified finer sandstone samples with parting lineation (Figs A5, A6, B, C) from the Rewan Group are consistent with those demonstrated by Moss (1972) to be indicative of the lower flow regime. The result of the measurement of the other sample 204 (Fig. A7) is not clear, because it does not appear to coincide with any normal upper or lower flow regime curves as derived by Moss (1972). A second curve for a different lamina from the same sample (Fig. A8) has the same basic shape, but the peak at 0.12 mm is subdued. A sample with rib-and-furrow marks (Pettijohn, 1957, pl. 4) yielded the same type of curve (Fig. A9). The form of this structure suggests that it is produced by the migration of small ripple trains, and the curve probably indicates deposition in the lower flow regime. Thus it is believed that sample 204 was deposited under similar flow conditions. The shape of the curve indicates a steep gradient in the elongation function of population B grains, reflecting a selection of only the most elongate of the larger population B grains to fill the interstices within the framework of population A grains.

Curves for parallel stratified sandstone samples from the Glenidal Formation and Expedition Sandstone in the southwestern part of the basin are also indicative of the lower flow regime (Figs A10-A13). The curves for samples 252 and 215 are the normal type, but those for samples 219 and 253 are more like the curves derived for samples 204 and 213 (Figs A7-A9).

Curves derived from the measurement of two samples from solitary cross-stratified units are not consistent with those of sediments deposited in the lower flow regime. It is therefore likely that the low elongation values of sample 214 at 0.25 mm (Fig. A14) represent 'Feature 1' of a sediment of the rheologic stage (Moss, 1968, 1972), which reflects the paucity of elongate population B grains at this point. The peak at 0.45 mm corresponds with 'Feature 2', and 'Feature 3' is present at 1.4 mm. In the second sample (217; Fig. A15) from a solitary cross-stratified unit 'Feature 1' appears to be absent, but this is probably the result of lack of measurements of grains finer than 0.1 mm. 'Feature 2' and 'Feature 3' are represented by peaks at about 0.2 and 0.5 mm. The results from these two samples indicate that at least some of the cross-stratified units were not deposited as dunes, but rather as isolated structures caused by local conditions (i.e. they are non-repetitive bed-forms). Furthermore, it appears that the movement of grains down the foreset of a microdelta is in some cases akin to the rheologic flow developed on a horizontal bed.

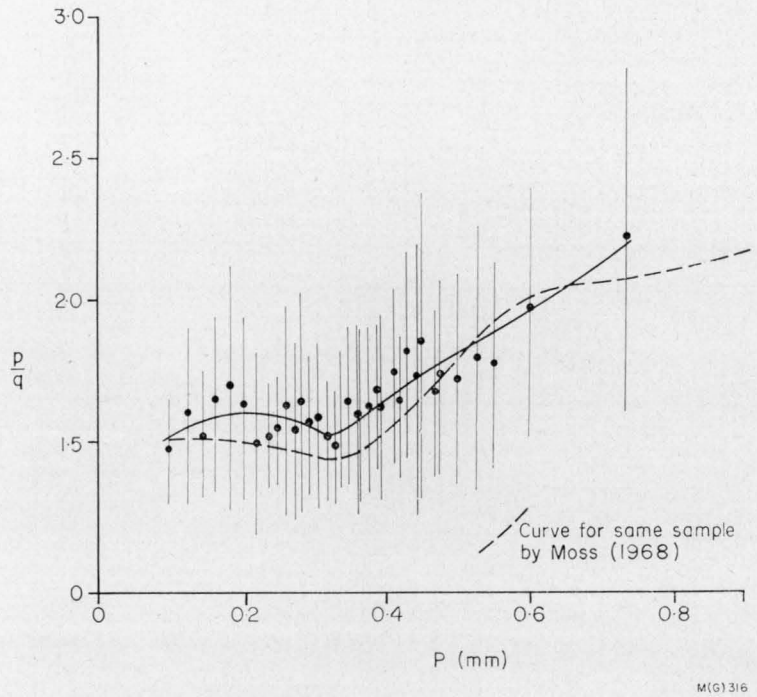


Fig. A1. Sample 1189, ripple stage. Means of groups of 30 measurements.

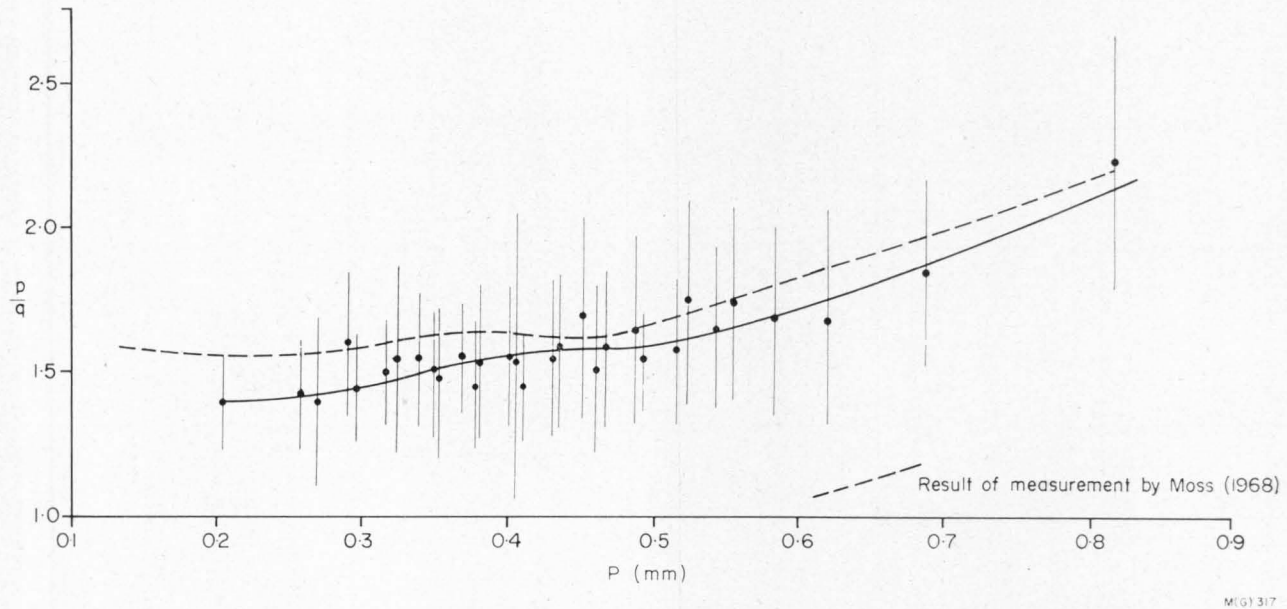


Fig. A2. Sample A44, a dune stage sand provided by Dr A. J. Moss. Means of groups of 30 measurements.

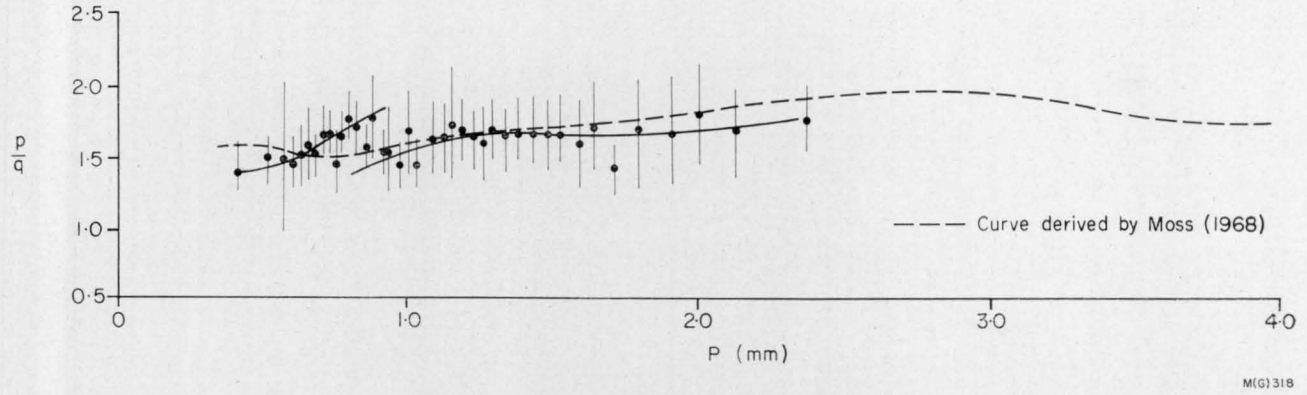


Fig. A.3. Sample 11775, ripple stage sand provided by Dr A. J. Moss. Means of groups of 30 measurements.

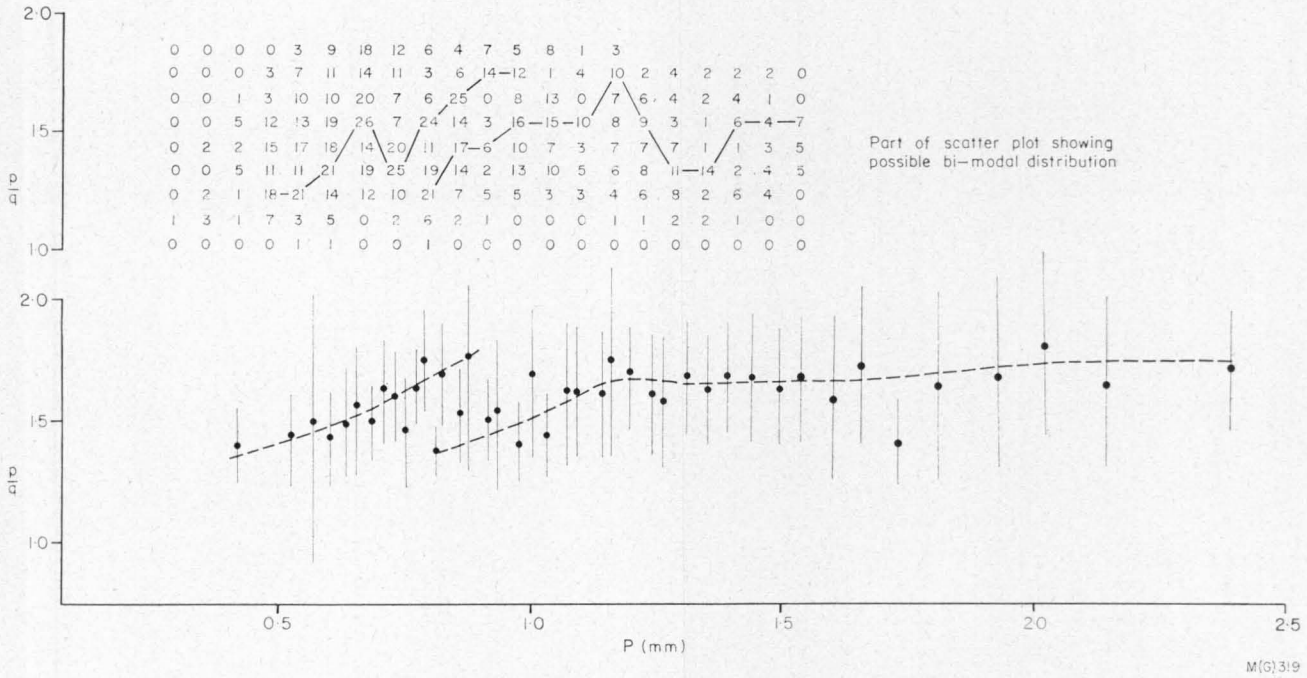


Fig. A4. Sample 1175, curve and scatter plot. Means of groups of 30 measurements.

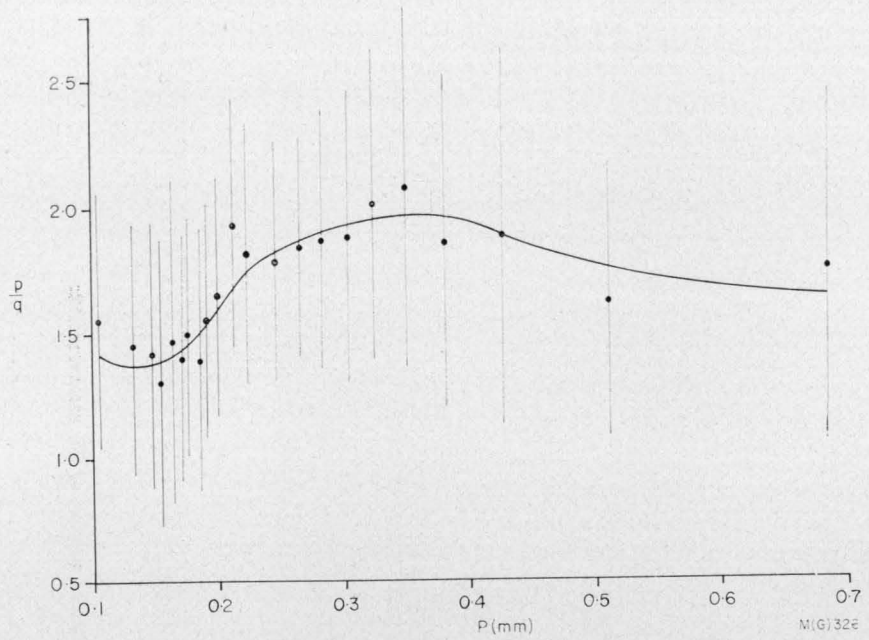


Fig. A5. Sample 220, planar stratification with parting lineation. Means of groups of 30 measurements.

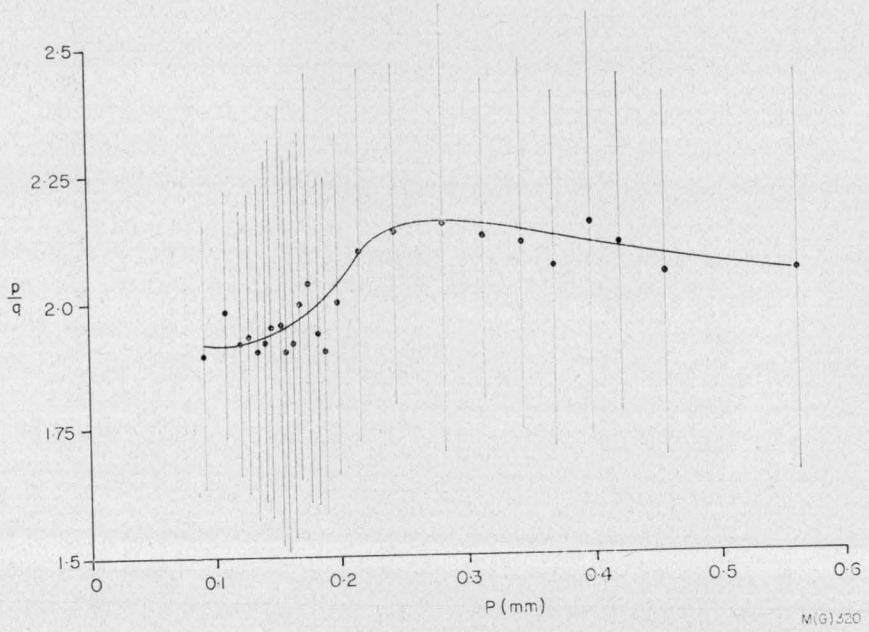


Fig. A6. Sample 218, planar stratification with parting lineation. Means of groups of 90 measurements.

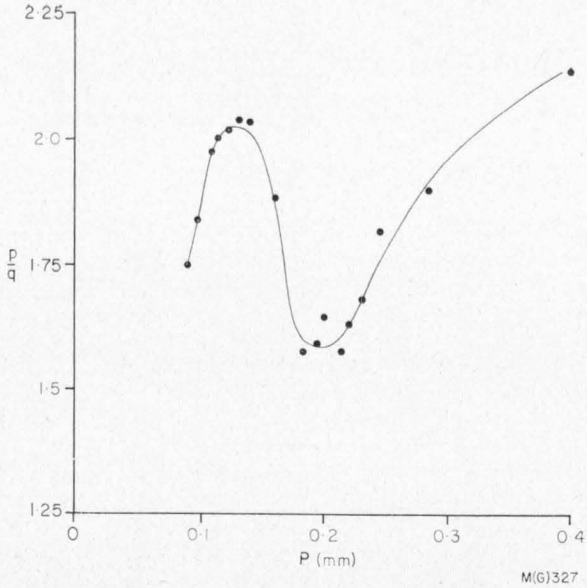


Fig. A7. Sample 204, planar stratification with parting lineation. Means of groups of 90 measurements.

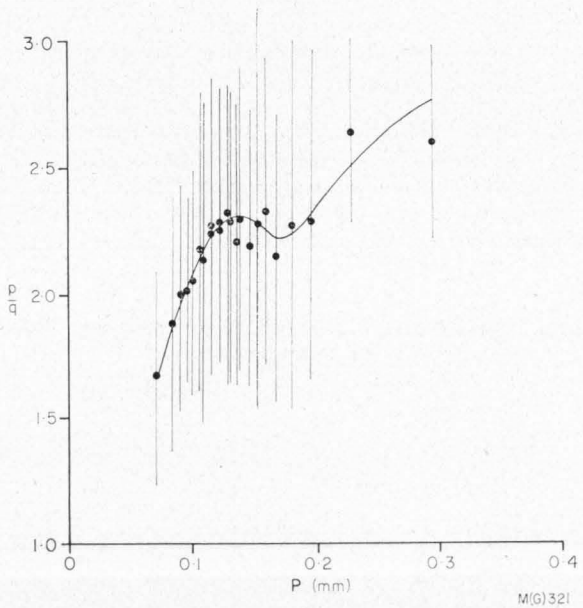


Fig. A8. Sample 204, different lamination. Means of groups of 90 measurements.

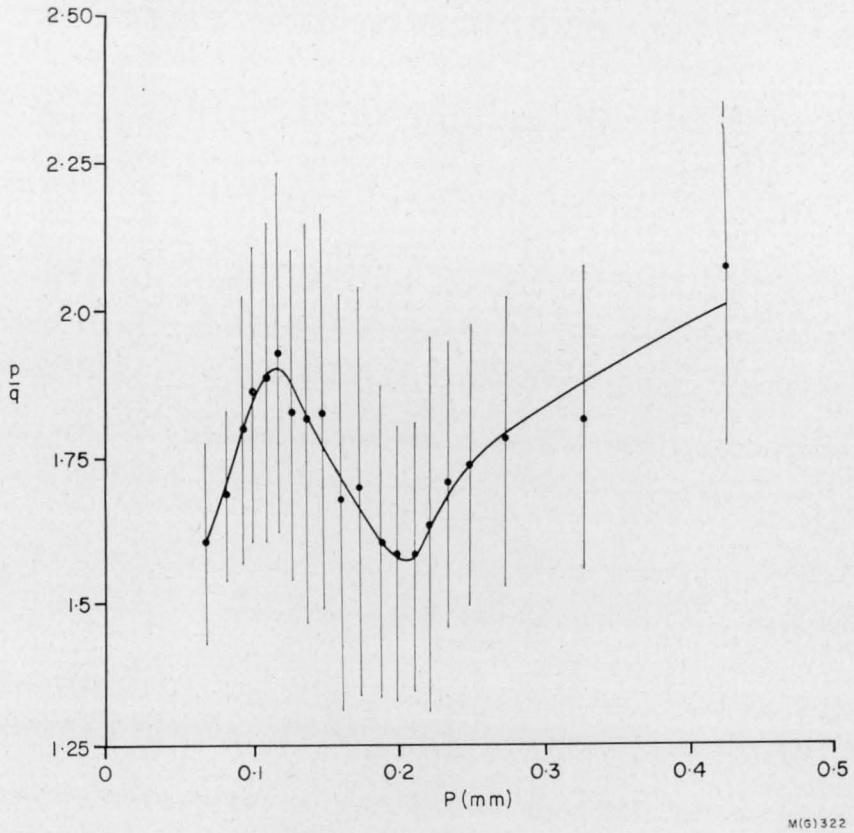


Fig. A9. Sample 213, sandstone with rib-and-furrow structure. Means of groups of 90 measurements.

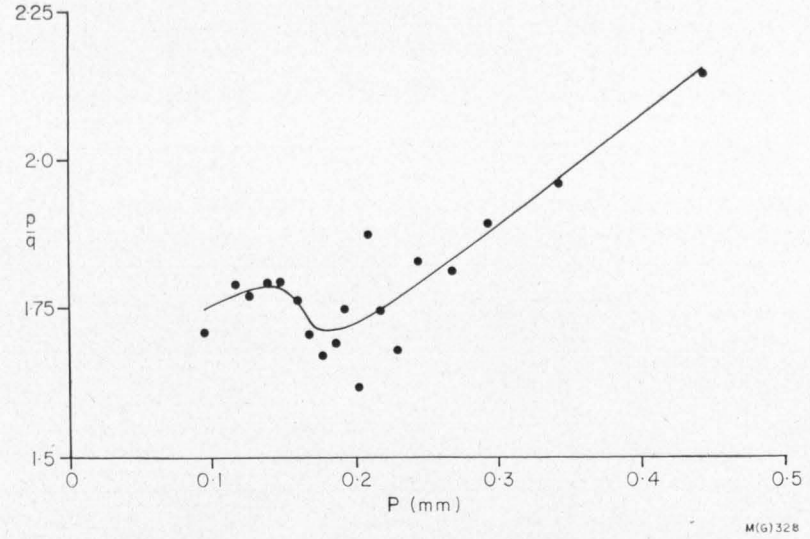


Fig. A10. Sample 219, planar stratification. Means of groups of 90 measurements.

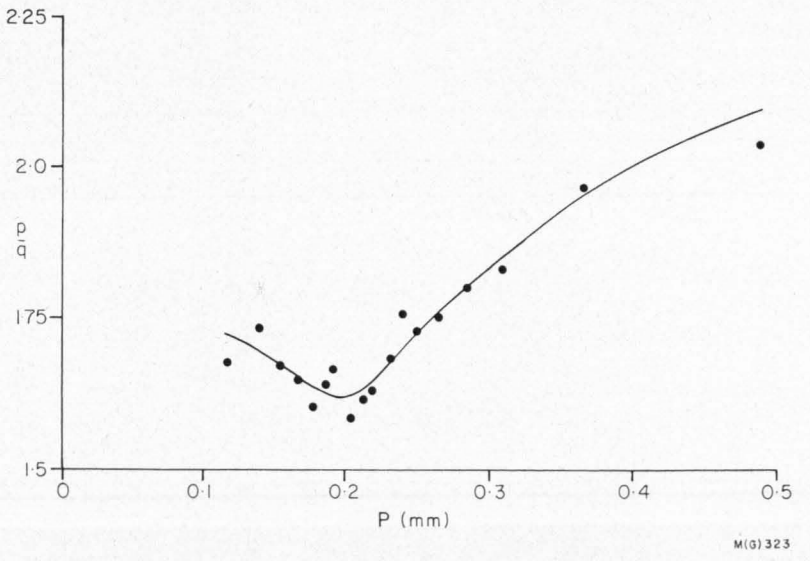


Fig. A11. Sample 252, planar stratification. Means of groups of 90 measurements.

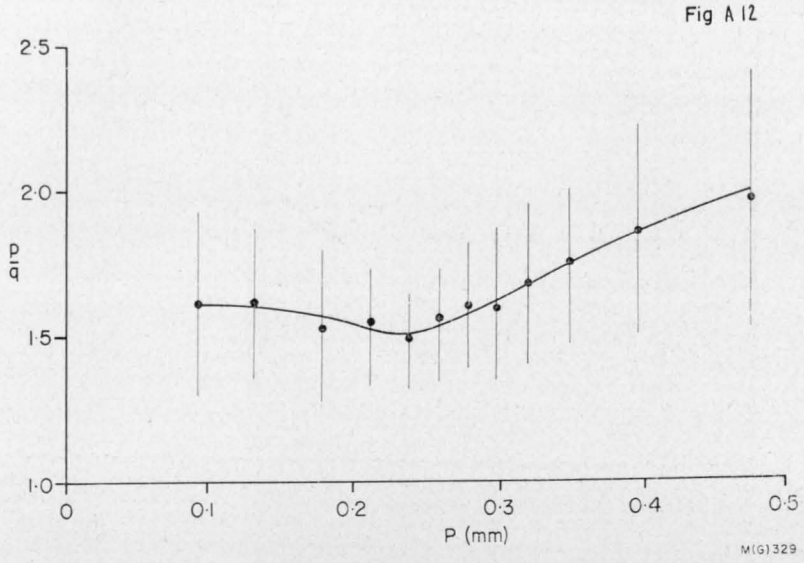


Fig. A12. Sample 215, planar stratification, Expedition Sandstone. Means of groups of 90 measurements.

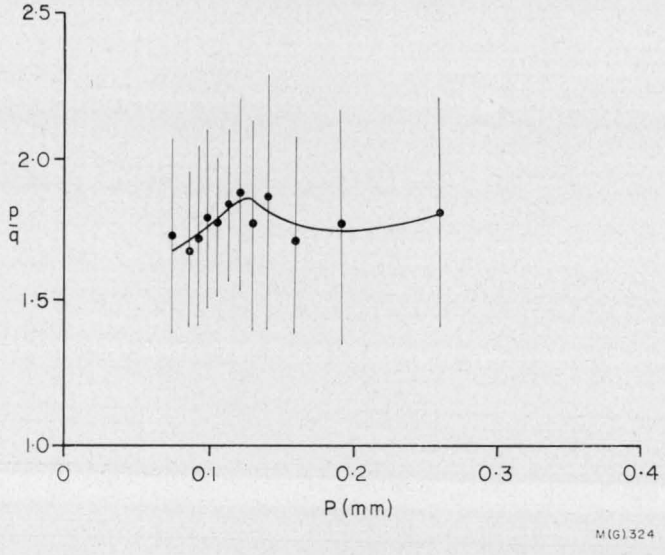


Fig. A13. Sample 253, planar stratification, Expedition Sandstone. Means of groups of 90 measurements.

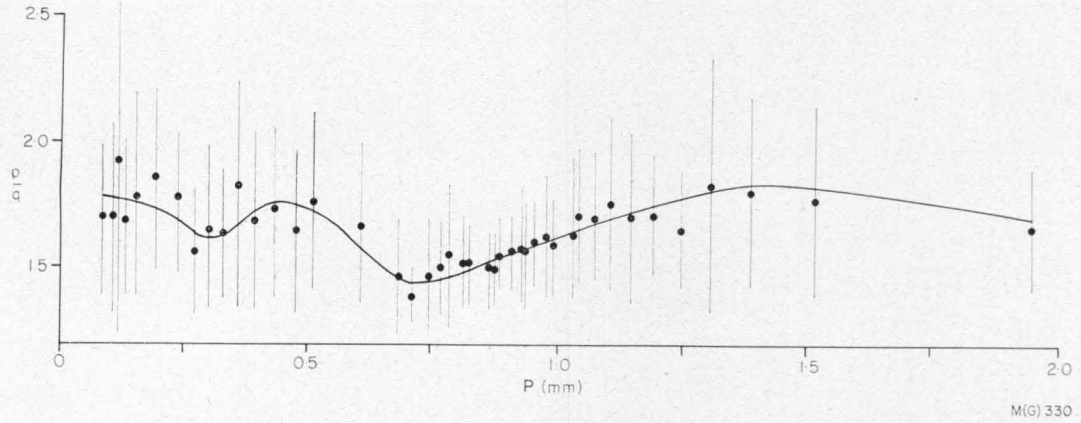


Fig. A14. Sample 214, sandstone with solitary cross-stratification. Means of groups of 30 measurements.

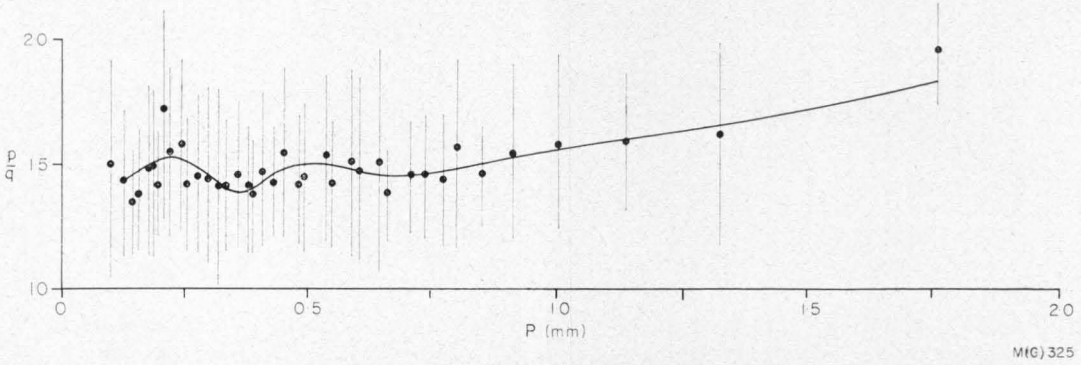


Fig. A15. Sample 217, sandstone with solitary cross-stratification. Means of groups of 30 measurements.



Fig. C. Parting lineation in the Sagittarius Sandstone. Sample 204, half natural scale. Central area.

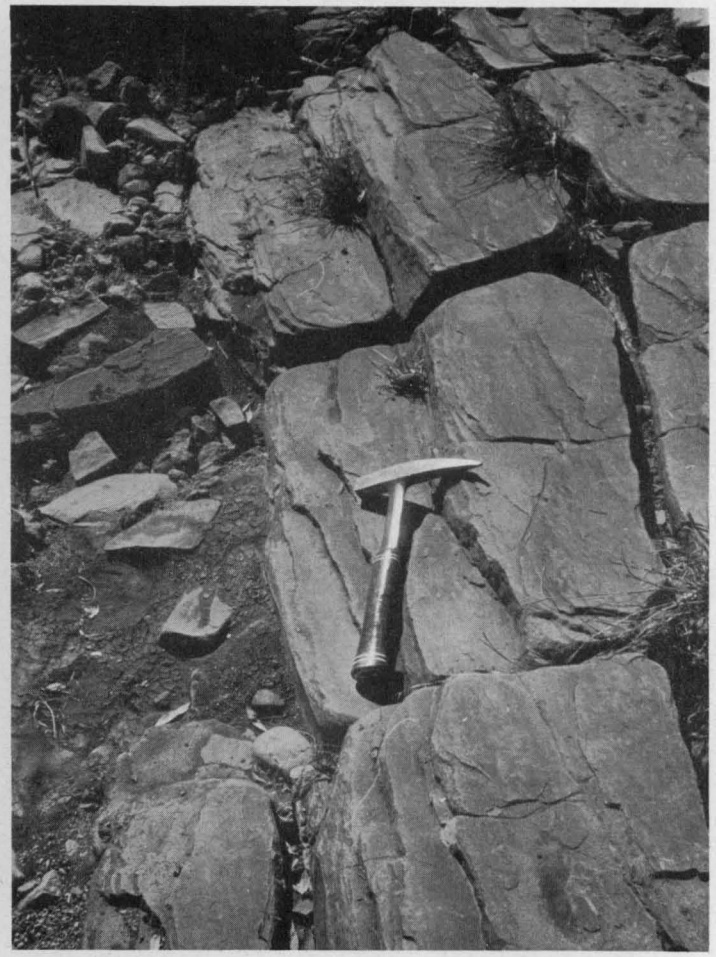


Fig. B. Sagittarius Sandstone showing planar stratification and marked parting lineation. Central area.

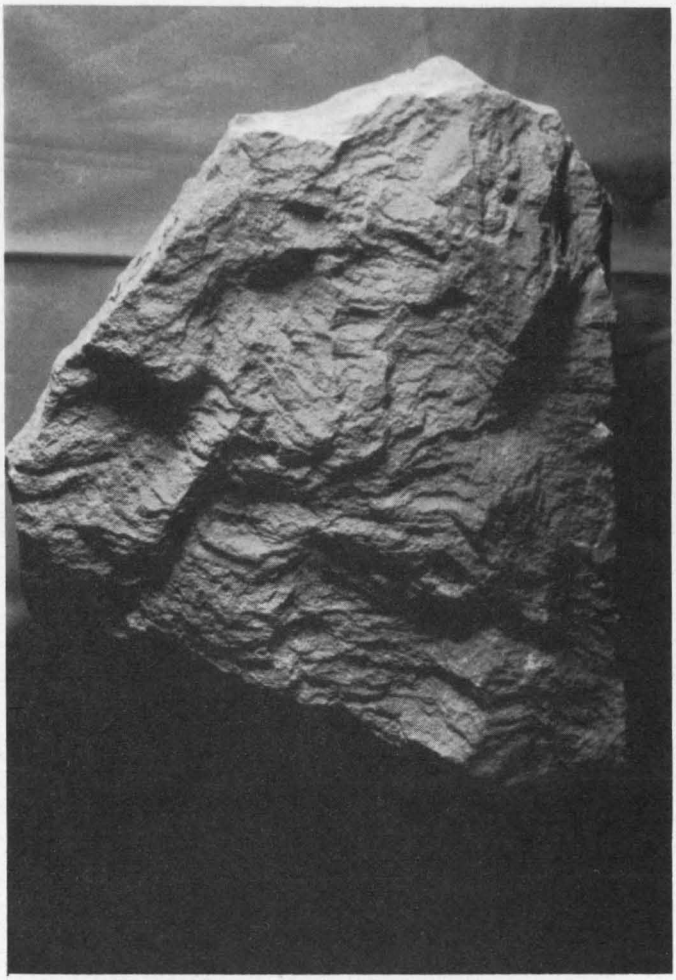


Fig. D. Rib-and-furrow marks in the Sagittarius Sandstone formed by the migration of small ripple trains in the lower flow regime. Half natural scale. Southwestern area.

REFERENCES

ALLEN, J. R. L., 1970—Studies in fluviatile sedimentation: a comparison of fining-upwards cyclothems, with special reference to coarse-member composition and interpretation. *J. sediment. Petrol.*, 40(1), 298-323.

Moss, A. J., 1962—The physical nature of common sandy and pebbly deposits, Part 1. *Amer. J. Sci.*, 260, 337-73.

Moss, A. J., 1963—The physical nature of common sandy and pebbly deposits, Part 2. *Ibid.*, 261, 297-343.

Moss, A. J., 1968—Bed-load deposits of shallow unidirectional currents. Ph.D. Thesis, *Aust. Nat. Univ.* (unpubl.).

Moss, A. J., 1972—Bed-load sediments. *Sedimentology*, 18, 159-219.

PETTIJOHN, F. J., 1957—SEDIMENTARY ROCKS. *N.Y., Harper*, 2nd Ed.

SIMONS, D. B., RICHARDSON, E. V., & ALBERTSON, M. L., 1961—Flume studies using medium sand (0.45 mm). *Wat. Supply Irrig. Pap. Wash.*, 1498A, 76 pp.

APPENDIX 2

Page

Table B. Location of samples 167

Table C. Modal analyses of arenite samples 176

Table D. Cross-stratification in Permian and Triassic units 183

TABLE B. LOCATION OF SAMPLES

Serial No.	*BMR No.*	*1:250 000 Sheet*	*Grid Reference*	*General Location*	*Stratigraphic Position*
1	69017137/8	Mt Coolon	64813152	L. Elphinstone	185 m
2	68012411/E	Mt Coolon	64843154	L. Elphinstone	190 m
3	65014318	Mt Coolon	65443066	L. Elphinstone	170 m
4	65014317	Mt Coolon	65443066	L. Elphinstone	105 m
5	69017137/6	Mt Coolon	64813152	L. Elphinstone	75 m — above base of Arcadia Fm
6	69017137/2	Mt Coolon	64813152	L. Elphinstone	45 m
7	65012402/2	Mt Coolon	65782066	L. Elphinstone	40 m
8	65014316	Mt Coolon	65373072	L. Elphinstone	40 m
9	68012303	Mt Coolon	65713075	L. Elphinstone	0 m
10	68012206	Mt Coolon	65883067	L. Elphinstone	Top
11	65010174	Mt Coolon	65502942	L. Elphinstone	175 m
12	68012205	Mt Coolon	65883067	L. Elphinstone	175 m
13	68012204	Mt Coolon	65883067	L. Elphinstone	170 m — above base of u. part of Sagittarius Sst
14	68012203	Mt Coolon	65883067	L. Elphinstone	150 m
15	68012201	Mt Coolon	65883067	L. Elphinstone	120 m
16	65010177	Mt Coolon	66163033	L. Elphinstone	115 m
17	65014314	Mt Coolon	65803096	L. Elphinstone	60 m
18	68012508	Mt Coolon	65833086	L. Elphinstone	15-30 m above base of Sagittarius Sst
19	68012505	Mt Coolon	65833086	L. Elphinstone	
20	68012504	Mt Coolon	65833086	L. Elphinstone	
21	68012503	Mt Coolon	65833086	L. Elphinstone	
22	65015507	Mt Coolon	67281580	L. Elphinstone	
23	65010167	Mt Coolon	66093052	L. Elphinstone	
24	65010169	Mt Coolon	66163023	L. Elphinstone	

TABLE B—*Continued*

Serial No.	*BMR No.*	*1:250 000 Sheet*	*Grid Reference*	*General Location*	*Stratigraphic Position*
25	65016418	Duaringa	16370431	49 m	218 m
26	65016419	Duaringa	16370431	92 m	176 m
27	65016421	Duaringa	16370431	128 m	138 m
28	65016422	Duaringa	16370431	156 m	115 m
29	65016423	Duaringa	16370431	179 m	89 m
30	65016424	Duaringa	16370431	211 m	56 m
				BHP No. 1 coal bore, Blackwater	above top of Permian coal meas.
31	65016427	Duaringa	16370431	315 m	46 m below top of Permian coal meas.
32	65016311	Duaringa	16530594	60 m	138 m
33	65016312	Duaringa	16530594	65 m	133 m
34	65016315	Duaringa	16530594	125 m	73 m
35	65016317	Duaringa	16530594	141 m	57 m
36	65016319	Duaringa	16530594	196 m	2 m
				BHP No. 2 coal bore, Blackwater	above top of Permian coal meas.
37	65016321	Duaringa	16530594	223 m	27 m
38	65016322	Duaringa	16530594	242 m	44 m
39	65016323	Duaringa	16530594	263 m	65 m
					below top of Permian coal meas.
40	69017146/6	Mt Coolon	65243505		
41	69017146/3	Mt Coolon	65243505		
42	72010038	Mt Coolon	64823589		Arcadia Fm
43	72010041	Mt Coolon	64843620	Blenheim area	
44	72010040	Mt Coolon	64873635		
45	72010039	Mt Coolon	64873635		Sagittarius Sst
46	R12544	Mt Coolon	65173586		
47	72010042	Mt Coolon	65173586		U. part of Arcadia Fm

TABLE B—*Continued*

Serial No.	*BMR No.*	*1:250 000 Sheet*	*Grid Reference*	*General Location*	*Stratigraphic Position*
48	68013806	Taroom	13298674	Moolayember Cr.	U. part of Arcadia Fm
49	68013401	Taroom	15808386	Basin Cr.	
50	69017111G	Taroom	13398669	Moolayember Cr.	
51	69017111C	Taroom	13398669	Moolayember Cr.	
52	68013801	Taroom	13298674	Moolayember Cr.	
53	69017126/8	Taroom	13298677	S. part of Arcadia	
54	69017126/5	Taroom	16358277	valley	
55	R17136	Springsure	66228990	Mt Carnarvon	280 m above base of Arcadia Fm
56	R17134	Springsure	66228990	Mt Carnarvon	130 m
57	68013640/A	Taroom	15958290	S. part of Arcadia	50 m
58	65012404	Taroom	15538515	Brumby Mountain	50 m
59	65012403	Taroom	15538515	Brumby Mountain	100 m above base of u. part of Sagittarius Sst
60	61012401	Taroom	15538515	Brumby Mountain	20 m
61	65012501	Taroom	15538515	Brumby Mountain	Base
62	65012504	Taroom	15358521	Brumby Mountain	100 m above base of Sagittarius Sst
63	65012505	Taroom	15358521	Brumby Mountain	100 m
64	65013601	Springsure	65969009	Mt Carnarvon	30 m
65	68010818	Baralaba	28228824	Glenmoral Gap	207 m above base of Glenidal Fm
66	68010817	Baralaba	28228824	Glenmoral Gap	133 m
67	68010814	Baralaba	28228824	Glenmoral Gap	119 m
68	68010812	Baralaba	28228824	Glenmoral Gap	98 m
69	68010811	Baralaba	28228824	Glenmoral Gap	95 m
70	**68010810**	Baralaba	28228824	Glenmoral Gap	89 m
71	68010809	Baralaba	28228824	Glenmoral Gap	80 m
72	68010807	Baralaba	28228824	Glenmoral Gap	64 m above base of Dawson Ra. Sst
73	68010805	Baralaba	28228824	Glenmoral Gap	49 m
74	68010802	Baralaba	28228824	Glenmoral Gap	34 m
75	68010801	Baralaba	28228824	Glenmoral Gap	25 m

TABLE B—*Continued*

Serial No.	*BMR No.*	*1:250 000 Sheet*	*Grid Reference*	*General Location*	*Stratigraphic Position*
76	68012436	Baralaba	28298940	E. of Dawson Ra. near Glenmoral Gap	460 m
77	68012434/A	Baralaba	28268951	E. of Dawson Ra. near Glenmoral Gap	225 m
78	68012446/8	Baralaba	28209039	E. of Dawson Ra. near Glenmoral Gap	210 m above base of Glenidal Fm
79	68012447/A	Baralaba	28209039	E. of Dawson Ra. near Glenmoral Gap	175 m
80	68012445/A	Baralaba	28388997	E. of Dawson Ra. near Glenmoral Gap	130 m
81	68012440/A	Baralaba	27859261	E. of Dawson Ra. near Glenmoral Gap	115 m
82	(DRD15)	Baralaba	28758918	E. of Dawson Ra. near Glenmoral Gap	1510 m
83	69017110/1	Baralaba	28659146	E. of Dawson Ra. near Glenmoral Gap	1200 m
84	69017110/2	Baralaba	28659146	E. of Dawson Ra. near Glenmoral Gap	1200 m
85	68012443/A	Baralaba	28659146	E. of Dawson Ra. near Glenmoral Gap	1200 m above base of Rewan Gp
86	68012443/B	Baralaba	28659146	E. of Dawson Ra. near Glenmoral Gap	1200 m
87	(BAR23)	Mundubbera	29528808	BMR Baralaba No. 23	400 m
88	(BAR24)	Mundubbera	30278722	BMR Baralaba No. 24	10 m
89	(BAR25)	Mundubbera	30208724	BMR Baralaba No. 25	20 m
90	68012604	Mt Coolon	65182876	Kerlong Ra.	460 m
91	68012603	Mt Coolon	65182876	Kerlong Ra.	420 m above base of Clematis Gp
92	68012602	Mt Coolon	65182876	Kerlong Ra.	190 m
93	68012601	Mt Coolon	65182876	Kerlong Ra.	90 m
94	68012908	Mt Coolon	64773553	Redcliffe Tableland	
95	68012907	Mt Coolon	64773553	Redcliffe Tableland	
96	68012906	Mt Coolon	64773553	Redcliffe Tableland	
97	68012905	Mt Coolon	64773553	Redcliffe Tableland	
98	68012103	Mt Coolon	65213082	Carborough Ra.	
99	68012101	Mt Coolon	65213082	Carborough Ra.	Clematis Gp
100	68012021	Mt Coolon	64773020	Kerlong Ra.	
101	68012010	Mt Coolon	64773020	Kerlong Ra.	
102	68012003	Mt Coolon	64773020	Kerlong Ra.	
103	68012001	Mt Coolon	64773020	Kerlong Ra.	
104	68012709	Mt Coolon	65242896	Kerlong Ra.	Moolayember Fm
105	68012706	Mt Coolon	65242896	Kerlong Ra.	130 m
106	68012705	Mt Coolon	65242896	Kerlong Ra.	120 m
107	68012704	Mt Coolon	65242896	Kerlong Ra.	100 m
108	68012703	Mt Coolon	65242896	Kerlong Ra.	55 m above base of u. part
109	68012702	Mt Coolon	65242896	Kerlong Ra.	30 m of Expedition SSt
110	68012605	Mt Coolon	65182876	Kerlong Ra.	20 m
111	68012614	Mt Coolon	65182876	Kerlong Ra.	15 m
112	68012613	Mt Coolon	65182876	Kerlong Ra.	10 m

TABLE B—*Continued*

Serial No.	*BMR No.*	*1:250 000 Sheet*	*Grid Reference*	*General Location*	*Stratigraphic Position*
113	68012612	Mt Coolon	65182876	Kerlong Ra.	145 m
114	68012611	Mt Coolon	65182876	Kerlong Ra.	140 m
115	68012610	Mt Coolon	65182876	Kerlong Ra.	125 m
116	68012609	Mt Coolon	65182876	Kerlong Ra.	110 m
117	68012608	Mt Coolon	65182876	Kerlong Ra.	90 m
118	68012607	Mt Coolon	65182876	Kerlong Ra.	60 m
119	68012606	Mt Coolon	65182876	Kerlong Ra.	20 m
120	68011807	Mt Coolon	64393562	Redcliffe Tableland	Moolayember Fm
121	68011805	Mt Coolon	64393562	Redcliffe Tableland	
122	68011802	Mt Coolon	64393562	Redcliffe Tableland	
123	68012810	Mt Coolon	64513562	Redcliffe Tableland	75 m
124	68012808	Mt Coolon	64513562	Redcliffe Tableland	170 m
125	68012806	Mt Coolon	64513562	Redcliffe Tableland	85 m
126	68012813	Mt Coolon	64513562	Redcliffe Tableland	30 m
127	68012811	Mt Coolon	64513562	Redcliffe Tableland	5 m
128	68012911	Mt Coolon	64773553	Redcliffe Tableland	L. part of Expedition Sst
129	68012909	Mt Coolon	64773553	Redcliffe Tableland	
130	68012125	Mt Coolon	65213082	Carborough Ra.	170 m
131	68012123	Mt Coolon	65213082	Carborough Ra.	155 m
132	68012120	Mt Coolon	65213082	Carborough Ra.	115 m
133	68012119	Mt Coolon	65213082	Carborough Ra.	90 m
134	68012118	Mt Coolon	65213082	Carborough Ra.	45 m
135	68012117	Mt Coolon	65213082	Carborough Ra.	20 m
136	68012114	Mt Coolon	65213082	Carborough Ra.	140 m
137	68012110	Mt Coolon	65213082	Carborough Ra.	110 m
138	68012107	Mt Coolon	65213082	Carborough Ra.	35 m
139	68010605	Duaringa	21930257	Raby Cr.	Expedition Sst (see Fig. 23)
140	68010603	Duaringa	21930257	Raby Cr.	
141	68010608	Duaringa	21930257	Raby Cr.	
142	68010507	Duaringa	21930257	Raby Cr.	
143	68010505	Duaringa	21930257	Raby Cr.	
144	68010503	Duaringa	21930257	Raby Cr.	
145	68010501	Duaringa	21930257	Raby Cr.	
146	68010207	Duaringa	21950289	Raby Cr.	

TABLE B—*Continued*

Serial No.	*BMR No.*	*1:250 000 Sheet*	*Grid Reference*	*General Location*	*Stratigraphic Position*
147	68010203	Duaringa	21950289	Raby Cr.	Glenidal Fm (see Fig. 23)
148	68012420	Duaringa	21810303	Raby Cr.	
149	68010201	Duaringa	21950289	Raby Cr.	
150	68010305	Duaringa	21520300	Raby Cr.	
151	68010304	Duaringa	21520300	Raby Cr.	
152	68010303	Duaringa	21520300	Raby Cr.	
153	68010301	Duaringa	21520300	Raby Cr.	
154	68010402	Duaringa	21540354	Raby Cr.	
155	68010401	Duaringa	21540354	Raby Cr.	
156		Taroom	19348655	core 2 at 868.7 m, Glenhaughton No. 1	Top of Expedition Sst
157	69017123/C	Baralaba	16408965	Clematis Cr.	Expedition Sst
158	68013423	Taroom	15808386	Basin Cr.	
159	68013422	Taroom	15808386	Basin Cr.	
160	68013420	Taroom	15808386	Basin Cr.	
161	68013418	Taroom	15808386	Basin Cr.	U. part of Expedition Sst
162	68013415	Taroom	15808386	Basin Cr.	
163	68013414	Taroom	15808386	Basin Cr.	
164	68013411	Taroom	15808386	Basin Cr.	
165	68013408	Taroom	15808386	Basin Cr.	
166	68013710	Baralaba	16469002	Clematis Cr.	
167	68013810	Taroom	13298674	Moolayember	
168	68013709	Baralaba	16469002	Clematis Cr.	L. part of Expedition Sst
169	68013708	Baralaba	16469002	Clematis Cr.	
170	68013205	Baralaba	16408964	Clematis Cr.	
171	68013706	Baralaba	16469002	Clematis Cr.	
172		Taroom	19348655	Core 3 at 784.9 m, Glenhaughton No. 1	
173	69017203	Baralaba	16408964	Clematis Cr.	Glenidal Fm
174	68013705	Baralaba	16649002	Clematis Cr.	
175	68013701	Baralaba	16649002	Clematis Cr.	
176	68013808	Taroom	13298674	Moolayember	
177	68013407	Taroom	15808386	Basin Cr.	
178	68013404	Taroom	15808386	Basin Cr.	
179	69017201	Baralaba	16408964	Clematis Cr.	

TABLE B—*Continued*

Serial No.	*BMR No.*	*1:250 000 Sheet*	*Grid Reference*	*General Location*	*Stratigraphic Position*
180	68012411/D	Mt Coolon	64843154	Carborough Ra.	200 m above base of Arcadia Fm
181	68012402	Mt Coolon	65783066	L. Elphinstone	55 m above base of Arcadia Fm
182	69017137/1	Mt Coolon	64843154	Carborough Ra.	55 m above base of Arcadia Fm
183	68012401	Mt Coolon	65833052	L. Elphinstone	Base of Arcadia Fm
184	68012409/H	Mt Coolon	63913038	Burton Ra.	Base of Arcadia Fm
185	68012016	Mt Coolon	64773020	Kerlong Ra.	Top of Glenidal Fm
186	65010259	Duaringa	15770407	Blackwater	Base of Sagittarius Sst
187	68010202	Duaringa	21950289	Raby Cr.	Top of Glenidal Fm
188	68010302	Duaringa	21520300	Raby Cr.	50 m above base of Glenidal Fm
189	69017104/3	Taroom	14318608	Spring Cr.	Expedition Sst
190	68013644/A	Springsure	66489060	Serocold homestead	Expedition Sst
191	69017105/9	Taroom	1438608	Spring Cr.	Expedition Sst
192	69017133/B	Taroom	13398669	Moolayember Dip	Glenidal Fm
193	69017133/M	Taroom	13398669	Moolayember Dip	Glenidal Fm
194	69017123/4	Taroom	16358277	S. end Arcadia valley	Arcadia Fm
195	69017126/3	Taroom	16358277	S. end Arcadia valley	Arcadia Fm
196	69017111/D	Taroom	13398669	Moolayember Dip	Arcadia Fm
197	68013302	Taroom	16358277	S. end Arcadia valley	Arcadia Fm
198	68013301	Taroom	16358277	S. end Arcadia valley	Arcadia Fm
199	68013104	Taroom	13288675	Moolayember Dip	Arcadia Fm
200	680113102	Taroom	13288675	Moolayember Dip	Arcadia Fm
201	68013640/B	Taroom	15958290	S. end Arcadia valley	Sagittarius Sst
202	68012443/D	Baralaba	28659146	Dawson R.	Rewan Gp
203	69017109/6	Baralaba	28228824	Glenmoral Gap	Dawson Ra. Sst
204	65010600	Duaringa	15770407	Blackwater	Sagittarius Sst
205		Mt Coolon	64953508	33.57 m Cores from BMR Mt Coolon No. 7	Glenidal Fm
206		Mt Coolon	64953508	33.76 m Cores from BMR Mt Coolon No. 7	Glenidal Fm
207		Mt Coolon	64953508	33.14 m Cores from BMR Mt Coolon No. 7	Glenidal Fm
208		Mt Coolon	64953508	34.39 m Cores from BMR Mt Coolon No. 7	Glenidal Fm
209		Mt Coolon	64953508	35.00 m Cores from BMR Mt Coolon No. 7	Glenidal Fm
210		Mt Coolon	64953508	35.46 m Cores from BMR Mt Coolon No. 7	Glenidal Fm
211		Mt Coolon	64953508	35.76 m Cores from BMR Mt Coolon No. 7	Glenidal Fm

TABLE B—*Continued*

Serial No.	*BMR No.*	*1:250 000 Sheet*	*Grid Reference*	*General Location*	*Stratigraphic Position*
212	68012402/K	Mt Coolon	65783060	L. Elphinstone	Arcadia Fm
213	65012506	Taroom	15358521	Brumby Mount	Sagittarius Sst
214	69017105/1	Taroom	14318608	Spring Cr.	Expedition Sst
215	69017105/2	Taroom	14318608	Spring Cr.	
216	69017106/4	Taroom	15808386	Basin Cr.	
217	69017114/6	Springsure	66489060	Serocold	
218	69017137/5	Mt Coolon	64843154	Carborough Ra.	Arcadia Fm
219	69017180	Taroom	13398669	Moolayember Dip	Glenidal Fm
220	68012401/F	Mt Coolon	65833052	L. Elphinstone	Arcadia Fm
221	65016801	Duaringa	15171022	5 km N of Cooroorah homestead	Near top of Fair Hill Fm
222	65016803	Duaringa	15171022	5	Near top
223	65010269	Duaringa	15241030	9	Near top
224	65013801	Duaringa	12961022	3	30 m below top
225	65010268	Duaringa	15201030	11	Middle
226	65015103	Duaringa	15040996	6	Near top
227	65010267	Duaringa	15161030	11	Base
228	65015102	Duaringa	15040996	6	Middle
229	65012103	Mundubbera	31138558	3 km SE of Gyranda homestead	30 m below top of Gyranda Fm
230	65012102	Mundubbera	31158506		60 m
231	65011402	Mundubbera	31228569		205 m
232	65011401	Mundubbera	31228569		205 m
233	65011301	Mundubbera	31288570		410 m
234	65015402	Mt Coolon	67643179	11 km N Fort Cooper homestead	450 m above base of Fair Hill Fm
235	65015401	Mt Coolon	67703281	11 km N Fort Cooper homestead	400 m
236	65015609	Bowen	64063776	2 km SW Exmoor homestead	240 m
237	65015607	Bowen	64083780	1 km SW Exmoor homestead	140 m
238	65015606	Bowen	64093782	1 km SW Exmoor homestead	14 m
239	65015605	Bowen	64103784	1 km SW Exmoor homestead	7 m
240	65014403	Mt Coolon	68163109	11 km NE Fort Cooper homestead	60 m
241	65014402	Mt Coolon	68193110	11 km NE Fort Cooper homestead	14 m

TABLE B—*Continued*

Serial No.	*BMR No.*	*1:250 000 Sheet*	*Grid Reference*	*General Location*	*Stratigraphic Position*
242	65010155	Mt Coolon	66233044	Nebo area	Elphinstone Coal Meas.
243	65010156	Mt Coolon	66283021	Nebo area	
244	65015505	Mt Coolon	67303164	Nebo area	360 m above base of Fort Cooper Coal Meas.
245	65015501	Mt Coolon	67363182	Nebo area	90 m above base of Fort Cooper Coal Meas.
246	65010287	Duaringa	15660384	7 km SW Taurus homestead	Rangal Coal Meas.
247	65010215	Monto	29569483	Moura open cut mine	
248	65016102	Baralaba	27889901	Dawson R., near Baralaba	
249	65010480	Baralaba	27889901	Dawson R., near Baralaba	
250	65011603	Mundubbera	29628842	4 km W Kia Ora homestead	
251	65010275	Duaringa	15241022	10 km N Cooroorah homestead	Burngrove Fm
252	69017133C	Taroom	13398669	Moolayember Dip	Glenidal Fm
253	69017106/5	Taroom		Basin Cr.	

TABLE C. MODAL ANALYSES OF ARENITE SAMPLES

Sample No.		Fabric		Composition										Lithic Fragments					Minor Constituents													
				Framework					Matrix		Cement																						
Serial	BMR	Grainsize (ϕ units)	Sorting (ϕ units)	Quartz	Lithic	K-Feldspar	Plagioclase	Others	Undifferentiated	Clay	Silica	Carbonate	Iron	Volcanic	Sedimentary	Plutonic	Metamorphic	Biotite	Muscovite	Garnet	Zircon	Tourmaline	Hornblende	Pyroxene	Epidote	Hematite	Limonite	Opaque	Apatite			
1	GA37-8	2.1	1.5	48.8	19.0	8.2	11.2	1.8	6.2	4.6	—	0.2	—	P	—	—	C	—	—	—	—	P	—	—	P	—	—	—	—			
2	BD11-E	2.3	1.3	31.0	31.6	0.4	7.4	5.5	5.9	11.8	1.1	—	5.5	—	C	—	P	—	—	—	—	—	—	—	—	C	—	—	—			
3	P3-18	3.8	1.4	29.1	20.2	8.0	8.3	2.9	8.4	17.2	2.0	—	3.9	P	C	—	P	—	—	—	—	—	—	—	—	—	—	—	—			
4	P3-17	3.0	1.1	32.5	24.9	4.0	10.4	6.3	5.0	14.6	1.3	—	1.0	P	—	—	P	—	—	—	—	—	—	—	—	A	P	P	—	C		
5	GA37-6	3.2	2.2	25.6	32.0	3.6	2.4	5.6	5.6	22.4	0.4	2.0	0.4	—	C	—	—	P	P	—	—	—	—	—	—	—	—	—	—			
6	GA37-2	2.8	1.2	37.5	34.3	1.3	9.8	4.4	6.4	5.6	—	0.3	—	P	—	—	—	P	P	—	—	—	—	—	—	P	—	—	—			
7	BD02-B	2.4	>3	19.5	47.8	—	4.0	0.8	1.8	25.7	—	0.4	—	P	C	—	P	P	—	—	—	P	—	—	C	—	—	—	P			
8	P3-16	4.4	1.1	27	24	5	6	7	20	11	—	—	—	P	P	—	P	C	P	—	—	—	—	—	—	—	—	—	—			
9	BC03	2.7	1.0	33.6	33.6	2.9	5.7	2.4	6.4	10.8	1.6	2.8	—	P	P	—	P	—	—	—	—	—	—	—	C	—	—	—	—			
10	BB06	2.6	1.7	33.1	25.8	4.0	4.8	10.3	15.5	3.7	2.5	0.2	—	P	—	—	P	A	—	—	—	—	—	—	C	—	—	—	—			
11	A74	4.0	1.5	30.9	14.5	3.8	6.8	2.2	10.4	23.7	—	3.4	4.3	P	—	P	P	—	—	—	P	P	—	—	A	—	—	—	P			
12	BB05	2.2	1.8	44	25	4	8	1	7	4	4	1	2	P	—	—	P	—	—	—	—	—	—	—	P	—	—	—	—			
13	BB04	2.8	1.1	43.8	19.6	8.0	10.0	5.4	3.6	6.8	2.0	0.8	—	P	P	—	—	C	—	—	—	—	—	P	A	—	—	P	A			
14	BB03	2.9	0.9	44.8	23.8	5.0	5.5	5.0	3.2	11.3	0.8	—	0.6	P	P	P	P	C	—	—	—	P	—	P	P	—	—	—	P			
15	BB01	2.7	1.6	39.8	27.4	4.2	6.6	0.6	11.4	2.6	4.8	0.6	2.0	P	P	P	P	P	—	—	—	—	—	—	P	—	—	—	—			
16	A77	3.2	2.0	30.0	8.7	4.8	2.0	10.6	4.8	32.8	—	6.2	—	C	P	—	—	—	—	—	P	—	—	—	—	—	P	—	—			
17	P3-14	3.2	1.8	40.4	13.6	8.6	9.0	2.9	7.0	18.5	—	—	—	P	P	C	—	C	P	—	—	—	—	—	—	—	—	—	—			
18	BE-08	2.8	1.8	27.3	36.8	2.4	7.8	2.2	11.1	4.2	3.9	—	4.3	P	P	P	P	P	—	—	—	—	—	—	—	—	—	—	—			
19	BE05	2.7	1.1	33	32	13	5	1	2	5	2	1	6	P	C	—	P	P	—	—	—	—	—	—	—	P	—	P	—			
20	BE04	3.0	2.1	21.9	41.8	—	9.0	3.4	18.0	5.1	0.6	0.2	—	C	C	P	P	C	—	—	—	—	—	—	—	—	—	P	P			
21	BE03	4.0	1.8	18	32	4	9	1	31	5	—	—	—	P	P	—	P	P	—	—	—	—	—	—	—	—	—	—	—			
22	Q5-7	1.5	0.5	13.2	39.4	2.0	2.6	12.3	—	11.9	—	18.6	—	P	C	—	—	—	—	—	—	—	—	—	—	C	A	—	—			
23	A67	1.3	2.1	27.0	41.0	3.2	2.0	—	3.3	11.9	12.1	—	—	C	P	—	—	—	—	—	—	—	—	—	—	—	—	—	—			
24	A69	1.8	3.4	14.1	42.8	0.6	0.6	15.9	19.9	4.8	—	1.2	—	C	C	P	P	—	—	—	—	—	—	—	—	C	A	—	—			
25	6418	m	m	8.0	35.5	—	1.3	14.5	3.0	2.6	—	27.6	8.4	—	P	—	—	—	—	—	—	—	—	—	—	C	C	—	—			
26	6419	f	p	15	32	—	6	5	—	39	—	3	—	P	P	P	—	P	—	—	—	—	—	—	—	—	—	—	—			
27	6421	f	p	22	19	—	9	3	—	43	—	4	—	P	P	—	?	P	P	—	—	—	—	—	—	—	—	—	—			
28	6422	m	m	26.2	21.4	—	9.9	2.9	—	25.0	—	14.6	—	P	—	?	C	—	—	—	—	—	—	—	—	—	—	—	P			
29	6423	m	m	14.1	47.4	—	7.5	1.6	1.4	—	—	28.0	—	P	P	—	P	—	P	—	—	—	—	—	—	—	—	—	—			
30	6424	m	m	27	30	—	5	—	15	17	—	6	—	P	—	—	—	—	P	—	P	—	—	—	—	—	P	—	—			
31	6427	c	m	14	20	—	15	1	7	25	—	18	—	P	—	—	P	—	—	—	P	—	—	—	—	—	—	—	—			
32	6311	f	m	17.8	17.3	—	1.1	2.1	13.6	4.7	—	44.4	—	—	P	—	P	P	—	—	—	—	—	—	—	—	—	—	—			

TABLE C—*Continued*

Sample No.		Fabric		Composition										Lithic Fragments				Minor Constituents												
				Framework					Matrix		Cement																			
Serial	BMR	Grainsize (φ units)	Sorting (φ units)	Quartz	Lithic	K-Feldspar	Plagioclase	Others	Undifferentiated	Clay	Silica	Carbonate	Iron	Volcanic	Sedimentary	Plutonic	Metamorphic	Biotite	Muscovite	Garnet	Zircon	Tourmaline	Hornblende	Pyroxene	Epidote	Hematite	Limonite	Opaque	Apatite
33	6312	f	p	18.3	20.1	—	1.5	1.7	3.7	12.8	1.0	40.9	—	—	—	—	—	P	—	—	—	P	—	—	—	—	—	—	—
34	6315	m	m	52.6	15.0	—	—	0.1	11.4	5.2	4.3	11.4	—	P	P	—	P	—	—	—	—	—	—	—	—	—	—	—	—
35	6317	f	p	24	39	—	3	1	12	9	—	12	—	—	—	—	—	—	—	—	—	—	—	—	—	—	—	—	—
36	6319	f	p	14.0	11.9	—	1.4	4.9	4.9	10.5	—	52.4	—	P	P	—	—	—	P	—	—	—	—	—	—	—	—	—	—
37	6321	f	m	12.7	25.7	—	9.1	0.5	1.1	—	—	50.9	—	P	—	—	—	—	—	—	—	—	—	—	—	—	—	—	—
38	6322	m	p	8	20	—	13	4	3.3	—	—	22	—	—	?	—	?	—	—	—	—	—	—	—	—	—	—	—	—
39	6323	c	m	18.5	22.8	—	17.7	0.7	7.3	10.6	3.3	19.1	—	P	?	P	P	—	—	—	—	—	—	—	—	—	—	—	—
40	GA46-6	m	m	34.0	40.0	7.2	1.6	1.0	12.0	1.8	0.6	0.4	—	P	P	—	P	P	P	—	—	—	—	—	P	—	—	P	—
41	FA46-3	m	m	44.3	41.5	1.4	6.4	2.8	2.2	0.8	0.6	—	0.6	P	P	—	P	P	P	—	—	—	—	—	A	—	P	P	—
42	676	f	p	35.0	27.4	1.6	6.6	6.9	21.6	—	0.2	0.6	—	P	—	—	P	P	P	—	—	—	—	—	P	—	—	—	—
43	1409	m	m	27.2	27.6	2.7	2.8	10.4	21.2	—	—	8.2	—	—	—	—	P	A	—	—	—	—	—	—	—	—	—	—	—
44	1405	m	m	50.6	21.8	2.6	8.0	5.2	6.8	4.0	—	1.0	—	P	—	—	—	P	—	—	—	P	—	—	A	—	—	P	—
45	1403	m	m	14.2	30.4	1.4	1.8	0.2	—	—	—	51.8	0.2	P	P	—	—	P	—	—	—	—	—	—	—	—	—	—	P
46	294e	m	m	17.2	42.4	0.1	0.3	5.6	14.0	12.0	0.8	7.6	—	C	P	—	—	—	P	P	P	—	—	—	—	—	—	—	P
47	294a	m	m	13.8	40.8	—	0.2	3.6	0.8	—	—	40.8	—	P	P	—	—	—	—	—	—	—	—	—	—	—	—	—	P
48	CH06	2.6	1.0	31.4	29.8	7.2	—	—	10.0	3.4	0.6	1.8	15.8	—	P	—	P	—	—	—	—	—	—	—	—	—	—	—	—
49	CD01	2.3	1.7	22	18	6	—	1	16	6	6	1	24	—	P	—	—	C	—	—	—	—	—	—	P	—	—	—	—
50	GA11G	2.0	0.5	13.1	50.2	6.0	0.9	0.2	16.3	1.7	0.4	3.0	8.2	C	C	—	P	P	—	—	—	—	—	—	—	C	C	—	P
51	GA11C	2.2	0.8	14.0	52.7	6.1	3.3	1.6	18.5	1.3	—	2.0	0.5	P	P	—	P	—	—	—	—	—	—	—	—	P	P	—	—
52	CH01	2.2	1.4	14.1	48.5	9.6	1.1	0.4	7.0	7.3	0.8	6.5	4.7	P	—	—	P	—	—	—	—	—	—	—	—	—	P	—	—
53	GA26/8	3.0	1.3	21.3	29.1	7.2	3.0	0.9	6.5	9.6	—	16.7	5.7	—	—	—	P	—	—	—	—	—	—	—	—	—	P	—	P
54	GA26/5	2.0	—	19.8	33.3	8.6	2.0	1.0	10.0	3.7	1.5	14.4	5.6	—	—	—	P	—	—	—	—	—	—	—	P	—	—	—	P
55	SP159/E	2.5	2.1	19.2	49.8	1.2	5.0	0.6	0.8	21.4	0.2	1.2	0.6	P	P	—	P	P	—	—	—	—	—	—	P	—	—	—	—
56	SP159/C	2.5	—	13.8	42.1	3.6	1.3	1.0	4.0	20.9	0.2	12.3	0.6	P	P	—	—	P	—	—	—	—	—	—	P	—	—	—	—
57	CF40A	2.5	1.0	7.0	41.0	3.6	0.6	1.0	1.0	2.0	—	43.6	0.2	P	P	—	—	P	—	—	—	—	—	—	—	—	—	—	—
58	2404	f	m	9.1	53.0	0.7	2.1	0.3	13.2	1.9	—	10.0	9.7	—	—	—	—	—	—	—	—	—	—	—	—	—	—	—	—
59	2403	vf	m	6.6	22.4	5.8	9.8	2.8	—	—	—	50.3	2.2	—	—	—	—	—	—	—	—	—	—	—	—	—	—	—	—
60	2401	f	m	18.1	20.9	2.3	2.0	—	2.1	7.9	—	38.0	8.7	P	P	—	P	—	—	—	—	—	—	—	P	—	—	—	—
61	2501	vc	m	13.8	42.1	3.6	1.3	1.0	4.0	20.9	0.2	12.3	0.6	P	P	—	—	P	—	—	—	—	—	—	—	—	—	—	—
62	2504	m	m	9.1	15.9	2.8	2.0	2.5	7.5	18.2	—	31.5	10.5	—	—	—	—	—	—	—	—	—	—	—	—	C	—	—	—
63	2505	c	m	22.3	32.9	2.4	2.0	—	—	10.9	—	22.8	6.7	P	P	—	—	P	P	—	—	—	P	—	P	—	—	—	—
64	3601	1.9	1.3	23.6	34.4	3.5	2.0	—	—	—	—	25.4	11.1	P	P	P	P	P	—	—	—	—	—	—	—	A	—	—	—

TABLE C—*Continued*

Sample No.		*Fabric*		*Composition*										*Lithic Fragments*				*Minor Constituents*												
				Framework					*Matrix*		*Cement*																			
Serial	BMR	Grainsize (ϕ units)	Sorting (ϕ units)	Quartz	Lithic	K-Feldspar	Plagioclase	Others	Undifferentiated	Clay	Silica	Carbonate	Iron	Volcanic	Sedimentary	Plutonic	Metamorphic	Biotite	Muscovite	Garnet	Zircon	Tourmaline	Hornblende	Pyroxene	Epidote	Hematite	Limonite	Opaque	Apatite
65	BR18	f	—	40.0	10.2	7.6	—	0.8	5.2	2.8	1.2	—	32.4	?	—	—	—	P	—	—	—	—	—	—	—	C	A	—	—
66	BR17	m	—	61.2	4.0	10.6	—	—	0.8	8.6	1.6	—	13.2	—	—	—	—	—	—	—	—	—	—	—	—	C	C	—	—
67	BR14	m	—	34.4	7.2	10.0	—	0.6	1.4	10.6	3.4	0.4	27.0	—	—	—	—	C	—	—	—	—	—	—	—	P	A	—	—
68	BR12	m	—	49.9	9.4	9.4	—	0.2	2.8	17.4	1.6	—	—	—	—	—	—	P	—	—	—	—	—	—	—	—	—	—	—
69	BR11	m	—	50.1	6.8	6.1	—	—	3.1	12.6	2.4	—	19.9	—	—	—	—	P	P	—	—	—	—	—	—	—	C	—	—
70	BR10	m	—	46.0	10.7	14.4	—	0.2	3.7	11.4	1.3	—	12.3	—	—	—	—	P	P	—	—	—	—	—	—	—	C	—	—
71	BR09	m	—	49.2	8.2	16.6	—	—	2.5	11.8	0.2	—	11.4	P	?	—	—	—	—	—	—	—	—	—	—	—	P	—	—
72	BR07	f	—	48.0	6.8	15.6	—	—	4.4	17.9	4.4	—	28.8	?	P	—	P	—	—	—	—	—	—	—	—	—	—	—	—
73	BR05	m	—	40.2	11.0	15.5	—	0.6	1.5	19.6	0.6	—	11.0	—	—	—	—	—	—	—	—	—	—	—	—	—	A	—	—
74	BR02	m	—	47.9	9.6	10.0	—	0.2	3.9	13.2	1.1	—	14.1	P	—	—	P	P	—	—	—	—	—	—	—	—	A	—	—
75	BR01	c	—	34.7	29.1	13.8	—	0.2	5.3	4.6	0.5	1.5	10.4	—	—	—	—	—	—	—	—	—	—	—	—	A	—	—	—
76	BD36	f	—	49.2	13.7	3.4	4.4	2.2	20.2	1.2	0.6	—	5.4	—	—	—	—	—	P	—	—	—	—	—	P	P	C	—	—
77	BD34A	m	—	27	14	9	1	—	3	4	—	21	2	P	—	—	P	A	—	—	—	—	P	—	—	—	—	—	—
78	BD46B	f	—	53.2	16.0	7.5	1.5	4.0	5.0	2.0	0.5	1.0	6.5	—	—	—	—	P	C	P	—	—	—	—	A	—	—	—	—
79	BD47-A	m	—	37.2	12.2	20.2	7.2	6.0	9.4	2.2	0.6	0.2	3.8	P	P	P	P	C	—	—	—	—	—	—	P	P	—	—	—
80	BD45-A	m	—	25.8	23.4	13.8	2.0	6.4	—	0.6	—	27.0	—	P	—	—	P	C	—	—	—	—	—	—	—	—	—	—	—
81	BD40-A	f	—	44.3	15.3	7.1	4.0	7.8	21.3	0.2	—	—	—	—	—	—	—	—	—	—	—	—	—	—	P	P	—	—	—
82	DRD15	m	—	12	39	12	2	1	19	6	—	—	2	P	C	—	—	P	—	P	—	—	—	—	P	P	—	—	—
83	GA10-1	m	—	17.7	22.6	6.7	11.4	8.7	30.7	0.9	0.4	1.0	—	—	—	—	—	—	—	—	—	—	—	C	A	—	—	—	—
84	GA10-2	f	—	19.9	28.8	12.8	9.4	4.1	22.0	—	1.6	0.4	—	P	—	P	—	—	—	—	—	—	—	—	A	—	—	—	—
85	BD43-A	m	—	13.4	39.4	13.2	7.0	3.0	18.2	3.8	0.2	1.8	—	P	P	—	—	C	—	—	—	—	—	—	—	—	—	P	—
86	BD43-B	m	—	9.2	34.0	6.8	4.6	1.4	0.2	—	—	43.8	—	P	P	P	P	P	P	—	—	—	—	—	C	—	—	—	—
87	BAR23	m	—	6.8	53.8	15.4	1.2	2.2	—	1.6	—	20.0	—	P	P	P	—	C	—	—	—	—	—	—	C	—	—	—	—
88	BAR24	m	—	5	45	10	10	—	2	—	—	28	—	C	—	—	—	—	—	—	—	—	—	—	—	—	—	—	—
89	BAR25	m	—	—	65	10	—	—	—	5	—	20	—	C	—	—	—	—	—	—	—	—	—	—	—	—	—	—	—
90	BF04	1.9	1.0	73.0	8.3	10.4	0.9	—	1.4	3.8	2.1	—	—	—	P	—	P	—	P	—	—	—	—	—	—	—	—	—	—
91	BF03	2.3	1.1	81.4	2.3	5.0	—	1.5	2.5	5.3	1.9	—	0.2	—	—	—	—	—	—	—	—	—	—	—	—	—	—	—	—
92	BF02	1.8	0.7	64.5	6.2	9.9	2.1	1.2	5.8	0.8	1.4	—	8.1	—	P	—	P	—	P	—	—	—	—	—	—	—	—	C	—
93	BF01	1.4	0.8	68.3	13.7	6.1	1.2	0.7	5.7	1.4	2.6	—	0.3	P	P	—	P	—	—	—	—	—	—	—	P	—	—	—	—
94	B108	m	—	55.8	17.4	12.7	3.6	0.4	0.5	6.1	2.7	—	0.8	P	P	—	P	—	—	—	—	—	—	—	P	—	—	—	—
95	B107	1.6	0.8	76.3	7.2	13.8	0.9	—	0.6	—	1.2	—	—	—	—	—	P	—	—	—	—	—	—	—	C	—	—	—	—
96	B106	1.4	1.2	70.9	8.0	11.4	1.7	0.7	2.9	2.9	0.7	—	0.8	—	—	—	—	—	—	—	—	—	—	—	P	—	—	—	—

TABLE C—*Continued*

Sample No.		Fabric		Composition										Lithic Fragments						Minor Constituents								
				Fragments					Matrix		Cement																	
Serial	BMR	Grainsize (ϕ units)	Sorting (ϕ units)	Quartz	Lithic	K-Feldspar	Plagioclase	Others	Undifferentiated	Clay	Silica	Carbonate	Iron	Volcanic	Sedimentary	Plutonic	Metamorphic	Biotite	Muscovite	Garnet	Zircon	Tourmaline	Hornblende	Pyroxene	Epidote	Hematite	Limonite	Opaque	Apatite
97	B105	1.7	0.9	75.4	6.0	7.7	—	—	0.3	10.6	—	—	—	—	P	—	P	—	P	—	—	—	—	—	C	—	—	—	—
98	BA03	m	—	71.9	8.2	5.9	0.6	0.8	0.6	7.6	2.3	—	2.1	—	—	—	P	—	P	—	—	—	P	—	—	—	—	—	—
99	BA01	m	—	68.8	8.0	7.8	0.5	—	1.5	11.6	0.5	—	1.3	—	—	—	—	—	—	—	—	—	—	—	—	—	—	—	—
100	BJ21	c	—	59.5	12.9	10.6	0.8	1.4	7.4	2.8	3.0	—	1.6	—	—	—	—	—	—	—	—	—	—	—	—	—	—	—	—
101	BJ10	m	—	51.8	8.9	1.1	2.6	5.2	4.7	8.8	1.7	1.7	13.5	—	—	—	—	—	—	—	—	—	—	—	—	—	—	—	—
102	BJ03	m	—	69.4	3.6	13.0	0.2	1.8	1.8	7.6	2.4	—	0.2	—	P	—	P	—	P	—	—	—	—	—	—	—	—	—	—
103	BJ01	m	—	70.2	7.4	4.2	0.4	1.8	4.2	5.0	3.2	—	3.6	—	P	—	P	—	P	—	—	—	—	—	—	—	—	P	—
104	BG09	m	—	76.3	4.1	5.7	0.2	1.3	6.8	3.4	0.2	—	2.1	—	—	—	P	P	P	—	—	—	—	—	—	C	—	—	—
105	BG06	1.6	0.9	70.7	5.6	8.6	0.6	0.2	6.2	4.1	3.6	—	0.4	—	—	—	P	P	P	—	—	—	—	—	—	—	—	—	—
106	BG03	1.7	—	66.0	5.1	7.5	1.7	1.5	10.3	2.8	3.6	—	1.5	—	P	—	P	P	P	—	—	—	—	—	—	—	—	—	—
107	BG04	1.5	1.0	66.5	6.6	8.9	1.1	2.0	6.4	6.4	1.3	—	0.8	—	—	—	P	P	P	—	—	—	—	—	—	—	P	—	—
108	BG03	m	—	72.2	3.0	7.5	0.5	0.2	4.3	10.3	1.0	—	1.0	—	P	—	P	P	P	—	—	—	—	—	—	—	—	—	—
109	BG02	1.2	1.2	68.9	5.8	11.8	0.4	0.8	4.1	4.1	2.1	—	1.9	—	—	?	P	P	P	—	—	—	—	—	—	—	—	—	—
110	BF15	1.0	—	66.4	3.2	9.2	—	0.2	9.2	9.6	1.6	—	0.6	—	—	P	P	P	—	—	—	—	—	—	—	—	—	—	—
111	BF14	m	—	72.6	4.7	4.3	—	0.4	4.0	8.0	0.6	—	5.5	—	—	—	P	P	—	—	—	—	—	—	—	—	—	—	—
112	BF13	1.5	1.0	69.9	10.6	6.4	—	0.7	2.9	8.2	1.2	—	—	—	—	P	P	—	—	—	—	—	—	—	—	—	—	—	—
113	BF12	1.7	0.7	63.9	4.1	8.9	—	2.5	2.1	11.4	6.9	—	0.2	P	—	P	P	P	P	—	—	—	—	—	—	—	—	—	—
114	BF11	m	—	77.8	3.6	—	—	0.8	6.7	6.3	4.8	—	—	—	—	—	—	—	C	—	—	—	—	—	—	—	—	—	—
115	BF10	1.2	0.9	77.1	3.0	—	—	1.0	2.2	12.0	4.7	—	—	—	—	—	P	—	—	—	—	—	—	—	—	—	—	—	—
116	BF09	2.0	1.8	69.8	4.0	0.4	—	0.2	2.0	14.8	8.8	—	—	—	P	—	—	P	P	—	—	—	—	—	—	—	—	—	—
117	BF08	1.2	0.9	76.1	3.2	—	—	0.2	1.7	5.9	5.5	—	7.4	—	—	—	—	—	—	—	—	—	—	—	—	A	—	C	—
118	BF07	1.6	0.9	76.1	4.5	4.5	—	0.4	3.8	8.9	1.7	—	—	—	—	—	P	—	P	—	—	—	—	—	P	—	—	—	—
119	BF06	1.6	1.1	68.4	8.5	11.1	0.1	0.1	0.9	5.4	5.0	—	0.4	—	—	—	—	—	P	—	—	—	—	—	—	—	—	—	—
120	AH07	m	—	55.8	8.1	8.1	6.5	3.7	6.7	6.3	2.8	—	2.0	—	—	—	—	—	—	—	—	—	—	—	—	—	—	—	—
121	AH05	m	—	53.4	6.9	7.7	4.4	0.6	11.3	10.6	3.0	—	2.1	—	—	—	—	—	—	—	—	—	—	—	—	—	—	—	—
122	AH02	c	—	75.5	2.2	7.2	1.1	7.2	3.7	—	2.4	—	0.7	—	—	—	—	—	—	—	—	—	—	—	—	—	—	—	—
123	BH10	f	—	49.8	10.4	9.2	2.0	5.2	11.5	4.3	2.3	—	5.3	—	—	—	—	C	—	—	—	—	—	—	—	—	—	—	—
124	BH08	vc	—	65.6	5.6	11.1	—	0.8	9.6	1.4	1.0	—	4.9	P	—	—	P	P	—	—	—	—	—	—	—	—	—	—	—
125	BH6	c	—	71.3	4.3	7.4	1.3	0.4	2.6	10.8	1.7	—	0.2	—	—	—	—	—	—	—	—	—	—	—	—	—	—	—	—
126	BH13	m	—	64.1	7.0	9.1	—	1.2	8.4	7.8	2.1	—	0.3	—	—	—	—	P	—	—	—	—	—	—	—	—	—	—	—
127	BH11	c	—	78.0	3.0	10.6	—	0.5	3.5	3.0	1.4	—	—	—	—	—	—	—	—	—	—	—	—	—	—	—	—	—	—
128	BI11	c	—	77.4	7.2	—	—	—	1.6	9.4	1.8	—	1.5	—	—	—	—	—	—	—	—	—	—	—	—	—	—	—	—

TABLE C—*Continued*

Sample No.		*Fabric*		*Composition*										*Lithic Fragments*				*Minor Constituents*											
				Framework					*Matrix*		*Cement*																		
Serial	BMR	Grainsize (ϕ units)	Sorting (ϕ units)	Quartz	Lithic	K-Feldspar	Plagioclase	Others	Undifferentiated	Clay	Silica	Carbonate	Iron	Volcanic	Sedimentary	Plutonic	Metamorphic	Biotite	Muscovite	Garnet	Zircon	Tourmaline	Hornblende	Pyroxene	Epidote	Hematite	Limonite	Opaque	Apatite
129	B109	m	—	71.0	4.1	9.0	0.4	—	5.1	4.4	1.4	—	4.6	—	—	—	—	—	—	—	—	—	—	—	—	—	—	—	—
130	BA25	m	—	62.6	9.9	8.4	0.2	2.8	3.7	7.8	3.2	—	1.3	P	—	—	P	—	—	—	—	—	—	—	—	—	—	—	—
131	BA23	m	—	39.6	12.1	12.6	2.3	1.4	2.3	5.0	0.8	22.7	1.2	P	—	—	P	—	—	—	—	—	—	—	—	—	—	—	—
132	BA20	f	—	74.3	3.2	11.6	—	—	0.4	9.2	1.3	—	—	—	—	—	—	—	—	—	—	—	—	—	—	—	—	—	—
133	BA19	c	—	84.2	3.7	0.2	—	0.2	0.5	6.5	4.7	—	—	?	—	—	P	—	—	—	—	—	—	—	—	—	—	—	—
134	BA18	m	—	70.9	6.3	4.9	—	0.8	3.4	8.0	2.7	—	3.0	—	—	—	P	—	—	—	—	—	—	—	—	—	—	—	—
135	BA17	m	—	72.4	5.8	0.9	—	0.4	3.8	14.9	1.8	—	—	—	—	—	—	—	—	—	—	—	—	—	—	—	—	—	—
136	BA14	c	—	85.1	4.9	—	—	—	1.7	1.5	3.8	—	3.0	—	—	—	—	—	—	—	—	—	—	—	—	—	—	—	—
137	BA10	m	—	62.7	8.7	6.5	0.2	0.4	3.3	4.0	3.5	—	10.6	—	—	—	P	P	P	—	P	—	—	—	—	—	—	C	—
138	BA07	m	—	55.7	18.0	10.3	1.8	1.8	2.0	8.8	0.4	—	1.1	P	P	—	P	P	P	—	—	—	—	—	—	—	—	—	—
139	BP05	1.6	1.1	87.4	2.6	1.0	—	—	0.2	6.3	2.5	—	—	—	—	—	—	—	—	—	—	—	—	—	—	—	—	—	—
140	BP03	1.1	0.8	90.0	2.0	—	—	0.4	—	3.7	3.7	—	0.2	—	—	—	—	P	P	—	—	—	—	—	—	—	P	—	—
141	BP01	1.2	0.7	85.4	1.6	2.6	—	—	—	1.4	6.4	—	2.6	—	—	—	—	—	—	—	—	—	—	—	—	—	—	—	—
142	BO07	1.6	0.7	79.2	5.1	—	—	—	0.4	2.8	8.8	—	3.7	—	—	—	—	—	—	—	—	P	—	—	—	—	—	—	—
143	BO05	2.5	1.0	66.4	4.9	1.0	—	1.6	0.4	5.7	6.1	—	13.9	—	—	—	—	P	—	—	—	—	—	—	—	A	A	—	—
144	BO03	1.7	1.0	79.6	4.8	—	0.2	—	0.2	7.8	2.8	—	4.2	—	—	—	—	—	—	—	—	—	—	—	—	—	—	—	—
145	BO01	1.6	0.7	84.8	1.4	—	—	0.2	0.2	2.6	6.0	—	4.8	—	—	—	—	P	P	—	—	—	—	—	—	P	P	—	—
146	BL07	m	—	79.3	3.4	0.2	—	1.2	0.4	7.1	6.5	—	1.9	—	—	—	—	—	—	—	—	—	—	—	—	—	—	—	—
147	BL03	2.7	0.8	64.4	9.5	5.6	—	0.8	4.1	6.0	3.1	—	6.4	—	—	—	—	—	P	—	—	—	—	—	—	—	A	—	—
148	BD20	2.6	1.4	48.9	14.0	4.5	0.2	1.8	3.3	13.6	2.7	—	11.1	—	—	—	—	C	P	—	—	—	—	—	—	P	P	—	—
149	BL01	2.5	0.8	62.0	7.2	7.5	—	0.6	2.4	0.6	1.1	—	18.6	—	—	—	—	P	P	—	—	—	—	—	—	A	A	—	—
150	BM05	2.5	0.8	63.4	11.3	—	0.8	0.2	1.9	3.2	1.0	—	18.1	—	—	—	—	P	P	—	—	—	P	—	—	A	A	—	—
151	BM04	2.5	1.3	73.8	8.7	2.0	—	0.7	0.4	11.1	3.4	—	—	—	—	—	P	—	P	—	—	P	—	—	—	—	—	—	—
152	BM03	2.6	0.8	70.3	7.8	2.1	—	1.2	1.2	1.4	4.9	—	10.9	—	—	—	—	—	—	—	—	P	—	—	—	A	A	—	—
153	BM01	1.4	1.3	81.8	2.8	2.7	—	1.2	0.2	6.9	4.4	—	—	—	—	—	—	—	P	—	—	P	—	—	—	A	A	—	—
154	BN02	2.6	0.9	57.4	14.3	5.0	0.2	1.5	4.4	4.4	3.6	—	9.2	—	—	—	—	P	P	—	—	P	—	—	—	A	A	—	—
155	BN01	2.6	0.8	78.5	5.8	0.2	—	1.2	1.2	4.3	4.8	—	3.6	—	—	—	—	P	P	—	P	P	—	—	—	—	A	—	—
156	2085	2.7	1.2	59.4	6.1	9.7	—	—	11.2	10.3	2.6	0.4	—	—	—	—	P	—	P	—	P	P	—	—	—	—	—	—	—
157	GA23-C	3.7	1.1	61.8	7.6	—	—	2.4	3.8	0.4	5.0	—	19.0	—	—	—	C	—	C	—	—	—	—	—	—	P	—	—	—
158	CD23	3.1	1.4	72.2	5.2	—	—	5.7	7.2	7.7	0.2	—	1.8	—	—	—	C	—	A	—	—	P	—	—	—	—	—	—	—
159	CD22	2.8	1.0	70.2	3.1	0.7	—	9.0	7.4	0.4	4.2	—	4.8	—	—	—	P	P	A	—	—	P	—	—	—	—	—	—	—
160	CD20	1.7	1.1	87.0	0.4	—	—	0.4	4.0	6.2	1.0	—	0.6	—	—	—	—	—	—	—	—	C	—	—	—	—	—	—	—

TABLE C—*Continued*

Sample No.		Fabric		Composition										Lithic Fragments														Minor Constituents											
				Framework					Matrix		Cement																											
Serial	BMR	Grainsize (φ units)	Sorting (φ units)	Quartz	Lithic	K-Feldspar	Plagioclase	Others	Undifferentiated	Clay	Silica	Carbonate	Iron	Volcanic	Sedimentary	Plutonic	Metamorphic	Biotite	Muscovite	Garnet	Zircon	Tourmaline	Hornblende	Pyroxene	Epidote	Hematite	Limonite	Opaque	Apatite									
161	CD18	0.8	1.2	93.2	—	—	—	0.8	1.4	1.0	1.6	—	2.0	—	—	—	—	P	—	—	—	—	—	—	—	—	—	—									
162	CD15	2.2	1.0	73.6	3.8	—	—	2.6	18.2	1.8	—	—	—	—	—	—	—	—	—	—	—	—	P	—	P	—	—	—									
163	CD14	1.0	0.8	92.0	0.6	—	—	0.2	1.4	4.2	1.6	—	—	—	—	—	—	—	—	—	—	—	—	—	—	—	—	—									
164	CD11	3.3	1.1	84.0	0.6	—	—	1.2	5.4	2.8	1.2	2.2	2.6	—	—	—	P	—	C	—	—	C	—	—	—	—	—	—									
165	CD08	1.5	0.8	91.8	0.7	—	—	—	5.0	0.9	1.1	—	0.4	—	—	—	—	—	—	—	—	—	—	—	—	—	—	—									
166	CG10	0.8	1.4	88.6	1.2	—	—	1.4	6.2	2.4	—	—	0.2	—	—	—	P	P	C	—	—	C	—	—	—	—	—	—									
167	CH10	3.3	1.3	71.8	4.0	—	—	7.6	11.6	3.4	1.2	—	—	—	—	—	P	P	A	—	—	C	—	—	—	—	—	—									
168	CG09	2.8	1.1	71.3	2.6	—	—	7.2	3.4	6.8	0.8	0.2	5.0	—	—	—	P	—	A	—	—	P	—	—	—	—	—	—									
169	CG08	2.8	—	83.6	2.0	—	—	1.0	8.8	3.0	—	—	1.6	—	—	—	—	—	—	—	—	C	—	—	—	—	—	—									
170	GB05	3.2	0.8	66.2	2.2	—	—	5.7	3.1	16.3	6.1	—	0.4	—	—	—	—	—	C	—	—	—	—	—	—	—	P	—									
171	CG06	2.2	1.0	65.5	4.9	—	—	1.9	6.3	0.4	3.7	—	17.3	—	—	—	P	—	—	—	—	P	—	—	—	—	P	—									
172	2515	2.4	0.9	81.1	3.3	2.6	—	1.4	4.2	1.7	4.6	0.7	0.2	—	—	—	P	P	—	—	—	P	—	—	—	—	—	—									
173	GB03	3.4	0.9	64.4	2.8	—	—	4.2	21.8	2.3	2.1	—	2.4	—	—	—	—	P	C	—	—	—	—	—	—	—	—	—									
174	CG05	3.0	0.8	57.4	12.2	1.8	—	—	4.6	2.8	2.0	0.2	12.8	—	—	—	P	—	P	—	—	P	—	—	P	—	—	—									
175	CH01	3.5	1.1	68.8	7.6	7.0	—	2.2	5.4	1.2	0.2	0.2	7.4	—	—	—	—	—	—	—	—	P	—	—	—	—	—	—									
176	CH08	2.6	1.3	73.9	10.8	—	—	1.4	7.9	9.6	—	—	0.4	—	—	—	—	—	C	—	—	P	—	—	—	—	—	—									
177	CD07	2.9	0.8	56.6	5.6	—	—	0.4	3.6	5.4	5.2	—	13.2	—	—	—	P	—	—	—	—	—	—	—	—	—	—	—									
178	CD04	2.7	1.0	71.1	12.5	—	—	0.8	4.3	7.3	1.5	—	2.5	—	—	—	P	—	—	—	—	—	—	—	—	—	—	—									
179	GB01	2.3	1.0	24.4	23.0	1.6	1.0	0.2	12.4	1.1	0.2	35.0	1.0	—	P	—	P	—	—	—	—	—	—	—	—	—	—	—									
221	U8/1	m	p	19	11	4	18	1	38	—	—	7	—	P	—	—	P	P	P	—	—	P	—	—	—	—	—	P									
222	U8/3	f	p	25	22	2	17	4	9	20	—	1	—	P	—	—	P	P	P	—	—	—	—	—	—	—	—	P									
223	B/69	f	m	20	32	2	16	1	—	18	—	11	—	P	P	—	P	P	—	—	P	—	—	—	—	—	—	P									
224	N8/1	f	m	38	9	1	9	1	12	21	3	—	6	—	P	—	P	—	—	—	—	—	—	—	P	P	—	—									
225	B/68	m	m	12	23	6	7	—	—	10	—	28	14	P	—	P	P	—	—	—	—	—	—	—	C	C	—	—									
226	Q1/3	m	m	10	20	3	4	—	—	3	1	48	11	P	P	—	P	—	—	—	—	—	—	—	C	C	—	—									
227	B/67	m	m	23	19	2	1	1	—	11	—	42	—	C	—	—	P	—	—	—	—	—	—	—	—	—	—	—									
228	Q1/2	c	m	5	35	5	9	—	2	4	—	22	18	C	P	P	—	—	—	—	—	—	—	—	—	—	C	—									
229	R1/3	m	w	8	30	4	8	8	—	—	—	42	—	—	—	—	—	—	—	—	—	—	—	C	—	—	—	—									
230	R1/2	m	p	—	34	8	21	1	—	36	—	—	—	—	—	—	—	—	—	—	C	P	—	P	P	—	—	—									
231	M4/2	c	m	—	50	1	13	2	—	—	—	34	—	—	—	—	—	—	—	—	—	—	—	C	—	—	—	—									
232	M4/1	m	m	—	33	11	24	1	7	24	—	—	—	—	—	—	—	—	—	—	—	—	—	C	P	—	P	—									
233	M3/1	m	w	—	55	1	6	1	—	—	—	37	—	—	—	—	—	—	—	—	—	—	—	P	—	—	—	—									

TABLE C—*Continued*

Sample No.		*Fabric*		*Composition*										*Lithic Fragments*				*Minor Constituents*													
				Framework					*Matrix*		*Cement*																					
Serial	BMR	Grainsize (ϕ units)	Sorting (ϕ units)	Quartz	Lithic	K-Feldspar	Plagioclase	Others	Undifferentiated	Clay	Silica	Carbonate	Iron	Volcanic	Sedimentary	Plutonic	Metamorphic	Biotite	Muscovite	Garnet	Zircon	Tourmaline	Hornblende	Pyroxene	Epidote	Hematite	Limonite	Opaque	Apatite		
234	Q4/2	c	w	2	66	1	2	—	—	—	—	19	10	C	P	P	—	—	—	—	—	—	—	—	—	—	C	—	—		
235	Q4/1	c	m	1	55	2	5	2	—	—	—	30	5	C	—	—	—	—	—	—	—	—	—	—	—	—	—	—	—		
236	Q6/9	f	m	12	38	3	8	1	4	—	—	10	24	C	C	—	—	P	P	—	—	—	—	P	P	P	—	—	—		
237	Q6/7	f-m	p	20	25	2	11	—	1	18	—	19	4	P	C	—	—	—	P	—	—	—	—	—	—	—	P	—	—		
238	Q6/6	m	m	18	24	12	11	—	4	21	—	10	—	P	—	—	P	C	C	—	—	P	—	—	—	—	—	—	P		
239	Q6/5	f	p	66	5	3	5	1	14	5	—	—	1	P	P	P	P	P	—	—	P	P	—	—	—	—	—	—	—		
240	P4/3	m	p	15	42	5	10	5	10	13	—	—	—	P	—	—	P	—	C	—	P	—	—	—	—	—	P	—	—		
241	P4/2	m	p	12	40	11	10	5	14	6	—	2	—	P	P	—	P	—	—	—	P	—	—	—	—	—	P	—	—		
242	A55	m	p	1	42	12	4	4	—	30	—	7	—	—	—	—	—	P	—	—	—	—	—	—	—	—	—	—	—		
243	A56	m	m	6	36	12	15	2	5	21	—	3	—	C	P	—	P	—	—	—	—	—	—	—	—	—	—	—	P		
244	Q5/5	m	m	2	29	9	29	—	—	30	—	1	—	C	P	—	P	—	—	—	—	—	—	—	—	—	—	—	P		
245	Q5/1	c	p	1	51	5	23	—	15	—	—	5	—	—	—	—	—	—	—	—	—	—	—	—	—	—	—	—	P		
246	B87	c	m	0.8	32.5	2.0	2.8	—	1.0	1.0	—	45.0	14.9	A	—	—	—	—	—	—	—	—	—	—	—	—	—	—	—		
247	B15	1.5	m	2	50	2	9	2	—	23	—	12	—	C	P	—	—	—	—	—	—	—	—	—	—	—	—	—	—		
248	U1/2	c	m	2	47	1	3	—	—	17	—	13	17	A	—	—	—	—	—	—	—	—	—	—	—	C	C	—	—		
249	D80	m	m	6.1	45.1	19.2	4.3	2.6	6.9	11.3	4.3	—	—	A	—	—	—	—	P	—	—	—	—	—	—	—	—	—	—		
250	M6/3	c	m	4	54	9	3	—	2	—	—	28	—	P	P	—	C	—	—	—	—	—	—	—	P	—	—	—	P		
251	B75	m	p	14	18	7	20	—	17	—	2	22	—	A	—	—	—	—	—	—	—	—	—	—	—	—	—	—	—		

* Numbers ϕ units. vc, very coarse; c, coarse; m, medium; f, fine; vf, very fine; p, poor; w, well.

† P, present; C, common; A, abundant.

TABLE D. CROSS-STRATIFICATION IN PERMIAN AND TRIASSIC UNITS

Unit	*Location*			*Number of Readings*	*Vector Trend*	*Vector Magnitude (%)*	*Standard Deviation*	*R Prob.**	*R Stat.†*	*Av. Dip*
	Point	*Lat.*	*Long.*							
Fair Hill Formation	P4	21°30′S	148°29′E	21	162	71	50	10.5	3.0	19
	C63	20°58′	148°08′	33	256	54	75	9.6	3.0	17
	Q6	20°58′	148°08′	17	151	59	64	5.6	3.0	19
	B67	23°13′	148°47′	42	165	57	—	—	—	16
	A20	23°41′	148°45′	76	195	46	—	—	—	14
Elphinstone Coal Measures	D6	21°09′	148°13′	34	222	30	—	2.85	2.9	15
	A80	21°39′	148°19′	19	151	85	—	13.9	3.0	13
	A79	21°43′	148°22′	9	157	95	—	8.2	2.9	23
	C46	21°32′	148°16′	16	186	31	—	1.5	2.9	20
	A78	21°47′	148°23′	25	139	96	—	23.1	3.0	30
	A72	21°38′	148°18′	12	124	91	—	9.9	2.9	16
	A56	21°35′	148°18′	23	357	84	—	16.4	3.0	21
	A52	21°33′	148°18′	19	274	72	—	9.8	3.0	16
	Q5	21°27′	148°25′	26	127	51	—	6.6	3.0	19
	All points	—	—	183	162	49	—	—	—	—
Fort Cooper Coal Measures	D7	21°08′	148°14′	21	333	19	—	0.8	3.0	11
	A82	21°33′	148°21′	23	195	71	—	11.8	3.0	18
	A83	21°33′	148°21′	21	138	93	—	18.4	3.0	18
	Q5	21°27′	148°25′	61	127	23	—	3.3	3.0	14
	All points	—	—	126	152	40	—	—	—	15
Baralaba Coal Measures	K1	24°31′	150°03′	15	40	80	24	—	—	—

* *R. Prob.*, Rayleigh probability (see Durand & Greenwood, 1958).
† *R. stat.*, Rayleigh statistic calculated at 5% confidence level (see Durand & Greenwood, 1958).

TABLE D—*Continued*

Unit	Location			Number of Readings	Vector Trend	Vector Magnitude (%)	Standard Deviation	R Prob.*	R Stat.†	Av. Dip
	Point	Lat.	Long.							
Rangal Coal Measures and Burngrove Formation (Blackwater area)	B48	23°48′	148°49′	15	281	26	—	0.9	2.9	11
	B50	23°48′	148°49′	12	328	41	—	2.0	2.9	12
	B58	23°15′	148°50′	8	282	75	—	4.5	2.9	19
	B87	23°46′	148°50′	14	260	87	—	10.5	2.9	17
	A24	23°37′	148°47′	17	213	72	—	8.9	3.0	16
	A25	23°46′	148°52′	23	230	30	—	2.0	3.0	17
	A31	23°17′	149°07′	20	172	22	—	0.9	3.0	16
	A46	23°10′	148°44′	22	27	89	—	17.3	3.0	20
	A47	23°10′	149°10′	22	27	57	—	7.2	3.0	15
	A48	23°10′	148°49′	19	359	73	—	10.3	3.0	12
	All points	—	—	172	291	40	—	—	—	16
Rangal Coal Measures (southwestern area)	B23	24°38′	148°21′	18	249	25	—	1.4	3.0	14
	B32	25°03′	148°18′	18	246	15	—	0.4	3.0	16
	B35	25°01′	148°16′	12	352	72	—	6.2	2.9	22
	A1	25°02′	148°15′	48	327	77	—	28.4	3.0	16
	A2	25°04′	148°17′	18	263	67	—	8.1	3.0	14
	A15	24°58′	148°16′	22	340	87	—	16.8	3.0	20
	A16	24°30′	148°04′	34	1	42	—	5.9	3.0	17
	A17	24°33′	148°03′	24	10	76	—	13.9	3.0	13
	A18	24°34′	148°02′	30	357	87	—	22.9	3.0	15
Sagittarius Sandstone	C55	21°29′	149°23′	14	165	70	47	5.9	2.9	23
	BD04	21°31′	149°15′	59	139	52	69	15.7	3.0	14
	Q5	21°28′	148°25′	17	123	81	39	11.1	3.0	21
	C64	20°59′	149°04′	12	154	95	19	10.9	2.9	18
	D34	21°03′	148°08′	22	268	39	78	3.3	2.9	12
	D1	21°12′	148°02′	75	204	72	48	39.2	3.0	15
	P3	21°31′	148°14′	38	142	64	58	15.6	3.0	17
	A74	21°39′	148°17′	70	169	76	46	40.9	3.0	17
	A6	25°06′	148°22′	69	336	78	44	41.5	3.0	21
	A8	25°01′	148°23′	60	349	85	37	43.3	3.0	18
	A12	24°54′	148°21′	33	329	41	77	5.5	3.0	21
	CF40	25°28′	148°52′	21	329	61	59	7.8	3.0	16
	B46	23°39′	148°55′	63	326	64	56	25.9	3.0	18
	B72	23°39′	148°55′	19	315	72	55	9.9	3.0	23
Arcadia Formation	P3	20°57′	148°01′	6	149	85	36	4.3	2.9	15
	GA37	21°09′	148°09′	58	151	52	66	15.4	3.0	15
	GA46	21°12′	148°12′	30	355	7	88	0.1	3.0	28
	GA49	21°56′	148°18′	84	264	44	75	17.0	3.0	15
	GA57	23°27′	149°05′	29	53	39	82	4.3	3.0	19

TABLE D—*Continued*

Unit	Location			Number of Readings	Vector Trend	Vector Magnitude (%)	Standard Deviation	R Prob.*	R Stat.†	Av. Dip
	Point	Lat.	Long.							
Arcadia Formation	GA17 18	25°02′	148°25′	30	309	70	48	15.0	3.0	25
	GA19	24°59′	148°27′	20	330	83	37	13.2	3.0	21
	CF01	24°55′	148°30′	9	310	93	23	7.8	2.9	23
	GA11	25°10′	148°35′	69	20	54	64	20.0	3.0	20
	CF26	25°48′	148°52′	30	118	67	52	13.6	3.0	17
	CD	25°25′	148°48′	6	266	58	79	2.0	2.8	23
	CH	25°09′	148°34′	11	210	74	47	5.9	2.9	24
Glenidal Formation	GA43	21°12′	148°12′	21	226	61	59	7.8	3.0	19
	BD16	21°29′	148°10′	44	145	81	42	28.9	3.0	22
	BA	21°33′	148°13′	30	153	68	54	13.9	3.0	22
	BD10	21°37′	148°07′	23	200	69	59	10.9	3.0	23
	BJ	21°38′	148°12′	41	153	74	44	22.8	3.0	21
	BF	21°47′	148°14′	15	120	80	38	9.6	2.9	15
	BD07	21°56′	148°18′	35	176	76	46	20.5	3.0	24
	GA52	22°09′	148°23′	32	141	73	45	17.1	3.0	20
	GA36	21°37′	148°07′	26	166	99	30	25.3	3.0	25
	BN-M	23°48′	149°23′	12	79	37	76	1.7	2.9	32
	GA63	23°48′	149°23′	46	125	31	81	4.5	3.0	22
	GA60	23°48′	149°23′	15	83	79	42	9.4	2.9	13
	BD20	23°48′	149°23′	81	89	69	51	39.5	2.9	14
	BL	23°48′	149°23′	11	184	61	60	4.1	3.0	21
	GA67-8	24°00′	149°31′	23	148	91	26	18.9	3.0	18
	GA71	24°31′	149°48′	27	252	51	63	6.9	3.0	13
	BD47-6	24°57′	149°56′	8	230	68	54	3.7	2.9	28
	BD45	24°59′	149°58′	6	254	75	46	3.4	2.9	22
	GA20	24°53′	148°52′	11	43	74	47	6.0	2.9	18
	CF49	25°00′	148°42′	9	48	61	71	3.4	2.9	14
	CF46	24°55′	148°30′	32	14	40	78	5.1	3.0	18
	GA82	24°45′	148°35′	22	120	65	56	9.2	3.0	16
	GA83	24°38′	148°35′	20	161	58	59	6.7	3.0	15
	CD	25°26′	148°48′	4	137	75	50	2.3	2.8	23
	CF43	24°48′	148°22′	16	37	20	95	0.6	2.9	22
	GA77	24°45′	148°35′	13	140	83	37	8.9	2.9	18
	CF13	24°32′	147°21′	7	288	88	31	5.4	2.9	29
	GA84	24°31′	147°13′	8	298	94	22	7.1	2.9	22
	CH	25°10′	148°33′	8	47	37	78	1.1	2.9	16
	GA85	24°31′	147°13′	20	292	78	41	12.3	3.0	20
	CF06	24°32′	147°17′	16	297	74	45	8.7	2.9	23
	GB	27°50′	148°48′	8	80	56	72	2.5	2.0	11

TABLE D—*Continued*

Unit	Location: Point	Location: Lat.	Location: Long.	Number of Readings	Vector Trend	Vector Magnitude (%)	Standard Deviation	R Prob.*	R Stat.†	Av. Dip
Glenidal Formation	BA08	25°01′	148°31′	32	332	48	70	7.5	3.0	19
	GA24	25°08′	148°52′	39	20	46	80	8.3	3.0	21
	GA25	24°44′	148°25′	19	30	74	44	10.3	3.0	16
	GA40	21°29′	148°08′	24	121	87	30	18.2	3.0	23
	BF-FG	21°42′	148°18′	10	105	61	58	3.8	2.9	17
	GA52	22°09′	148°23′	25	156	73	46	13.2	3.0	21
	BA	21°33′	148°12′	9	181	42	85	1.6	2.9	19
	GA66	23°58′	149°28′	60	128	70	51	29.0	3.0	20
	GA64	23°51′	149°22′	11	131	94	20	9.8	2.9	25
	GA65	23°51′	149°22′	15	133	85	33	10.8	2.9	20
Dawson Range	BD37	24°33′	148°48′	10	151	94	19	9.0	2.9	26
	GA72	24°26′	149°45′	43	179	39	75	6.5	3.0	19
	BD38	24°26′	149°45′	8	141	68	59	3.7	2.9	20
	BD39	24°26′	149°45′	10	209	77	43	5.9	2.9	22
	BR	24°58′	149°56′	29	159	43	72	5.5	3.0	21
	BD28	24°57′	149°56′	12	177	75	45	6.7	2.9	20
	BK	24°55′	149°56′	4	160	97	17	3.8	2.8	20
	BD18	24°55′	149°56′	6	179	94	23	5.3	2.9	24
	BD17	24°57′	149°56′	6	175	78	44	3.6	2.9	18
	GA09	24°58′	149°56′	21	168	61	63	7.8	3.0	16
	BD30	25°08′	149°59′	15	189	70	49	7.4	2.9	18
	BD31	25°09′	149°59′	9	194	71	49	4.6	2.9	14
Expedition Sandstone	CF36	24°17′	148°59′	33	134	65	53	13.7	3.0	20
	CF37	24°17′	148°59′	33	134	65	53	13.7	3.0	20
	GB	24°50′	148°52′	12	62	77	45	7.3	2.9	20
	CG	24°53′	148°52′	3	124	64	63	1.2	2.8	21
	GA21	24°58′	148°52′	3	124	64	63	1.2	2.8	21
	CF49	24°59′	148°42′	21	108	18	34	15.0	3.0	21
	GA77	25°10′	148°35′	13	174	7	70	3.7	2.9	16
	GA76	24°36′	149°02′	29	159	60	57	10.6	3.0	20
	GA22	24°56′	148°52′	23	56	59	66	7.9	3.0	22
	CG	24°53′	148°52′	20	133	57	59	6.4	3.0	23
	CF27	25°12′	148°37′	15	128	44	70	3.0	2.9	20
	GA05	25°12′	148°37′	26	72	71	52	13.0	2.9	24
	GA02	25°12′	148°37′	26	52	82	37	17.4	3.0	23
	GA01	25°12′	148°37′	13	67	57	71	4.3	2.9	21
	GA30	25°12′	148°37′	15	5	67	65	6.7	2.9	21
	CD	25°25′	148°47′	30	139	31	84	2.9	3.0	25
	GA06	25°25′	148°47′	17	319	34	81	2.0	3.0	24
	GA07	25°25′	148°47′	29	130	18	95	1.0	3.0	19
	GA28	25°23′	148°52′	24	351	59	63	8.6	3.0	24

TABLE D—*Continued*

Unit	Location			Number of Readings	Vector Trend	Vector Magnitude (%)	Standard Deviation	R Prob.*	R Stat.†	Av. Dip
	Point	Lat.	Long.							
Expedition Sandstone	CF51	25°06′	148°15′	15	17	43	69	2.8	2.9	17
	BD08	21°42′	148°18′	20	223	73	46	10.5	3.0	17
	GA40	21°29′	148°09′	19	153	87	31	14.4	3.0	23
	GA70	24°09′	149°40′	30	146	80	45	19.0	3.0	24
	GA62	23°38′	149°03′	32	99	63	54	12.9	3.0	20
	GA61	23°38′	149°03′	32	99	63	54	12.9	3.0	20
	GA69	23°58′	149°29′	44	140	40	76	7.0	3.0	20
	BO	23°52′	148°23′	11	105	85	33	8.0	3.0	25
	BP	23°52′	149°23′	8	164	62	57	3.1	3.0	22
	BQ	23°52′	149°23′	7	197	73	49	3.7	2.9	23
	GA55	23°52′	149°23′	26	169	76	44	14.9	3.0	20
	GA54	23°52′	149°23′	23	176	97	15	21.5	3.0	21
	GA53	23°52′	149°23′	8	183	84	35	5.7	2.9	20
	GA56	23°52′	149°23′	30	241	57	60	9.9	2.9	19
	CF28	24°17′	149°03′	26	202	79	47	16.4	3.0	15
	CF29	24°13′	149°03′	13	236	76	43	7.5	3.0	18
	CB	24°13′	149°03′	12	164	57	59	3.9	3.0	23
	CF31	24°13′	149°03′	14	125	95	20	12.6	3.0	20
	CF32	24°10′	149°03′	20	111	93	23	17.1	3.0	26
	CF34	24°10′	149°03′	24	133	85	33	17.2	3.0	23
	CF22	24°37′	149°04′	21	193	40	77	3.4	3.0	20
	GA73	24°37′	149°04′	8	229	66	53	3.5	2.9	21
	GA75	24°37′	149°04′	75	186	45	71	15.0	3.0	22
	CF52	25°06′	148°15′	5	69	14	118	0.1	2.8	22
	CE	24°50′	148°23′	7	159	76	44	4.1	2.9	20
	CF45	24°50′	148°23′	7	79	48	72	1.6	2.9	23
	GA14	24°50′	148°23′	34	36	62	59	13.2	3.0	24
	GA15	24°50′	148°23′	21	159	82	37	13.9	3.0	25
	CF03	24°54′	148°30′	18	108	62	56	6.8	3.0	21
	CF07	24°29′	147°05′	8	48	87	32	6.1	2.9	22
	CF10	24°29′	147°05′	8	137	87	32	6.0	2.9	20
	GA86	24°29′	147°05′	16	58	91	49	8.6	2.9	20
	CF12	24°32′	147°09′	7	72	61	27	5.8	2.9	21
	CF14	24°37′	147°30′	15	146	73	68	5.6	2.9	20
	GA88	23°36′	146°41′	29	75	81	46	19.0	3.0	20
	GA90	23°21′	146°44′	29	69	61	62	10.7	3.0	21
	GA91	22°51′	146°44′	31	40	82	37	20.8	3.0	24
	GA94	22°32′	146°50′	30	123	55	59	9.0	3.0	22
	GA99	22°04′	146°47′	21	114	30	85	1.8	3.0	23
	BD13	20°57′	148°01′	23	192	52	66	6.2	3.0	19
	BH	21°09′	148°09′	21	134	47	71	4.7	3.0	25
	BD05	21°37′	148°07′	12	171	87	32	9.0	3.0	22
	BF-BG	21°44′	148°13′	9	104	66	63	3.9	3.0	17